

“Synthesis & Evaluation of Polymeric Drug Delivery Systems”

A thesis submitted to the
University of Mumbai
for the degree of
Doctor of Philosophy (Technology)
in Chemical Engineering

Submitted by
Jitendra J. Gangwal

Under the guidance of
Dr. M.G. Kulkarni

Polymer Science and Engineering Division
National Chemical Laboratory
Pune - 411008 (India)

July 2010

STATEMENT BY THE CANDIDATE

As required by the University ordinances 770, I wish to state that the work embodied in this thesis titled “**Synthesis & Evaluation of Polymeric Drug Delivery Systems**” forms my own contribution to the research work carried out under the guidance of **Dr. M. G. Kulkarni**, at National Chemical Laboratory, Pune. This work has not been submitted for any other degree of this or any other University. Whenever references have been made to previous works of other, it has been clearly indicated as such and included in the Bibliography.

(Signature of the Candidate)

Name: Jitendra J. Gangwal

Certified by

(Signature of the Guide)

Name: Dr. M.G. Kulkarni

Dedicated to my family

TABLE OF CONTENTS

List of Figures	XIII
List of Tables	XIX
Chapter 1	1
Literature survey	1
1.1. Introduction	2
1.2. Polymers	4
1.2.1. Polymerization and its types	4
1.2.2. Polymerization techniques	4
1.2.3. Classification of polymers	5
1.2.4. Polymer architecture	5
1.2.5. Polymers in pharmaceutical applications	8
1.2.5.1. Acrylate polymers	8
1.2.5.2. Polyethers	9
1.2.5.3. Polyesters	9
1.2.5.4. Polyanhydrides	10
1.2.5.5. Polyamino acids	10
1.2.5.6. Polysaccharides	11
1.2.6. Biodegradation of polymers	11
1.2.7. Mechanism of degradation of biodegradable polymers	12
1.2.8. Polymers in drug delivery and criteria for selection	14
1.3. Drug delivery	14
1.3.1. Routes of drug delivery	15
1.3.2. Significance of new drug delivery systems	15
1.4. Design criteria for drug delivery systems	18
1.5. Self assembly and development of polymeric drug delivery systems	18
1.5.1. Self-assembling materials	19
1.5.2. Polymeric micelles based drug delivery systems	20
1.5.2.1. Preparation methods	22
1.5.2.2. Characterization of micellar systems	23

1.5.2.3. Types of polymeric micelles	24
a) Cross-linked polymeric micelles	24
b) Functionalized polymeric micelles for targeting	25
c) Filamentous micelles	26
d) Polymeric micelles with controlled instability	26
1.5.2.4. Classification of micelles based on composition	28
a) PEG - polypeptide micelle	28
b) PEG - polyester Micelle	28
c) Lipid polymer conjugates	29
1.5.3. Polymeric vesicle based drug delivery systems	29
1.5.3.1. Factors affecting vesicle formation	32
1.5.3.2. Preparation methods	33
1.5.3.3. Vesicles and applications	34
1.5.4. Dendrimer and dendritic polymer nanocarriers	35
1.5.5. Polymeric particles (microparticles, nanospheres and nanocapsules)	36
1.5.5.1. Polymeric nanoparticles	37
1.5.5.2. Nanocapsules	37
1.5.6. Polymeric hydrogel based delivery system	38
1.5.6.1. Photopolymerizable hydrogels	39
1.5.6.2. Self-assembling hydrogels	39
a) Ionic cross-linking mediated gels	39
b) Temperature-sensitive hydrogel	40
c) Peptide-based supramolecular hydrogels	40
d) Polymer inclusion complex based hydrogels	40
e) Stereocomplex based hydrogels	40
f) Enzyme-mediated gelation	41
1.5.6.3. Chemical cross-linking of complementary groups mediated gelation	41
a) Schiffs base mediated gels	41
b) Michael addition mediated gels	41
1.5.7. Polymer mediated metal Nps synthesis, self assembly and applications	42
1.5.7.1. Gold nanoparticles	43
1.5.7.2. Silver nanoparticles	48
1.6. Bile acid: A building block, its structure, properties and polymerization	49
1.6.1.1. Polymerization of bile acid monomers	50

1.6.1.2. Bile acid based acrylated polymers	50
1.6.1.3. Polycondensates of bile acids	50
1.6.1.4. Bile acid polymer conjugates	51
1.6.2. Applications of bile acid based polymers	52
1.7. Summary and learning	53
1.8. References	55
Chapter 2	61
Objectives and scope of work	61
2.1. Preamble	62
2.2. Objectives	62
Chapter 3	66
Synthetic biloproteins: synthesis and characterization	66
3.1. Introduction	68
3.2. Experimental	70
3.2.1. Materials	70
3.2.2. Synthesis of polymer backbone Polysuccinimide (PSI)	70
3.2.3. Synthesis of hydrophobe AEDOCA	71
3.2.4. Synthesis of AEDOCA substituted polyaspartic acid (P2K-A, P14K-A)	71
3.2.5. Preparation of biloprotein aggregates	72
3.2.6. Molecular weight determination	72
3.2.7. Differential scanning calorimetry	73
3.2.8. Characterization of biloprotein aggregates	73
3.2.8.1. Fluorescence studies	73
3.2.8.2. Static light scattering	74
3.2.8.3. Turbidity measurements	75
3.2.8.4. Zeta potential measurements	75
3.2.8.5. Transmission electron microscopy	75
3.3. Results and discussion	75
3.3.1. Synthesis and characterization of PSI - AEDOCA conjugate	76
3.3.2. Preparation and characterization of PASP -AEDOCA aggregates	79

3.3.2.1. Macroscopic analysis	80
3.3.2.2. Microscopic analysis	82
3.3.3. Vesicle formation index (F)	90
3.3.4. Morphology and size	91
3.4. Conclusions	94
3.5. References	94
Chapter 4	97
Manipulating self assembly in synthetic biloprotein: role of hydrophilic functional substitution	97
4.1. Introduction	98
4.2. Experimental	101
4.2.1. Materials	101
4.2.2. Synthesis of polymer backbone polysuccinimide (PSI)	101
4.2.3. Synthesis of hydrophobe AEDOCA	101
4.2.4. Synthesis of reactive polymer conjugates	102
4.2.5. Hydrophilic functionalization of reactive polymer conjugate	102
4.2.6. Preparation of self assemblies	102
4.2.7. Characterization of self assemblies	103
4.2.7.1. Static light scattering / Particle size determination	103
4.2.7.2. Turbidity measurements	103
4.2.7.3. Zeta potential measurements	103
4.2.7.4. Fluorescence spectroscopy	103
4.2.7.5. Surface tension measurements	104
4.2.7.6. TEM of aggregate	104
4.3. Results and discussion	104
4.3.1 ¹ H NMR spectroscopy	106
4.3.2. IR spectroscopy	108
4.3.3. Circular dichroism (CD) spectroscopy	108
4.3.4. DSC studies	109
4.3.5. Fluorescence spectroscopy	111
4.3.6. Static light scattering studies	114
4.3.7. Microscopic investigations	114

4.3.8. Mechanism of self assembly	116
4.4. Conclusions	121
4.5. References	122
Chapter 5	125
Drug encapsulation in biloprotein self assemblies for solubilization and toxicity reduction	125
5.1. Introduction	127
5.2. Experimental	128
5.2.1. Synthesis and characterization of synthetic Biloproteins	128
5.2.2. Ampho B encapsulation in synthetic Biloprotein	129
5.2.3. Ampho B content determination	129
5.2.4. Ampho B loaded biloprotein nano aggregate characterization	129
5.2.5. Study of drug aggregation by UV, CD and fluorescence spectroscopy	130
5.2.6. In vitro antifungal activity	131
5.2.7. Hemolytic activity	131
5.3. Results and discussion	132
5.3.1. Synthesis and characterization of synthetic biloprotein	132
5.3.2. Ampho B encapsulation in Biloprotein	135
5.3.3. State of Ampho B before and after heat treatment	136
5.3.3.1. UV spectroscopy	137
5.3.3.2. Circular dichroism spectroscopy	138
5.3.3.3. Fluorescence spectroscopy	140
5.3.4. Effect of freeze drying and heat treatment on particle size and zeta potential	143

5.3.5. In vitro efficacy and RBC toxicity study	145
5.4. Conclusions	147
5.5. References	147
Chapter 6	150
Biloprotein based preparation of gold and silver nanoparticles	150
6.1. Introduction	152
6.2. Experimental	154
6.2.1. Synthesis and characterization of synthetic biloproteins	154
6.2.2. Preparation of Au and Ag Nps	155
6.2.3. Characterization	156
6.3. Results and discussion	156
6.3.1. Synthetic biloproteins	157
6.3.2. Silver nanoparticles	157
6.3.2.1. Sodium borohydride reduction method	157
6.3.2.2. UV irradiation method	161
6.3.2.3. IR spectra of composites	164
6.3.2.4. XRD analysis	165
6.3.2.5. TEM of nanoparticles	168
6.3.1. Nano-patterning of silver Nps	169
6.3.2. Gold nanoparticles	172
6.4. Conclusions	175
6.5. References	176

Chapter 7	182
In situ biodegradable hydrogels from surface cross-linked supramolecular self assemblies	182
7.1. Reactive micelle based in situ hydrogels	183
7.1. Introduction	184
7.1.2. Experimental	187
7.1.2.1. General	187
7.1.2.2. Synthesis of polysuccinimide (PSI)	187
7.1.2.3. Synthesis of amino ethyl deoxycholamide (AEDOCA)	187
7.1.2.4. Synthesis of reactive bilo / fatty polymer conjugates	187
7.1.2.5. Preparation of bilo / lipoprotein nanoaggregates	189
7.1.2.6. Bilo / lipoprotein characterization	189
7.1.2.7. In situ gel preparation and its characterization	189
a) Gelation time	189
b) Rheological study	190
c) Morphological analysis by ESEM	190
d) CLSM study	190
7.1.2.8. Degradation study	190
7.1.2.9. Drug encapsulation and release	191
7.1.3. Results and discussion	191
7.1.3.1. Synthesis and characterization of AEDOCA and fatty amine PSI conjugates	192
7.1.3.2. Synthesis and characterization of synthetic bilo / lipoproteins	193
7.1.3.3. Preparation and characterization of bilo / lipoprotein aggregates	194
7.1.3.4. In situ Hydrogel Formation and characterization	200
a) Confocal microscopy	202
b) ESEM analysis	203
c) Rheological characterization	204
7.1.3.5. Mechanism of gel formation.	210
7.1.3.6. Hydrogel degradation study	211
7.1.3.7. TCN release from in situ hydrogels	212
7.1.4. Conclusions	214

7.2. Reactive emulsion based in-situ hydrogels (Emulhydrogels)	216
7.2.1. Introduction	217
7.2.2. Experimental	219
7.2.2.1. Materials	219
7.2.2.2. Synthesis and characterization of aminated bilo / lipoproteins	219
7.2.2.3. Preparation of reactive emulsion	220
7.2.2.4. Characterization of reactive emulsion	220
7.2.2.5. Preparation of emulhydrogel and its characterization	220
7.2.2.6. Emulhydrogel degradation study	221
7.2.2.7. Drug encapsulation and release from emulhydrogel	221
7.2.3. Results and discussion	222
7.2.3.1. Synthesis and characterization of bilo / lipoproteins	222
7.2.3.2. Preparation and characterization of biloprotein or lipoproteins	223
7.2.3.3. Preparation of reactive emulsion	224
7.2.3.4. Emulhydrogel preparation and characterization	226
a) Confocal microscopy	228
b) Rheological studies	229
c) Morphological analysis of emulhydrogel using ESEM	230
7.2.3.5. Emulhydrogel degradation study	231
7.2.3.6. PTX release from emulhydrogels	232
7.2.4. Conclusions	233
7.2.5. References	234
Chapter 8	238
Synthesis and characterization of bile acid based oligo β amino esters for drug delivery system	238
8.1. Introduction	240
8.2. Experimental	243
8.2.1. Materials	243
8.2.2. Synthesis of bile acid based poly β amino ester	243

8.2.2.1. Poly (Deoxycholyly glycol β amino ester) (C ₃ -C ₂₄ Head to tail conjugation)	243
8.2.2.2. Poly (methyl deoxycholate β amino ester) (C ₃ -C ₁₂ Head to side conjugation)	245
8.2.2.3. Poly (trimethylolpropane deoxycholate β amino ester) (TMP-DOCA Pendent through tail)	247
8.2.3. Characterization	249
8.2.3.1. ¹ H NMR study	249
8.2.3.2. Size exclusion chromatography	250
8.2.3.3. IR spectroscopy	250
8.2.3.4. XRD	250
8.2.3.5. Thermogravimetric analysis	250
8.2.3.6. Differential scanning calorimetry	250
8.2.3.7. Polymer degradation study	251
8.2.3.8. Drug encapsulation in polymeric nanoparticles	251
8.2.3.9. Scanning electron microscopy	252
8.2.3.10. Particle size and zeta potential determination	252
8.2.3.11. Drug content determination	252
8.2.3.12. Drug release studies	253
8.3. Results and discussion	253
8.3.1. Synthesis and characterization of poly bilo β amino esters	253
8.3.1.1. C ₃ -C ₂₄ polyaddition	254
8.3.1.2. C ₃ -C ₁₂ polyaddition	255
8.3.1.3. TMP-DOCA polyaddition	256
8.3.2. Degradation studies	259
8.3.3. Preparation of PTX loaded nanoparticles and characterization	261
8.3.4. Drug loading and release	262
8.4. Conclusions	263
8.5. References	264
Chapter 9	266
Conclusions and suggestions for future work	266

List of Figures

Chapter 1

Figure 1.1. Type of polymers based on origin, composition, linkage and structure	5
Figure 1.2. Polymer architectures (Source: Qiu 2006)	6
Figure 1.3. Chemical structure of different acrylate polymers	8
Figure 1.4. Chemical structures of different polyesters	9
Figure 1.5. Chemical structures of different polysaccharides	11
Figure 1.6. Schematic illustration of polymer matrix bulk and surface erosion	13
Figure 1.7. Schematic illustration of factors affecting polymer degradation.	13
Figure 1.8. Schematic representation of self assembled pharmaceutical carriers	20
Figure 1.9. Schematic representation of graft and block copolymer micelles	21
Figure 1.10. Schematic representation of core, shell and core shell crosslinked micelles prepared from graft (G) and block (B) copolymers	24
Figure 1.11. Functionalized micelles from (a) graft and (b) block copolymers; (c) filamentous micelles.	25
Figure 1.12 Schematic representation of self-assembling vesicle-forming polymers. (Uchegbu 2006)	30
Figure 1.13. Schematic representation of vesicles from a) Block copolymers and b) polymer conjugates. (Uchegbu 2006)	31
Figure 1.14. Schematics of michael addition mediated in situ crosslinked hydrogel formation.	42
Figure 1.15. Schematic representation of polymer-mediated assembly of AuNPs.(Ofir 2008).	44
Figure 1.16. Applications of gold nanoparticles.	47
Figure 1.17. Chemical structures of different bile acids.	49

Chapter 3

Figure 3.1. Synthesis AEDOCA substituted Polyaspartic acid sodium.	72
Figure 3.2. ¹ H NMR spectrum of PSI14K-AEDOCA in DMSO d6.	77
Figure 3.3. DS of AEDOCA on PSI as a function of feed composition in P2k-A conjugates	78

Figure 3.4. DSC endotherms of reactive polymer conjugate, polysuccinimide, AEDCOA.	79
Figure 3.5. ¹ H NMR of P14K-A at different DS in D ₂ O.	81
Figure 3.6. Emission and excitation spectra of Pyrene in P2K-A40 in water.	82
Figure 3.7. CAC of P2K-A and P14K-A as function of DS; b) Effect of morphological transition and dependence of CAC on DS of P2K-A.	83
Figure 3.8. Log CAC of literature reviewed polymer conjugates as a function of DS.	84
Figure 3.9. Plots of $(F - F_{\min}) / (F_{\max} - F)$ vs [P14K-A] with different DS and at different concentration of polymer conjugate.	85
Figure 3.10. Log (I_0 / I) of Pyrene 6.0×10^{-7} M fluorescence as a function of CPC concentration in the presence of polymer conjugates P2K-A at the conc. of 2 mg / ml.	87
Figure 3.11. TEM images of P2K-A [a) DS 10, b) DS 20, c) DS 40, d) DS 60] and P14K-A [e) DS 10, f) DS 20, g) DS 40, h) DS 60] self aggregate with varying DS	93

Chapter 4

Figure 4.1. Schematic representation of functional manipulation of polymer conjugate guiding self assembly	105
Figure 4.2. ¹ H NMR spectrum of PSI and PSI-AEDOCA (DS 10-60) in DMSO d ₆ .	106
Figure 4.3. ¹ H NMR of synthetic biloproteins (60 mole % functionalized) in D ₂ O.	107
Figure 4.4. IR spectra of polymer conjugate with 60 mole % functionalized biloproteins 1) Hydroxyl, 2) Carboxylate, 3) Hydrazide and 4) Amide	108
Figure 4.5. Circular dichroism spectra of functionalized biloproteins.	109
Figure 4.6. DSC endotherms of 40 mole % functionalized Biloprotein solutions.	110
Figure 4.7. DSC endotherms of 40 mole % functionalized Biloprotein solutions.	110
Figure 4.8. CAC determination of functionalized biloproteins: a) Hydroxyl, b) Hydrazide, c) Amide, d) carboxylate	111
Figure 4.9. Optical image of tubular structures of A40 at 50X (a); ESEM image	

of A40 in water (b); Confocal image of A40 at 40X using Rhodamine as hydrophilic marker (c); Phase contrast image at 40X(d)	114
Figure 4.10. TEM images of functionalized biloproteins (90 to 40 mole %): a-d Carboxylate; e-h Hydrazide; i- l Hydroxyl; m-p Amide.	116
Figure 4.11. Structure of AEDOCA conjugated to Aspartic acid trimer as representative backbone.	117
Figure 4.12. Spacefill model for functionalized PASP-AEDOCA unit of biloprotein.	118
Figure 4.13. Chemdraw 3D view of functional groups in Biloproteins.	119
Figure 4.14. Schematic cross sectional view of lamella formed by AEDOCA in biloproteins	120
Figure 4.15. Models of lamella formation A) Juxtaposed; B) Interdigitated; C) model (Blue rectangles represent AEDOCA and black wire represent functionalized backbone)	121

Chapter 5

Figure 5.1. Reaction scheme for preparation of Biloproteins.	133
Figure 5.2. TEM images of synthetic Biloprotein (DS 10 to 60).	135
Figure 5.3. TEM images of Ampho B loaded synthetic Biloproteins (DS 10 and 60).	136
Figure 5.4. UV-vis absorption spectrum of aggregated and heat induced super aggregated form of Ampho B in SD and Biloprotein self assemblies at 0.01 mM in PBS pH 7.4.	137
Figure 5.5. CD spectrum of aggregated and heat induced super aggregated form of Ampho B in SD and Biloprotein self assemblies at 29 mM in PBS pH 7.4.	139
Figure 5.6. Fluorescence spectra (a) Excitation scan (Em. 560 nm), Emission scan (Ex. 408 nm); (b) Excitation scan (Em.471 nm.), Emission scan (Ex. 350 nm), (c) Emission scan (Ex. 325 nm) of aggregated and heat induced super aggregated form of Ampho B in PBS pH 7.4	141
Figure 5.7. Hemolysis induced by Ampho B as a function of type of biloprotein and heat treatment in isotonic PBS, pH 7.4 at 37 ° C.	146

Chapter 6

Figure 6.1. UV-visible spectra of Ag Nps in carboxylated biloproteins (NaBH ₄ method).	158
Figure 6.2. UV-visible spectra of Ag Nps in carboxylated biloproteins (Reflux method).	160
Figure 6.3. UV-visible spectra of silver Nps in functionalized biloproteins (NaBH ₄ method).	161
Figure 6.4. UV-visible spectra of Ag Nps in functionalized biloproteins (UV method).	163
Figure 6.5. FTIR spectra of silver Nps in functionalized biloproteins (DS 10 and 60).	164
Figure 6.6. XRD pattern of silver Nps in functionalized biloproteins (DS 10 and 60).	165
Figure 6.7. C 1s, N 1s and Ag 3d XPS spectra of Ag Nps in functionalized biloproteins.	167
Figure 6.8. TEM of silver Nps capped by functionalized biloproteins at DS 10.	169
Figure 6.9. Schematic illustration of nanopatterned silver nanoparticles in biloproteins.	170
Figure 6.10. TEM of nano-patterned silver Nps in hydrazide, amide and hydroxyl functionalized biloproteins.	171
Figure 6.11. UV-visible spectra of Au Nps in carboxylated biloproteins (Reflux and NaBH ₄ method).	173
Figure 6.12. XRD spectra of Gold Nps with carboxylated biloproteins prepared by reflux method.	174
Figure 6.13. XPS spectra of Gold Nps with carboxylated biloproteins prepared by reflux and Chemical reduction (NaBH ₄) method.	174
Figure 6.14. TEM of Au Nps capped by carboxylated biloproteins.	175

Chapter 7

Figure 7.1. Synthesis of aminated bilo / lipoproteins.	188
Figure 7.2. Synthetic biloprotein and lipoproteins.	194
Figure 7.3. ¹ H NMR of biloproteins at different DS in D ₂ O.	195

Figure 7.4. CAC of bilo / lipoprotein C ₁₈ with DS 10-60	196
Figure 7.5. Effect of DS on CAC of bilo / lipoproteins.	196
Figure 7.6. TEM of aminated lipoproteins and biloprotein at DS 40.	199
Figure 7.7. Schematic of in situ hydrogel Formation.	201
Figure 7.8. Bilo / lipoprotein aggregate dispersions and b) cross-linked Gels 10% w/v.	202
Figure 7.9. Confocal photomicrograph of Lp DS 40 gel stained with Nile red and FITC dextran.	203
Figure 7.10. ESEM of bilo / lipoprotein in situ gels: a) hydrated b) freeze dried and freeze-fractured.	203
Figure 7.11. Storage and loss modulus of bilo / lipoproteins at DS 10.	205
Figure 7.12. Storage and loss modulus of lipoproteins at DS 40	206
Figure 7.13. Storage and loss modulus of in situ lipoprotein gels: a) C ₁₂ , b) C ₁₆ , c) C ₁₈	207
Figure 7.14. Storage and loss modulus of in situ biloprotein hydrogel at DS 10 and 20, with PEGDA at 10 % w / v.	208
Figure 7.15. Effect of DS of type of hydrophobe in proteins on storage modulus (G') of in situ hydrogels.	208
Figure 7.16. Schematics of gelation mechanism of bilo / lipoproteins with PEGDA	210
Figure 7.17. Effect of type of hydrophobe and its content on degradation of hydrogels	212
Figure 7.18. TCN release from lipo / biloprotein hydrogels prepared by cross linking with a) PEGDA 700, b) Jeffamine 600 diacrylamide, in PBS with 2% SDS (pH 7.4) at 37 ° C	213
Figure 7.19. Effect of DS on CAC of synthetic bilo / lipoproteins.	223
Figure 7.20. Synthetic biloprotein and lipoproteins.	225
Figure 7.21. Schematic of emulhydrogel preparation.	227
Figure 7.22. a) Synthetic bilo / lipoprotein based emulsion; b) Emulhydrogels.	228
Figure 7.23. Confocal photomicrographs of emulhydrogels stained with Nile red and FITC dextran: a) C ₁₂ -10E; b) C ₁₆ -10E; c) C ₁₈ -10E; d) DOCA-10E; e) C ₁₂ -20E; f) C ₁₆ -20E; g) C ₁₈ -20E; h) DOCA-20E.	229
Figure 7.24. Storage and loss modulus of bilo / lipoprotein based emulhydrogels.	230

Figure 7.25. Morphological analysis of gels containing self assemblies.	231
Figure 7.26. Emulhydrogel formation and degradation in phosphate buffer (pH 7.4).	231
Figure 7.27. Degradation study of bilo / lipoprotein DS10 – 20 emulhydrogels.	232
Figure 7.28. PTX release from bilo / lipoproteins (C ₁₂) DS 20	233

Chapter 8

Figure 8.1. Synthesis of Poly (Deoxycholyl glycol β amino ester)	244
Figure 8.2. Synthesis of Poly (methyl Deoxycholate β amino ester).	246
Figure 8.3. Synthesis of Poly (trimethylolpropane deoxycholate β amino ester).	248
Figure 8.4. IR spectra of poly deoxycholyl TMDP β amino esters	257
Figure 8.5. XRD spectra of poly deoxycholyl TMDP β amino esters	257
Figure 8.6. TGA curves of poly deoxycholyl TMDP β amino esters	258
Figure 8.7. DSC thermograms of poly deoxycholyl TMDP β amino esters.	259
Figure 8.8. Release of p- nitro aniline from poly deoxycholyl – TMDP β amino esters.	260
Figure 8.9. Mechanism of p- nitro aniline release from bile acid based poly (β amino esters).	260
Figure 8.10. SEM micrograph of nanoparticles prepared from poly deoxycholyl – TMDP β amino esters a) C ₃ C ₂₄ , b) C ₃ C ₁₂ , c) TMP-DOCA.	261
Figure 8.11. PTX release from nanoparticles prepared from bile acid based β amino esters of C ₃ C ₂₄ , C ₃ C ₁₂ , TMP-DOCA polymers by solvent evaporation (SE) and solvent diffusion (SD) methods.	263

List of Tables

Chapter 1

Table 1.1. Role of polymer architecture in drug delivery	7
Table 1.2. Methacrylate polymers and their applications	8
Table 1.3. Biodegradable polymers and their degradation rate	12
Table 1.4. Commercialized NDDS	17

Chapter 3

Table 3.1. Characterization of PSI - AEDOCA Conjugates	78
Table 3.2. Binding (K) and Equilibrium constant (K _v) of Pyrene	86
Table 3.3. Effect of DS on CAC, N _{agg} and Anisotropy	88
Table 3.4. Effect of molecular weight and DS on Vesicle formation index	91
Table 3.5. Effect of molecular weight and DS on particle size, zeta potential and pH	92

Chapter 4

Table 4.1. Characterization of PSI – AEDOCA conjugate by ¹ H NMR in DMSO d ₆	107
Table 4.2. Effect of type and extent of functionalization on CAC, Microviscosity and morphology	112
Table 4.3. Hydrophilicity factor (f _{hydrophilic}), surface tension, size and zeta potential of functionalized biloproteins	113

Chapter 5

Table 5.1. Physico - chemical properties of Biloproteins	135
Table 5.2. Preparation of Ampho B loaded Biloprotein nanoaggregates	136
Table 5.3. Effect of freeze drying on Ampho B loaded Biloprotein nanoaggregates	144
Table 5.4. Effect of heat treatment on particle size distribution	144
Table 5.5. In vitro efficacy of Amphotericin B in Biloprotein nanoaggregates	145

Chapter 6

Table 6.1. Silver Nps synthesized by carboxylated biloproteins	158
Table 6.2. Mechanism of metal capping by different functionalities	162
Table 6.3. XRD angles of functionalized biloproteins coated silver Nps	165

Chapter 7

Table 7.1. Bilo / lipoproteins characterization	197
Table 7. 2. Size and stability of bilo / lipoproteins	199
Table 7.3. Gel characteristics of synthetic bilo / lipoproteins	201
Table 7.4. Comparison of storage modulus of in situ gels in literature	209
Table 7.5. CAC and surface tension of synthetic lipo and biloproteins	224
Table 7.6. Characterization of synthetic bilo and lipoprotein based emulsions	226
Table 7.7. Gel characteristics of synthetic bilo / lipoprotein Emulhydrogel	227

Chapter 8

Table 8.1. Partical size and zeta potential of PTX loaded nanoparticles	262
Table 8.2. PTX content in bile acid based poly (β amino ester) nanoparticles	262

Chapter 1

Literature survey

1.1 Introduction

A pronounced increase in lifespan during the last century has been due to the revolution made since the discovery of drugs like Penicillin for the treatment of infectious diseases. This progress has been sustained by the rational design and search for novel therapeutic alternatives. Technological and industrial developments enabled production and distribution of formulations on large scale and made drugs commercially available to almost every social stratus. Now with the emergence of new life style diseases and increasing resistance to existing medicines coupled with delays in introduction of new molecules due to stringent FDA requirements, high cost and increased risk of failure, judicious delivery of existing drugs is the option which makes drug delivery an extremely challenging science.

Research in drug delivery seeks to address two issues

- a) Maximize drug activity
- b) Minimize side effects

Due to high hydrophobicity, more than 50% of the drugs approved for use exhibit poor aqueous solubility, which poses one of the main hurdles to attain convenient absorption and bioavailability. Thus, limited water solubility represents a serious drawback in the design of formulations not only for oral but also for parenteral and topical administration. Another concern stems from the limited chemical or biological stability of the drugs in the physiological environment. In sync with drug discovery science, drug delivery researchers adopted different strategies for efficient utilization of molecules for better therapeutic effects. Many approaches over the last decade were focused on improving therapeutic index. The portion of the dose which causes adverse events should be directed away from site where the event occurs. Recent focus in therapy is that no portion of drug is wasted. Drug is delivered where it is needed, at the time when needed and the rate desired for effective therapeutic action.

Drug delivery systems have to be precise in their control of drug distribution and, preferably, respond directly to the local environment of the pathology in order to ensure a dynamic and beneficial interaction with the host pathology or

physiology. Different technological strategies have been investigated in order to prolong the exposure to the drug.

The multiple benefits of employing new drug delivery systems like polymeric micelle, vesicles, tubes, nanoparticles, hydrogels and drug conjugates for innovative drug formulations are being increasingly recognized and are now better understood. Studies have shown that innovative drug delivery systems can improve drug therapy by

- Efficient targeting of drugs to the site of action;
- Use of drug therapy that would otherwise be impossible;
- Use of new, more convenient / comfortable routes of administration;
- Timed release of a drug when pharmacological action is needed;
- Improving patient compliance with medication; and
- Increasing comfort to the patient and improving health-related quality of life.

This chapter compiles different polymer classes, their synthesis and degradability. It also describes designing of polymeric architectures investigated for the preparation of self assembly mediated drug delivery vehicles such as micelles, vesicles, tubes, nanoparticles, hydrogels etc. Evolution of different drug delivery systems, their preparation, characterization, drug encapsulation methodologies and commercial successes with upcoming research approaches have been reviewed. Utility of these different constrained environments for nano-patterning of metal nanoparticles has also been reviewed. Use of bile acid as a building block for polymers and its significance has been highlighted. Following a critical review of the relevant literature, the perceived gaps have been summarised under “Summary and learning” which formed the basis of the different approaches described in subsequent chapters.

1.2 Polymers

1.2.1 Polymerization and its types

Polymerization is a process which allows low molecular weight compounds named monomer to combine and form complex high molecular weight compounds named polymer. Depending upon the functionality of the monomer and polymerization technique, it is possible to synthesize linear, branched or cross-linked polymers. Based upon the mechanism through which polymers are formed, polymerization can be classified as chain growth polymerization and step growth polymerization.

In chain growth polymerization, self addition of the monomer molecules takes place very rapidly through a chain reaction. Based on the nature of growing species, polymerisation can be classified as a) free radical polymerisation, b) ionic polymerization and c) coordination polymerization.

In step growth polymerization, the polymer build-up proceeds in stepwise manner through the reaction between functional groups of the monomers. Based on the reaction mechanism, it can be classified as a) polycondensation, b) polyaddition and c) ring – opening polymerization.

1.2.2 Polymerization techniques

Factors such as the nature of the monomer, mechanism of polymerization, requirement of physical form of polymer and viability of industrial production dictate the conditions under which polymerization is performed. The techniques of chain growth polymerization can be classified as

- a) Bulk polymerization
- b) Solution polymerization
- c) Suspension polymerization
- and d) Emulsion polymerization

Similarly, the techniques of step growth polymerization can be classified as

- a) Melt polycondensation
- b) Solution polycondensation
- c) Interfacial polycondensation
- and d) Solid or dry polycondensation

1.2.3 Classification of polymers

Polymers can be classified based on various parameters which include origin, composition, response to environment and the linkage between the monomeric units as shown in chart below.

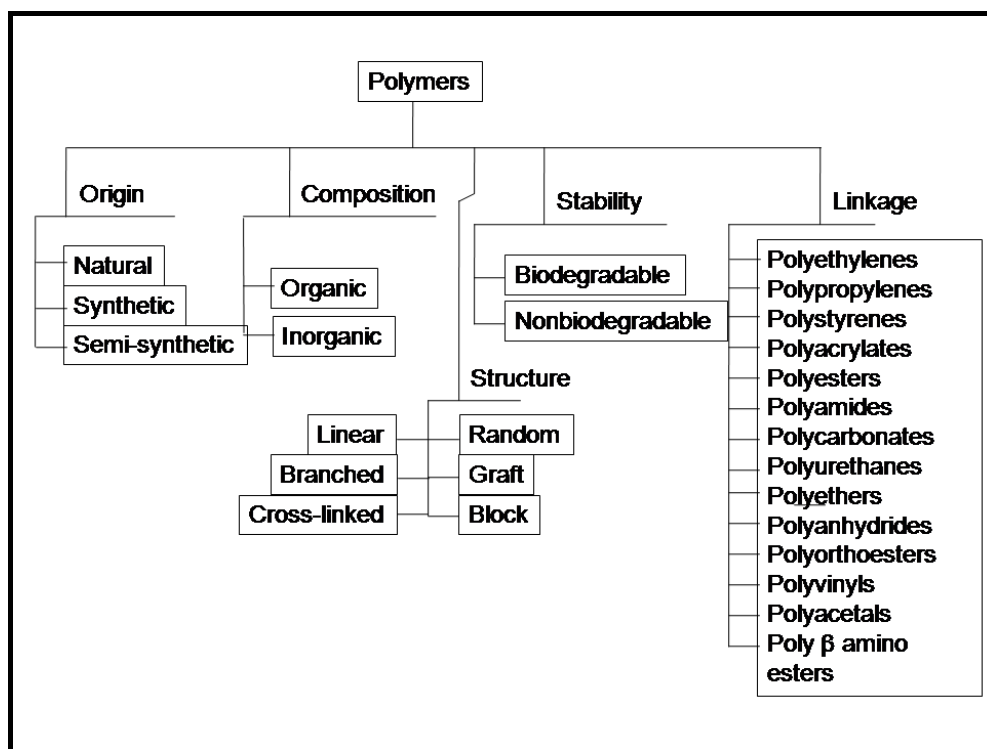


Figure 1.1. Type of polymers based on origin, composition, linkage and structure

1.2.4 Polymer architecture

Polymer architecture describes the shape of a single polymer molecule, which often determines its physicochemical properties. Controlled polymer architectures are of considerable interest for the delivery of drugs, therapeutic biopolymers, such as DNA and proteins, to their site of action.

Polymers that can respond with a change in conformation to biologically relevant stimuli, such as temperature and pH, are being designed to take advantage of the change in environmental conditions the polymer-drug conjugate encounters upon progression from large scale systems in the body to subcellular compartments. Viruses respond to changes in the cellular environment to gain access to their desired region of cells, and much can be learned from the mechanisms they employ in this effort. (Qiu 2006)

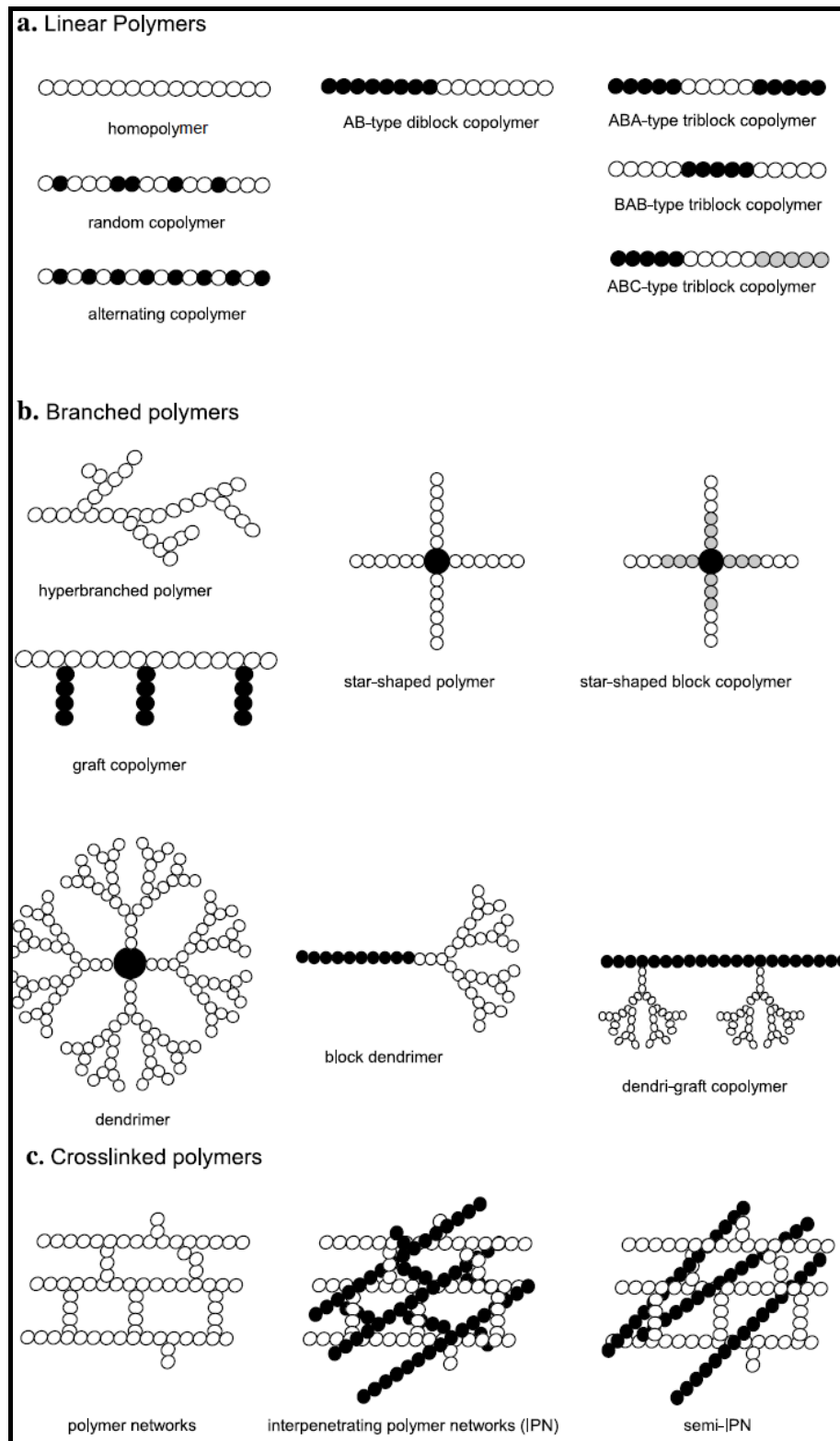


Figure 1.2. Polymer architectures (Source: Qiu 2006)

Table 1.1. Role of polymer architecture in drug delivery (Qiu 2006).

Architecture	Drug carrier	Property	Controlling factor
Water-soluble linear polymer	Drug conjugate	Solubility	Chain hydrophilicity Solubilizing moiety Drug content
		Bio-distribution and Cytotoxicity	Molecular weight Electrical charge Targeting groups
		Degradation	Backbone Spacer
		Drug release	Spacer
Block copolymer	Micelle	Shape, critical micelle concentration, and size	Proportion of A block to B block Electrical charge
		Drug encapsulation	Intrinsic affinity between drug and hydrophobic block
		Bio-distribution	Molecular weight Proportion of A block to B block Electrical charge Surface hydrophilicity Targeting groups
		Drug release	Interaction between drug and hydrophobic block Conjugation bond between drug and polymer
	Injectable hydrogel (sol-gel transition)	Sol-gel transition temperature and critical gel concentration	Molecular weight Proportion of A block to B block
	Polymersome	Polymersome	Shape
Membrane thickness			Length of hydrophobic chain
Hyperbranched polymer	Micelle	Shape, critical micelle concentration, size	Proportion of hydrophilic to hydrophobic domain Electrical charge Complexed Drug content
		Cytotoxicity and gene transfection efficiency	Molecular weight Electrical charge Surface hydrophilicity
Graft polymer	Injectable hydrogel (sol-gel transition)	Lower critical solution temperature	Graft ratio Molecular weight
	Micelle	Critical micelle concentration	Graft ratio
Star polymer	Unimolecular micelle	Drug encapsulation	Dimension of hydrophobic core Arm number
	Injectable hydrogel (sol-gel transition)	Lower critical solution temperature and gel strength	Arm number
Dendrimer	Unimolecular micelle	Size, drug-loading capability, and efficiency	Generation number Electrical charge

1.2.5 Polymers in pharmaceutical applications

1.2.5.1 Acrylate polymers

These are from the class of non-biodegradable polymers of synthetic origin in which functional monomer alone or with suitable hydrophobic monomers have been copolymerized by free radical polymerization. These constitute broad range of homopolymers, copolymers and cross-linked polymers with broad range of pharmaceutical applications. (Ray, 2000)

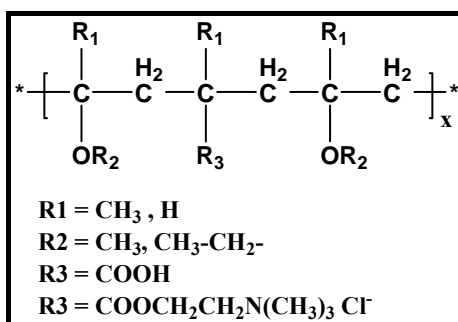


Figure 1.3. Chemical structure of different acrylate polymers

Table 1.2. Methacrylate polymers and their applications (Ray 2000)

Polymer	Trade name	Characteristics	Application
Anionic copolymer of MAA and EA	EUDRAGIT® L 30 D-55 and L 100-55	Dissolution above pH 5.5 and 6 resp.	Enteric drug delivery systems
Anionic copolymer of MAA and MA	EUDRAGIT® L 100, L 12.5, S 100, S 12.5	Dissolution above pH 7.0	
Anionic copolymer of MA, MMA and MAA	EUDRAGIT® FS 30D		
Cationic copolymer of DMAEMA, BMA, and MMA.	EUDRAGIT® E 100 and E 12.5, E PO	Soluble in up to pH 5.5, swellable and permeable above pH 5.0	Moisture or light protection
Copolymer of EA, MMA and a low content of quaternary salt of 2-TMAEMA	EUDRAGIT® RL 100 RL PO, RL 30 D, RL 12,5, RS 100, RS PO, RS 30 D, RS 12,5	Insoluble High permeability pH-independent swelling	Sustained release drug delivery systems
Neutral copolymer of EA and MMA	EUDRAGIT® NE 30 D, NE 40 D, NM 30D	Insoluble, low permeability, pH-independent swelling	
High molecular wt. Cross-linked PAA	Carbomer 934/974	Swells at neutral pH	Topical gels, suspender

1.2.5.2 Polyethers

Polyethers represent non-biodegradable but biocompatible class of polymers which include polyethylene oxide (PEO), polypropylene oxide and polytetrahydrofuran. They are formed by the joining of monomers through ether linkages.

Base-catalyzed, ring-opening polymerization is employed for ethylene and propylene oxides, while acid catalysis is used with tetrahydrofuran. Since they have alcohol groups at the chain ends, they are also called as polyethylene glycol (PEG) and polypropylene glycol (PPG). Depending on molecular weight, these polyethers range from viscous liquids to waxy solids. PEG being biocompatible is FDA approved polymer and has been useful in pharmaceutical applications like prodrug preparation, long circulating drug delivery systems, oral controlled release formulations and topical formulations. Triblock polymer i.e. PEO- PPO- PEO (Pluronic[®]) is an important FDA approved polymers useful for development of thermo sensitive drug delivery systems. (Bailey 1976)

1.2.5.3 Polyesters

Aliphatic polyesters are useful as drug carriers due to their biocompatibility and biodegradability (Kissel 2002). These polymers degrade via the hydrolytic cleavage of the ester bonds in their backbone, with or without aid of enzymes. Poly(lactic-co-glycolic acid) (PLGA) copolymers have been most widely used because their degradation rate and mechanical properties which can be precisely controlled by varying the lactic / glycolic acid ratio and by altering the molecular weight of the polymers.

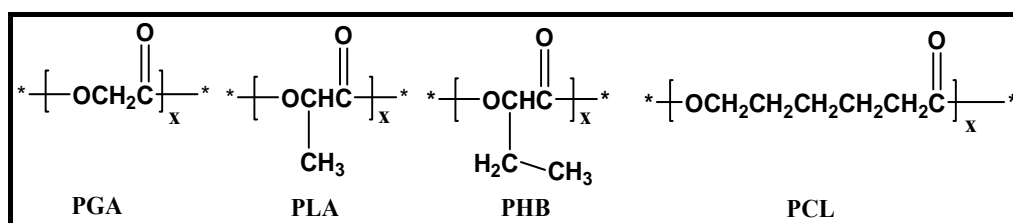


Figure 1.4. Chemical structures of different polyesters

PLGA polymers on hydrolysis yield monomeric acids (i.e., lactic and glycolic acids) which are eliminated from the body as carbon dioxide and water.

Poly(ϵ -caprolactone) (PCL) is a biodegradable, semi-crystalline polymer with low glass transition temperature (~ 60 °C). Due to its crystallinity and hydrophobicity, degradation is very slow which makes it suitable for long-term delivery over a period of more than one year (Sinha 2004).

1.2.5.4 Polyanhydrides

Polyanhydrides are hydrophobic polymers containing hydrolytically labile anhydride linkages. The degradation rate can be manipulated by varying polymer composition. These polymers show minimal inflammatory reaction *in vivo* and degrade into monomeric acids which are non-mutagenic and non-cytotoxic products (Kumar 2002). Only drawback of polyanhydrides is hydrolytic instability of the anhydride bond because of which most of them have to be stored in frozen state under the anhydrous condition. Polyanhydrides undergo surface erosion, and yield near zero-order drug release profile (Katti 2002). Polyanhydride degradation is dependent upon rate of water uptake guided by hydrophilicity and crystallinity of the polymer. US FDA has approved the use of the polyanhydride of sebacic acid and 1,3-bis(*p*-carboxyphenoxy) propane for delivery of antitumor agents in brain cancer (Park 2005)

1.2.5.5 Polyamino acids

Poly(amino acids) (PAAs) are of synthetic origin and biodegradable in nature. These are synthesized by dry and melt polycondensation of amino acids or ring opening polymerization method. They are of considerable commercial interest due to their ease of synthesis and biodegradable nature.

PAAs offer several advantages in biomedical applications and in others such as in diagnostics, sustained release matrices, microencapsulation, for plasma membrane isolation and chromosomal preparations, carriers for therapeutic protein conjugates and drug delivery systems (Li 1998). PAA exhibits very low toxicities and immunogenicities e.g., the acute toxicity of poly(aspartic acid) M_w 1,500-3,000 is $LD_{50} > 2,000$ mg/L, [rat, oral]. *In vivo* degradation rate of PAA can be modulated by varying the hydrophilicity of branch residues (Hayashi 1990).

1.2.5.6 Polysaccharides

Use of natural biodegradable polymers remains attractive for biomedical applications because of their abundance in nature, good biocompatibility, easy FDA approval and tunability. Most of the drug delivery systems that use natural polymers use proteins (e.g., collagen, gelatin, and albumin) and polysaccharides (e.g., starch, dextran, hyaluronic acid, and chitosan).

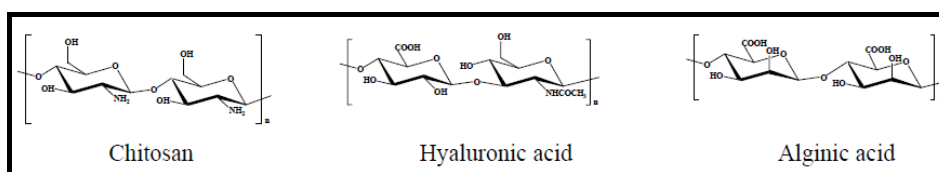


Figure 1.5. Chemical structures of different polysaccharides

For the delivery of protein drugs, use of natural proteins has been limited due to their poor mechanical properties, low elasticity, possibility of an antigenic response, and high cost (Sinha 2003). Polysaccharides due to commercial availability at low cost, tunability for specific applications and broad range of physicochemical properties are gaining importance. e.g. Chitosan and its derivatives are biocompatible, biodegradable and low immunogenic (Park 2003).

1.2.6 Biodegradation of polymers

A number of polymers used in pharmaceutical applications are biodegradable, which degrade either by chemical or enzymatic action, or both. Polymers are characterized by stability toward degradation like polyanhydrides are very labile and degrade within minutes or hours, others are much more stable.

Biodegradable polymers for drug delivery are generally chosen such that the degradation products are essentially harmless, and ideally naturally occurring in the human metabolism. Pharmaceutically useful polymers should exhibit degradation patterns from hours to weeks based upon the need of application. Highly unstable polymers (polyanhydrides) are not favoured since their controlled preparation and storage would be difficult, while more stable polymers (polyamides) are effectively not biodegradable in the context of drug delivery. Polyesters which fall in between these two extremes are most explored class of biodegradable polymers in drug

delivery. The rate of the degradation is mainly controlled by linkage as well as monomer structure or monomer mixture composition.

Table 1.3. Biodegradable polymers and their degradation rate

Sr.no	Polymers	Hydrolysis rate*
1.	Polyanhydride	0.1 hours
2.	Polyketal	3 hours
3.	Polyorthoester	4 hours
4.	Polyacetal	0.8 years
5.	Polyester	3.3 years
6.	Polyurea	33 years
7.	Polycarbonate	42,000 years
8.	Polyurethane	42,000 years
9.	Polyamide	83,000 years

* Time required for 50% hydrolysis at pH 7 and 25°C (Pierre 1986).

1.2.7 Mechanism of degradation of biodegradable polymers

In recent years synthetic biodegradable polymers has been getting lot of attention as carrier material for delivery of drugs and antigens (Park 1993). These materials are advantageous as they degrade within the body due to natural biological processes, eliminating the need to remove a drug delivery system after release of the active agent has been completed. In general, biodegradable polymers can be defined as macromolecular materials which are capable of conversion into less complex products through in situ hydrolysis of labile links (ester, amide, carbonate or urethane) by simple or enzyme catalyzed hydrolysis over a reasonable period of time (Park 1993). Such chemical changes usually result in the dissolution of the previously insoluble material due to alterations in polymer side groups or destruction of the macromolecular backbone leading to generation of shorter chain segments and low molecular- mass products. Polyesters like PLA, PLGA, PCL, polyamino acids like polyaspartic acid, polyglutamic acid, polyurethanes and

polycarbonates all represent biodegradable polymers. In all these polymers degradation takes place through bulk hydrolysis, in which the polymer degrades in a fairly uniform manner throughout the matrix. (Figure 1.6)

Another class of polymers which are bioerodible has been explored since long for the development of drug delivery systems (Park 1993). In these systems the release of the drug is accomplished through a decrease in the integrity and a subsequent dissolution of the polymeric matrix, but not necessarily complete chemical degradation. In poly anhydrides and poly ortho esters, the degradation occurs only at the surface of the polymer, resulting in a release rate that is proportional to the surface area of the drug delivery system, as shown in Figure below.

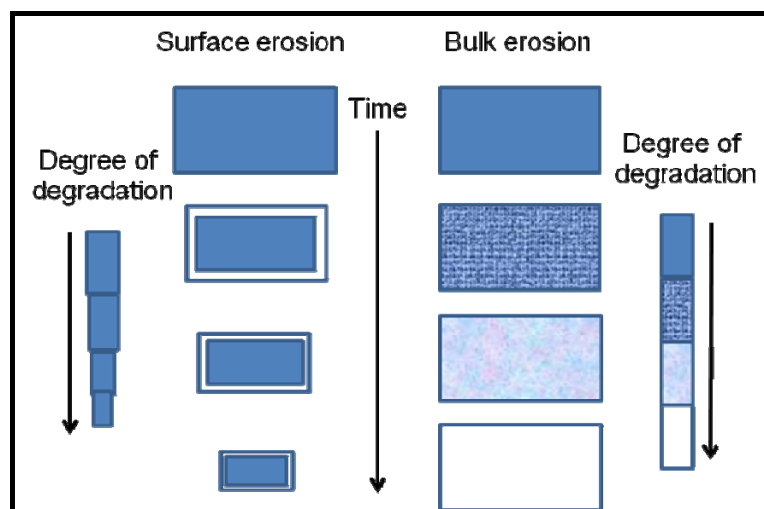


Figure 1.6. Schematic illustration of polymer matrix bulk and surface erosion (Winzenburg 2004).

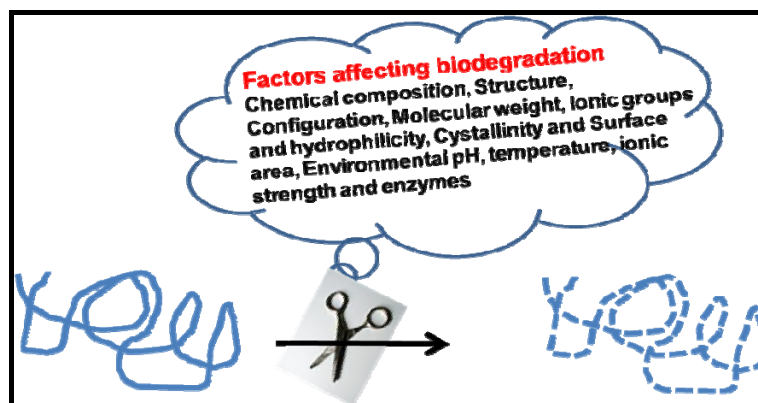


Figure 1.7. Schematic illustration of factors affecting polymer degradation.

Degradation of biodegradable polymers mostly depends on the type of linkage and environment of degradation but many other factors which also contribute indirectly to degradation are represented schematically above (Figure 1.7) (Huang 1986).

1.2.8 Polymers in drug delivery and criteria for selection

Polymers are becoming increasingly important in the field of drug delivery. The pharmaceutical applications of polymers range from their use as binders in tablets to viscosity, flow controlling agents in solutions, suspensions and emulsions. Polymers can be used in oral dosage forms as film coatings to disguise the unpleasant taste of a drug, to enhance drug stability, to modify drug release characteristics, in oral and parenteral dosage forms to solubilize drug, in parenteral dosage forms to protect drug in circulation or deliver it to desired site at desired time at desired rate.

Depending upon the application of polymers in the type and site of drug delivery system, performance requirements of polymers vary but overall following properties are desirable. An ideal polymer should be

1) biocompatible; 2) non-immunogenic, non-pyrogenic or nontoxic; 3) with desired functionalities for better biocompatibility; 4) stable with high glass transition temperature (T_g); 5) bio-resorbable; 6) amenable to synthesis on large scale; 7) readily soluble in common solvents.

1.3 Drug delivery

The science of drug delivery can be defined as the application of chemical and biological principles to control the in vivo temporal and spatial location of drug molecules for clinical benefits. When the drugs are administered, only a small fraction of the dose actually reaches relevant receptors or sites of action which indicate that most of the dose gets wasted due to undesired uptake by “wrong” tissue or gets removed from the “right” tissue too quickly, or gets destroyed during transit. Hence the holy grail of drug delivery researchers has been to maximize drug efficacy and reduce side effects (Uchegbu 2006).

1.3.1 Routes of drug delivery

For most drugs, there exists relationship between pharmacological response and concentration at the receptor. Thus to be biologically active, the drug must get into the systemic circulation. Plasma drug concentration depends on both drug kinetics and the design of the drug delivery system. Not only the magnitude of drug that comes into the systemic circulation but also the rate at which it is absorbed is important.

A drug that is completely absorbed but at slower rate may fail to show therapeutic response since the plasma concentration never reaches desired level to exhibit therapeutic effect. On the contrary, a drug which gets rapidly absorbed attains the therapeutic level easily and elicits pharmacological effect. Thus both the rate and the extent of absorption are important. Drugs that have to enter the systemic circulation to exert their effect can be administered by three major routes:

1. **Enteral Route:** This includes peroral i.e. gastrointestinal, sublingual or buccal and rectal routes. The GI route is the most common for administration of majority of drugs.
2. **Parenteral Route:** This class includes all routes of administration through or under one or more layers of skin. No absorption is required when the drug is administered intravenously (i. v.) hence this route has 100 % bioavailability. Absorption is necessary for extravascular parenteral routes like subcutaneous and intramuscular routes.
3. **Topical Route:** This class includes skin, eyes or other specific membranes. The intranasal, inhalation, intravaginal and transdermal routes are subtypes of this route.

1.3.2 Significance of new drug delivery systems

Control and manipulation of structures at the molecular level in polymers leads to the creation of novel surface architectures and materials. Biomedical applications make use of nanotechnology in biosensors, tissue engineering, intelligent systems and nanocomposites used for implant design and controlled release (Hasirci 2006).

In order to improve performance of drugs nanoparticles engineering (Overhoffa 2007) approach was adopted which dramatically enhanced dissolution rates and bioavailabilities of drugs. For development of nanocarrier vehicles, newer macromolecular architectures such as nanoparticles, dendrimers, polymeric micelles and polymersomes along with noble metal nanoparticles have been developed for parenteral applications. There are several small hydrophobic drugs which have limited water solubility, poor oral bioavailability, and / or short half lives. These molecules can be encapsulated and delivered from vehicles that have hydrophobic interiors to increase their efficacy. Typical examples of these drugs are Paclitaxel (for cancer treatment), levonorgestrol (for female birth control), and morphine (for anti-inflammatory care or pain relief)

Water soluble drugs, such as the anticancer molecule doxorubicin, that are nonspecific in their action are best delivered to specific locations to reduce adverse side effects. Delivery vehicles that can target specific tissue types improve the effectiveness of these types of drugs. Design of nanocarriers has thus seen milestones like Doxil[®] a PEG coated liposome containing Doxorubicin for tumour therapy from the stage of liposomes developed by Gregoriadis and colleagues more than three decades ago (Gregoriadis 1974). Biopharmaceuticals, such as proteins and peptides, have benefited by the designing of drug delivery vehicles which increase long-term structural stability when formulated at high concentrations, which improve their shelf life and slow delivery reduces susceptibility to biodegradation at release site. Chronic hormone treatment (human growth hormone, leuprolide) has been simplified due to vehicles like Lupron[®] a microsphere based depot of leuprolide acetate (1, 3, 6 12 month) for prostate cancer and diabetic drugs (insulin) that show improved efficacy when delivered from a Basulin[®] a leucine – glutamate micellar vehicle.

Delivery vehicles for the above therapeutics and the others listed in Table 1.4 are commercially available. However, many other methods of delivery for other promising therapies are currently being developed or still need to be addressed. Furthermore, emerging tissue-engineering strategies that involve the localized

delivery of cells would benefit from a vehicle that mimics the extracellular matrix and results in the acute retention of cells at the delivery site (Branco 2009).

Table 1.4. Commercialized NDDS (Branco 2009)

Delivery system	Material composition	Product name	Drug / Bioactive
Micelles	Leucine–glutamate copolymer	Basulin	Insulin
Vesicles	Lipid	Abelcet Allovectin-7 AmBisome Amphocil Amphotec DaunoXome	Amphotericin B HLA-B7 plasmid Amphotericin B Amphotericin B Amphotericin B Daunorubicin
		Depocyt Depodur Doxil	Cytarabine Morphine sulfate Doxorubicin
		MiKasome	Amikacin
		Myocet Stealth	Doxorubicin Doxorubicin
Micro-spheres	Crosslinked albumin PLA (polylactic acid) PL-ethylphosphate PLG (polylactide-glycolide) PLGA-glucose Polybutylene terephthalate	LeuProMax Lupron Depot Paclimer Eligard Risperdal Consta Trelstar LA Sandostatin LAR Locteron	Leuprolide Leuprolide acetate Paclitaxel Leuprolide acetate Risperidone Triptorelin pamoate Octreotide rh IGN-a
Gels	Hydroxyl methacrylate PLGA	Vantas Oncogel	Histrelin Paclitaxel
Implants	Collagen PLGA Polyanhydride Silicon rubber Titanium mechanical device	CollaRx Durin Zoladex Gliadel Wafer Implanon Jadelle Viadur	Gentamicin Leuprolide Goserelin acetate Carmustine Levonorgesterol Levonorgesterol Leuprolide acetate

1.4 Design criteria for drug delivery systems

The criteria for the design of new delivery vehicles are designed are highly dependent on the type of drug and the route for intended application. However, there are general criteria that drug delivery system must meet. Drug delivery system should

(1) be constructed with materials that are non cytotoxic, biocompatible and, in most cases, biodegradable. (2) provide solubilizing environment with high loading capacity in order to lower frequency of administration and increase patient compliance needed for long term therapies. (3) provide spatial distribution of drug in order to control and achieve consistently defined release profiles. (4) use the method which load the vehicle without damaging or altering therapeutic agent. (5) protect the drug from physical and chemical degradation, as well as antibody neutralization on administration. (6) be capable of targeting if needed and being retained at the desired site of action, in order to release the therapeutic with defined and reproducible temporal resolution. (7) be easy to administer with little discomfort. (8) be easy to fabricate in quantities commensurate with the market size at an acceptable cost (Branco 2009)

1.5 Self assembly and development of polymeric drug delivery systems

Molecular synthesis is a method that chemists use to make small or large molecules by forming covalent bonds between atoms giving due attention towards stereochemistry. Molecular self-assembly is a spontaneous process in which molecules (or parts of molecules) form ordered aggregates mainly by non covalent interactions. In molecular self-assembly, the assembling molecular structure determines the structure of the assembly (1). Synthesis makes molecules; self-assembly makes ordered ensembles of molecules (or ordered forms of macromolecules). The structures generated in molecular self-assembly are usually in equilibrium state (or at least in meta-stable states). Molecular self-assembly is ubiquitous in chemistry, materials science, and biology and has been existent long before becoming a discrete field of study and as a synthetic strategy. The formation of molecular crystals, colloids, lipid bilayer, phase separated polymers, folding of

polypeptide chains into proteins, folding of nucleic acids into their functional forms association of a ligand with a receptor and self-assembled monolayers are all examples of molecular self-assembly (Whitesides 2002).

1.5.1 Self-assembling materials

Most self-assembling molecules are amphiphilic in structure, containing both hydrophobic and hydrophilic domains. The hydrophilic portion can be charged (anionic, cationic, or zwitterionic) or uncharged (Tu 2004). Amphiphilicity is imparted to a molecule by spatially segregating the hydrophobic and hydrophilic portions either along the length of the molecule or on distinct faces of a structured molecule. The concept of using amphiphilicity to drive molecular assembly is inspired from nature, where amphiphilic molecules such as lipids, peptides, and proteins serve as building blocks for the construction of functional assemblies like cellular membranes, the cytoskeleton, and the extracellular matrix.

Under aqueous conditions, these amphiphilic molecules associate through weak, non-covalent interactions and form ordered assemblies with sizes in range from nanometers to microns (Tu 2004). The thermodynamic driving force for the most self-assembly events are provided by the desolvation, collapse, and intermolecular association of the hydrophobic portions of monomers. Intermolecular polar interactions, such as electrostatics and hydrogen bonding, can also occur and help define the structural specificity. For lipids, the area of the head group, the length of the extended hydrocarbon chain, and the volume occupied by the hydrocarbon tail(s) also control the final assembled structure (Tu 2004). The morphology of the final assembled structure is dependent not only on the structure of the monomer but also on the external environment in which self-assembly occurs (Whitesides 2002). The temperature, pH, and ionic strength of the solution, as well as the concentration of the monomer, can dictate the formation of a variety of structures formed by a single, distinct amphiphile. Self-assembly is a dynamic process, and therefore can be triggered or reversed by these external stimuli, offering the possibility of forming the assembly before delivery and disassembling the final supramolecular structure after delivery to the site of interest (Whitesides 2002, Tu 2004). Molecular amphiphiles self-assemble to form a variety of nano- and microscale structures

under aqueous solution. The most common three-dimensional structures include micelles, vesicles, tubules, fibrils, fibers and molecular gels (Branco 2009).

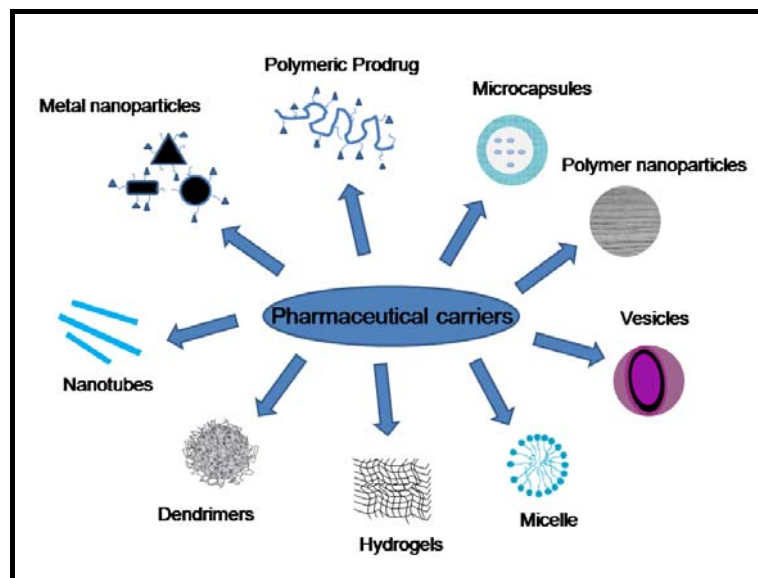


Figure 1.8. Schematic representation of self assembled pharmaceutical carriers

1.5.2 Polymeric micelles based drug delivery systems

Micelles are colloidal dispersions of particle sizes between 5 and 50 - 200 nm. Among colloidal dispersions, micelles belong to a group of associating or amphiphilic colloids, which, under certain conditions of concentration and temperature amphiphilic or surface-active agents (surfactants) spontaneously form. These molecules consist of two clearly distinct hydrophobic and hydrophilic regions which exhibit opposite affinities towards water (Duncan 2003). At low concentrations, they exist separately; however, as their concentration is increased, aggregation takes place within a narrow concentration interval. Those aggregates, micelles, consist of several dozens of amphiphilic molecules and usually have a spherical shape. The concentration of a monomeric amphiphile at which micelles form is called the critical micelle concentration (CMC), whereas the number of individual molecules forming a micelle is called the aggregation number (N_{agg}) of the micelle.

In aqueous media, amphiphilic copolymers i.e. block or graft copolymers with large solubility difference between the hydrophilic and hydrophobic segments,

spontaneously form polymeric micelles with a distinct core-shell structure in which a hydrophobic inner core is surrounded by a hydrophilic shell or corona. Systematic control of the core-forming block structure provides micelle stability and a wide variety of materials for drug loading, release and activation. Thermodynamic and kinetic stability of the polymeric micelles is important because their fast dissociation in the blood compartment would result in the burst release of loaded drugs causing systemic toxicity. In contrast to micelles from small surfactant molecules (e.g., polyethoxylated castor oil or Cremophor[®] EL, polysorbate 80 or Tween[®] 80), polymeric micelles are generally more stable and can retain the loaded drug for a prolonged period of time even in a very diluted condition in the body due to appreciably lowered critical micelle concentration, particularly for polymeric micelles like unimers, cross-linked micelles or highly regulated block copolymers with distinct core-shell structure

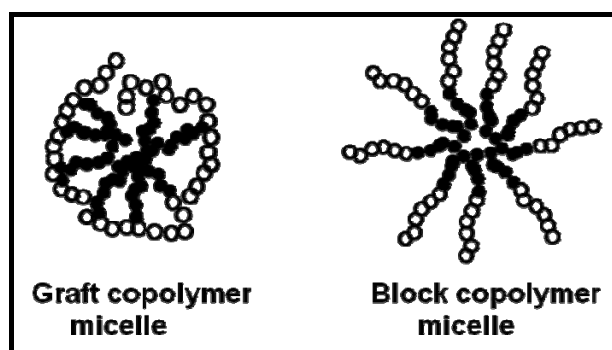


Figure 1.9. Schematic representation of graft and block copolymer micelles

For poorly-water-soluble pharmaceuticals, micelles act as preferred drug carrier since they offer following advantages.

- They can efficiently solubilize water-insoluble drugs inside the hydrophobic core by the inclusion of hydrophobic drugs by physical means or chemical conjugation and their dispersion at the molecular level, resulting in enhanced water-solubility and thus increase their bioavailability.
- The isolating effect (from the environment) of the polymeric entity can protect molecules sensitive to chemical or biological triggers from degradation and metabolism thus prevent the incorporated drug from the inactivation in biological environment.

- Polymeric micelles containing poly(ethylene oxide) as the hydrophilic component evade opsonisation and uptake by the macrophages of the reticulo-endothelial system (RES), which prolong circulation times in blood leading to increased residence time in the circulation causing gradual accumulation in body regions with leaky vasculature via the enhanced permeability and retention effect, EPR, known also as a “passive” targeting or accumulation via an impaired filtration mechanism, and enhance drug delivery in those areas
- They can be targeted by attaching a specific ligand to their external surface.
- They have ability to inhibit the activity of efflux transporters like PGP which are known to pump out circulating drug from the system.

The “ideal” pharmaceutical micelle should possess a suitable size (10 to 100 nm), and high stability towards *in vitro* and *in vivo* conditions by virtue of low CMC value and high kinetic stability. They should be long-circulating and still able to eventually disintegrate into inert and nontoxic unimers that should be easily cleared from the body. The core of the polymeric micelle should demonstrate a high loading capacity, controlled-release profile for the incorporated drug, and good compatibility between the core-forming block and incorporated drug. The effective steric protection offered by the micellar corona depends on the length and density of hydrophilic blocks. They also impart hydrophilicity, charge, and sites for reactive groups suitable for further micelle derivatization through attachment of targeting moieties. The micellar corona properties thus control important biological properties of a micellar carrier, such as its pharmacokinetics, biodistribution, biocompatibility, longevity, surface adsorption of biomacromolecules, adhesion to biosurfaces, and targetability (Torchilin 2007 and Uchegbu 2006).

1.5.2.1 Preparation methods

Polymeric micelles are mostly prepared by following four methods

- Solvent injection method: In this method polymer and drug are both dissolved in common solvent and then slowly added to water or buffer under vigorous condition to form micelle.

- Dialysis method: In this method solution of polymer and drug is placed in dialysis bag and dialyzed against distilled water. Slowly water penetrates inside and the solvent moves out forcing polymer to form micellar structures.
- Film hydration method: In this method both the polymer and drug are dissolved in solvent and slowly a film is formed in round bottom flask. After complete removal of solvent hydrating medium like water or buffer is added and vigorously mixed to form micellar structures.
- Sonication method: In this method polymer and drug are added as solid in dispersion medium and energy is provided to disperse them by sonication. Sonication causes de-aggregation of polymers chains and allows penetration of drug inside hydrophobic core. It is also used in case of other method to reduce particle size of formed micelles.

1.5.2.2 Characterization of micellar systems

Micelles prepared from block and graft copolymers are interesting to characterize in order to learn more about a particular system. Micelles can be characterized for the concentration at which aggregation takes place (CMC), the temperature at which aggregation takes place (C_t), number of molecules constituting micelle (N_{agg}), environment inside micelle (micropolarity), rigidity of micelle core (microviscosity), density of hydrophilic coat, size and shape of micelles are some of the characteristics to be investigated which largely influence their physical and biological stability. These features depend primarily on the chemical nature and the molecular weight of the segments of the block copolymers and hydrophobe content and type of hydrophobe in graft copolymers. Polymeric micelles are usually smaller in size (10 to 60 nm) with narrower size distribution (polydispersity index < 0.1) than liposomes and nanoparticles, but some polymeric micelles exhibit a bimodal size population due to high polydispersity of polymer backbone in graft copolymers and secondary aggregation of exposed hydrophobic cores (Cammis 1997). Polymeric micelles are mostly spherical but other shapes like ellipsoid and rod-like micelles can also be observed depending on the hydrophilic-hydrophobic balance in

block copolymer (Allen 1999), hydrophobic content and head group size in graft copolymer and polymer conjugates.

The molecular level investigation of polymeric micelles (CAC, Nagg, microviscosity) can be probed by fluorescence spectroscopy. The morphological aspects like size and shape can be determined by light scattering experiments, microscopic techniques, e.g. transmission electron microscopy (TEM), and atomic force microscopy (AFM). Using the Stokes-Einstein relation for colloidal particles, diffusion coefficient of the micelles can be calculated to determine hydrodynamic diameter by DLS technique. The state of hydration, the counter ion binding and the location of solubilized molecules in micelles can be probed by NMR spectroscopy (Uchegbu 2006).

1.5.2.3 Types of polymeric micelles

a) Cross-linked polymeric micelles

One of the major problems with micellar systems has been, once in circulation they open prematurely before reaching to the desired site due to dilution below CAC. The performance of self-assembled drug delivery systems can be improved by designing functional block or graft copolymers. These architectures can be cross-linked to become stable towards dilution and release components on reaching site.

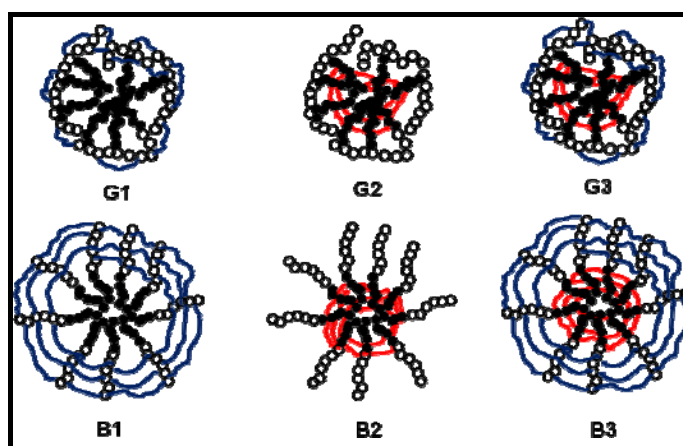


Figure 1.10. Schematic representation of core, shell and core shell cross-linked micelles prepared from graft (G) and block (B) copolymers
The first approach has been synthesis of copolymers which contain one or more functional groups on the hydrophobic block which allow cross-linking of the core of

the micelle eg. PBD - PEO. Second approach involves copolymers in which the reactive substituents are located on the hydrophilic part of the molecule which enable cross-linking of the micellar corona eg. PSS – PAA. Third approach involves synthesis of copolymers which have reactive functionalities in both the hydrophilic and hydrophobic segments which leads to generation of core and corona cross-linked micelles useful for controlling the release of actives from the micelles e.g. PBD - PAA (Uchebu 2006b).

b) Functionalized polymeric micelles for targeting

This involves synthesis of copolymers which have ligands conjugated on hydrophilic corona for directing the drug delivery device to the specific site of interest. Some of the examples of directing ligands are antibodies, sugar moieties, transferrin, and folate residues. The last two ligands are especially useful in targeting to cancer cells, since many cancer cells over-express transferrin and folate receptors on their surface. Transferrin - modified micelles based on PEG and polyethyleneimine with the size between 70 and 100 are expected to target tumors with over-expressed transferrin receptors.

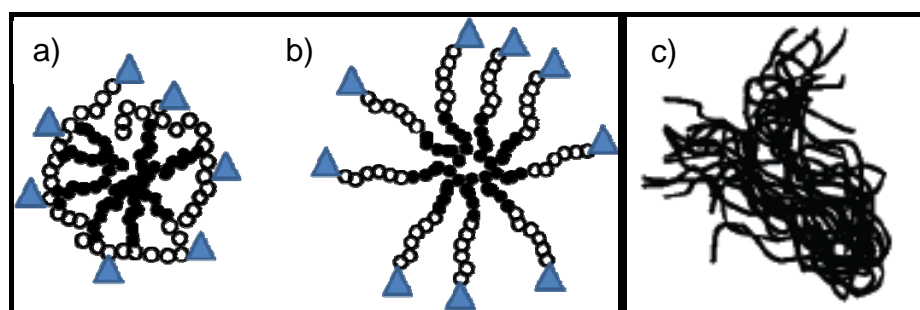


Figure 1.11. Functionalized micelles from (a) graft and (b) block copolymers; (c) filamentous micelles.

Similar approach has been adopted for Poly(L-histidine) - PEG and PLA - PEG with folate residue on their surface. These ensured efficient delivery of adriamycin to tumor cells in vitro useful for targetable and pH sensitive solid tumor treatment. Galactose- and lactose-modified PEG - polylactide copolymers form micelles which specifically interact with lectins for targeted delivery of the micelles to liver (Torchilin 2007).

c) Filamentous micelles

In nature, numerous viruses which infect animals are filamentous. This has motivated the development and study of soft filamentous vehicles. The distinctive in vivo circulation behaviour of such filaments for comparison with spheres of similar surface chemistry has been investigated by Geng et.al. The lipid bilayer represents successfully mimicked cell biological structure. Poly(ethylene oxide)- polybutadiene (PEO-PBD) and / or poly(ethylene oxide)-polyethylethylene (PEO-PEE), self-assemble in water to yield highly stable vesicles compared to natural systems. Many related systems and copolymers have been developed in recent years. Both PEO-PBD and PEO-PEE of higher PEO weight fraction than those used to make vesicles form worm like micelles which are many micrometers long and highly stable in flow but only 10 nm in diameter. Free-radical polymerization of PBD in the hydrophobic cores of PEO-PBD and PEO-PEE blended worms provided means of control over flexibility. The copolymers used were more symmetric than lipids in their hydrophilic / hydrophobic ratio, which lead to the cylindrical shapes. The copolymers also had higher molecular weights than lipids, which imparted physical stability and aggregate lifetimes of weeks or longer (Geng 2005a, 2005b, 2007). Another copolymer studied had hydrophilic polyethyleneglycol (PEG) and hydrophobic inert polyethylethylene or biodegradable polycaprolactone segment, which hydrolyses over hours to days in these micelles. Shape, size and flexibility of micelles have to be taken into consideration while devising new filamentous carriers for higher longevity in circulation inside body (Geng 2005a, 2005b, 2007).

d) Polymeric micelles with controlled instability

The ideal polymeric micellar system should retain the entrapped drug in the bloodstream, and release it in a relatively short time preferably only after reaching the site of action. In order to achieve responsive drug delivery system light, pH, or temperature have been used as stimuli for site-specific drug delivery.

pH sensitive micelles exploit mildly acidic pH in tumor and inflammatory tissues (pH 6.5) as well as in the endosomal intracellular compartments (pH 4.5 – 6.5) to trigger drug release upon their arrival at the targeted disease site. e.g. polyacetal core micelles developed by Fréchet and coworkers demonstrated pH dependent micelle

that release encapsulated cargos significantly faster at pH 5 than at pH 7.4.(Gillies 2003) Another approach by Kataoka and coworkers makes use of an acid-labile hydrozone linker to conjugate Doxorubicin to pAsp (Bae 2003). The release of Doxorubicin resembled to that observed in Fre'chet's pH-sensitive micelles.

Light sensitivity is an alternative trigger which makes use of infrared light. The amphiphilic structure has an oligo(ethylene glycol) as the hydrophilic block and 2-diazo-1,2-naphthoquinones as the terminal hydrophobic end which on light exposure through Wolf rearrangement turns hydrophilic and releases encapsulated Nile red (Goodwin 2005).

Thermosensitive polymers exhibiting a lower critical solution temperature (LCST) have been under investigation for biomedical and pharmaceutical applications. The temperature at which the phase transition (precipitation of the polymers) occurs is called the cloud point (CP). Poly(N-isopropylacrylamide) (PNIPAAm) has a reversible and sharp phase transition around 32 °C in water which has been explored for most of the LCST polymers (Pelton 2000). A major disadvantage of PNIPAAm-based systems is that thermal treatment (hyperthermia or hypothermia) is required for the controlled destabilization of the micelles and concurrent drug release, which is not always feasible in clinical practice. PNIPAAm exhibits thermal stimulated insolubility which might cause some serious adverse effects due to its non biodegradable and inconclusive biocompatible nature.

Thermo-sensitive polymeric micelles which spontaneously destabilize at physiological conditions are more promising since the use of external stimuli is not possible in clinical practice. There are two possible approaches for destabilization of thermo-sensitive polymeric micelles: 1) Degradation of the backbone of thermo-sensitive polymers. 2) Degradation of the side chains of thermo-sensitive polymer so that the hydrophilicity of the polymer increases and results in the increase of the CP of the polymers with time. Novel class of thermo-sensitive and biodegradable polymers, poly(HydroxyPropylMethacrylamide-lactate), and polymeric micellar system consisting of pHPMAmDL-b-PEG block copolymers have been explored (Soga 2005).

1.5.2.4 Classification of micelles based on composition

a) PEG - polypeptide micelle

One of the most explored micellar drug delivery system has been reported by Kataoka and co-workers based on PEG-b-poly(aspartic acid) [PEG-b-pAsp] and their Doxorubicin conjugates (NK911). In this approach Doxorubicin molecules were conjugated to the copolymers to form micelles having diameters in the range 15–60 nm. Drug molecules covalently conjugated to the pAsp side chain did not have therapeutic activity but could promote the formation of stable p–p interaction with encapsulated DOXO molecules. In a Phase I study, the toxicity of NK911 was same as that of free DOXO, and the dose-limiting toxicity was neutropenia. NK911 is currently being evaluated in a phase II clinical trial. PEG-b-polypeptide micelles have also been used for the delivery of Cisplatin and Paclitaxel. Amphiphilic copolymer containing pAsp and pGlu have been used to complex with anticancer platinum compounds like Cisplatin since carboxylate groups can chelate with multivalent metal ions, Kwon et.al. (2003) reported that synthetic lipoproteins based PEG-PHASA micelles which contain stearyl chains for interaction and solubilization of Amphotericin B inside fatty core was useful in lowering the hemo and nephrotoxicity (Adams 2003, Tong 2007).

b) PEG - polyester Micelle

Biodegradable polyesters like polycaprolactone (PCL), poly(lactic acid) (PLA), poly(glycolic acid) (PGA), and poly(lactide-co-glycolide) (PLGA) have been approved by the FDA in various clinical applications and being hydrophobic in nature have been used as core forming block in micellar drug delivery. The drug release from these polymers can be tuned based upon the degradation rate of polymers. Unlike peptides, these polymers are devoid of functionality which makes drug loading totally dependent on the hydrophobic interactions. Low M_w methoxy-PEG-b-PLA has recently been employed to encapsulate Paclitaxel. In vivo antitumor efficacy in SKOV-3 human ovarian cancer implanted xenograft mice of these micelles at its maximum tolerable dose (60 mg/kg), demonstrated significantly enhanced antitumor activity as compared to free Paclitaxel with no detectable tumor on Day 18 after administration. After 1 month, all mice remained tumor - free.

Currently, these Paclitaxel-containing methoxy-PEG-b-PLA micellar vehicles are under Phase II clinical evaluation. PEG-b-(PCL-TMC) and PEG-b-PLA have also been explored for delivery of Amphotericin B with reduction in haemolytic potential and higher loading. (Tong 2007).

c) Lipid polymer conjugates

The use of lipid moieties as hydrophobic blocks with capped hydrophilic polymer (such as PEG) chains provides additional advantages for particle stability when compared with conventional amphiphilic polymer micelles because of the presence of two fatty acid acyls useful for an increase in the hydrophobic interactions between the polymeric chains in the micelle core. Conjugates of lipids with water-soluble polymers are commercially available and can be easily synthesized. Phospholipid-PEG conjugates have been explored for the controlled drug delivery for preparation of PEGylated liposomes containing Doxorubicin. These phospholipid - PEG conjugates represent a characteristic amphiphilic polymer with a bulky hydrophilic (PEG) portion and a very short but very hydrophobic diacyllipid part which were useful to form micelles of size 7 to 35 nm and CAC of 1 µg/ml which is at least 100-fold lower than those of conventional detergents in an aqueous environment. These micelles also retained the size of micelles even after 48 h incubation in the blood plasma, without getting affected by components of biological fluids upon parenteral administration (Torchilin 2007).

1.5.3 Polymeric vesicle based drug delivery systems

Liposomes were the first synthetic self-assembling vesicular systems based on phospholipids to be described in literature. Liposome-encapsulated doxorubicin, known as Doxil[®] or Caelyx[®] (Gabizon 2001), contains lipid polymer conjugate i.e. DSPE-PEG 2000, hence it is considered to be the first polymeric vesicle in therapeutics used by cancer patients. Polymeric vesicles were first prepared for stabilizing the meta-stable vesicles formed from low-molecular-weight amphiphiles, through polymer linkage acting as trap for the self assembled phospholipids. Numerous polymer architectures like block copolymers, random graft copolymers, polymerized self-assembling monomers, and polymers-bearing lipid pendant groups are known to assemble into vesicles. Self-assembly of amphiphilic polymers and

lipids or amphiphilic polymers and surfactants also form vesicle like structures known as niosomes (Wang 2001, Discher 2002, Antonietti 2003, Uchegbu 1995). There is a clear relationship between the hydrophobic content of polymers and self-assembly.

Block copolymers: The self assembly of block copolymers and polymers bearing hydrophobic pendant groups into vesicles is governed by the hydrophobic–lipophilic balance in a manner similar to that found in liposomes and niosomes. In case of block copolymers it has been established that generally the surfactant parameter (v/al) should approach unity for vesicular self-assemblies to prevail. Here v is the volume of the hydrophobic block; l , the length of the hydrophobic block; and a , the area of the hydrophilic block (Antonietti 2003).

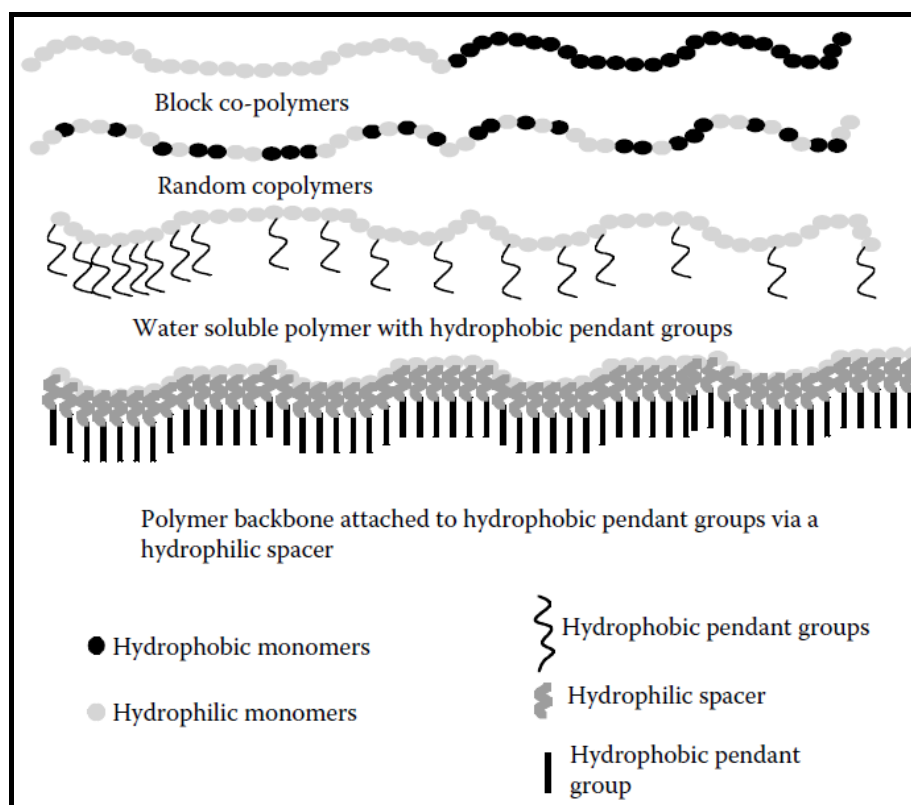


Figure 1.12 Schematic representation of self-assembling vesicle-forming polymers. (Uchegbu 2006)

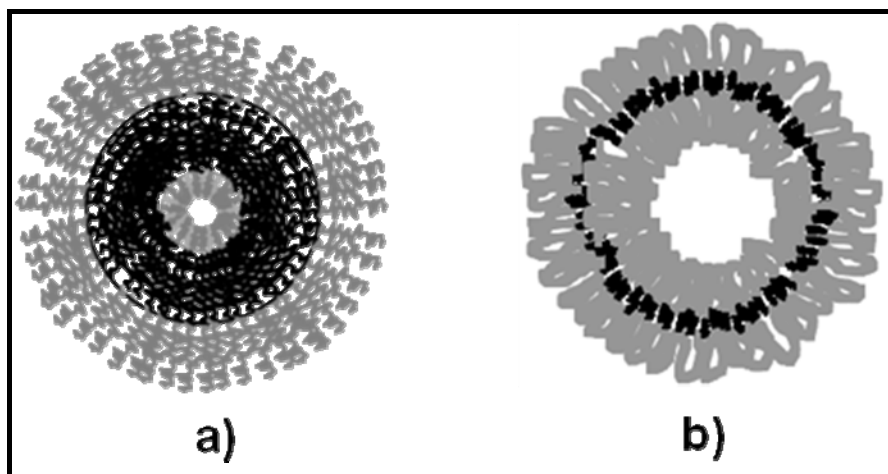


Figure 1.13. Schematic representation of vesicles from a) Block copolymers and b) polymer conjugates. (Uchegbu 2006)

Some polymer-specific factors also determine vesicle-forming ability in self assembly. Very high degrees of polymerization prevent vesicle formation. The flexibility of the hydrophobic block in block copolymers determines type of self-assemblies. For instance more flexible hydrophobic portions of the polymer favour formation of vesicles and the more rigid polymers yield flat lamella, being unable to self-assemble into three-dimensional structures. Polymeric vesicles when compared to monomeric vesicles are mostly unilamellar with superior mechanical stability. They exhibit lower permeability for low molecular weight solutes and are more stable towards organic solvents and surfactants (Antonietti 2003).

Polymeric vesicles are more stable than liposomes because the membrane-making polymers form much stronger hydrophobic interactions than the short hydrocarbon segments of liposomes. Block copolymers self-assemble into vesicles by forming bilayer through the close packing of amorphous polymer hydrophobic segments in a way similar as phospholipids. Polybutadiene (PBD) constitute hydrophobic block whose length determines thickness of bilayer and can be cross-linked subsequently for enhanced vesicle stability. Biodegradable PLA and PCL in PEO-PCL and PEO-PLA also form bilayer and vesicle for controlled drug release (Ahmed 2004). Polypeptides also form conformation-specific vesicle assembly. Block copolymers forming polymeric vesicles include non ionic PEG or oligo(ethylene-oxide) modified polypeptide and ionic poly(acrylic acid) or polypeptides (Discher 2006).

Polypeptides due to amino acid interactions exhibit more diverse conformations like coils, α -helices and β -sheets hence compared to synthetic polymers, they are very versatile building blocks for polymeric vesicles. This highlights importance of conformation in addition to hydrophilic lipophilic balance for vesicle formation. Conventional uncharged amphiphilic block copolymer vesicles require high hydrophobic contents (approximately 30 – 60 mol%) to form stable vesicles (Discher 2000) but the block copolypeptides can form vesicles with 10–40 mol % hydrophobic domains. This difference can be attributed to rigid chain conformations of polypeptides and strong intermolecular interactions as compared to flexible polymer segments of PBD-PEG or PLA-PEG. Copolypeptides used in vesicle formation can be designed to adopt rod-like conformations in both hydrophobic and hydrophilic domains due to the strong α -helix forming tendencies which provide a flat interface on hydrophobic association in aqueous solution for driving the self-assembly into vesicle structures (Tong 2007).

Amphiphilic polymer: First report on the use of preformed polymers to prepare polymeric bilayer vesicles was presented in 1981 by Kunitake and others (Kunitake 1981). In this study, bilayer vesicles were prepared from a hydrophilic polyacrylamide backbone bearing dialkyl hydrophobic pendant groups and hydrophilic oligooxyethylene spacers. The hydrophilic spacer group between the dialkyl moieties was essential for vesicle formation for these polyacrylamide-type polymers (Ringsdorf 1988). The introduction of essentially water-soluble carbohydrate, polyamine, and polyamino acid polymer backbones bearing hydrophobic pendant groups is a fairly recent development. Poly(ethylenimine) and poly(L-lysine) based amphiphiles indicated that the level of lipid pendant groups determined vesicle formation. Hydrophobically modified poly(ethylenimines), formed dense nanoparticles, bilayer vesicles, or micellar self assemblies, depending upon their hydrophobic content (Wang 2004).

1.5.3.1 Factors affecting vesicle formation

Hydrophobic content

In graft copolymers like hydrophobically modified poly(ethylenimine) amphiphiles, hydrophobic content of 58% and above favor dense nanoparticle self-assemblies,

whereas a hydrophobic content of 43 to 58% favors bilayer vesicle assemblies and a hydrophobic content of less than 43% favors the formation of micellar assemblies (Wang 2004). Similar trend has been reported for the poly(oxyethylene)- block - poly(lactic acid) system in that a poly(lactic acid) fraction equal to or more than 80% favors dense nanoparticles, whereas a poly(lactic acid) fraction of 58 to 80% favors bilayer vesicle assemblies and a poly(lactic acid) fraction of less than 50% favors the production of micellar self-assemblies (Ahmed 2004).

Molecular weight

Molecular weight of polymer determines the ability of polymer to create curvature for vesicle formation. In graft copolymers or polymers with pendent hydrophobes, higher molecular weight leads to larger size of vesicles.

Block lengths

In case of block copolymers block lengths determine the thickness of bilayer. Maintaining the ratio of hydrophilicity to hydrophobicity, increase in length of hydrophobic block leads to increase in bilayer thickness e.g. PEO-PBD.

Nature of blocks

In case of peptidic block copolymers both the block are rigid in nature to form interactions and lamellae formation and closure to yield vesicles. In other vesicle forming block copolymers both the block should be amorphous in nature with high flexibility. (Uchegbu 2006)

1.5.3.2 Preparation methods

Instead of directly dissolving block copolymer in water, specific techniques are generally required to fabricate polymersomes. Electroformation has been useful for preparing the giant polymeric vesicles with diameters in the range 10 - 200 nm. Vesicle size can be readily controlled by varying the voltage and frequency of the electric field. Polymersomes of nanometer range can be prepared by film hydration method much alike liposomes. The size distribution of polymersomes can be regulated by further sonication or extrusion or even with several freeze - thaw

cycles. Another method is injection of organic polymer solution into the aqueous solution to precipitate the polymersome (Qiu 2006).

1.5.3.3 Vesicles and applications

Polymersomes have been used for the delivery of small hydrophobic drugs and DNA/RNA molecules and display similar drug delivery characteristics like liposomes. (Uchegbu 2006b). Hydrophobic drugs can be solubilized into the lamellar bilayer of the vesicle, protecting the therapeutic from external degradation e.g. Paclitaxel, while hydrophilic drugs can be loaded inside water filled core e.g. Doxorubicin. The loading capacities of polymersomes are high as seen with diblock vesicles of PEG-PCL and PEG-PLA which show loading ratios of approximately 1:1 of copolymer to drug. Since polymersomes can encapsulate both hydrophilic and hydrophobic molecules, they are ideal vehicles for dual delivery of drugs like Paclitaxel and Doxorubicin which shrank tumors in mice more successfully than a combination of the drugs administered without the carrier (Ahmed 2004, 2006a, 2006b).

Stimuli responsive vesicles have also been designed to release the payload in response to environmental changes of pH, temperature, and redox potential. Temperature responsive vesicles composed of copolymers of PEG and the temperature-sensitive PNIPAAm undergo phase transitions in response to temperature. When incorporated into a diblock with PEG, vesicles are formed at temperatures above the LCST. When the temperature is decreased below the LCST, the PNIPAAm block solubilizes and the vesicle disassembles and releases entrapped molecules. Redox - responsive vesicles undergo phase transitions in response to oxidative potential. A triblock copolymer consisting a hydrophobic block of polypropylene sulfide (PPS) sandwiched between two hydrophilic blocks of PEG forms vesicles. Under reducing conditions, the PPS block maintains thioether moieties that are hydrophobic and stabilize the vesicular bilayer. When subjected to an oxidant, such as hydrogen peroxide, these functionalities oxidize and form relatively hydrophilic sulfoxide and sulfone functionalities. This change in hydrophobic content destabilizes the lamellar bilayer and the vesicle ruptures releasing contents (Branco 2009).

Polymeric vesicles are recent but promising advancement in controlling drug loading, systemic bio-distribution, and drug release (Ahmed 2004, Geng 2007). One of the major challenges in particle-based delivery systems has been control of drug release kinetics. Polymeric nanoparticles can release more than 50% of the encapsulated drugs within the first several or tens of hours due to burst effect (Musumeci 2006). In contrast, hydrolyzable copolymers (e.g., PLAPEG) based polymeric vesicle can be formed for precise tuning of the drug release rates. Polymeric vesicles also offer hydrophilic, hollow interior space for application in encapsulation and delivery of hydrophilic therapeutics, such as DNA and proteins (Tong 2007).

1.5.4 Dendrimer and dendritic polymer nanocarriers

Dendrimers (reported in the late 1970 and early 1980) represent a class of monodisperse macromolecules with highly branched, symmetric, three-dimensional architectures (Tomalia 1985). Dendrimers contain layered structures or generations that extend outwards from a multifunctional core on which dendritic subunits are attached. The sizes of dendrimers are in the range 1–15 nm. These can also be called as unimers since their self assembly is not concentration dependent.

The synthetic strategies can be classified depending upon the direction in which dendrimer grows, as divergent or convergent. The initial efforts in dendrimer research focused primarily on the development of various synthetic methods and the investigation of the physical and chemical properties of dendrimers. In the past 10 years, significant efforts have been devoted towards potential applications of dendrimer in drug delivery. (Yang 2006) Drug molecules can either be conjugated on the surface or encapsulated inside a dendrimer. The periphery of a dendrimer presents multiple functional groups for the conjugation of drug molecules or targeting ligands. Thus conjugation through surface functionality is straightforward and easy to control. Hence majority of dendrimer-based drug delivery is based on this covalent conjugation approach. Despite numerous designs of dendrimers based carriers, only a few of them have been evaluated for their *in vivo* antitumor activities. Carboxylated G-3.5 polyamidoamine (PAMAM) dendrimer Cisplatin conjugate (20–25 wt%) administered to treat a subcutaneous B16F10 melanoma, the

dendrimer- Pt conjugate displayed significantly enhanced antitumor activity as compared to free cisplatin. Acetylated G-5 PAMAM dendrimers loaded with methotrexate and targeted to cancer cells through folate ligand also indicated significant activity (Tong 2007).

Recently an asymmetric dendrimer based on degradable polyester was reported for small molecule delivery (Lee 2006a, 2006 b). In contrast to the non-degradable PAMAM that forms globular structures, these had bow-tie shaped molecular architecture. The number and size of the PEG chains, and the number of drug conjugation sites were tailorable. Bow-tie dendrimers with MW over 40 kDa exhibit plasma clearance half-lives greater than 24 h. Dendrimer-DOXO was found to be much more efficacious than free DOXO and had toxicity and in vivo efficacy comparable to Doxil, an FDA approved, liposome-based DOXO delivery vehicle which was presumably related to enhanced tumor-uptake. Compared to liposomes and micelles, dendrimer-drug conjugates seem to be more stable due to their unimolecular structures, and thus are easier to formulate and sterilize (Tong 2007).

1.5.5 Polymeric particles (microparticles, nanospheres and nanocapsules)

Biodegradable polymer particles (e.g., microspheres, microcapsules, and nanoparticles) are stable and easy to formulate and administer. A variety of drugs, regardless of their molecular weights and water solubility, can be loaded in these biodegradable microparticles using different manufacturing techniques (Nelson 2009). Nanoparticles (including nanospheres and nanocapsules of size 10-200 nm) are solid and are amorphous or crystalline with ability to adsorb and/or encapsulate a drug, protecting it from chemical and enzymatic degradation. Nanocapsules are vesicular systems in which the drug is confined into a cavity surrounded by polymer coat, while nanospheres are matrix systems in which the drug is physically and uniformly dispersed. Nanoparticles as drug carriers can be formed from both biodegradable polymers and non-biodegradable polymers. In recent years, biodegradable polymeric nanoparticles have attracted considerable attention due to their applications in the controlled release of drugs, in targeting particular organs / tissues, as carriers of DNA in gene therapy, and in their ability to deliver proteins, peptides and genes through the peroral route.

1.5.5.1 Polymeric nanoparticles

These are colloidal solids of size 10 to 1000 nm with spherical, branched or shell structures. About 35 years ago, nanoparticles were developed as carriers for vaccines and cancer chemotherapeutics. They are developed from non-biodegradable and biodegradable polymers with small sizes useful for penetration in capillaries and to be taken up by cells, thereby increasing the accumulation of drugs at target sites. Drugs are incorporated into nanoparticles by dissolution, entrapment, adsorption, attachment or by encapsulation, and the nanoparticles provide sustained release of the drugs for longer periods, e.g., days and weeks. Nanoparticles also enhance immunization by prevention of degradation of the vaccine and increased uptake by immune cells. To target drugs to site of action, the drug can be conjugated to a tissue or cell specific ligand or coupled to macromolecules that reach the target organs. Some other applications of nanoparticles include possible recognition of vascular endothelial dysfunction, oral delivery of cyclosporine and peptides like Insulin and Calcitonin, brain targeting for Alzheimer's disease; topical administration to enhance penetration and distribution in and across the skin barrier. Polymers like chitosan, alginate, albumin, gelatin, polyacrylates, polycaprolactones, poly(D, L-lactide-co-glycolide) and poly (D, L-lactide) can be used for preparation of nanoparticles (Kingsley 2006 and Nelson 2009).

1.5.5.2 Nanocapsules

These are spherical hollow structures in which the drug is confined in the cavity and is surrounded by a polymer membrane. Sizes between 50 and 300 nm are preferred for drug delivery and they may be filled with oil which can dissolve lipophilic drugs. They have low density, high loading capacity and are taken up by the mononuclear phagocyte system, and accumulate in target organs such as liver and spleen (Jiang 2006 a, 2006 b). Nanocapsules have been useful as protective shell for cells or enzymes, confined reaction vessels, transfection vectors in gene therapy, dye dispersants, carriers in heterogenous catalysis, imaging and drug carriers (Meier 2000 and Reinhold 2007). They are known to improve the oral bioavailability of protein and peptides like insulin, calcitonin and salmon calcitonin (Jiang 2006 a, 2006 b). Encapsulation of drugs such as ibuprofen (Jiang 2006 a, 2006 b) within

nanocapsules protect labile drugs from degradation, reduce systemic toxicity, provide controlled release and mask unpleasant taste. Due to their high stability and low permeability, loading of drugs into the capsules after formulation and release of the drug at target site becomes difficult which can be overcome by the use of stimuli sensitive polymers. (Nelson 2009)

There are a number of techniques available for microencapsulation of drugs such as the emulsion solvent evaporation / extraction method, spray drying, phase separation-coacervation, interfacial deposition, and in situ polymerization. Each method has its own advantages and disadvantages. The choice of a particular technique depends on the attributes of the polymer and the drug, the site of the drug action, and the duration of the therapy (Soppimath 2001). For preparation of microparticles using biodegradable polymers, it is important to choose an appropriate encapsulation process which meets the following requirements. (1) During encapsulation process the chemical stability and biological activity of the incorporated drugs should be maintained. eg. Proteins are denatured in the presence of solvents. (2) The encapsulation efficiency and the yield of the microparticles should be high enough for mass production. (3) The microparticles produced should have reasonable size range ($< 250 \mu\text{m}$) that can be administered using the syringe needle via the parenteral pathway. (4) The release profile of the drug should be reproducible without significant initial burst. (5) The process employed should produce free-flowing microparticles, thus making it easy to prepare uniform suspension of the microparticles.

1.5.6 Polymeric hydrogel based delivery system

Hydrogels are three-dimensional, hydrophilic polymeric networks capable of holding large amounts of water or biological fluids. The networks are composed of homopolymers or copolymers, and are insoluble due to the presence of chemical or physical cross-links. In-situ forming implants are getting a lot of attention due to their ease and utility and biocompatibility aspects. Liquid formulations which turn to a solid or semisolid depot after subcutaneous injection are useful as in situ forming implant based drug delivery system for parenteral application because they are less painful and non-invasive compared to surgical implants. Localized or systemic drug

delivery can be achieved for prolonged periods of time from one to several months. Parenteral depot systems have been developed to minimize side effects by achieving constant plasma levels of proteins and drugs with narrow therapeutic indices. In-situ forming depot systems are advantageous to formulate on larger scale due to simple manufacturing procedure from polymers (Van Tomme 2008).

According to the mechanism of depot formation, injectable in-situ forming implants can be classified into four categories as (i) thermoplastic pastes, (ii) in-situ cross-linked polymer systems, (iii) in-situ polymer precipitation, and (iv) thermally induced gelling systems.

In situ gelling hydrogels can be further subdivided into two main categories a) Externally induced cross-linked gel and b) Spontaneously self assembled gel. Externally induced cross-linked gels need triggers like light to trigger cross-linking for gel formation. In spontaneously self assembled gel, as the name suggests gelation needs no triggers. This gelation can be the result of physical or chemical cross-linking mechanisms spontaneously or in response to triggers like temperature, pH etc.

1.5.6.1 Photo-polymerizable hydrogels

In situ photo-polymerization has been used in biomedical applications for over more than a decade. Photo-polymerizable hydrogels were formed *in situ* wherein poly(ethylene glycol) (PEG) acted as central block, functionalized with terminal oligo(α -hydroxy acids) and acrylate groups (Sawhney 1993). The acrylate end-groups showed rapid polymerization upon irradiation with visible light in the presence of a suitable photo-initiator to yield a hydrogel structure.

1.5.6.2 Self-assembling hydrogels

a) Ionic cross-linking mediated gels

Three-dimensional hydrogels are formed by the complexation of bi- or polyvalent cations with the Glucuronic moieties in alginates. Alginate hydrogels act as gel forming matrices for controlled release of pilocarpine in the eye for 24 hrs (Cohen 1997). Chitosan cross-linked with triphosphate formed hydrogels which have potential applications in the biomedical field (Berger 2004). Ionic interactions

between oppositely charged dextran microspheres (Van Tomme 2005) led to gel formation.

b) Temperature-sensitive hydrogel

Temperature increase results in dehydration of polymer chains causing formation of hydrophobic domains and eventually transition of an aqueous liquid to a hydrogel network. Most studied materials are block copolymers of poly(ethylene oxide) (PEO) and poly(propylene oxide) (PPO), well known as Pluronics®, and PEO-PLGA or other polyesters (Jeong 1997).

c) Peptide-based supramolecular hydrogels

There is a growing interest in formation of supramolecular peptide-based or hybrid hydrogels because of the biocompatibility and gelation mechanism (Xu 2005; Kopecek 2007 a). A reversible stimuli-responsive hydrogel has been reported which is composed of genetically engineered protein block copolymers containing a central water soluble random coil polyelectrolyte with two coiled-coil domains (Xu 2005).

d) Polymer inclusion complex based hydrogels

In situ hydrogel formation occurs through the supramolecular assembly of Cyclodextrin modified polymeric host and hydrophobic low molecular weight guests. PEG and poly (propylene glycol) (PPG) form inclusion complexes with α -CDs and β -CDs, respectively. If they are grafted to a dextran backbone and subsequently mixed with a CD solution, threading of the latter onto the PEG and PPG chains takes place which is followed by gelation. The concentration of the graft copolymer and the PEG/PPG content, i.e. the graft density on the dextran chains guides gelation time (Choi 2002).

e) Stereocomplex based hydrogels

Earlier reports indicated that physically cross-linked dextran hydrogels can be formed by stereo complexation between oligolactates of opposite chirality (De Jong 2000).

Rheological analysis revealed that mixing of aqueous solutions of dex-l-lactate and dex-d-lactate formed elastic hydrogels. A novel in situ gelling system based on

stereo-complexed star block copolymers has also been reported. PEG - octa (PLLA) and PEG- octa (PDLA) star block copolymers were synthesized by ring-opening polymerization of either l-lactide or d-lactate in the presence of eight-arm PEG and a catalyst. The aqueous solutions of equimolar amounts of both copolymers, in the concentration range 5 – 25 % (w/v) and 6 – 8 % (w/v) for PEG 21,800 and PEG 43,500 respectively formed hydrogels on mixing. Lysozyme and IgG release were studied (Hiemstra 2007a). The same polymers were methacrylated and physical gels were formed which were cross-linked by UV irradiation to fix the formed gels.

f) Enzyme-mediated gelation

Dextran-tyramine (dex-TA) conjugates were in situ cross-linked in the presence of H₂O₂ and horseradish peroxidase (HRP), yielding chemically cross-linked, highly elastic and degradable hydrogels (Jin 2007). Degradation of the gels took several months due to the slow hydrolysis of the urethane bonds.

1.5.6.3 Chemical cross-linking of complementary groups mediated gelation

a) Schiff's base mediated gels

Dextran is an interesting polysaccharide for the preparation of in situ cross-linked hydrogels because of its biocompatible nature. Oxidation of dextrans with sodium periodate yielded DexOx. Subsequent reaction of this aldehyde-functionalized Dextran with hydrazide groups of adipic acid dihydrazide (AAD) resulted in the formation of injectable hydrogels (Maia 2005).

b) Michael addition mediated gels

PEG has been frequently used for the preparation of hydrogels, mainly because of its proven safety and its FDA approved status. PEG functionalized with thiol groups, could form self-assembling chemically cross-linked hydrogels (Qiu 2003). Diamino-PEG was reacted with 2- mercaptosuccinic acid to yield an amide-linked copolymer bearing pendant thiol groups, which on mixing reacted rapidly with vinylsulfone groups on PEG under mild conditions (pH 7, RT) to yield gel which had water content above 90%. Fluorescein labeled BSA released over 25 days with no significant burst release and inflammation of surrounding tissues.

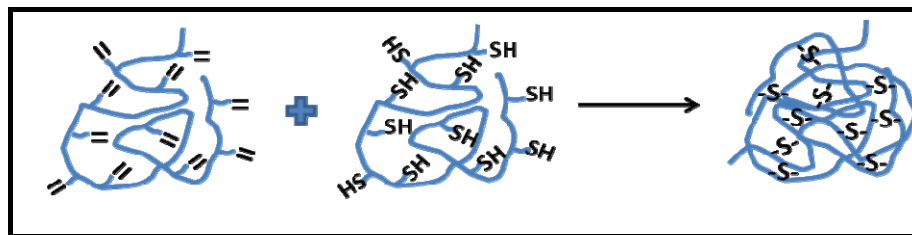


Figure 1.14. Schematics of Michael addition mediated in situ crosslinked hydrogel formation.

Heparin has also been functionalized with thiol groups and subsequently reacted with PEG-diacrylate to form a hydrogel (Tae 2007). It was shown that the mechanical properties (storage modulus) and gelation kinetics could be tailored by varying the degree of thiolation and the total precursor concentration (both heparin-SH and PEG-diacrylate). Keeping the applicability as in situ forming gelation system in mind, it was concluded that at least 30% thiolation was required for gelation time of approximately 5 mins.

Dextran-based in situ gels formed through Michael addition mechanism were also reported. Dextran was functionalized with vinyl sulfone which on mixing with 4-arm mercapto-PEG (PEG-4-SH) formed gels through Michael-type addition reaction at physiological conditions. The gelation time decreased from 7 to 0.5 min when the degree of VS substitution (DS, i.e. number of VS groups per 100 glucopyranose units) increased from 4 to 13. Rheological analysis showed that highly elastic hydrogels were formed. Gel strength could be tailored from 3 to 46 kPa and so was degradation time from 3 – 21 days, by varying the DS, concentration and dextran molecular weight. (Hiemstra 2007a, Van Tomme 2008).

1.5.7 Polymer mediated metal Nps synthesis, self assembly and applications

Nanomaterials are being studied for a wide range of applications in sensors, electronics, and optical materials. The nano size provides unique physical properties that are often completely different than those observed for their respective bulk materials. Metal and semiconductor nanoparticles (NPs) display interesting and useful quantum-confined properties including novel electronic, optical and chemical characteristics. These NPs are generally capped by an organic monolayer which

prevents agglomeration and tailors chemical properties through organic synthesis. Colloid properties like size, shape, type of core material and features like inter-particle spacing and dielectric environment control the physic-chemical properties of nanoparticles. (Spadavecchia 2005)

For practical utility array of nanoparticles are needed. Numerous attempts have been made to organize them into one, two and three dimensions. The ability to create NP networks, arrays and composites, however, depends on understanding and control of the assembly. The patterning and controlling the spatial assembly of these NPs and their composites involves both “bottom-up” i.e. self-assembly and “top-down” i.e. lithographic techniques. New functional materials and devices could be designed through the synergy between these two approaches (Xu 2007). Self-assembly requires interactions favourable enough so that stable equilibrium or near-equilibrium structures are formed, but not so strong that materials become irreversibly structured. The intermolecular forces like hydrogen bonding, metal coordination, electrostatic attraction/repulsion, dipolar interactions, Van der Waals forces, and hydrophobic interactions can both induce NPs into controlled structures and modulate their physical responses. Biomolecular assembly can thus be utilized to incorporate the intrinsic properties of biomolecules into nanocomposite structures. In NP–polymer composites, polymeric templates can serve three purposes: (1) assemble the NPs into composite material, (2) serve as a matrix that induces order and anisotropic orientation in clusters and on surfaces, and (3) act as a functional element (e.g. possess an electronic property). The chemical approach for the construction of these composites allows the polymers to serve any or all of these functions (Ofir 2008).

1.5.7.1 Gold nanoparticles

Gold nanomaterials have attracted particular interest owing to their ease of synthesis and functionalization, chemical stability, low inherent toxicity (biocompatibility), and tunable optical and electronic properties (absorption, fluorescence and conductivity). Polymer-mediated ‘bricks and mortar’ assembly of gold NPs (AuNPs) through self assembly using linear, branched, and block copolymers and biopolymers such as proteins and DNA has been an interesting approach.

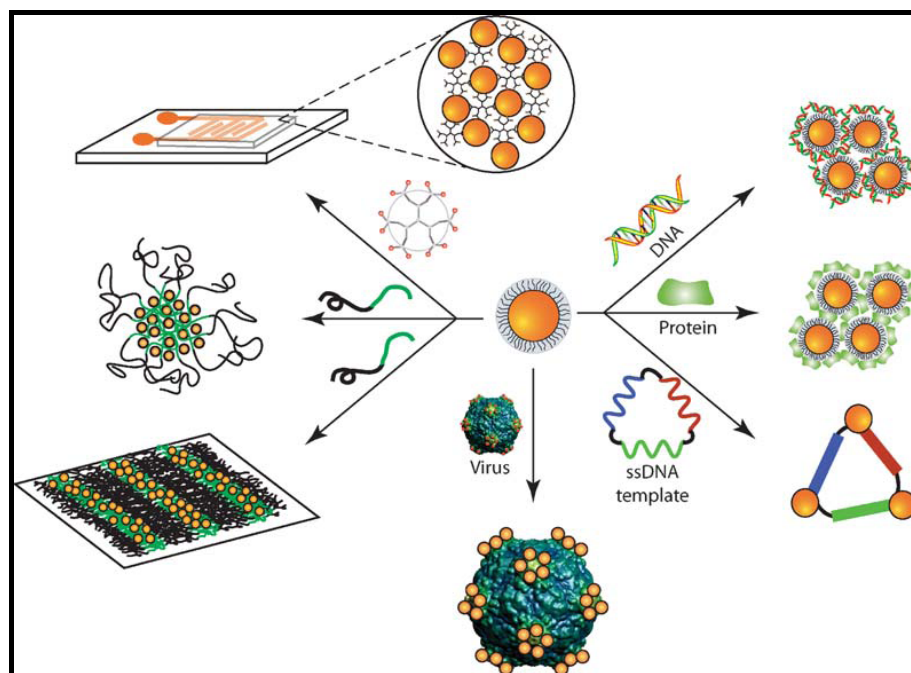


Figure 1.15. Schematic representation of polymer-mediated assembly of AuNPs.(Ofir 2008).

Supramolecular chemists have developed numerous synthetic methods to attach non-covalent host–guest complexes to nanoparticle ‘bricks’ and a wide variety of ‘mortars’ e.g. dendrimers, polymers, surfaces, proteins, nucleic acids and drug molecules. Each of these systems brings both structural and physical properties for the creation of functional nanosystems (Ofir 2008).

Layer-by-layer (LbL) assembly

This is a simple technique for fabrication of structural and functional thin films on both flat and curved substrates. LbL uses sequential adsorption of complementary materials using electrostatics, hydrogen bonding and other complementary interactions. e.g. polymer assembled NP films on cyclodextrin (CD)-functionalized self-assembled monolayers (SAMs) through host–guest (CD– adamantyl (Ad)) interactions. (Crespo-Biel 2006)

Dendrimers

Numerous assemblies between poly(amidoamine) (PAMAM) dendrimers and AuNPs have been explored in order to control the inter particle spacing and hence dipole coupling between particles. Dendrimers act as a capping agent, ligand on AuNPs or ionic complexing agent for AuNps (Frankamp 2002a).

Linear and block copolymer self assemblies

For microelectronic applications NPs needs to be self-assembled in well-ordered 2D arrays as addressable components for high density memory devices and integrated circuits. e.g. Sulfonic acid-functionalized AuNPs on poly(ethylene imine) (PEI) yield cubic and hexagonal packing arrangements. AuNPs and polymer scaffolds functionalized with complementary hydrogen bonding recognition units formed ordered arrays (Schmid 2000).

Phase segregated block copolymers like Polystyrene-b-poly(methyl methacrylate) (PS-b-PMMA) form periodic structure which exhibit cylindrical PMMA features surrounded by hydrophobic PS matrix which electively deposits AuNP through interaction and forms interesting hexagonal nano-patterns (Zehner 1998). The use of recognition functionalized diblock copolymer provided not only the formation of nano sized aggregates but also precise control of the size of AuNP aggregates by varying the length of the diblock copolymer (Frankamp 2002b). Another approach to control the structures of self assembled block copolymers and AuNPs was recently illustrated wherein amphiphilic triblock copolymers poly (acrylic acid)-block-poly (methyl acrylate)-block-polystyrene (PAA-b-PMA-b-PS) resulted in diverse nanoscale structures (Cui 2007). Amphiphilic Au nanorods bound to PS were assembled into structures exhibiting varying geometries. The hydrophilic nanorods tethered with hydrophobic polymer chains at both ends which behaves like triblock copolymer. Depending upon the difference in obtained triblock composition and structure, the Au nanorod species could be organized into a range of different structures (e.g. rings, linear, bundled chains and nanospheres with two dimensional walls (Nie 2007).

DNA mediated self assembly

ssDNA labeled AuNPs can be used to create multimeric networks and chain-like structures through sequence-specific DNA hybridization. This approach leads to assemblies of AuNPs exhibiting controlled spatial arrangement of two or more distinct populations of AuNPs. AuNPs modified with ssDNA could be arranged into homodimeric and homotrimeric assemblies based on Watson–Crick base-pairing interactions. Another approach to create DNA–AuNP assemblies employs strong electrostatic interactions between cationic NPs and anionic DNA, aligned along the DNA scaffold (Deng 2005).

Protein-mediated assembly

The interaction between proteins and monolayer-protected NPs can be engineered to generate highly organized assemblies exhibiting structural diversity. These superstructures combine tunable Np features with unique physical and chemical properties of the proteins and therefore provide a potential route to a wide array of materials and devices. A variety of assemblies have been created using biotin–streptavidin and antigen–antibody interactions. Viral capsids and other multi-protein assemblies provide a useful tool for the assembly of nanomaterials. A mutant viral protein cage has been used to control AuNP assembly onto virus capsids to generate 3D conductive molecular networks. More recently His-tagged 20S proteasome has been demonstrated as a building block to provide ordered assemblies, with AuNPs attached to the exterior of these large proteins. In all these cases, protein is larger than the Nps hence drives the order in the resultant material (Ofir 2008).

Applications

With the control on morphologies and the resultant physical properties of AuNPs assembly demonstrated, a deeper understanding of fundamental principles of self-assembly is needed. Advances in NP and polymer synthesis will help designing of intricate nano-architecture needed for the devices of the future which will have applications in fields ranging from electronics and materials science to molecular biology like biosensors and memory chips etc. (Ofir 2008)

Gold nanoparticles due to their lower toxicity and hyperthermic effect have also been useful as drug delivery vehicles. Tumor necrosis factor- α (TNF- α), a cytokine exhibits excellent anticancer efficacy but is systemically toxic which limits its therapeutic applications. PEG coated gold nanoparticle loaded with TNF- α , exhibited therapeutic efficacy, high tumor damage and reduced systemic toxicity of TNF- α . This system named “CYT-6091” (Visaria 2007) has been in Phase I clinical trials for evaluation of safety, pharmacokinetics, and clinical efficacy. Nanoshells have been tested for small and macromolecular drug delivery triggered by hyperthermic effect. When irradiated with light of 1064 nm, nanoshells are heated causing the collapse of the hydrogel triggering drug release. (Sershen 2000). Modulated drug delivery of methylene blue, insulin, and lysozyme has been achieved. The release rate depends upon the molecular weight of the therapeutic molecule (Bikram 2007).

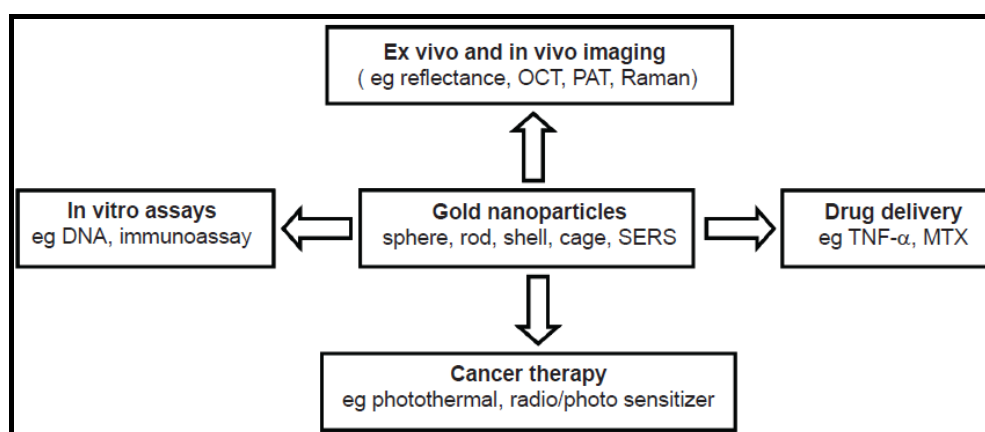


Figure 1.16. Applications of gold nanoparticles.

Physical dimensions like size and shape of gold nanoparticles determine intracellular uptake (Chithrani 2006). Gold nanoparticles can be classified as nanospheres, nanoshells, and nanorods which exhibit different absorption / scattering efficiency and optical resonance wavelengths (Jain 2006). Nanospheres exhibit peak in narrow SPR range 520–550 nm which limits their utility for in vivo applications. The SPR peaks of gold nanoshells lie in the NIR region while nanorods exhibit excellent optical properties at much smaller effective size. They exhibit absorption and scattering coefficients an order of magnitude higher than those exhibited by nanoshells and nanospheres. Nanorod with a higher aspect ratio and a smaller

effective radius acts as good photoabsorbing nanoparticle useful for therapeutic applications, while the one which has larger effective radius is useful for imaging purposes.

Nanoparticle stability is directly proportional to PEG molecular weight, PEG content and inversely proportional to size of nanoparticles. (Liu 2007). Molecular cancer markers over-expressed on the tumor vasculature may be the targets of choice. The efficacy of gold nanoparticles as drug delivery vehicle can be further enhanced by targeting to diseased site. (Cai 2008).

1.5.7.2 Silver nanoparticles

The synthesis of silver NPs is of a considerable interest in both research and technology because of its highest conductivity, reflectivity and antibacterial properties compared to all metals. Optical, magnetic, catalytic, and electrochemical properties of silver NPs are strongly dependent on their size, shape, and media composition. This dependence has been explored for practical use in novel biosensors, chemical sensors, electro-optical devices, and data storage media, in surface enhanced Raman spectroscopy, and in biological imaging.

Silver NPs have been used for surface modification of polyelectrolyte multilayer capsules fabricated by the layer by layer (LbL) technique by alternately absorbing oppositely charged polyelectrolytes on colloidal template cores followed by core dissolution. Control on the capsule permeability allows one to fill its interior with drug or essential chemicals for their delivery into biological tissues. The release of the encapsulated compound from the modified polyelectrolyte capsules can be stimulated by microwave, ultrasonic, laser light, and magnetic field. The efficiency of the irradiation-stimulated release of the encapsulated compound has been further enhanced by encapsulation of silver NPs. Thus as a light sensitive component in the vis/IR region, they enhance the interaction of the laser beam with the modified polyelectrolyte shell and remotely release encapsulated compound from the capsule inside the cell. e.g. Silver in layer by layer coatings of [poly(sodium 4-styrenesulfonate) / poly(allylamine hydrochloride), PSS/PAH] bilayers is sensitive to laser light of wavelength 830 nm. Laser exposure results in the deformation and rupture of the shell due to the local heating of NPs. Thus remote release of the

encapsulated material from microcapsules inside the living tissue can be achieved (Skirtach 2006, Radziuk 2007).

1.6 Bile acid: A building block, its structure, properties and polymerization

These natural compounds are synthesized in the liver from cholesterol. These are stored in the gall bladder, and released in the small intestine for the digestion of fats and lipids. They are reabsorbed into the liver through the ileum membrane. The enterohepatic circulation of the bile acids holds key to biological processes, such as emulsification and membrane transport of cholesterol, vitamins, retinol, β -carotene, etc. Structurally all bile acids are rigid due to the presence of steroidal nucleus and belong to coprostane family, where the *cis* connection between ring A and ring B imparts a curvature to the steroid skeleton, which makes the formation of a cavity possible. The cavity has two faces which exhibit very different properties.

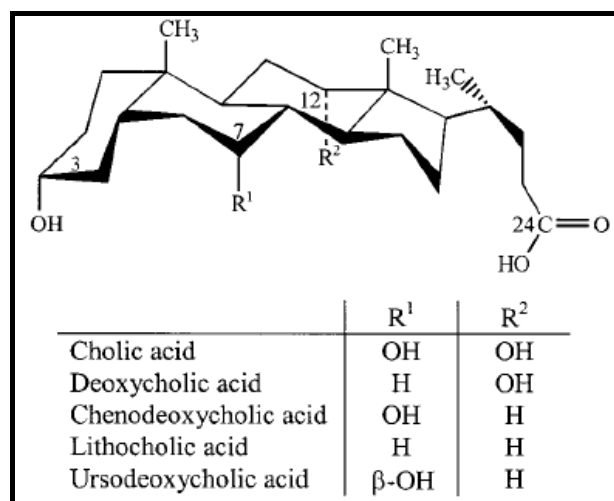


Figure 1.17. Chemical structures of different bile acids.

α face has several hydroxyl groups directed convergently towards the concavity which forms the hydrophilic part together with the carboxylic side chain. At convex side, there exists a completely hydrophobic β face where three methyl groups are present. Bile acids also possess several chiral centres. Because of this facial amphiphilicity, bile acids form micelles and other supramolecular structures in a stepwise manner. The organization is induced by the back-to-back hydrophobic interactions aided by hydrogen bonding in between OH-OH and OH-COOH groups present on steroidal nucleus. Bile acids exist in salt form to act as surfactant which

exhibit biological activity. They can also form mixed micelles with water-insoluble compounds. From the synthetic point of view carboxylic and hydroxyl groups are easy to modify. The interesting properties of bile acids and their derivatives have prompted researchers to use these compounds in the design of new polymeric materials. These polymers could preserve some properties of bile acids, such as facial amphiphilicity, chirality, self assembling abilities, and high chemical stability of the steroid nucleus combined with the reactivity of the side groups, and could impart new properties because of the higher molecular weights. (Zhu 2002)

1.6.1.1 Polymerization of bile acid monomers

Modification of hydroxyl groups or carboxylic side chain of bile acids has been used to introduce functional groups capable of free radical polymerization or polycondensation. The new materials exhibit good mechanical properties or a high degree of water uptake (hydrogels), with varying degree of biodegradability under physiological conditions.

1.6.1.2 Bile acid based acrylated polymers

Bile acid methacrylates and methacrylamides could easily polymerize to yield homo and copolymers. (Benrebouh 2001) Polymerization of bile acids through carboxyl side chain end by preparation of acrylate esters like Cholic acid coupled to a methacryloyl group via a spacer has been reported (Zhu 2002).

1.6.1.3 Polycondensates of bile acids

Bile acid (deoxycholic and cholic acids) polycondensation using p-toluenesulfonic acid as a catalyst at high reaction temperatures yielded branched polymers. Later linear polymers could be achieved using an enzyme (lipase). These polymers had a good thermal stability and partial crystallinity but were poorly soluble in common organic solvents due to their rigid structure (Noll 1996).

Polycondensation of the dimers of lithocholic acids obtained by linking the C₃-OH groups via alkylene diester or diether spacers yielded high molecular weight homo- or copolyanhydrides. The T_g of the homopolymer was high (85 °C) which reduced to 13 °C when copolymerized with 90 mole % sebacic acid. Degradation studies

indicated surface erosion mechanism and tailorable degradation pattern depending upon comonomer content (Gouin 1998).

Entropy-driven ring-opening metathesis polymerization (EDROMP) of bile acid based macrocycles led to formation of polymers of high molecular weight. The polymers displayed low T_g and hence exhibited typical rubberlike elasticity, with elongation moduli that favorably compared to those of soft tissues and elastin. The polymers degraded slowly over a period of several months at 37 °C in phosphate-buffered saline solutions (Gautrot 2006).

Recently bile acids have also been polymerized by aza - alkyne click reaction. Polymers obtained were of high molecular weight and high T_g . These polymers displayed remarkable ability to stabilize silver nanoparticles that showed selective colorimetric sensing for the iodide ion. However, potential of these polymers for drug delivery was not explored (Kumar 2010).

1.6.1.4 Bile acid polymer conjugates

Polymers bearing reactive groups such as OH or NH₂ were chemically modified with bile acids, mainly through the COOH groups at C₂₄ position. Modification of the OH groups of polymers was performed with the help of coupling reagents, such as carbodiimides or carbonyldiimidazole. Coupling of the bile acid to the NH₂ groups of polymers was realized also in the presence of carbodiimides or by using activated esters of bile acid, for instance, 24-hydroxysuccinimide esters. (Zhu 2002)

Pendent bile acid polymer conjugates

The reactive groups containing polymers, such as polysaccharides like dextran, aminohexylamino agarose, chitosan, and partially N-desulfated heparin, proteins like bovine serum albumin, BSA and polymers like poly(p-aminomethylstyrene) have been hydrophobically modified with Bile acids through amide and ester linkages. The extent of modification depended upon application and was low at 5-15 mol % in order to ensure water-solubility. These hydrophobically modified polysaccharides aggregated in aqueous solutions and formed nanoparticles with a mean diameter of 20-200 nm and could solubilize hydrophobic drugs. (Nichifor 1999)

Telechelic polymers with bile acids

Monomethoxy PEG amine was chemically modified with deoxycholic or cholic acid at only one chain end the other end being a methoxy group or a sugar moiety. The resulting amphiphilic polymers were water-soluble and formed self-aggregates in aqueous solutions. The CACs were 0.04-0.05 mg/mL which are much lower than the critical micellar concentration (CMC) of the corresponding bile salts. (Huh 2000)

1.6.2 Applications of bile acid based polymers

Bile acids based polymers are useful for biological purposes as they are product of biocompatible and nontoxic natural compounds. Polymers prepared from bile acids have been tested as potential drug delivery systems, either in the form of physical mixtures with the drug, or as drug polymer conjugates. Their amphiphilicity has been exploited for entrapping and delivery of hydrophobic bioactive compounds like Amphotericin B in fungizone[®]. Chitosan and heparin modified with bile acids form nanoparticles in water useful as colloidal delivery systems for hydrophobic drugs. These systems have an advantage of a longer circulation time, since they are not taken up by the reticulo-endothelial system. Cationic nature, mucoadhesive properties and possibility of bile acid aided transport makes Chitosan modified bile acids as potential candidates for transport of these carriers across intestinal mucosa for delivery of encapsulated peptides (Zhu 2002).

Bile acid based polyanhydrides showed a near-zero-order erosion rate profile for upto 100 days and the release of a model compound, such as p-nitroaniline also had a quasi-zero order rate that was almost parallel to the erosion profile. Thus polyanhydrides can be used as implants for prolonged release of active drug (Gouin 1998). The ursodeoxycholic acid-PEG conjugates released the drug by a stepwise hydrolysis of the ester bond connecting the drug to the polymer. After the oral administration it was found that the half-life of the drug in the blood was longer, and the concentration in the blood was more stable than after administration of an equivalent dose of free drugs. This indicates that the ursodeoxycholic acid-PEG conjugate might have a better therapeutic efficacy than the free drug (Zhu 2002).

1.7 Summary and learning

Designing of diverse morphologies has been long time quest of researchers since these can modify drug solubilization and disposition in the body. In order to achieve this, different approaches have been adopted in development of drug delivery systems based on polymer architecture. The self assembly route has been explored by using block copolymers, graft copolymers, dendrimers and polymer conjugates for preparation of micelles. In order to achieve morphologies other than micelles, block copolymers have been explored. Many non-biodegradable and biodegradable block copolymers like PSS-PAA, PEO-PBD, PEO-PLA, PEO-PCL show promise. Peptidic block copolymers exhibit different morphologies and do not follow $f_{\text{hydrophilic}}$ rule, which can be attributed to the interactions between functionalities. In Chitosan-g-PCL graft copolymers different morphologies could be achieved but there is a need for other biocompatible and biodegradable polymers. Recently polyamino acid and polyethyleneimine hydrophobic conjugates of fatty chains have been shown to form micelles, vesicles and nanoparticles based upon the hydrophobic content. In nature, post translational modifications of proteins also alter protein structure and function. Hence mimicking nature, role of functionalities in guiding morphologies needs to be investigated to devise new strategy for structuring self assemblies. The suitability of these self assembly environments for drug solubilization and drug delivery also needs to be explored.

Bile salts constitute intestinal bile which ensures solubilization and uptake of fats by forming mixed micelles with phospholipids. Deoxycholic acid is one of the important components of bile. Deoxycholic acid contains hydroxyl functionalities along with steroidal nucleus and carboxylate group which aids in its hydrophobic and hydrophilic interactions. Deoxycholic acid sodium salt forms micelles in which different hydrophobic drugs have been solubilized. Fungizone[®] is Amphotericin based sodium deoxycholate micelle formulation available in market in freeze dried form. Even though bile acid based system has reached market and has been in clinical practice since decades, its potential for development of other formulations or drug delivery systems remains unexplored because of its high critical micellar concentration, instability towards ions and tendency to form secondary micelle led larger aggregates. In order to overcome these limitations, bile acids (Deoxycholic

acid and Cholic acid) have been conjugated to different polysaccharides like dextran, chitosan and heparin. The level of conjugation was always lower hence formed micelles. These micelles exhibited low CMC but remained unexplored due to their inability to solubilize drugs and exhibit acceptable biocompatibility. Chitosan – deoxycholate conjugates formed micelles which were mucoadhesive and absorbable from intestinal region. Other monomeric bile acid conjugates like adamantyl or p – tert butylphenyl group modified β aminated cholic acid formed vesicle and tubes which has evoked new interest in bile acid usage for development of new drug delivery applications. Judicious selection of peptide backbone and conjugation with bile acid could yield interesting self assembly patterns.

Metal nanoparticles have been synthesized using different capping agents like polysaccharides, proteins, polyols, polyamines etc. They have also been making inroads in drug delivery systems owing to their useful physical properties and high surface area for surface drug conjugation and targeted drug delivery as a result of hyperthermic properties. Synthesis of nanoparticles in different self assembly environment created by synthetic peptides needs to be explored. Role of functionalities in capping nanoparticles needs to be explored to determine most favoured functionality for capping and stabilization of nanoparticles.

In-situ hydrogels have been attracting attention for localized drug delivery because of biocompatibility and soft tissue like nature. Spontaneous in situ cross-linking led gel formation through the reaction between complimentary functionalities is an interesting and practicable approach. Mimicking natural peptide led self assembly, incorporation of hydrophobic functionalities could aid cross-linking process. Judicious use of complimentary biocompatible functionality through self assembly principles of hydrophobic hydrophilic segregation needs to be explored. Efficient use of this approach for hydrophobic drug delivery by incorporation of hydrophobic pockets inside gel matrix needs to be studied and explored for hydrophobic drugs.

Oral delivery of anticancer drugs, peptides and large molecules through nanoparticles and micelles is promising in need of high patient compliance today due to high patient compliance and ease of administration. High uptake of bile acid -

Chitosan conjugate based micelles containing Calcitonin and Insulin indicates utility of mucoadhesive carrier bearing positive charge and need of bile acid hydrophobe. Thus a review of the literature highlights need for bile acid based polymers and polymer conjugates for drug solubilization, toxicity reduction of water insoluble antifungal and anticancer drugs through passive targeting and localized drug delivery approaches. Absorption enhancement of peptides and anticancer drugs from oral route through bile acid based carriers is also worth to be investigated.

The objectives and scope of the proposed investigation in the light of the current status of research in this area have been summarised in the next chapter.

1.8 References

1. Adams M. L., Andes D. R., Kwon G. S., *Biomacromolecules*, 2003, 4, 750-757.
2. Ahmed F., Pakunlu R. I., Brannan A., Bates F., Minko T., Discher D. E. J. *Control Release*, 2006 a, 116, 150–158.
3. Ahmed F., Pakunlu R. I., Srinivas G., Brannan A., Bates F., Klein M. L., et al. *Mol. Pharm.*, 2006b, 3, 340–350.
4. Ahmed F., Discher D. E., *J. Controlled Release*, 2004, 96, 37–53.
5. Allen C., Maysinger D., Eisenberg A. *Colloids Surf B: Biointerfaces*, 1999, 16, 3-27.
6. Antonietti M., Forster S., *Adv.Mater.*, 2003, 15, 1323–1333.
7. Bae Y., Fukushima S., Harada A., Kataoka K. *Angew. Chem. Int. Ed.* 2003, 42, 4640–4643.
8. Berger J., Mayer J.M., Felt O., Gurny R., *Eur. J. Pharm. Biopharm.* 2004, 57, 35–52.
9. Bikram M., Gobin A. M., Whitmire R. E., *J. Control. Release* 2007, 123, 219–27.
10. Branco M. C., Schneider J. P., *Acta Biomater.* 2009, 5, 3, 817 - 831.
11. Cai W., Gao T., Hong H., Sun J. *Nanotechnology, Science and Applications* 2008, 1, 17–32.
12. Cammas S., Suzuki K., Sone C., Sakurai Y., Kataoka K., Okano. T., *J Control Release* 1997, 48,157-164.
13. Chithrani B. D., Ghazani A. A., Chan W. C., *Nano Lett.* 2006, 6, 662–8.

14. Choi H. S., Kontani K., Huh K. M., Sasaki S., Ooya T., Lee W. K., Yui, N., ,
Macromol.Biosci. 2002, 2, 298–303.
15. Cohen S., Lobel E., Trevgoda A., Peled Y., J. Control. Release 1997, 44, 201–
208.
16. Crespo-Biel O., Dordi B., Maury P. Peter, M., Reinhoudt D. N., Huskens, J.,
Chem. Mater. 2006, 18, 2545–2551.
17. Cui H., Chen Z., Zhong S., Wooley K. L., Pochan D. J., Science 2007, 317, 647–
650.
18. De Jong S.J., De Smedt S.C., Wahls M.W.C., Demeester J., Kettenes-van den
Bosch J.J., Hennink W.E., Macromolecules 2000, 33, 3680–3686.
19. Decher G. Science 1997, 277, 1232-1237.
20. Deng Z. X., Tian Y., Lee S. H., Ribbe A. E., Mao C. D. Angew. Chem. Int. Ed.
2005, 44, 3582–3585.
21. Discher B. M., Hammer D. A., Bates F. S., Discher D. E. Curr. Opin. Colloid
Interface Sci. 2000, 5, 125–131.
22. Discher D. E., Ahmed F., Annu. Rev. Biomed. Eng. 2006, 8, 323–341.
23. Discher D.E., Eisenberg A., Science 2002, 297, 967–973.
24. Duncan R., Nat. Rev. Drug Discovery 2003, 2, 347–360.
25. Frankamp B. L., Boal A. K., Rotello V. M., J. Am. Chem. Soc. 2002a, 124,
15146–15147.
26. Frankamp B. L., Uzun O., Ilhan F., Boal A. K., Rotello V. M., J. Am. Chem.
Soc., 2002b, 124, 892–893.
27. Gabizon A.A., Cancer Invest. 2001,19, 424–436.
28. Gautrot J. E., Zhu X. X., Angew. Chem. Int. Ed. 2006, 45, 6872 – 6874.
29. Geng Y., Discher D. E., J. Am. Chem. Soc. 2005a, 127, 12780-12781.
30. Geng Y., Ahmed F., Bhasin N. Discher, D. E., J. Phys. Chem. B 2005b, 109,
3772-3779.
31. Geng Y., Dalhaimer P., Cai S., Tsai R., Tewari M., Minko T., Discher D. E.,
Nature nanotechnology 2007, 2, 249-255.
32. Gillies E. R., Frechet J. M., J. Chem. Comm. 2003, 1640–1641.
33. Goodwin A. P., Mynar J. L., Ma Y. Z., Fleming G. R., Frechet J. M. J., J. Am.
Chem. Soc. 2005, 127, 9952–9953.
34. Gouin S., Zhu X. X., Langmuir 1998, 14, 4025-4029.

35. Gregoriadis G., Wills E. J., Swain C. P., Tavill A. S., *Lancet* 1974, 1, 1313-1316.
36. Hasirci V., Vrana E., Zorlutuna P., *J. Biomater Sci. Polym. Ed.* 2006, 17, 1241-1268.
37. Hayashi T., Iwatsuki M., *Biopolymers* 1990, 29, 549-557.
38. Hiemstra C., vanderAa, L. J., Zhong Z., Dijkstra P. J., Feijen J., *Macromolecules* 2007a, 40, 1165–1173.
39. Huang S. J., Roby M. S., *J. Bioact., Compat. Polym.* 1986, 1, 61-71.
40. Huh K. M., Lee K. Y., Kwon I. C., Kim Y. H., Kim C., Jeong Y., *Langmuir* 2000, 16, 10566-10568.
41. Jain P. K., Lee K. S., El-Sayed I. H., *J. Phys. Chem. B* 2006, 110, 7238–48.
42. Jeong B., Bae Y. H., Lee D. S., Kim S. W., *Nature* 1997, 388, 860–862.
43. Jiang B., Hu L., Gao C., Shen J., *Acta Biomaterialia*, 2006a, 2, 9-18.
44. Jiang G. B., Quan D., Liao K., Wang H., *Mol. Pharmacol.* 2006b, 3, 152-160.
45. Jin R., Hiemstra C., Zhong Z., Feijen, J., *Biomaterials* 2007, 28, 2791–2800.
46. Katti D. S., Lakshmi S., Langer R., Laurencin C. T., *Adv. Drug. Deliv. Rev.* 2002, 54, 933-961.
47. Kingsley J. D., Dou H., Morehead J., Rabinow B., Gendelman H. E., Destache C. J., *J. Neuroimmune Pharmacol.*, 2006; 1: 340-35.
48. Kissel T., Li Y., Unger F., *Adv. Drug. Deliv. Rev.* 2002, 54, 99-134.
49. Kopecek J., *Biomaterials* 2007, 28, 5185–5192.
50. Kumar A., Chhatra R. K., Pandey P. S., *Org. Lett.*, 2010, 12, 1, 24 - 27.
51. Kumar, N., Langer, R. S., Domb, A. J., *Adv. Drug Deliv. Rev.* 2002, 54, 889-910.
52. Kunitake T., Nakashima K., Takarabe M., Nagai A., Tsuge A., Yanagi H. J., *Am. Chem. Soc.*, 1981, 103, 5945–5947.
53. Lee C. C., Gillies E. R., Fox M. E., Guillaudeu S. J., Frechet J. M. J., Dy E. E., Szoka F. C. *Proc. Natl. Acad. Sci. U.S.A.* 2006a, 103, 16649–16654.
54. Lee J., Bae Y. H., Sohn Y. S., Jeong B., *Biomacromolecules* 2006b, 7, 1729–1734.
55. Li C., Yu D. F., Newman R. A., *Cancer Res.* 1998, 58, 11, 2404-9.
56. Liu Y., Shipton M. K., Ryan J., *Anal Chem.* 2007, 79, 2221–9.

57. Maia J., Ferreira L., Carvalho R., Ramos M. A., Gil M. H., *Polymer* 2005, 46, 9604–9614.
58. Meier W., *Chem. Soc.Rev.*, 2000, 29, 295-303.
59. Nelson A., Ochekepe L., Olorunfemi, P. O., Ngwuluka N. C., *Tropical Journal of Pharmaceutical Research* 2009, 8, 3, 275-287.
60. Nichifor M., Carpov A., *Eur. Polym. J.* 1999, 35, 2125-2129.
61. Nie Z., Fava D., Kumacheva E., Zou S., Walker G. C., Rubinstein M. *Nat. Mater.* 2007, 6, 609–614.
62. Noll O., Ritter H., *Macromol. Rapid Commun.* 1996, 17, 553-557.
63. Ofir Y., Samanta B., Rotello V. M., *Chem. Soc. Rev.* 2008, 37, 1814–1825.
64. Overhoffa K. A., Engstromb J. D., Chenc B., *Eur. J. Pharm. Biopharm.* 2007, 65, 57-67.
65. Park K., Shalaby W. S. W., Park H., “Biodegradable Hydrogels for Drug Delivery”, Technomic Publishing, Lancaster-Basel, 1993
66. Park J. H., Cho Y. W., Chung H., Kwon I. C., Jeong, S. Y., *Biomacromolecules* 2003, 4, 1087-1091.
67. Park J. H., Ye M., Park K., *Molecules* 2005, 10, 146-161
68. Pelton R., *Adv Colloid Interface Sci.* 2000, 85, 1-33.
69. Qiu L. Y., Bae Y. H., *Pharmaceutical Research* 2006, 23, 1, 1-30
70. Qiu B., Stefanos S., Ma J., Lalloo A., Perry B.A., Leibowitz M.J., Sinko P.J., Stein S., *Biomaterials* 2003, 24, 11–18.
71. Radziuk D., Shchukin D. G., Skirtach A., Mõhwald H., Sukhorukov G. *Langmuir* 2007, 23, 4612-4617.
72. Reinhold C., *NanoToday*, 2007; 2, 2, 13.
73. Ringsdorf H., Schlarb B., and Venzmer J., *Angew. Chem., Int. Ed. Engl.*, 1988, 27, 113–158.
74. Rowe R. C., Sheskey P. J., Weller P. J., *Hand Book of Pharmaceutical excipients*, American Pharmaceutical Association Washington DC, USA & Pharmaceutical press, London U.K. 2000, 3rd ed.
75. Sawhney A. S., Pathak C. P., Hubbell J. A., *Macromolecules* 1993, 26, 581–587.
76. Schmid G., Bãumle M., Beyer N., *Angew. Chem., Int. Ed.* 2000, 39, 181–183.
77. Sershen S. R., Westcott S. L., Halas N. J., J., *Biomed. Mater. Res.* 2000, 51, 293–8.

78. Sinha V. R., Bansal K., Kaushik R., Kumria R., Trehan A., *Int. J. Pharm.* 2004, 278, 1-23.
79. Skirtach A., Javier A., Kreft O., Köhler, K., Alberola A., Möhwald H., Parak, W., Sukhorukov G., *Angew. Chem. Int. Ed.* 2006, 45, 4612-4617.
80. Soga O., van Nostrum C.F., Fens M.H.A.M., Rijcken C.J.F., Schiffelers R.M., Storm G., Hennink W.E., *Journal of Controlled Release* 2005, 103, 341-353.
81. Soppimath KS, Aminabhavi TM, Kulkarni AR Rudzinski WE. *J. Controlled Release* 2001, 70,1-2, 1-20.
82. Spadavecchia J., Prete P., Lovergine N., Tapfer L., Rella R., *J. Phys. Chem. B* 2005, 109, 17347–17349.
83. St.Pierre T., Chiellini E. J., *Bioact. Compatible Polym.* 1986, 1, 467-497.
84. Tae G., Kim Y. J., Choi W. I., Kim M., Stayton P. S., Hoffman A. S., 2007. *Biomacromolecules* 8, 1979–1986.
85. Tomalia D. A., Baker H., Dewald J., Hall M., Kallos G., Martin S., Roeck J., Ryder J., Smith P., *Polym. J.* 1985, 17, 117–132.
86. Tong R., Cheng J., *Polymer Reviews* 2007, 47, 345–381.
87. Torchilin V. P., *Pharmaceutical Research*, 2007, 24, 1, 1-16.
88. Tu R.S., Tirrell M., *Adv. Drug Deliv. Rev.* 2004, 56, 1537– 1563.
89. Uchegbu I. F., Schätzlein A. G., *Polymers in Drug Delivery* published by CRC press 2006
90. Uchegbu I. F., Florence A. T., *Adv. Coll. Interf. Sci.* 1995, 58, 1–55.
91. Van Tomme S. R., Storm G., Hennink, W. E., *International Journal of Pharmaceutics* 2008, 355, 1–18.
92. Van Tomme S.R., van Steenberg M.J., De Smedt S. C., van Nostrum C. F., Hennink W. E., *Biomaterials* 2005, 26, 2129–2135.
93. Visaria R., Bischof J. C., Loren M., *Int. J. Hyperthermia* 2007, 23, 501–11.
94. Wang W., Qu X., Gray A. I., Tetley L., Uchegbu I. F., *Macromolecules* 2004, 37, 9114–9122.
95. Wang W., Tetley L., Uchegbu I. F., *J. Coll. Interf. Sci.* 2001, 237, 200–207.
96. Whitesides G. M., Boncheva M., *PNAS* 2002, 99, 8, 4769 - 4774.
97. Winzenburg G., Schmidt C., Fuchs S., Kissel T., *Advanced Drug Delivery Reviews* 2004, 56, 1453.
98. Xu C., Breedveld V., Kopecek J., *Biomacromolecules* 2005, 6, 1739–1749.

99. Xu H., Srivastava S., Rotello V. M., *Adv. Polym. Sci.* 2007, 207, 179–198.
100. Yang H., Kao W. Y. J., *J. Biomater. Sci. Polym. Ed.* 2006, 17, 3–19.
101. Zehner R. W., Lopes W. A., Morkved T. L., Jaeger H., Sita L. R., *Langmuir*, 1998, 14, 241–244.
102. Zhu X., Nichifor M., *Acc. Chem. Res.* 2002, 35, 539-546

Chapter 2

Objectives and scope of work

2.1 Preamble

More than 50% of the drugs approved for use exhibit poor aqueous solubility, which poses a major hurdle in ensuring better absorption and bioavailability. This also poses a serious challenge in the design of formulations not only for oral but also for parenteral and topical administration. Polymeric excipients enhance solubilization and mitigate toxicity through self assembly mediated formation of nanoaggregates like micelles, vesicles and nanospheres. Another approach to reduce drug toxicity is to use implants or depots for sustained drug delivery. *In situ* hydrogels are attracting attention because of their high biocompatibility, ease of synthesis and ability to act as depots.

For the preparation of diverse morphologies mainly block copolymers have been explored. Very few reports deal with graft and polymer conjugates. The driving force for self assembly is hydrophilic lipophilic balance or hydrophilicity parameter $f_{\text{hydrophilic}}$. In nature, post translational modification of proteins modify the protein structure and hence the function through altered hydrogen bonding and secondary valence interactions. Taking inspiration from nature, self assemblies can be guided through hydrophilic functionalization of polymer conjugates.

Even though *in situ* hydrogels are very versatile systems for localized drug delivery, hydrophobic drugs cannot be distributed uniformly within the hydrogel matrix. Thus there is a need for hydrogel systems containing hydrophobic domains within which the hydrophobic drugs can be solubilized and released over longer duration.

2.2 Objectives

The major focus of this work has been to enhance drug efficacy through increased solubilization of drug and reduce toxicity through localized delivery. In order to overcome these limitations, work has been mainly focused on the design and evaluation of polymeric self assemblies which exhibit diverse morphologies for applications in drug delivery. This includes choice of hydrophobe, choice of biodegradable and biocompatible polymer backbone, synthesis of polymer conjugates, characterization of supramolecular self assemblies and drug loading in these self assemblies. Diverse morphologies are proposed to offer different

environment and functionalities on the surface which could be explored for nano-patterning of silver and gold nanoparticles useful for stimuli sensitive drug delivery system. Some of these morphologies would be explored for loading of Amphotericin B (Ampho B) for reduction in toxicity. Incorporation of reactive amine functionality on the surface of these self assemblies was explored for in situ hydrogel formation and Paclitaxel delivery.

The major objectives and scope of the proposed investigation are summarized below.

1. To identify rigid biocompatible and biodegradable polymer and conjugate bile acid to it at different degrees of substitution in order to study the effect of hydrophobicity. e.g. Polysuccinimide an active analogue of polyaspartic acid.
2. To incorporate different functionalities on bile acid conjugated polyaspartate backbone in order to study the effect of head group size in guiding self assembly and identify resulting morphologies.
3. To characterize different morphologies for size, critical aggregation concentration, hydrophobic environment and rigidity of the system.
4. To study Amphotericin B loading in these self assemblies and its aggregation, solubilization and toxicity. Investigate the effect of different parameters like hydrophobe content, type of self assembly and heat on drug aggregation and toxicity.
5. To investigate the capping abilities of different functionalities like hydroxyl, carboxyl, amide and hydrazide on polyaspartic acid bile acid conjugates through interaction with gold and silver.
6. To explore functionalized polyaspartic acid bile acid conjugate morphologies like micelles, vesicles, tubes and nanospheres as templates for nano-patterning of silver and gold nanoparticles.
7. To study in situ hydrogel formation using reactive self assemblies formed by various polymer conjugates. Characterize these hydrogels containing hydrophobic domains for gelation time, degradation and modulus.

8. To study solubilization of a model hydrophobic compound (Triclosan) by encapsulation in reactive self assemblies.
9. To investigate in situ gelation by cross linking the self assemblies. Characterize in situ hydrogels with hydrophobic pockets and study release of encapsulated Triclosan.
10. To explore the possibility of forming the reactive emulsion using soya bean oil or α tocopherol as oil phase and reactive polymer conjugates as emulsifier.
11. To monitor in situ cross linking of reactive emulsion droplets resulting in hydrogels containing oil pockets. Characterize these products for gelation time, degradation time, rheology etc. and finally investigate the potential of these for the release of hydrophobic drug.
12. To explore polymerizability of bile acid using Michael type addition between diacrylated monomers of bile acids and Trimethylene dipiperazine (TMDP). Characterize Oligo β amino esters for mol. Wt., degradability and drug loading.
13. To study hydrophobic drug loading and release from particulate drug delivery systems (nanospheres and microspheres) prepared from Oligo β amino esters. Characterize particles for size and zeta potential.

A bird's eye view of the thesis is presented below

In order to achieve these goals, bile acid – polyaspartic acid conjugates have been synthesized. These conjugates exhibited hydrophilic functionality guided self assembly resulting in morphologies like micelles, vesicles, tubules and nanospheres which are investigated in details in chapter 3 and 4. Amphotericin B encapsulation and its toxicity reduction in micelles and vesicles has been investigated in chapter 5. These morphologies also acted as templates for nanopatterning of silver and gold nanoparticles in ring and necklace forms as discussed in chapter 6. In order to reduce drug toxicity, localized drug delivery which is most preferred approach has

been investigated. Aza-Michael addition led *in situ* hydrogels with hydrophobic domains have been studied. Additionally *in situ* hydrogels with oil pockets have also been conceptualized and explored for Triclosan delivery as described in chapter 7. Bile acid based poly (β amino esters) have also been synthesized in all structural planes of steroidal nucleus. These polymers formed nanoparticles in the range 70 - 500 nm which were investigated for Paclitaxel delivery as discussed in chapter 8.

Chapter 3

Synthetic biloproteins: synthesis and characterization

Summary

The potential of bile acid self assembly has been limited by high CMC and secondary aggregation led instability. In order to overcome these limitations, Deoxycholic acid was conjugated with rigid Polyaspartic acid in the range 10 - 60 mole %. These conjugates referred to as Biloproteins; exhibit a morphological transition from micelle to vesicle with increasing degree of substitution (DS) between 20 to 40 mole %. Both morphologies bear polyaspartate shell, exhibit zeta (ξ) potential -17 to -64 mV and average diameter 140-230 nm. Critical aggregation concentration (CAC) of polymer conjugates was in the range 3.65×10^{-2} to 1.297 mg/ml depending on DS. The aggregation number of Deoxycholic acid groups per hydrophobic microdomain (N_{AEDOCA}) indicated dependence on molecular weight and DS. Number of chains forming a domain in an aggregate (N_{chain}) suggests that an increase in molecular weight favored intramolecular association. Fluorescence quenching experiment indicated possibility of multiple hydrophobic microdomains in the aggregate. The morphological transition was confirmed by molecular anisotropy measurements and Transmission electron microscopy. Pyrene binding constant and equilibrium partition constant indicate suitability of biloproteins as a carrier for hydrophobic drug delivery.

3.1 Introduction

Synthetic block and graft copolymers exhibit a wide range of biomimetic morphologies such as micelles, vesicles and tubes driven by the secondary valence forces as in natural biomacromolecules. The factors which govern the morphologies have been extensively investigated in view of their applications in nanolithography, as nanoreactors for chemical reactions and nanocontainers for biomedical applications including drug delivery. (Burke 2000, Pasparakis 2010) The morphologies of block copolymers are governed primarily by polymer molecular weight, hydrophilic content, segment length and distribution (Discher 2002, Blanazs 2009), while those of graft copolymers are governed by inter or intra molecular associations, which depend upon the molecular weight of polymer backbone, its flexibility, hydrophobic segment length, grafting frequency and dispersion medium.(Wang 2004)

Polymeric nanoaggregates have been explored for drug delivery mostly because of the advantages conferred like low CMC, high stability, high drug loading and encapsulation efficiency, slow release and better control over aggregate characteristics like size, shape and charge. (Kataoka 2001, Torchilin 2007) Especially water-soluble polymers and natural polysaccharides such as Pullulan, Heparin, Dextran and deacylated Chitosan have been modified with Cholesterol and Cholic / Deoxycholic acid. All conjugates formed micellar structures deeming applications in drug delivery systems. (Akiyoshi 1993, Park 2004, Nichifor 1999, Lee 1998)

Polymeric aggregates like micelles and vesicles have also been formed by grafting long chain alkyl hydrophobes on hydrophilic polymers like Hydroxyethyl starch (Besheer 2007), Glycol Chitosan, Polylysine and Polyethylenimine. (Wang 2001a, 2001b, 2004)¹ Polyethylenimine containing Cetyl groups formed micelles (DS < 18), vesicles (18 < DS < 37) and solid nanoparticles (DS > 37). In poly-L-lysine Palmitic acid conjugates, bilayer formation was observed at DS 43 – 58. Recently, hydroxy ethyl starch was hydrophobically modified with Lauric, Palmitic and Stearic acids at DS 10 to 30. The conjugates formed micelles and vesicles depending upon DS and length of hydrophobe

(Besheer 2007). Thus DS and backbone play an important role in determining morphology (Wang 2001a, 2001b, 2004).

Cholesterol is an important membrane additive in the formation and / or stabilization of phospholipids and nonionic surfactant assemblies like liposomes and niosomes (New 1990, Uchegbu 1995). The importance of bulky steroidal compound like cholesterol was also stressed in polymer conjugate based vesicle formation (Wang 2001a, 2001b, 2004). Vesicular structures were also reported to result from bile acids and cholesterol mixture, useful for encapsulation of drugs or proteins (Martin 2003, 2005). Deoxycholic acid is a major constituent of bile, which plays a key role in the solubilization of hydrophobic components of food by micelle formation in GI tract. It contains a steroidal head and a flexible tail with a carboxylate end. Bile acid usage for solubilization of many hydrophobic drugs has been explored extensively because of its biocompatibility. Its usage has been limited due to high CMC, instability towards ions and tendency to form larger secondary aggregates (Zhu 2005).

Although the polymers used for bile acid conjugation reported hitherto are biocompatible and potentially biodegradable, their degradation behavior is not readily predicted. Polyaspartic acid is one of the most versatile synthetic polypeptides known to be biodegradable, biocompatible and tailorable (Roweton 1997, Nakato 1998, Tabata 2000, Shinoda 2003).

The hydrophobic drug delivery systems based on fatty chain modified polyaspartic acid has been explored earlier (Yokoyama 1998, Kwon 1996). Poly hydroxyethyl aspartamide conjugates containing Dehydrocholic acid formed stable uncharged micelles upto DS 10, but aggregated at higher DS (Yang 2003). Thus there is a need to enhance the DS of bile acid which would overcome stability problems and exhibit low CAC.

In this chapter we report in detail the self assembly behavior of carboxylated Biloproteins and micelle to vesicle transition as a function of DS. The influence of rigid peptide backbone, its molecular weight, number of hydrophobes forming domain,

minimal concentration for hydrophobe association, nature of hydrophobic environment, binding with Pyrene and type of association (intra / intermolecular) which in turn guide micelle to vesicle transition has been investigated.

3.2 Experimental

3.2.1 Materials

L- aspartic acid, Deoxycholic acid, Pyrene, Diphenyl hexatriene (DPH), Dicyclohexyl carbodidimide (DCC) [Aldrich], Dry Methanol, N hydroxy succinimide (NHS), Cetyl pyridinium chloride (CPC) [SD fine India], Ethylene diamine (SRL, India), o-Phosphoric acid (85%), Hydrochloric acid, Sodium hydroxide, Acetone, Dimethyl formamide (DMF) [Merck, India] dried and stored on molecular sieves.

3.2.2 Synthesis of polymer backbone Polysuccinimide (PSI)

Low and high Mol.Wt. PSI were synthesized using o-Phosphoric acid as catalyst by dry blending and melt polycondensation method respectively. In dry blending, 200 g of aspartic acid and 20 g of o-phosphoric acid were added to three neck round bottom flask. Mixture was kneaded well at room temperature and subjected to heating at 180 °C under nitrogen flow. After 1 hr, dry lumps were ground in mixer grinder to fine powder and reheated for 3 hrs at 180 °C under nitrogen flow. Polymer was then washed with deionized water till neutrality and finally with methanol to dry at 60 °C in vacuum oven overnight.

In melt condensation, 25 g of aspartic acid and 15 g of o-Phosphoric acid were added to round bottom flask and stirred to form homogeneous paste which was heated to 180 °C with distillation condenser. After 1 hour it was subjected to vacuum of 5 mbar for 4 hrs at 180 °C to yield brownish polymer which was dissolved in 100 ml of Dimethylformamide and precipitated in 1 L of methanol to yield powder. It was then purified by dissolution in Dimethylformamide and precipitation in water followed by washing with methanol and drying at 60 °C overnight.

3.2.3 Synthesis of hydrophobe AEDOCA

Deoxycholic acid being anionic in nature could not be conjugated with PSI hence an amine analogue of it was needed for grafting on Polysuccinimide. Amino ethyl Deoxycholamide was synthesized through an intermediate NHS analogue prepared by DCC chemistry. Briefly Deoxycholic acid (23.6 g, 60 mmol) was mixed with DCC (14.8 g, 77.8 mmol) and N-hydroxy succinimide (9 g, 76.4 mmol) in 200 ml of dry Tetrahydrofuran. The mixture was stirred for 12 hrs at room temperature under nitrogen atmosphere and precipitated dicyclohexylurea was removed by filtration. The concentrated filtrate was precipitated in n-Hexane. The succinimide ester of Deoxycholic acid was filtered off and washed thoroughly with n-Hexane, followed by vacuum-drying at room temperature. Succinimide ester (10 g, 20 mmol) was dissolved in THF (50 ml), and the solution was slowly added drop wise to ethylene diamine (134 ml, 2 mol) solution. After reaction for 6 hrs, the mixture was precipitated in distilled water. AEDOCA was obtained after three washes of distilled water and drying in vacuum desiccator.

3.2.4 Synthesis of AEDOCA substituted polyaspartic acid (P2K-A, P14K-A)

4 g PSI (41 mM) was dissolved in 40 ml dry DMF and different amounts of AEDOCA were added to achieve varying degrees of substitution. Reaction mixture was stirred for 24 hrs at 65 ° C under Nitrogen and then concentrated and precipitated in excess Acetone. AEDOCA conjugated PSI was washed thrice with Acetone and then dried in vacuum desiccator. Reactive conjugates were added slowly to 1.5 equivalent Sodium hydroxide solutions with stirring at 5-10 ° C. After 3 hrs the reaction mass was dialyzed in spectrapor dialysis bag (Mol.wt. cut off 2000) against deionized water till complete removal of sodium hydroxide was achieved as confirmed by pH of water. Dialyzate was then freeze dried to yield AEDOCA substituted Polyaspartic acid sodium referred to as Biloproteins. (Figure 3.1)

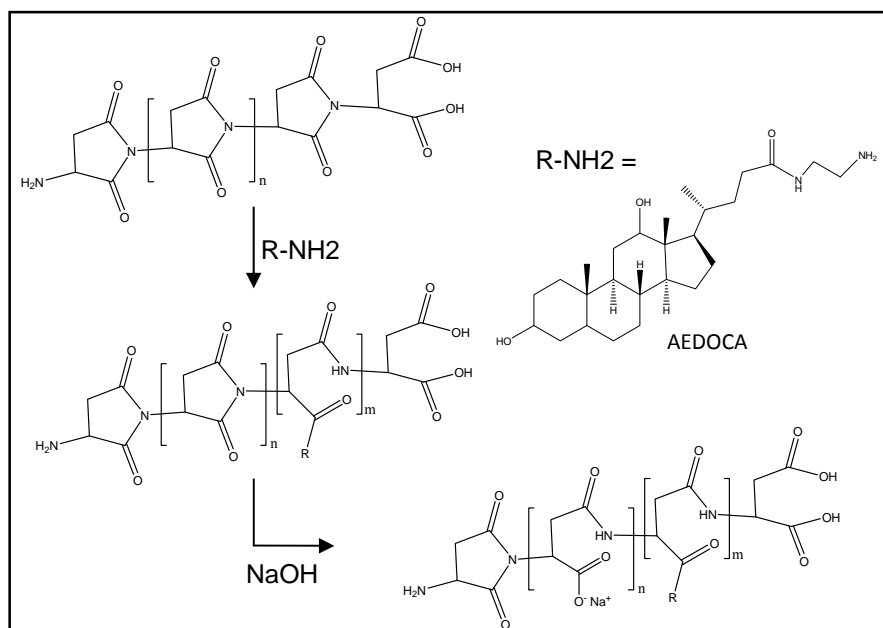


Figure 3.1. Synthesis AEDOCA substituted Polyaspartic acid sodium.

3.2.5 Preparation of biloprotein aggregates

AEDOCA substituted Polyaspartic acid sodium was added in deionized water, on Spinix vertex stirrer and sonicated for 5 minutes in bath sonicator at room temperature. Aggregate solution was filtered through 0.8 / 0.45 μ filter and used for further characterizations.

3.2.6 Molecular weight determination

PSI was reacted with ethanolamine at 5-10 ° C in Dimethylformamide to obtain Poly hydroxyl ethyl aspartamide, a water soluble analogue. Molecular weights were determined at 25 ° C by aqueous Gel permeation chromatography (GPC), equipped with TSK- GEL columns using 0.2 M NaNO₃ at a flow rate of 1 ml/min. The columns were calibrated using PEO standards.

3.2.7 Differential scanning calorimetry

Absence of free AEDOCA in polymer conjugate was confirmed using DSC. PSI, AEDOCA and PSI-AEDOCA conjugates were subjected to DSC analysis in the temperature range 40 °C to 200 °C at 10 °C / min.

3.2.8 Characterization of biloprotein aggregates

Biloprotein aggregates were characterized for size and stability by static light scattering studies, zeta potential measurement and turbidity measurements. Size and shape were probed using transmission electron microscopy. Self assembly was characterized in terms of critical aggregation concentration (CAC), aggregation number (N_{agg}), microviscosity, Pyrene binding and equilibrium partition constant using fluorescence spectroscopy.

3.2.8.1 Fluorescence studies

Steady-state fluorescence experiments were carried out using Edinburgh luminescence spectrophotometer. Fluorophore molecules form complex with cyclodextrins and amphiphiles or amphiphilic polymers hence are useful to understand self assembly process (Akiyoshi 1993). We used Pyrene, a hydrophobic fluorescent probe as guest molecule, which exhibited change in fluorescence intensity as a function of concentrations of polymer conjugate. Critical aggregation concentration (CAC) of polymer conjugates and binding constant (K) were deduced from the results. Pyrene being sparingly soluble in water, a stock solution (6.0×10^{-4} M) was prepared in acetone and added to the polymer dispersion to attain 6.0×10^{-7} M concentration. The mixture was then stirred at room temperature for 24 h. All samples were excited at 339 nm while the emission spectra were recorded at 390 nm with slit width of 2 nm. The intensities of peaks at 373 nm and 385 nm were monitored as I_1 and I_3 peaks respectively to monitor encapsulation of Pyrene within the hydrophobic interior of polymer aggregates.

The binding constant between the Pyrene and polymer conjugate was determined using Benesi- Hildebrand equation as described by Akiyoshi et.al (1993).

$$I_0 / I = (1 / \text{Polymer conjugate}) * (I_0 / K * I_\infty) + I_0 / I_\infty \text{ ----- Equation 1}$$

Where K is binding constant, I_0 / I is relative fluorescence intensity of Pyrene in the absence and presence of polymer conjugate. I_∞ is the fluorescence intensity when all Pyrene would be complexed with polymer conjugate. The plot of I_0/I vs $1/\text{Polymer conjugate}$ yields a straight line. The binding constant (K) was calculated from the ratio of intercept to slope. Aggregation number (N_{agg}) was determined using Cetyl pyridinium chloride (CPC) as Pyrene fluorescence quencher.

Edinburgh luminescence spectrometer equipped with filter polarizers in L-format configuration was used to determined microviscosity. DPH is insoluble in water hence 1.0 mM stock solution of the probe in Tetrahydrofuran was prepared. The final concentration of the probe was adjusted to 1.0 μM by adding appropriate amount of the stock solution to the polymer aggregate. The anisotropy measurements were carried out at 20, 40 and 55 °C. The samples containing DPH were excited at 350 nm, and the emission intensity was measured in range 370-550 nm using excitation and emission slit width of 2.5 nm each. Integration time of 10 seconds was used for data collection.

The r -value was calculated using equation

$$r = [(G * I_{VV}) - I_{VH}] / [(G * I_{VV}) + 2 I_{VH}] \text{ ----- Equation 2}$$

Where I_{VV} and I_{VH} are the fluorescence intensities polarized parallel and perpendicular to the excitation light and G is the instrumental correction factor ($G = I_{HH} / I_{HV}$).

3.2.8.2 Static light scattering

The static light scattering (SLS) measurements were performed using a Brookhaven Instruments corporation UK 90 Plus particle size analyzer. The scattering intensity was measured at 90 ° angle. All polymer aggregate solutions were prepared in double distilled water at 2 mg/ml concentration. The solutions were filtered through a Pall Gellman PES syringe filter (0.45 μ) directly into the scattering cell. Prior to the

measurements, the scattering cell was rinsed thrice with the filtered solution. All the experiments were performed at room temperature in triplicate.

3.2.8.3 Turbidity measurements

Samples of polymer aggregates were checked for turbidity using UV spectrophotometer at 500 nm, in the range 1×10^{-4} mg/ml to 10 mg/ml.

3.2.8.4 Zeta potential measurements

The electrode probe was dipped in the polymer aggregate solutions at 2 mg/ml. Electric field of 7.0 V/cm was applied across the two electrodes. Zeta potential was determined with inputs of pH and particle size. For each measurement 5 runs were averaged with each run employing 10 cycles for 3 minutes. The data was analyzed using zeta pals software of Brookhaven instruments.

3.2.8.5 Transmission electron microscopy

The morphology of nanoaggregates was investigated using a high-resolution transmission electron microscope (HR-TEM) at 300 kV (Technai- FEI). A drop of self-aggregate solution (2 mg/ml) was placed on a polymer coated copper grid. The grid was held horizontally for 5 minutes to allow the aggregates to settle and then blotted with tissue paper from one edge point to allow the excess fluid to drain. Grid was then allowed to dry in air and stored in desiccator before visualization.

3.3 Results and discussion

Morphological behavior of a wide range of block copolymers has been extensively investigated in the past (Discher 2002, Kataoka 2001). The graft copolymers investigated so far are natural polymers such as Pullulan, Chitosan, Heparin and synthetic ones like Polyethylenimine. It was concluded that the incorporation of cholesterol in Polyethylenimine grafted Palmitic acid was necessary to form and stabilize vesicles (Wang 2001a, 2001b, 2004). Bile acids and their derivatives are known to self organize in both solid state and in aqueous solutions to micelles, gels, fibers and nanotubes. Bile salts exhibit micellar structures but have drawbacks like high

CMC (1.25 mg/ml), instability towards ions and aggregation on storage (Zhu 2002). We therefore chose to synthesize Polyaspartic acid – deoxycholic acid conjugates through an amide spacer so as to achieve higher degree of conjugation than that reported in the past which would lead to lower CAC. The presence of anionic charge is expected to enhance stability of the self assembly.

The conjugates were characterized for composition, aggregation behavior and morphology as a function of degree of conjugation and molecular weight. Our results show that the polymer conjugates having DS as high as 60 can be synthesized. These amphiphilic polymer conjugates undergo micelle to vesicle transition with increasing DS. In case of Polyaspartic acid of lower molecular weight (P2K-A) the domain formations is a result of both intra and inter chain association, whereas in case of high molecular weight (P14K-A), intra chain association predominated.

3.3.1 Synthesis and characterization of PSI - AEDOCA conjugate

Apart from DS of hydrophobe, molecular weight of polymer is an important parameter governing aggregate formation. High molecular weight polymers form larger aggregates compared to low molecular weight polymers (Wang 2001a, 2001b, 2004). To confirm if this holds true for the present system, we investigated both low and high molecular weight polymers. In synthesis of Polysuccinimide, dry blending yielded lower molecular weight while melt condensation yielded higher molecular weight (Neri 1973). Low molecular weight Polysuccinimide was synthesized and characterized by Vapor pressure osmometry (VPO) to yield M_n 2263. This was further confirmed by aqueous gel permeation chromatography (GPC), by converting PSI to Polyhydroxyethyl aspartamide. The estimated M_w and M_n were 5171 and 2498 respectively. Corresponding values for Polysuccinimide synthesized by the melt polycondensation were 22,200 and 14,300 respectively.

Poly (succinimide) (PSI), cannot be directly conjugated with Deoxycholic acid but is highly reactive towards amine because of the presence of imide groups. Compared to ester link between hydrophobe and polymer backbone, amide linkage bearing short

spacer has been reported to favor intramolecular association guided by hydrogen bonding (Yamamoto 1998, Suwa 2000, Hu 1995). Deoxycholic acid was reacted with ethylene diamine through an NHS ester intermediate to yield AEDOCA, which was then conjugated, to Polysuccinimide yielding poly (Deoxycholamidoethyl aspartamide – co -succinimide).

^1H NMR in $\text{DMSO } d_6$ was used to quantify the DS of AEDOCA. The characteristic proton peak of Polysuccinimide, a single methine proton at 5.21δ and the proton peaks of DOCA, including 18- CH_3 (0.60δ), 19- CH_3 (0.86δ), 21- CH_3 (0.94δ), and methylene-methine envelope ($1 - 2.3\delta$), were completely resolved. It can also be observed from NMR spectra (Figure 3.2) that with an increase in DS, the intensity of methyl protons in AEDOCA at 0.60δ increased because of conjugation of AEDOCA with Polysuccinimide.

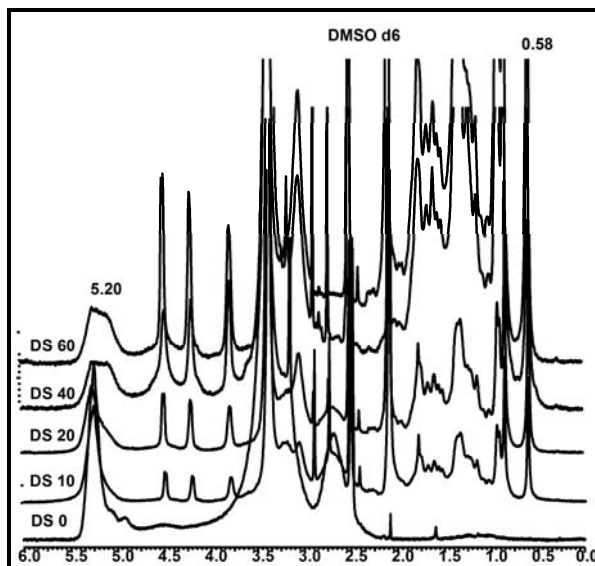


Figure 3.2. ^1H NMR spectrum of PSI14K-AEDOCA in $\text{DMSO } d_6$.

The DS was quantified using a peak at 5.21δ of methine proton of PSI to protons of methyl group of AEDOCA at 0.60δ . DS of AEDOCA in the range 7 to 58 mole % was achieved when AEDOCA in feed was varied from 10 to 60 mole %. Thus a linear relationship existed between DS and AEDOCA in feed (Figure 3.3), which is in

accordance with findings of Nakato et.al wherein DS of Octadecyl amine on PSI ranged from 0 to 50 mole % (Nakato 2000).

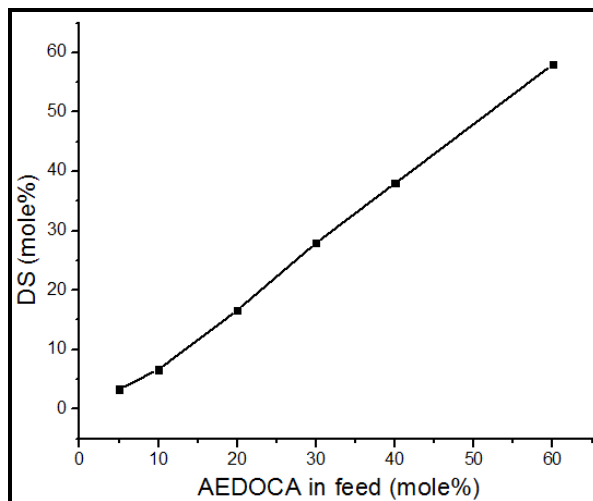


Figure 3.3. DS of AEDOCA on PSI as a function of feed composition in P2k-A conjugates

Table 3.1. Characterization of PSI - AEDOCA Conjugates

DOCA in feed (mole %)	DS # (mole %)	No. of DOCA per chain	DOCA content weight (%)	M _n [#]
PSI 2k-AEDOCA				
0	00.00	00.00	00.00	2263
10	06.66	01.50	28.21	2906
20	16.60	03.80	52.82	3945
40	38.00	08.75	77.56	6164
60	58.00	13.34	88.62	8234
PSI 14k-AEDOCA				
0	00.00	00.00	00.00	14310
10	09.00	13.23	35.80	20211
20	19.00	27.93	56.95	26827
40	39.00	57.33	78.28	40056
60	55.00	80.85	87.32	50641

Molecular weight of reactive polymer conjugate i.e. PSI – AEDOCA was calculated using molecular weight of PSI and DS of AEDOCA. (Table 3.1)

Differential scanning calorimetric technique was used to confirm that no unreacted AEDOCA was present in the conjugate. AEDOCA yielded broad melting (a) at 115 °C while PSI (b) and PSI-g-AEDOCA (c) showed no melting around 115 °C. Thus there was no free AEDOCA residue in Polymer conjugate. (Figure 3.4)

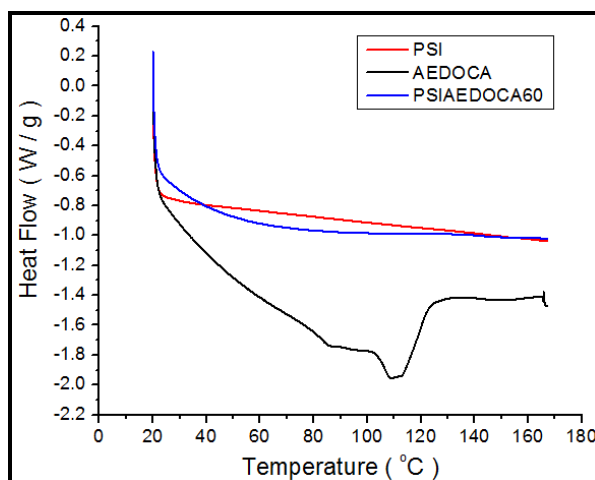


Figure 3.4. DSC endotherms of reactive polymer conjugate, polysuccinimide, AEDCOA.

3.3.2 Preparation and characterization of PASP -AEDOCA aggregates

Succinimide rings in PSI – AEDOCA conjugates were opened with aqueous sodium hydroxide treatment which yielded hydrophobically modified polyaspartic acids referred to as PASP – AEDOCA. These were recovered by freeze-drying. The aggregates were prepared by dispersing PASP - AEDOCA in water by bath sonication for five minutes. Self aggregates of PASP - AEDOCA in water were evaluated at macroscopic and microscopic levels. Macroscopic investigations involved turbidity studies, zeta potential measurements, ¹H NMR analysis to confirm aggregate formation, quantify charge and evaluate stability. Microscopic investigations like fluorescence studies, light scattering and TEM measurements were used to quantify aggregate

formation, understand mechanism of formation, environment within the aggregate, ability to bind with hydrophobic compounds and morphology of aggregates.

3.3.2.1 Macroscopic analysis

a) Formation of stable aggregates: turbidity measurements

Absorbance of PASP-AEDOCA conjugates in the concentration range 1×10^{-4} mg/ml to 10 mg/ml was measured at 500 nm using UV spectrophotometer. The solutions were optically clear and transparent at polymer concentrations upto 10 mg/ml and had an absorbance less than 0.02 (data not shown) This is in contrast to previous report on Dehydrocholic acid (DHA) - Polyhydroxyethyl aspartamide (PHEA) conjugates in the DS range 8 to 34 mole % containing ester linkage. These solutions at 10 mg/ml were optically clear below DS 10 and turbid at or above DS 12. The said conjugates at high DS formed large aggregates in aqueous solution, apparently due to the high density of DHA groups having a large exclusive volume. PHEA - DHA having DS greater than 12 could not form the layer curvature enough to stabilize self-aggregates. It was concluded that interaction between neighboring DHA groups stabilized the primary self-aggregates at low DS, while at high DS, the stiffness of the PHEA backbone destabilized primary aggregates to form irreversible interfused large aggregates. In the present case negative surface charge generated by PASP corona resulted in better dispersion and prevention of reunion of smaller aggregates resulting in optically transparent solutions even at high DS. The results are consistent with earlier reports for alkyl grafts (Suwa 2000).

b) Surface charge and stability: Zeta potential (ξ) measurements

Zeta potential (ξ) values for all polymer conjugates were negative indicating that the polymer conjugates were coated with anionic PASP corona. Polymer conjugates P2K-A and P14K-A exhibited more negative zeta potential at higher DS as shown in Table 3.4. P2K-A at DS 10 and 20 exhibited ξ values -25 and -41 respectively, indicating negatively charged particles having weak aggregate structure. At DS 40 and 60, ξ values were -69 and -68 respectively, which indicated compact negatively charged particles exhibiting high stability. At same DS, ξ values of high molecular weight

polymer conjugate were more negative than those for low molecular weight polymer conjugate.

c) Aggregate formation: ^1H NMR in D_2O

The peaks of methyl protons in AEDOCA at 0.6δ and 0.8δ are very sharp in $\text{DMSO } d_6$ and broaden and decrease in intensity in D_2O . In $\text{DMSO } d_6$, both polymer backbone and AEDOCA are soluble hence homogeneously solvated enabling all the protons in structure to spin in response to magnetic field applied. In D_2O , only PASP is soluble, hence AEDOCA segments remain dispersed in the interior away from D_2O , causing fewer protons in structure to spin in conformity with applied field resulting in decrease in intensity of methyl protons at 0.6δ and 0.8δ . (Figure 3.5) Thus NMR study revealed aggregation of PASP -AEDOCA in D_2O wherein AEDOCA is shielded as micro segregated segment and PASP segment is exposed to solvent. Similar decrease in intensity of AEDOCA peaks was observed earlier in Heparin - DOCA conjugate aggregates (Park 2004).

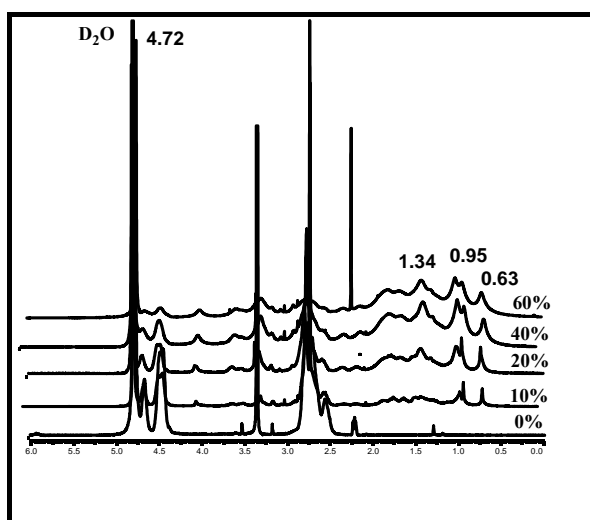


Figure 3.5. ^1H NMR of P14K-A at different DS in D_2O .

3.3.2.2 Microscopic analysis

a) Critical aggregation concentration (CAC)

Excitation and emission spectra of Pyrene in PASP-AEDOCA solutions reveal characteristic vibrionic peaks of Pyrene I_1 at 373 nm and I_3 at 385 which are a measure of hydrophobicity in microdomains of aggregate [Figures 3.6a) and 3.6b)].

The intensities of the vibrionic bands strongly depend on the compactness of hydrophobic environment. Figure 3.6 shows, sigmoidal plots of intensity ratio (I_1/I_3) of Pyrene as a function of PASP-AEDOCA concentration on a logarithmic scale. At very low concentration below CAC, the intensity ratio was 1.8, indicating very low hydrophobicity. Further at this concentration, with increasing DS of AEDOCA, the intensity ratio decreased to 1.7, indicating increasing hydrophobic environment as a result of hydrophobic association. The concentration at which intensity ratio (I_1/I_3) showed an abrupt decrease was denoted critical aggregation concentration (CAC). The CAC of polymer conjugates decreases with an increase in DS (Figure 3.7). Previous reports indicate a linear relationship existed between DS and log CAC but in most of these polymer conjugates, DS was restricted to 10.

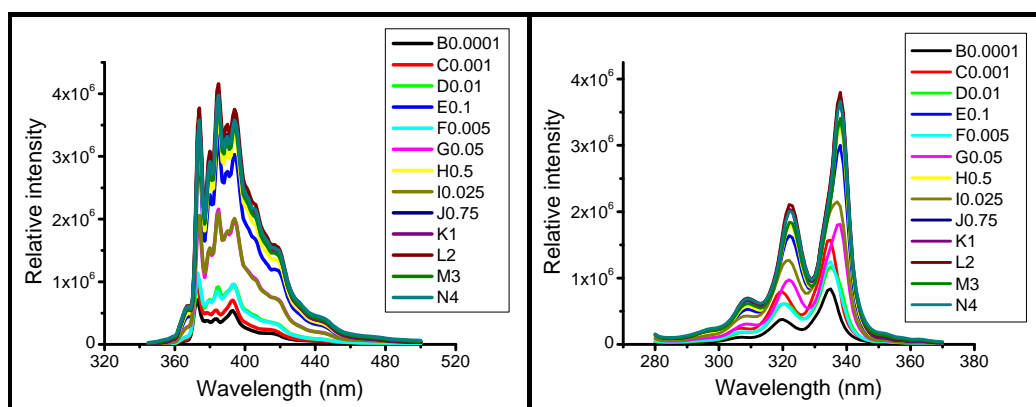


Figure 3.6. Emission and excitation spectra of Pyrene in P2K-A40 in water.

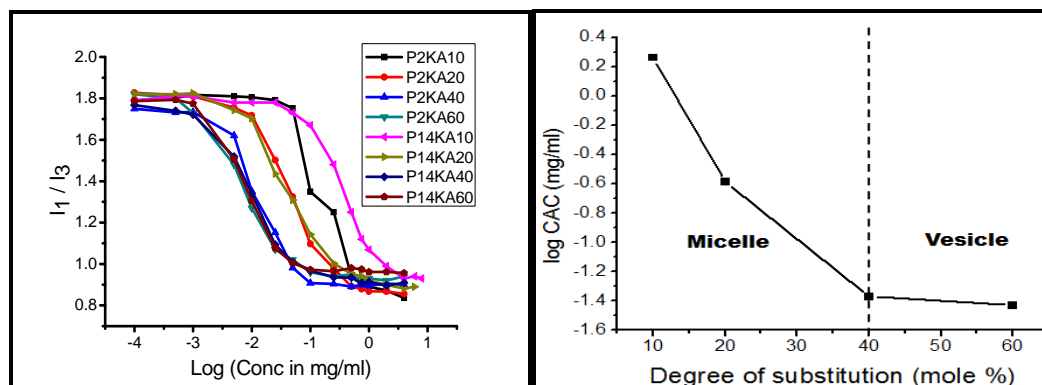


Figure 3.7. CAC of P2K-A and P14K-A as function of DS; b) Effect of morphological transition and dependence of CAC on DS of P2K-A.

In case of Biloproteins too, when DS increased from 10 to 20, log CAC decreased. Further increase in DS from 20 to 40 caused a steeper decrease in log CAC value which then plateaued at DS 60. We attribute this behavior to a change in the morphology of the aggregate from micelle to vesicle, since in the same range micelle to vesicle transition has been observed by TEM later. (Figure 3.7)

A comparison of log CAC vs DS for different polymer steroid conjugates highlights the importance of effect of hydrophobe type, backbone structure and DS on CAC values. (Figure 3.8) At DS 2 to 4, Dextran – Cholic acid exhibited higher CAC (0.35 mg/ml) than that of Dextran - Deoxycholic acid (0.18 mg/ml) as a result of higher hydrophobicity of Deoxycholate graft (Nichifor 1999). At DS 3 to 5, Chitosan – Deoxycholic acid (3×10^{-2} mg/ml) exhibited 10 fold lower CAC than Dextran – Deoxycholic acid, owing to higher hydrophobicity of Chitosan backbone. (Lee 1998) At DS 6 to 10, Heparin – Deoxycholic acid exhibited lowest CAC (3×10^{-3} mg/ml), which could be ascribed to the effect of DS and amide linkage. (Park 2004) At DS 3 to 10, Polyhydroxyethyl aspartamide – Dehydrocholic acid exhibited higher CAC (5×10^{-3} mg/ml) than that of Heparin – Deoxycholic acid. (Park 2004, Yang 2003) Compared to flexible polysaccharide Heparin, Polyhydroxyethyl aspartamide is a rigid polypeptide which might have countered hydrophobe association.

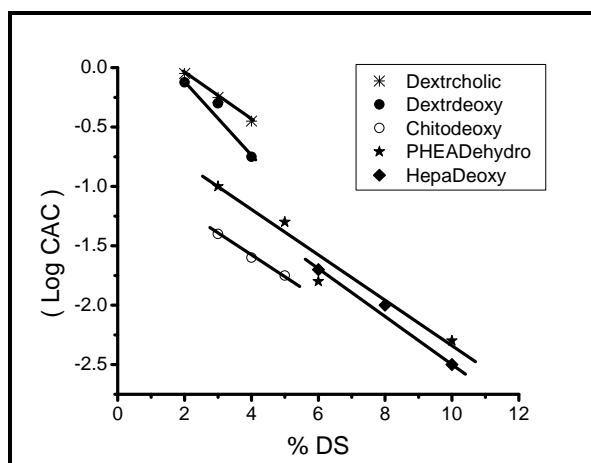


Figure 3.8. Log CAC of literature reviewed polymer conjugates as a function of DS.

Polyaspartate backbone is rigid and charged hence even at DS 60, P2K-A and P14K-A formed aggregates at 7 fold higher CAC value (3.65×10^{-2} mg/ml) than Poly hydroxy ethyl aspartamide – Dehydrocholic acid. Thus ionized corona repelled polar groups countering hydrophobic association (Yang 2003, Suwa 2000, Kang 2001).

b) Pyrene binding constant (K)

A plot of (I / I_0) vs [PASP-AEDOCA] shows that Pyrene complexes with polymer conjugate even below CAC leading to significant quenching of Pyrene. At Pyrene concentration of 6×10^{-7} M, relative fluorescence intensity (I / I_0) decreased in the order P-A60 > P-A40 > P-A20 > P-A10. The binding constant (K) values of Pyrene are summarized as in Table 3.2.

c) Pyrene partitioning constant (K_v)

Pyrene distribution in aggregate can be explained by estimating partitioning constant using binding equilibrium method (Lee 1998). Above CAC, fluorescence signal intensity is enhanced due to Pyrene binding. Pyrene interacts with individual polymeric amphiphiles prior to self-aggregation, followed by partitioning into the inner core of self-aggregates. Assuming simple partition equilibrium, the equilibrium constant (K_v) for partitioning of Pyrene between water and micellar phases can be calculated as follows

$$[\text{Py}]_m / [\text{Py}]_w = K_v V_m / V_w \text{ ----- Equation 3}$$

Where $[\text{Py}]_m$ and $[\text{Py}]_w$ represent Pyrene in micellar and aqueous phase and V_m, V_w are volumes of the two phases respectively. Above equation can be rewritten as

$$[\text{Py}]_m / [\text{Py}]_w = K_v x c / 1000\rho \text{ ----- Equation 4}$$

Where x is the weight fraction of deoxycholic acid in polymer conjugate and ρ is the density of the inner core of self-aggregates and can be assumed to be the same as of Deoxycholic acid in water (1.31 mg/ml). In the intermediate concentration range, $[\text{Py}]_m / [\text{Py}]_w$ can be obtained from the excitation spectrum of Pyrene as

$$[\text{Py}]_m / [\text{Py}]_w = (F - F_{\min}) / (F_{\max} - F) \text{ ----- Equation 5}$$

where F is the intensity ratio I_{336} / I_{333} at a specific polymer conjugate concentration and F_{\min} and F_{\max} are the minimum and maximum intensity ratios. Combining equation 3 and 4, a plot of $(F - F_{\min}) / (F_{\max} - F)$ versus concentration yields K_v (Figure 3.9).

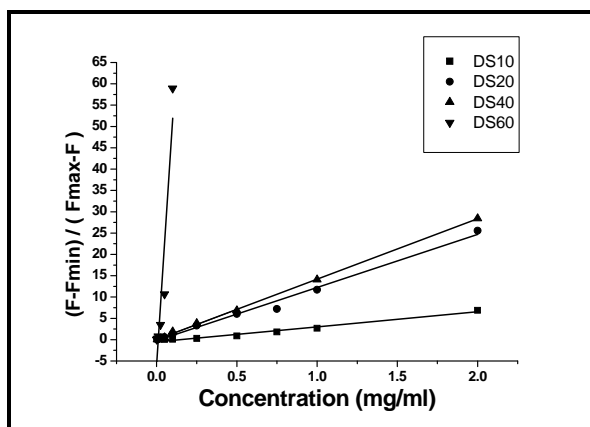


Figure 3.9. Plots of $(F - F_{\min}) / (F_{\max} - F)$ vs [P14K-A] with different DS and at different concentration of polymer conjugate.

The values increased with DS of AEDOCA, (Table 3.2) indicating that number of polar microdomains in the inner core of self-aggregates was much lower. The corresponding values for SDS, poly (styrene-ethylene oxide) (PS-PEO) block copolymer and

Deoxycholate grafted Chitosan are shown in Table 3.2 (Park 2004). K_v values increased with DS in polymer conjugate. Since the K_v values for P2K-A40 and P2K-A60 are higher, it may be concluded that Pyrene is preferentially partitioned into the interior of PASP-AEDOCA microdomains. This association was favored in low molecular weight P2K-A polymer conjugates as indicated by high K_v values. In contrast, the aggregates of high molecular weight P14K-A conjugate at all DS exhibited lower K_v values indicating lower association.

Table 3.2. Binding (K) and Equilibrium constant (K_v) of Pyrene

Sr.no	Polymer conjugate	$K * 10^7$	$K_v * 10^5$
1.	P2K-A10	5.46	0.65
2.	P2K-A20	6.92	0.54
3.	P2K-A40	47.56	6.84
4.	P2K-A60	43.55	3.31
5.	P14K-A10	1.53	0.21
6.	P14K-A20	8.87	0.34
7.	P14K-A40	34.73	0.26
8.	P14K-A60	65.00	1.80
9.	SDS	-	1.2
10.	PS-b-PEO	-	3
11.	Deoxychol - Chitosan	-	5

d) Aggregation number (N_{agg})

This investigation was undertaken to estimate the number of AEDOCA units as well as the number of polymer conjugate chains in the microdomains revealing if association was intra or intermolecular. Multiple chains constituting the domain would yield loose i.e. less compact aggregates because of the incorporation of more polar hydrophilic

groups within the hydrophobic segments. Cetyl Pyridinium Chloride (CPC) was used as a fluorescence quencher (Chu 1987, Alami 1996, Kratochvil 1986). For aqueous polymeric aggregate solutions, the steady state quenching data fit quenching kinetics as

$$\ln (I_0 / I) = [Q] / [M] \quad \text{----- Equation 6}$$

Where I_0 and I denote the fluorescence intensity in the absence and presence of a quencher, $[Q]$ is concentration of the quencher, and $[M]$ concentration of AEDOCA microdomains in polymer aggregates. From the slope of $\ln (I_0 / I)$ Vs $[Q]$, $[M]$ was obtained (Figure 3.10) and the aggregation number per domain $N_{(AEDOCA)}$ was calculated

$$N_{AEDOCA} = [AEDOCA] / [M] \quad \text{----- Equation 7}$$

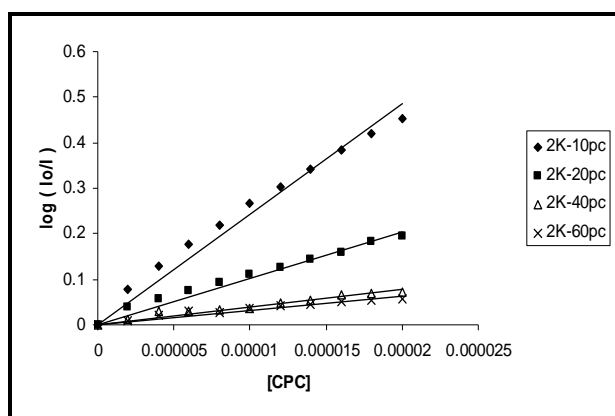


Figure 3.10. Log (I_0 / I) of Pyrene 6.0×10^{-7} M fluorescence as a function of CPC concentration in the presence of polymer conjugates P2K-A at the conc. of 2 mg / ml.

Deoxycholic acid micelle comprises 6-10 molecules (Jover 1997, Morishima 1995). In case of low molecular weight P2K-A ($M_n = 2260$) 2, 4, 6, 8 and 10 AEDOCA units are conjugated to the single polymer chain for DS 10, 20, 30, 40 and 60 respectively. At low DS, lower hydrophobicity in the polymer conjugate favors intermolecular associations. At high DS, fewer chains take part in forming more compact structures through inter and intramolecular associations. The number of AEDOCA units in high molecular weight P14K-A ($M_n = 14310$) are greater than 13 and hence at any DS, polymer conjugate favors intramolecular association during aggregation.

With increasing DS from 10 to 60, N_{AEDOCA} decreased from 77 to 11 for P2K-A while for P14K-A the decrease was from 31 to 10. Thus loose and large hydrophobic domains formed at low DS while compact smaller hydrophobic domains were formed at high DS.

For P2K-A10 domain comprised 77 AEDOCA units. Since each chain has only 1.5 AEDOCA units number of chains required would be approximately 50, i.e. $N_{\text{chain}} \approx 50$, indicating intermolecular association. This would lead to incorporation of some aspartate units (out of remaining 22 units) along with AEDOCA in the hydrophobic domain. As PASP is anionic in nature, it would counter hydrophobic associations through electrostatic repulsion, yielding loose domains in an aggregate structure. In case of Heparin - Deoxycholic acid (DS 6-10), loose aggregate structures were formed because of limited mobility, charge repulsion and steric hindrance in hydrophobes (Park 2004).

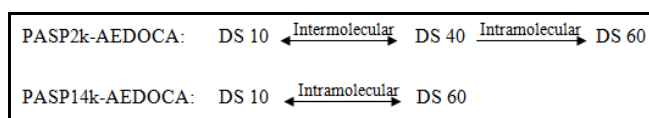
Table 3.3. Effect of DS on CAC, N_{agg} and Anisotropy

Polymer conjugate	CAC (mg/ml)	Aggregation number (N_{agg}) in one hydrophobic domain at 2.0 mg/ml			Anisotropy (r)		
		N_{Chain}	N_{AEDOCA}	Association	20°C	40°C	55°C
P2K-A10	0.270	50.10	77	Inter	-	-	-
P2K-A20	0.201	8.85	34	Inter	0.182	0.151	0.118
P2K-A40	0.063	1.58	14	Inter	0.205	0.171	0.152
P2K-A60	0.036	0.85	11	Intra	0.226	0.175	0.156
P14K-A10	1.297	2.38	31	Inter	-	-	-
P14K-A20	0.257	0.90	25	Intra	0.206	0.182	0.170
P14K-A40	0.042	0.19	10	Intra	0.218	0.190	0.173
P14K-A60	0.037	0.13	10	Intra	0.219	0.198	0.200

Anisotropy values (r) at 20° C for SDS, Poly(ethylene-co-maleic acid), Deoxycholated chitosan, Sodium *N*-(4-Dodecyl oxybenzoyl)-L-valinate were 0.073, 0.273, 0.3 and 0.23 respectively.

According to DS calculations P2K-A60 has 13 AEDOCA units on each chain. Since N_{agg} is 11, each domain is formed by 11 AEDOCA units. Hence all AEDOCA units contributing would be from the same chain, i.e. $N_{chain} \approx 0.86$, suggesting intramolecular association. These domains formed can be expected to be more compact yielding stable aggregates. In case of high molecular weight polymer conjugate P14K-A at DS from 10 to 60; each domain comprised less than one chain ($N_{chain} = 0.9 - 0.133$) indicating preferential intramolecular association during domain formation.

The effect of molecular weight and DS on intra / inter molecular association leading to micro domain formation in an aggregate has been reported in Table 3.4 and can be summarized as follows



According to literature, randomness and DS of bulky hydrophobe with amide linkage having short spacer favors intramolecular association in the domain formation (Yamamoto 1998, Suwa 2000, Hu 1995, Morishima 1995, Akiyoshi 1997). Our results show that in addition to these, molecular weight of the polymer conjugate plays significant role in governing intra / intermolecular association.

e) Microviscosity

The microviscosity of self assembled structures can be determined by measuring molecular anisotropy resulting from rotational diffusion of a probe molecule such as DPH since its fluorescence quantum depends on medium viscosity (Cehelnik 1975). The anisotropy values (r) of PASP-AEDOCA conjugates of two different molecular weights and DS are listed in Table 3.3. In PASP-AEDOCA as DS increased from 10 to 60, anisotropy values increased from 0.182 to 0.226. These findings are in agreement

with earlier reports wherein anisotropy values in case of Chitosan – Deoxycholic acid increased from 0.300 to 0.314 as the DS increased from 2.8 to 5.1 (Lee 1998). Higher molecular weight polymer conjugate P14K-A yielded higher anisotropy values compared to P2K-A at all DS.

The effect of temperature on microviscosity was also studied since structural rigidity depends on temperature. The maximum value (approx. 0.226) of r was obtained at 20 ° C. A similar value has been reported for liposomes (0.230) and Vesicle of N acylamino acid chiral surfactant (Zachariasse 1980, Mohanty 2004). Aggregates of high molecular weight polymer conjugate were more resistant to temperature effect compared to aggregates of low molecular weight polymer conjugate. In both cases anisotropy values decreased on increase in temperature which indicated that phase transition temperature of these aggregates was low.

The lower anisotropy values at lower DS were due to decrease in packing of AEODCA units suggestive of micellar structure. High anisotropy values with increasing DS indicate an increase in packing as a result of bilayer structure formation i.e. a transformation from micelles to vesicles. High anisotropy value of probe suggests that the probe is solubilized in a rigid environment. An increase in rigidity (i.e. microviscosity) of the microenvironment results from tight packing of the steroidal moieties of the polymer conjugates.

3.3.3 Vesicle formation index (F)

Polymeric vesicle formation is governed by molecular weight, hydrophilicity and degree of hydrophobic substitution (Wang 2001a, 2001b, 2004). Vesicle formation index F can be computed using correlation

$$F \propto H / LDP \quad \text{----- Equation 8}$$

Where H represents Carboxyl sodium (mole %), L indicates mole % of substituted AEDOCA units, and DP is the square root of the degree of polymerization of the polymer Wang et.al. (2001a). presumed that vesicle formation is dependent on the

square root of the polymer chain length, expressed as the degree of polymerization. Incorporating the proportionality constant within the vesicle formation index yields

$$F' = H / LDP \quad \text{----- Equation 9}$$

F' is specific for the particular type of polymer backbone.

Vesicle formation index values calculated for Biloproteins varied in the range 0.068 to 0.8455 for P14K-A and 0.15 to 2.922 for P2K-A with decreasing DS from 60 to 10.

Table 3.4. Effect of molecular weight and DS on Vesicle formation index

Sr.No.	Polymer conjugate	Vesicle formation index (F')
1.	P2K-A10	2.922
2.	P2K-A20	1.047
3.	P2K-A40	0.34
4.	P2K-A60	0.15
5.	P14K-A10	0.8455
6.	P14K-A20	0.356
7.	P14K-A40	0.130
8.	P14K-A60	0.068

Results obtained with other techniques like fluorescence spectroscopy, TEM and light scattering studies and correlation of data with F' values indicated that at DS 40 and 60, P2K-A yield vesicles at 0.34 and 0.15 while P14K-A yield vesicles at 0.130 and 0.068 respectively. Thus for polyaspartate backbone with same AEDOCA hydrophobe content (DS), vesicle formation index (F') decreased with an increase in molecular weight.

3.3.4 Morphology and size

Particle size of aggregate was determined using light scattering technique. P2K-A10 to 40 exhibited size 154 to 142 nm, but at DS 60 size increased to 152 nm. (Table 3.5) In P14K-A10 to 40, size decreased from 234 to 148 nm but again increased to 213 nm for

DS 60. Thus Polymer conjugates exhibit size reduction on increase in DS till DS 40 which is consistent with the previous reports (Nichifor 1999, Yokoyama 1998, Yang 2003).

Table 3.5. Effect of molecular weight and DS on particle size, zeta potential and pH.

DS	Size (nm)	PD	ξ	pH
P2K-AEDOCA				
10%	154.7	0.298	-24.98	7.73
20%	142.5	0.208	-40.89	7.68
40%	142.4	0.333	-69.30	7.48
60%	151.9	0.304	-67.94	7.50
P14K-AEDOCA				
10%	234.3	0.198	-47.96	7.90
20%	163.1	0.272	-43.43	7.79
40%	147.7	0.319	-60.93	7.80
60%	212.5	0.185	-74.36	7.65

Further increase in DS to 60 caused size to increase again. This can be attributed to inability to incorporate more hydrophobes in the structure at high DS. DS exhibited same effect in both low and high molecular weight polymer conjugates. The effect of molecular weight was in agreement with earlier findings which reported increase in aggregate size with molecular weight (Wang 2001a, 2001b, 2004).

The particle size distribution was multimodal having polydispersity 0.198 - 0.333. This could be because of high polydispersity index of polymer backbone (PDI \approx 2) and tendency to form multiple aggregates by deoxycholate hydrophobe. Earlier reports suggested sodium deoxycholate micelle in 0.5M sodium chloride exhibited size of 7.4 nm, (D'alagni 1997) while size of these polymeric aggregates is in range 150 - 180 nm. This could be attributed to the formation of higher aggregates like large compound micelle or vesicles.

Morphological analysis by TEM confirmed findings of static light scattering experiments. At low DS, spongy and flower like interpenetrating structures were seen. As DS increased, structures became more compact and at high DS 40, a morphological transition from micelle to vesicle was observed. (Figure 3.11) With further increase in DS to 60, structures became even more compact demonstrating formation of unilamellar vesicles. DS has more pronounced effect than molecular weight on micelle to vesicle transition.

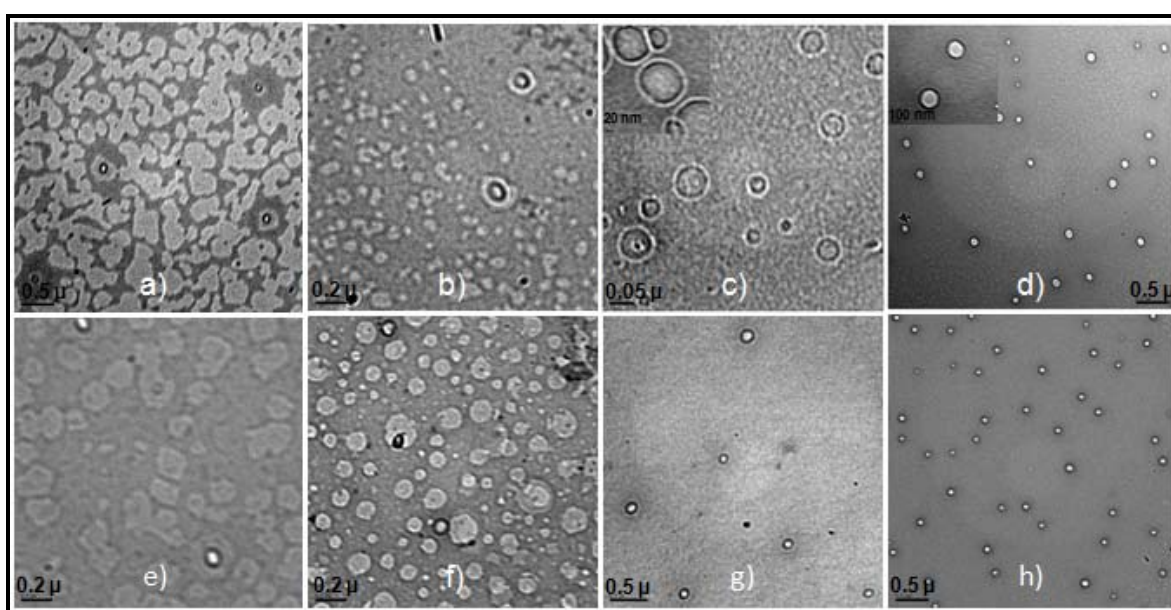


Figure 3.11. TEM images of P2K-A [a) DS 10, b) DS 20, c) DS 40, d) DS 60] and P14K-A [e) DS 10, f) DS 20, g) DS 40, h) DS 60] self aggregate with varying DS

Further investigation of vesicular structures of PASP2k – AEDOCA40 revealed a unilamellar vesicle of 110 nm size having 80 nm inner core and bilayer thickness of 15 nm. The compactness of vesicle bilayer increased with an increase in DS. The observed particle size by TEM was smaller than that obtained by static light scattering experiments. This was because in static light scattering, particles were in hydrated swollen state while in TEM samples were in dried shrunken state.

3.4 Conclusions

Deoxycholic acid was conjugated to polyaspartic acid using Amino ethyl Deoxycholamide (AEDOCA) through amide linkage. These amphiphilic polymer conjugates having DS 10 to 60 formed nanoaggregates in aqueous medium. Transition from loose micelle to vesicle like aggregate was clearly evident at and above DS 40. The critical aggregation concentrations of aggregates (CAC) were determined by fluorescence spectroscopy which indicated decrease in CAC with an increase in DS from 1.297 mg/ml to 3.65×10^{-2} to 2 mg/ml. Equilibrium binding constant revealed ability of aggregate to complex hydrophobic compounds. The size distribution of aggregates was poly disperse in the range 142-234 nm. Negatively charged aggregates had Polyaspartate shells, which exhibited zeta (ξ) potential of -25 to -64 mV. The polymeric micelles and vesicles described herein have been explored for the solubilization and toxicity reduction of hydrophobic drug Amphotericin B.

3.5 References

1. Akiyoshi K., Deguchi S., Moriguchi N., Yamaguchi S., Sunamoto J., *Macromolecules* 1993, 26, 3062.
2. Akiyoshi K., Deguchi S., Tajima H., Nishikawa T., Sunamoto J., *Macromolecules* 1997, 30, 857.
3. Alami E., Almgren M., Brown W., Francüois J., *Macromolecules* 1996, 29, 2229.
4. Besheer A., Hause G., Kressler J., Mader K., *Biomacromolecules* 2007, 8, 359.
5. Blanazs A., Armes S. P., Ryan A. J., *Macromol. Rapid. Comm.* 2009, 267.
6. Burke S., Eisenberg A., *High Perform. Polym.* 2000, 12, 535.
7. Cehelnik E. D., Cundall R. B., Lockwood J. R.; Palmer T. F. *The Journal of Physical Chemistry* 1975, 79, 14, 1369.
8. Chu D. Y., Thomas J. K., *Macromolecules*, 1987, 20, 2133.
9. D'alagni M., D'Archivio A. A., Galantini L., Giglio E., *Langmuir*, 1997, 13, 5811.

10. Discher D.E., Eisenberg A., *Science* 2002, 297, 967.
11. Hu Y., Kramer M. C., Boudreaux C. J., McCormick C. L., *Macromolecules* 1995, 28, 7100.
12. Jover A., Meijide F., Nunez E. R., Tato J. V., Mosquera M., *Langmuir* 1997, 13, 161.
13. Kang H. S., Yang S. R., Kim J. D., Han S.H., Chang I.S., *Langmuir* 2001, 17, 7501.
14. Kataoka K., Harada A., Nagasaki Y., *Advanced Drug Delivery Reviews* 2001, 47,113.
15. Kratochvil J. P., Hsu W. P., Kwok D. I., *Langmuir* 1986, 2, 256.
16. Kwon G. S., Okano T., *Adv. Drug Del. Rev.* 1996, 21,107.
17. Lee K. Y., Jo W. H., Kwon I. C., Kim Y., Jeong S. Y. *Macromolecules* 1998, 31, 378.
18. Martin C., Thongborisute J., Takeuchi H., Yamamoto H., Kawashima Y., Alpar H.O., *Int. J. Pharm.* 2005, 298, 339.
19. Martin C., Thongborisute J., Takeuchi H.; Yamamoto H.; Kawashima Y.; Alpar H.O., *Proc. Int. Symp. Cont. Rel. Bioact. Mater.* 2003, 31, 288.
20. Mohanty A., Dey J., *Langmuir* 2004, 20, 8452.
21. Morishima Y., Saegusa K., Kamachi M., *Macromolecules* 1995, 28, 1203.
22. Nakato T., Tomida M., Suwa M., Morishima Y., Kusuno A., Kakuchi T., *Polym. Bull.* 2000, 44, 385.
23. Nakato T., Yoshitake M., Matsubara K., Tomida M., Kakuchi T., *Macromolecules* 1998, 31, 2107.
24. Neri P., Antoni G., Benvenuti F., Cocoda F., Gazze G., *J. Med. Chem.* 1973, 16, 893.
25. New R. R. C., *Liposomes: A Practical Approach: Practical Approach Series*, Oxford University Press 1990.
26. Nichifor M., Lopes A., Carpov A., Melo E. *Macromolecules* 1999, 32, 7078.
27. Park K., Kim K., Kwon I. C., Kim S. K., Lee S., Lee D. Y., Byun Y. *Langmuir*, 2004, 20, 11726.

28. Pasparakis G., Krasnogor N., Cronin L., Davis B. G., Alexander C. *Chem. Soc. Rev.* 2010, 39, 286.
29. Roweton S., Huang S. J., Swift, G. J., *Environ. Polym. Degrad.* 1997, 5, 175.
30. Shinoda H., Asou Y., Suetsugu A., Tanaka K., *Macromol. Biosci.* 2003, 3, 34.
31. Suwa M., Hashidzume A., Morishima Y., Nakato T., Tomida M., *Macromolecules* 2000, 33, 7884.
32. Tabata K., Abe H., Doi Y., *Biomacromolecules* 2000, 1, 157.
33. Torchilin V. P., *Pharmaceutical Research* 2007, 24, 1.
34. Turro N. J., Yekta A., *J. Am. Chem. Soc.* 1978, 1, 5951.
35. Uchegbu I. F., Florence A.T., *Advances in Colloid and Interface Science*, 1995, 58, 1.
36. Wang W., McConaghy A. M., Tetley L., Uchegbu I. F., *Langmuir* 2001, 17, 631.
37. Wang W., Qu X., Gray A. I., Tetley L., Uchegbu I. F., *Macromolecules* 2004, 37, 9114.
38. Wang W., Tetley L., Uchegbu I., F., *J. Colloid and Interface Science* 2001, 237, 200.
39. Yamamoto H., Mizusaki M., Yoda K., Morishima Y., *Macromolecules* 1998, 31, 3588.
40. Yang S. R., Jeong J. H., Park K., Kim J. D., *Colloid Polym. Sci.* 2003, 281, 852.
41. Yokoyama M., Fukushima S., Uehara R., Okamoto K., Kataoka K., Sakurai Y., Okano T., *J. Controlled Rel.* 1998, 50, 79.
42. Zachariasse K. A., Kuhnle W., Wellaer A., *Chem. Phys. Lett.* 1980, 73, 1, 6.
43. Zhu X., Nichifor M., *Acc. Chem. Res.* 2002, 35, 539.

Chapter 4

Manipulating self assembly in synthetic biloprotein: role of hydrophilic functional substitution

4.1 Introduction

Molecular self assembly is an important strategy for designing nano structures. (Whitesides 2002, Service 2002, Chen 2005) Self assembly processes are manifest in nature in diverse forms and are responsible for the formation of complex biomembranes in bacteria, viruses and human cells. These involve amphiphilic biomacromolecules such as phospholipids, lipoproteins and polysaccharides which regulate fluidity, functionality and stability.(Zimmerberg 2006,Gallop Nature 2005, Zimmerberg 2006) It is intriguing that small differences in hydrophilicity of these biomacromolecules resulting from minor differences in chemical composition result in major microstructural modifications and morphologies which regulate their function in diverse biological processes. (Iozzo 2000, Nelson 2004, Montreuil 1995, Griel 1969) Self assembly in peptides, lipids and polysaccharides in lipoproteins, glycoproteins, lipoglycoproteins yields supramolecular structures responsible for recognition in receptors, enzyme activity, interaction motif in uptake and transport (Wasan 2008, Gutteridge 2005, Ross 2004).

Self assembly is a result of co-operative interplay between three effects: (i) alteration of hydrogen-bonding in water by sequestration of non-polar side chains (ii) replacement of bonds made in the unfolded state with the solvent by the formation of hydrogen bonds within secondary structure; and (iii) extensive van der Waals interactions between atoms (Worrall 2007). Any imbalance in cooperative interplay leads to alteration in protein structure. Chemical alterations of protein side chains and main-chain peptide-bond incorporate new functionalities in addition to those already present in the side chains of the proteins leading to a set of changes referred as the posttranslational modifications. These result in new conformations, morphologies and functions such as new recognition patterns for partner molecules, switching of enzyme activity, control of lifetime and location of proteins in cells.

The enabling chemistries include phosphorylation, glycation, methylation, acetylation, hydroxylation and ubiquitination etc (Walsh 2006). The post translational modification is a result of actions of enzymes and small molecules on proteins at particular sites which if misplaced leads to malfunction. Nonenzymatic

glycation of skeletal muscle myosin has a significant effect on both the structural and functional properties of the protein leading to impairment in muscle function associated with aging and diabetes (Brownlee 1995). Phosphorylation on the first microtubule-binding repeat domain of tau protein (R1) determines its aggregation dynamics. Fibrils formed by R1 are long and smooth while fibrils formed by Ser 262 phosphorylated R1 (pR1) are short. The later causes extracellular amyloid plaques and the intracellular neurofibrillary tangles (NFTs) leading to Alzheimer's disease. In murine estrogen receptor β (mER- β) site, O phosphorylation imparts more flexibility to the active site region while O-GlcNAcylation promotes type II β turns. Thus functionalization of particular site influences performance and morphology of self assembled protein. Proteins rich in glutamine and asparagine aggregate into a self-propagating, fibrillar protein aggregate known as amyloid structures due to β pleated sheets structure rich in hydrogen bonds.(Nelson 2005, Weichenberger 2006) These are considered to be responsible for neurological disorders such as Huntington's, Alzheimer's and Parkinson's diseases. (Perutz 1994, Perutz 1999, Perutz 2001)

To simulate nature in self assembly for achieving diverse morphologies, different architectural approaches have been explored like block copolymers, graft copolymers, dendrimers, cyclic structures and hyperbranched polymers, highlighting importance of type block segments, molecular weight of block segments, graft type, degree of grafting, type of branching unit and degree of branching etc. (Zhang 1995, Azzam 2006, Lim 2009, Wang 2005, Persec 1998, Yan 2004) Highly asymmetric amphiphilic block copolymers can self assemble in selective solvents to form crew-cut aggregates of a wide range of morphologies, such as spherical micelles, rods, vesicles, and others. In these aggregates, the long hydrophobic block forms either the core in micelles and rods, or the wall in bilayer structures, whereas the short hydrophilic block forms the corona. (Zhang 1995, Zhang 1996)

In comparison reports of graft copolymers forming diverse morphologies are few, even though they offer versatility towards functional modification, simple and economical synthesis. Synthesis and self-assembly of graft copolymer focus on the traditional comb-shaped or brush-shaped graft copolymer composed of longer main

chain as backbone with shorter side chains as graft segments leading to inter or intramolecular association favoring spherical micelle formation. This creates an impression that morphological diversity cannot be achieved through graft copolymers unlike block counterpart. However an insightful designing of structure of amphiphilic graft copolymer might help in decreasing the above mentioned influence yielding abundant morphologies like micelle, vesicle, rod, tubules etc.

Recently wang et.al highlighted importance of designing architecture in synthesis of chitosan-g-PCL, using short rigid chitosan backbone for grafting flexible hydrophobic PCL imparting varied graft hydrophobicity yielding different morphologies from micelle to fibres. (Wang 2005)

Polyaspartic acid has been used in its imide form i.e. Polysuccinimide which is highly reactive towards amine substitution. Polyaspartic acid is synthetic polypeptide which is biodegradable, biocompatible and easy to synthesize. (Roweton 1997, Tabata 2000, Shinoda 2003) Herein we prepared conjugates of Polysuccinimide with an amine analogue of Deoxycholic acid (Amino ethyl Deoxycholamide) a well known bile acid from bile in human intestine. Earlier reports indicated that the incorporation of bulky steroidal compound like cholesterol was necessary to either form or stabilize vesicles, highlighting the importance of steroidal molecules in bilayer formation (Wang 2001, 2004). Cholesterol has been extensively used in liposome and noisome preparations Polymer conjugates are with very reactive imide groups making them versatile in functional group modification. The said conjugates on reaction with different bases like sodium hydroxide, amino ethanol, ammonia and hydrazine yielded “synthetic biloproteins” with charge or hydrophilicity tuned exclusively as per need. The prepared conjugates are referred as “synthetic biloproteins” as they are composed of bile acid and peptide which on dispersion in water attained different 3D structures like protein in nature. This is first attempt in a way that on the same backbone with same hydrophobic substitution, different functionalities can be achieved. The said functionalities seem to exert different magnitude of forces like hydrogen bonding, charge interactions along with hydrophobic interactions in self assemblies in an aqueous medium leading to diverse morphologies like micelle, vesicle, tubule and compact nanoparticles. Thus

amphiphilicity, architecture and the shape of the building units when tuned appropriately influenced the self-assembly behaviour. The most interesting aspect of this approach is once a bulk of polymer conjugate is prepared diverse synthetic biloproteins can be obtained by reaction with functionality bearing amine. Thus diverse functional synthetic biloproteins can be achieved in one step keeping its hydrophobic components constant.

In this chapter synthesis and characterization of different functionalized biloproteins has been achieved. The self assemblies were characterized adequately to demonstrate the role of size of head group in governing different interactions which guided morphologies in addition to hydrophilic and hydrophobic content. Different possible models have been suggested to explain this phenomenon of hydrophilic functionality driven self assembly.

4.2 Experimental

4.2.1 Materials

L- aspartic acid, Deoxycholic acid, Pyrene, Diphenyl hexatriene (DPH), Dicyclohexyl carbodidimide (DCC) [Aldrich], Amino ethanol, Ammonia, Hydrazine hydrate, Dry Methanol, N hydroxy succinimide (NHS), Cetyl pyridinium chloride (CPC) [SD fine India], Ethylene diamine (SRL, India), o-Phosphoric acid (85%), Hydrochloric acid, Sodium hydroxide, Acetone, Dimethyl formamide (DMF) [Merck, India] dried and stored on molecular sieves.

4.2.2 Synthesis of polymer backbone polysuccinimide (PSI)

PSI was synthesized using o-Phosphoric acid as catalyst by melt polycondensation method as discussed in chapter 3.

4.2.3 Synthesis of hydrophobe AEDOCA

AEDOCA was synthesized from Deoxycholic acid and excess of ethylene diamine through NHS ester intermediate as described in chapter 3.

4.2.4 Synthesis of reactive polymer conjugates

Reactive polymer conjugates were prepared by stirring AEDOCA with PSI in dry DMF at 70 °C for 24 hrs and recovered and purified as described in chapter 3.

4.2.5 Hydrophilic functionalization of reactive polymer conjugate

Reactive AEDOCA polymer conjugates of different DS were dissolved in dry DMF and each DS sample solution was divided into 4 portions and chilled to 5 - 10 °C. Different functionalizing agents like amino ethanol, ammonia, hydrazine were diluted with dry DMF and added to each of three portions and stirred overnight at RT then dialyzed against deionized water for 48 hrs using spectrapor 2K dialysis bags. For carboxylate functionalization, reactive polymer conjugate DMF solution was added to chilled aqueous sodium hydroxide solution and stirred for 3 hrs till clarity and dialyzed as mentioned above for other functionalities. Thus all the functionalized biloproteins were prepared in one step at the same time. Biloprotein self assemblies were recovered by freeze drying and stored at RT in desiccators.

Re-dispersion of freeze dried self assemblies was achieved by simple sonication of functionalized biloprotein in water using bath sonicator for 5-10 minutes. Clear transparent samples were filtered to remove dust while larger aggregate samples were used as such. Samples with higher particle size were visualized using optical or confocal microscopy while transparent samples were imaged by TEM.

4.2.6 Preparation of self assemblies

Different self assemblies were prepared by simple dispersion of functionalized biloprotein in water using bath sonicator for 5-10 minutes. Clear transparent samples were filtered to remove dust while samples with larger particle size were used as such. Samples with higher particle size were visualized using optical or confocal microscopy while transparent samples were imaged by TEM.

4.2.7 Characterization of self assemblies

Biloprotein self assemblies were characterized by Dynamic light scattering studies, Zeta Potential measurements, Differential scanning calorimetry (DSC), Transmission electron microscopy and Turbidity measurements

4.2.7.1. Static light scattering / Particle size determination

The static light scattering (SLS) measurements were performed using a Brookhaven Instruments corporation UK 90 Plus particle size analyzer. The scattering intensity was measured at 90 °. Polymer aggregate solutions were prepared in double distilled water. The solution was filtered through a Pall Gellman PES syringe filter (0.45 μ) directly into the scattering cell. Prior to the measurements, the scattering cell was rinsed thrice with the filtered solution. The particle size measurements were carried out at room temperature in triplicate.

4.2.7.2. Turbidity measurements

Samples of polymer aggregates were checked for turbidity using UV spectrophotometer at 500 nm. Different samples were analyzed at 2 mg/ml for comparing change in aggregation and its effect on turbidity of solution.

4.2.7.3. Zeta potential measurements

Samples of polymer aggregate solution were prepared at 2 mg/ml and probe was dipped in sample to apply potential. Electric field of 7.0 V/cm was applied across 2 electrodes and with inputs of pH and particle size, zeta potential was determined. For each measurement 5 runs were averaged with each run employing 10 cycles for 3 minutes. For analyzing data Zeta pals software of Brookhaven instruments was used.

4.2.7.4. Fluorescence spectroscopy

Steady-state fluorescence experiments were carried out with Edinburgh luminescence spectrometer. Using Pyrene as a hydrophobic fluorescent probe, critical aggregation concentration (CAC) of polymer conjugates were deduced from the results. Plot of log C vs I_1 / I_3 yield sigmoidal curve to which 2 tangents

intersection point yielded CAC value. For microviscosity experiments, Edinburgh luminescence spectrometer equipped with filter polarizers with L-format configuration was used for fluorescence depolarization measurements of DPH using a 1 cm² quartz cuvette.

4.2.7.5. Surface tension measurements

A stock solution of polymer conjugate (0.8 mg/ml) was prepared in Milli-Q water (18.2 M Ω). 25 ml of this solution was transferred to a beaker and surface tension was measured by Wilhelmy plate. For each measurement, at least three readings were taken and the mean γ (mN/m) value was recorded. Before each experiment, the instrument was calibrated and checked by measuring the surface tension of distilled water. Before every experiment Platinum plate was cleaned with deionized water and activated on gas burner to remove any adsorbed contaminant.

4.2.7.6. TEM of aggregate

The morphology of nanoaggregates was studied using a high resolution transmission electron microscopy (HR-TEM) at 300 kV with Technai- FEI machine. A drop of self-aggregates solution (2 mg/ml) was placed on a copper grid coated with a carbon and polymer film. The grid was held horizontally for 5 minutes to allow the aggregates to settle and then blotted with tissue paper from one edge point to allow the excess fluid to drain. Grid was then allowed to dry in air and stored in desiccator before visualization.

4.3 Results and discussion

Block and graft copolymers, dendrimers, cyclic and hyperbranched polymers, have been explored for designing of self assemblies of different shape and size. The influence of type and molecular weight of block segments, graft type and frequency etc has been investigated (Zhang 1995, Azzam 2006, Lim 2009, Wang 2005). In synthetic polymers, structural regulation of self assemblies exploiting amphiphilic and charge interactions has been explored in great detail (Zhang 1995, Azzam 2006, Lim 2009, Wang 2005, Persec 1998, Yan 2004, Wang 2008). However, the role of

functional groups in governing these interactions and hence the morphology has not been clearly brought out.

In this work to bring out role of different functional groups present in nature we conjugated polysuccinimide, a reactive analogue of polyaspartic acid with Amino ethyl Deoxycholamide, an amine derivative of Deoxycholic acid.

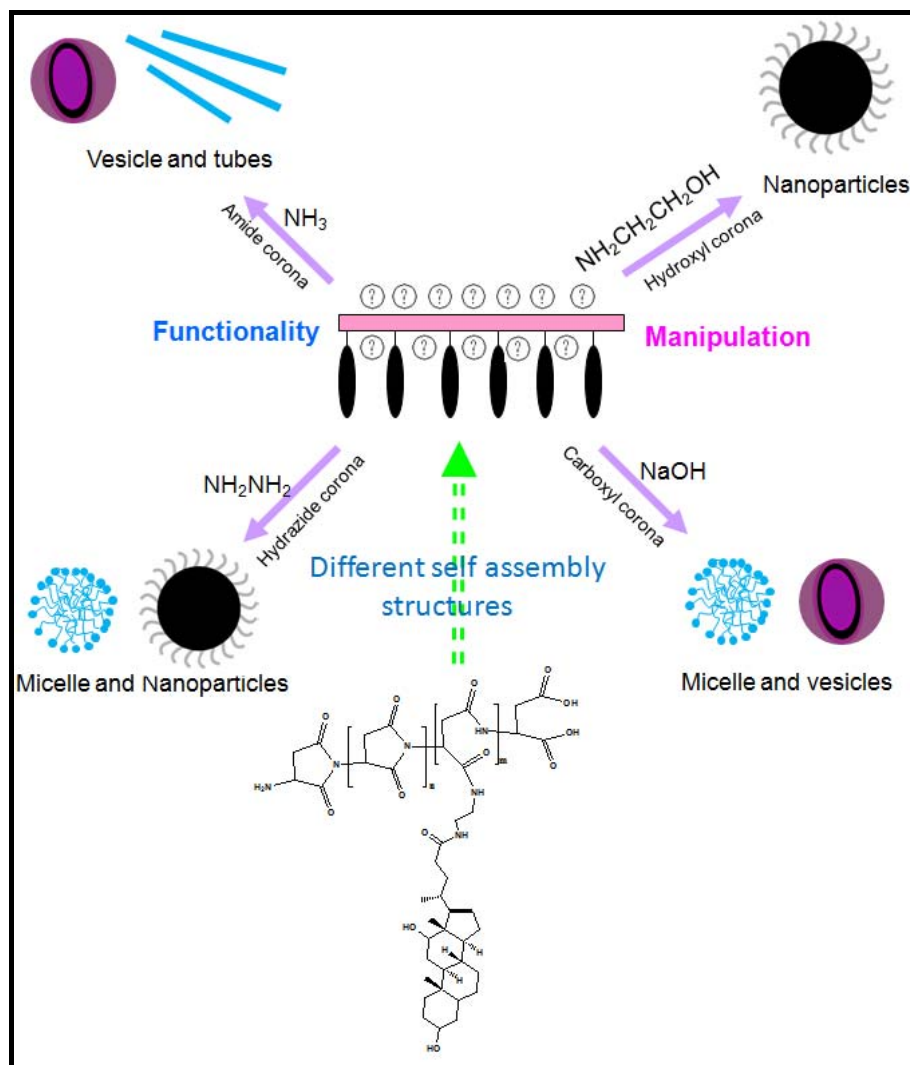


Figure 4.1. Schematic representation of functional manipulation of polymer conjugate guiding self assembly

Amine functionality was necessary for conjugation with polysuccinimide, and also acted as a spacer between the steroidal nucleus and polymer backbone.

Incorporation of bulky steroidal moiety like cholesterol assists in forming and / or stabilizing vesicles (New 1990, Uchegbu 1995, Wang 2004).

The conjugates on incubation with different bases like sodium hydroxide, amino ethanol, ammonia and hydrazine yielded “synthetic biloproteins” composed of bile acid and peptide backbone. This step in a way mimics post translational modification of proteins. The functionalities aid in secondary valence interactions like hydrogen bonding, charge interactions in addition to hydrophobic interactions during formation of self assemblies in an aqueous medium leading to micelles, vesicles, tubules and compact nanospheres as shown in Scheme 1.

4.3.1 ^1H NMR spectroscopy

The degree of substitution (DS) of AEDOCA was determined from ratio of the intensity of protons in hydrophobic region [18- CH_3 , (0.71 δ)] to methine proton in PSI at 5.2 δ . (Table 4.1, Figure 4.2)

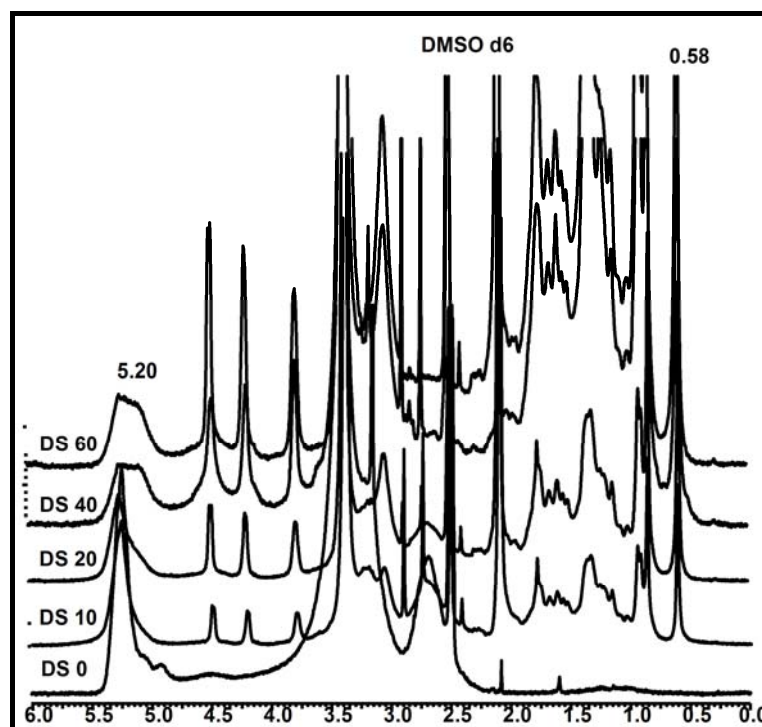


Figure 4.2. ^1H NMR spectrum of PSI and PSI-AEDOCA (DS 10-60) in $\text{DMSO } d_6$.

Formation of self assembly in aqueous medium was confirmed by the observed decrease in peak intensity of protons in the hydrophobic region i.e. 18- CH₃ (0.71 δ) by ¹H NMR studies in D₂O. (Figure 4.3)

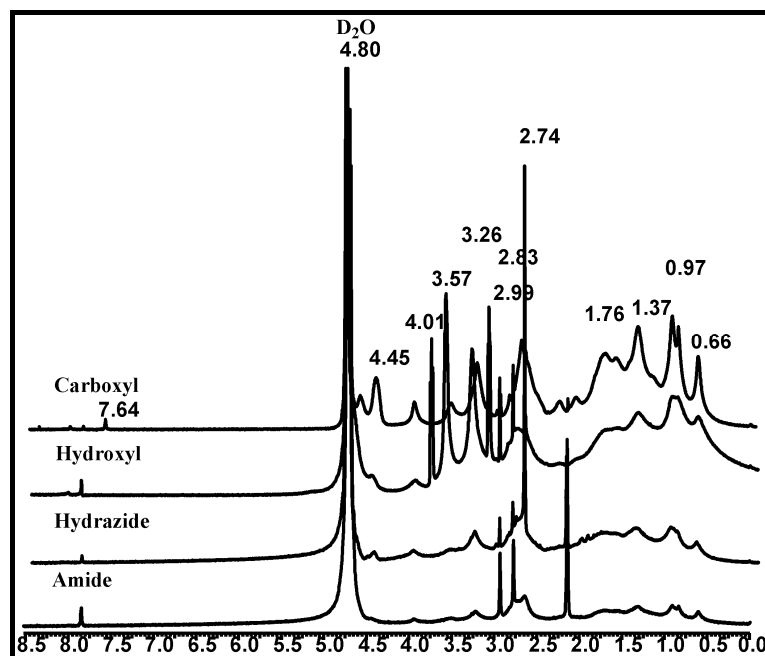


Figure 4.3. ¹H NMR of synthetic biloproteins (60 mole% functionalized) in D₂O.

The intensity of protons in hydrophobic region [18- CH₃, (0.71 δ)] showed that the degree of compactness inside self assembly decreased in the order Amide > Hydrazide > Hydroxyl > Carboxylate.

Table 4.1. Characterization of PSI – AEDOCA conjugate by ¹H NMR in DMSO d₆.

Sample	AEDOCA in feed (mole %)	AEDOCA conjugated (mole %)
DS10	10	09
DS20	20	19
DS40	40	39
DS60	60	55

4.3.2 IR spectroscopy

The IR spectra of biloproteins indicate bands of Amide III, Amide II and Amide I at 1200, 1445, 1655 cm^{-1} respectively (Figure 4.4). In all cases peak at 620 cm^{-1} was observed which corresponds to amide V representative of α helix. Peak at 1250 cm^{-1} for amide III indicated unordered or α helix structure (Saudek 1982). The peak at 1591 cm^{-1} for ionized COO^- was present only in carboxylated biloprotein and absent in all others. This confirmed complete functionalization of polyaspartic acid amino ethyl deoxycholamide by the respective reagent.

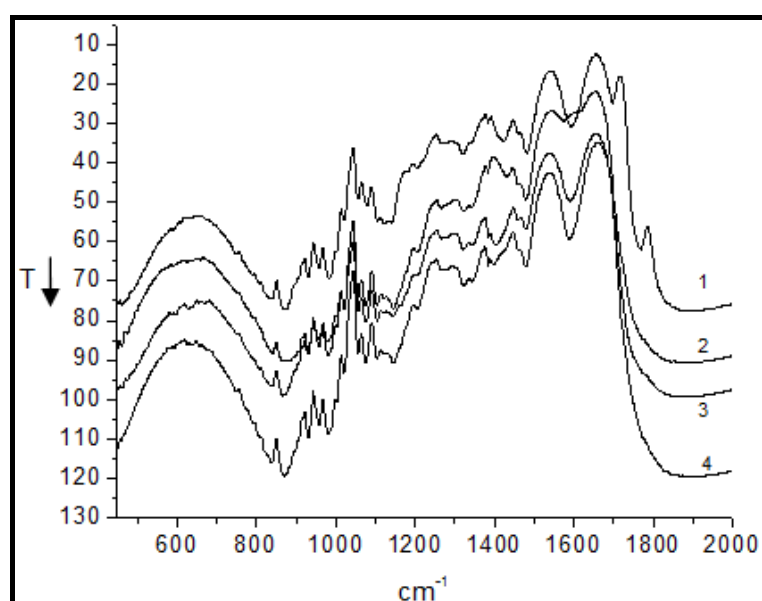


Figure 4.4. IR spectra of polymer conjugate with 60 mole% functionalized biloproteins 1) Hydroxyl, 2) Carboxylate, 3) Hydrazide and 4) Amide

All polymer conjugates displayed maximum at 3310 cm^{-1} indicative of hydrogen bonding between $\text{OH} \cdots \text{OH}$, $\text{OH} \cdots \text{COOH}$, $\text{OH} \cdots \text{CO}$, $\text{CONH}_2 \cdots \text{CO}$ and $\text{CONH}_2 \cdots \text{OH}$ groups. Hydrogen bonding in the hydrophobic bile acid has also been reported to exhibit maxima at 3310 cm^{-1} . (Mohanty 2004)

4.3.3 Circular dichroism (CD) spectroscopy

CD spectra for all synthetic biloproteins were very weak in intensity with absence of helix, pleated or random folding patterns as expected for polyaspartic acid in ionized form (Saudek 1982, Lamcharfi 1997). (Figure 4.5) Deoxycholic acid has been

reported to form micellar aggregates, which exhibit rotational ability in circular dichroism studies. The contribution of Deoxycholic acid unit to overall biloprotein ellipticity seems to be practically negligible due to unavailability of carboxylate group which has now been utilized for conjugation (Campanelli 1989, D'alagni 1997).

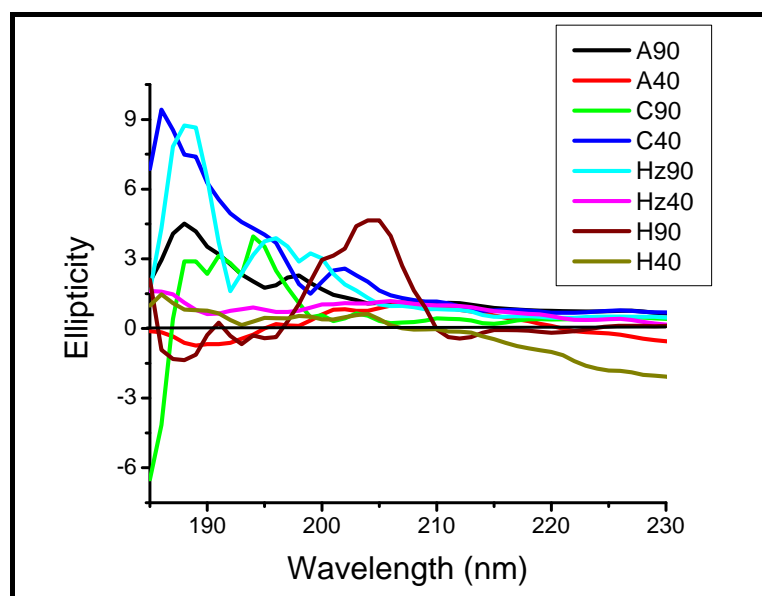


Figure 4.5. Circular dichroism spectra of functionalized biloproteins.

The origin of self assembled microstructures in the present case is thus different from that in case of peptide based block copolymers and amphiphiles which exhibited high circular dichroism (Checot 2001, Yan 2007, Matsuura 2005).

4.3.4 DSC studies

The DSC melting endotherms of biloprotein solutions (Figure 4.6) reveal the presence of both bound and free water (Samuni 1998, Saito 1996). Functionalities hydrate biloprotein to different extents because of differences in polarity and follow the trend Carboxylate > Hydroxyl > Amide \geq Hydrazide. This has implications in guiding self assembly are discussed later.

When these solutions are heated from 20 ° C to 80 ° C, phase transition temperatures were observed due to mobility in self assembled structures. Amide functional biloproteins (60 mole %) exhibited drastic change in heat flow in range 40 - 60 ° C

indicating phase transition of ordered structures analogous to structural reassemblies and increased fluidity as observed in liposomes. (Malcolmson, 1997, Torchilin, 2003, Taylor 1995) In carboxylated biloproteins (60 mole %), peaks at 35 °C and 65 °C indicated pre transition and main transition respectively. (Figure 4.7)

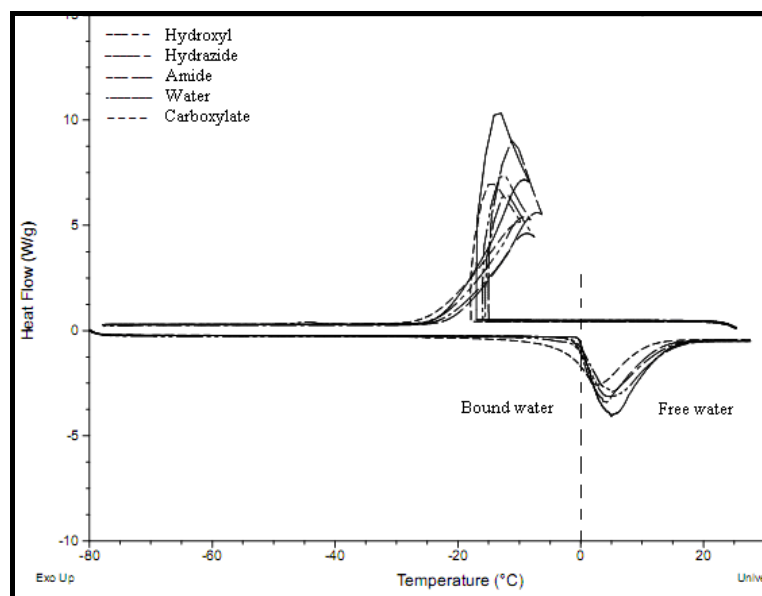


Figure 4.6. DSC endotherms of 40 mole% functionalized Biloprotein solutions.

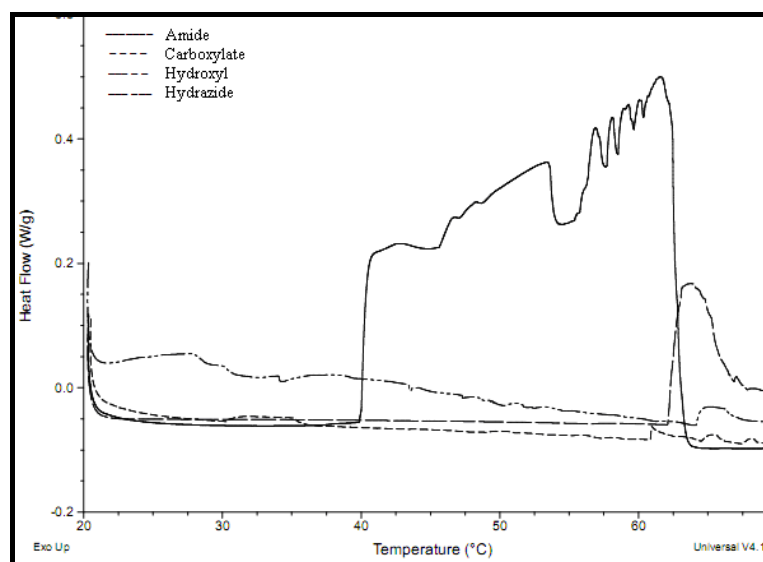


Figure 4.7. DSC endotherms of 40 mole% functionalized Biloprotein solutions.

For other biloproteins weak peak at 64 - 65 °C indicated small changes in compact structures suggestive of nanoparticles. (Figure 4.7)

4.3.5 Fluorescence spectroscopy

Hydrophobicity in the biloprotein self assembly was further probed by fluorescence spectroscopy using Pyrene. A red-shift in Pyrene (0, 0) band from 335.5 nm to 339 nm was observed with increasing biloprotein concentration. The ratio of intensity of the signals at 373 nm and 385 nm (I_1 / I_3) remained constant at about 2.22 when Pyrene was dissolved in water. In contrast when the biloprotein was added to the aqueous solutions, the intensity ratio decreased to 0.9 - 1.1 indicating transfer of Pyrene from aqueous to hydrophobic environment of biloprotein self assemblies.

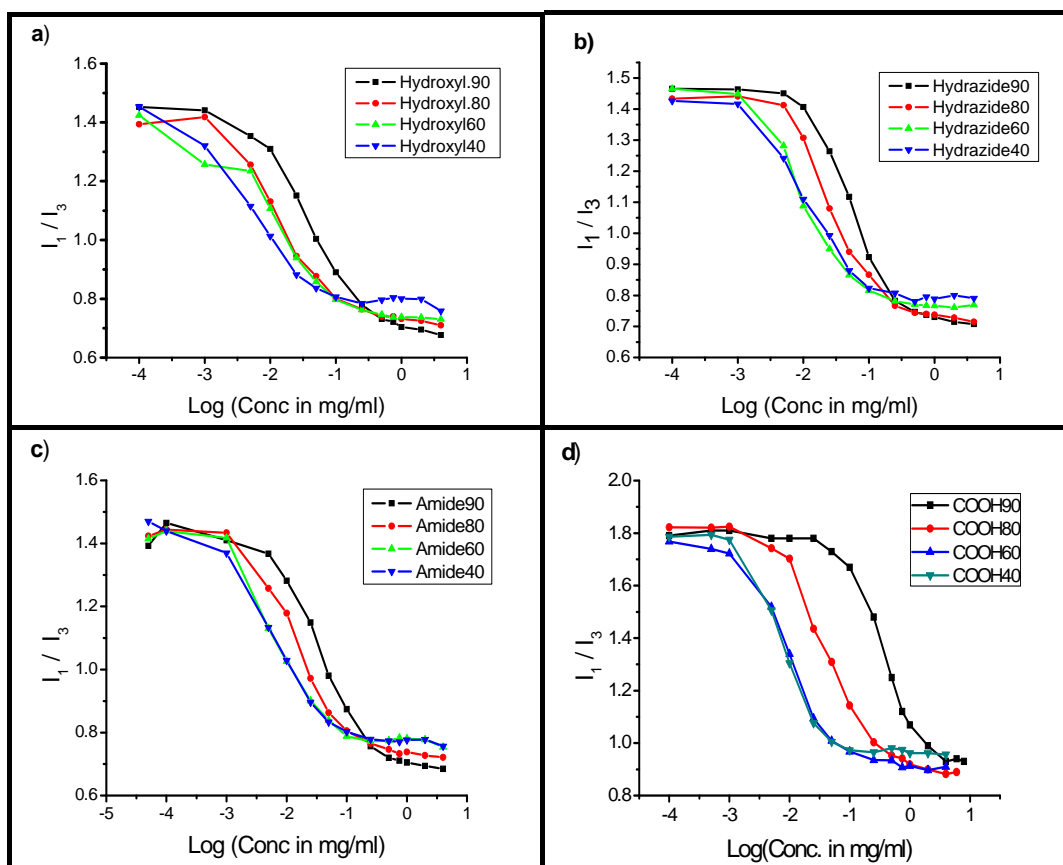


Figure 4.8. CAC determination of functionalized biloproteins: a) Hydroxyl, b) Hydrazide, c) Amide, d) carboxylate.

The importance of functionality and extent of functionalization in self assembly is evident from CAC values determined using fluorescence spectroscopy (Table 4.2). Thus for polyaspartic acid bile acid conjugate, CAC can be tuned by the extent and choice of hydrophilic functionality. (Figure 4.8)

Surface tension measurements (Wilhelmy Plate method) of all biloproteins indicated surfactant activity. (Table 4.3)

Table 4.2. Effect of type and extent of functionalization on CAC, Microviscosity and morphology

Sample	Self assembly #	CAC (mg/ml)	Micro viscosity
C90	LM	1.297	0.201
C80	M	0.257	0.206
C60	V	0.042	0.218
C40	V	0.037	0.219
A90	V	0.184	0.209
A80	V	0.069	0.228
A60	T	0.053	*
A40	T	0.049	*
Hz90	M	0.205	0.181
Hz80	M	0.113	0.216
Hz60	N	0.090	0.235
Hz40	N	0.059	0.266
H90	CM	0.196	0.229
H80	M	0.069	0.220
H60	N	0.057	0.254
H40	N	0.040	*

(C- Carboxylate, - Amide, Hz - Hydrazide, H- Hydroxyl group) (M = Micelle, V= Vesicle, T = Tubule, LM = Loose micelle, CM = compound micelle, N = Nanospheres) (* Indicate samples could not be analyzed due to high turbidity) (# Based on TEM data)

The microviscosity of self assembled structures was determined by measuring molecular anisotropy of Diphenyl hexatriene (DPH). (Cehelnik 1975) Anisotropy values of DPH in biloproteins indicate rigidity at molecular level inside self assembly, which in turn suggest type of self assembly. (Table 4.2) In biloproteins, as the degree of functionalization was increased from 40 to 90 mole %, anisotropy values decreased. The lower anisotropy values at higher degree of functionalization were due to the decrease in packing of AEODCA units suggestive of micellar structure, while higher anisotropy values indicated compact nanoparticles. Intermediate values suggested bilayered vesicular or tubular structures (Mohanty 2005).

Table 4.3. $f_{\text{hydrophilic}}$, surface tension, size and ξ of functionalized biloproteins

Sample	$f_{\text{hydrophilic}}$ (%)	Surface tension (γ)	Effective diameter (nm)	Poly- dispersity	Zeta pot. ξ
C90	77.70	46.72 \pm 1.50	298	0.282	-53
C80	55.54	46.60 \pm 0.63	242	0.281	-68
C60	28.86	45.56 \pm 1.70	245	0.279	-64
C40	15.26	48.15 \pm 0.66	306	0.298	-64
A90	74.33	47.45 \pm 1.57	291	0.297	-65
A80	50.93	46.90 \pm 0.72	211	0.310	-61
A60	25.21	48.85 \pm 2.47	331	0.296	-50
A40	13.01	51.08 \pm 2.30	482	0.216	-42
Hz90	76.63	42.57 \pm 0.20	161	0.314	-50
Hz80	54.04	44.37 \pm 0.87	194	0.355	-55
Hz60	27.63	42.48 \pm 0.94	128	0.346	-71
Hz40	14.49	41.41 \pm 1.23	337	0.280	-54
H90	80.09	44.31 \pm 0.96	183	0.296	-26
H80	59.05	45.50 \pm 0.76	210	0.323	-34
H60	31.89	46.44 \pm 2.40	198	0.265	-40
H40	17.21	52.87 \pm 0.87	450	0.182	-33

4.3.6 Static light scattering studies

Sodium deoxycholate formed micelles in 0.5 M sodium chloride of size 7.4 nm. (Campanelli 1989, D'alagni 1997) however static light scattering studies of functionalized biloproteins indicated size 183 to 482 nm, which indicated possible higher aggregate structures. (Table 4.3)

The overall particle size distribution was multimodal in nature and exhibited high polydispersity (0.182-0.346). This can be attributed to high polydispersity index of the polymer backbone ($PDI \approx 2$). All the biloproteins exhibited high negative zeta potential indicating stability (Table 4.3).

4.3.7 Microscopic investigations

The optical microscopy studies of biloprotein self assemblies bearing amide corona at 2 mg/ml concentration in an aqueous medium indicated tubular structure as shown in Figure 4.9. Tubules seem to be open at both ends.

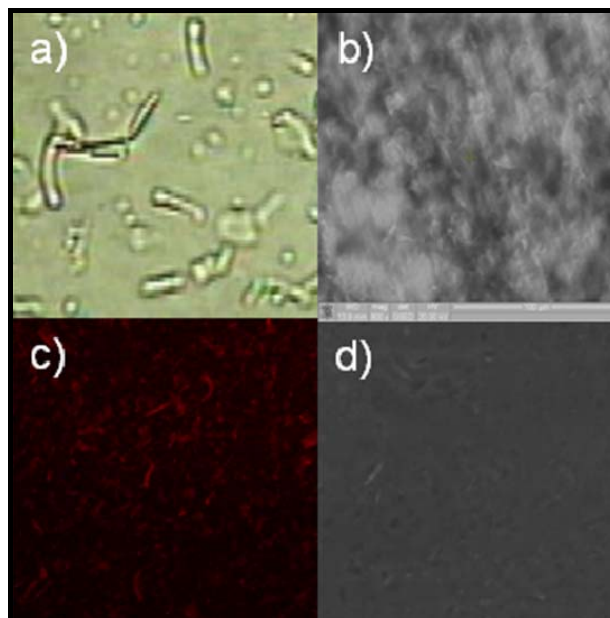


Figure 4.9. Optical image of tubular structures of A40 at 50X (a); ESEM image of A40 in water (b); Confocal image of A40 at 40X using Rhodamine as hydrophilic marker (c); Phase contrast image at 40X(d)

ESEM imaging of A40 in water indicated tubular structures supporting findings of optical microscopy. Characterization by confocal microscopy using Rhodamine as hydrophilic fluorescent marker indicated presence of hollow tubules. Phase contrast imaging further confirmed the findings.

Other biloproteins formed self assemblies in nanometre range and were probed using transmission electron microscopy. (Figure 4.10)

- (1) “Neutral biloproteins” containing 90 to 80 mole % amides yielded vesicles (Figure 4.10 m, n) of size 170 - 200 nm of bilayer thickness 30 - 40 nm and 100 – 120 nm aqueous core. Tubular structures resulted at 60 and 40 mole % amide content (Figure 4.10 o, p). The Average external diameter of the tubules was 80 nm .This is greater than values for monomeric Lithocholic tubules (52 nm) in alkaline solution, but smaller than the value (450 nm) reported for Cholic acid derivative (Terech 2002, Tellini 2007). Biloprotein tube lengths were as large as 1.4 - 2 μ . Some tubules were single-walled, while most others were double walled indicating bilayer formation. The collapse or shrinkage of the tubule could result in compartmentalization. Double walled tubules displayed outer and inner diameter of 80 nm and 68 nm respectively, indicating bilayer thickness of 12 nm. Larger diameter tubules exhibited greater contrast than the smaller diameter tubules while two superimposed tubes also exhibited high contrast confirming above hypothesis (Coldren 2003).
- (2) Loose micelles were observed when hydroxyl groups were conjugated at 90 and 80 mole % (“Neutral biloprotein”) (Figure 4.10 i , j). Compact nanoparticles were observed at 60 and 40 mole % hydroxylation (Figure 4.10 k, l). The micelle size ranged between 100 nm and 1 μ .. Honeycomb type aggregates were observed at 90% hydroxylation (Figure 4.10 m).
- (3) “Basic biloproteins” containing weakly basic hydrazide groups formed micelles having either loose or highly compact core depending upon hydrazide content. The particle size distribution was highly polydispersed and the size varied between 100 nm to 5 μ (Figure 4.10 e, f, g, h).

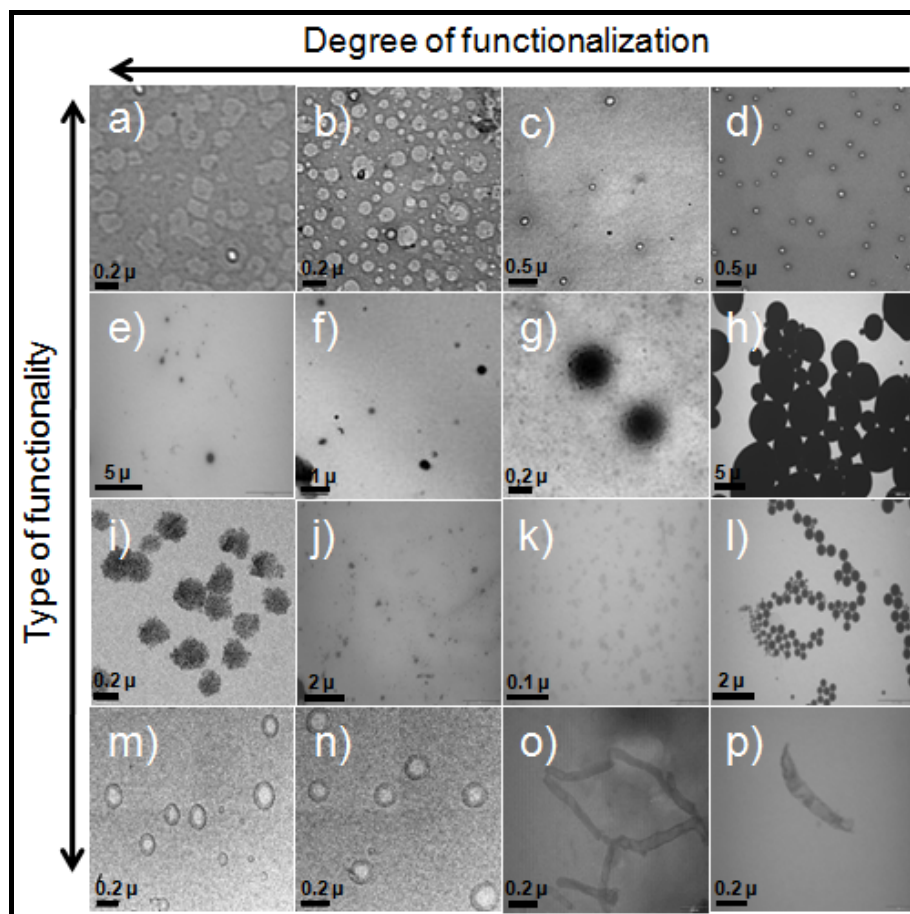


Figure 4.10. TEM images of functionalized biloproteins (90 to 40 mole %): a-d Carboxylate; e-h Hydrazide; i-l Hydroxyl; m-p Amide.

(4) “Anionic biloproteins” had carboxylate groups which repelled each other leading to core segregation and corona formation yielding micellar structures. Repulsion of few ionized carboxyl groups present in core would yield loose core, and aggregates 200 to 300 nm in size. (Figure 4.10 a, b) hydrophobic interactions dominated over carboxyl repulsion at lower carboxyl content, leading to compact 120 nm vesicles having 80 nm aqueous core and 20 nm bilayer thickness. (Figure 4.10 c, d)

4.3.8 Mechanism of self assembly

The amphiphilicity factor $f_{\text{hydrophilic}}$ (Discher 2002) used to rationalize aggregation behaviour of block copolymers, could not predict the morphologies of functionalized biloproteins, just as it was found inadequate in the case of hyper

branched multi armed (HBPO - star PEO) copolymer (Yan 2004) (Table 4.3). This is because in addition to gross hydrophilicity, the interactions of the hydrophilic functional groups and the bile acid bilayer guided the morphology of the aggregates.

The morphologies of the polymer aggregates are governed by the membrane curvature. Low curvature favours vesicle formation, high curvature favours tubules, while core segregation results in micelles (Wang 2008). AEDOCA conjugated functionalized polyaspartamide consists of three regions; 1) hydrophobic steroidal nucleus, 2) linear flexible aliphatic spacer chain through which the bile acid is conjugated, 3) Aspartamide backbone repeat unit to which a hydrophilic functional group is conjugated. Thus the structure incorporates both rigid and flexible components. (Figure 4.11)

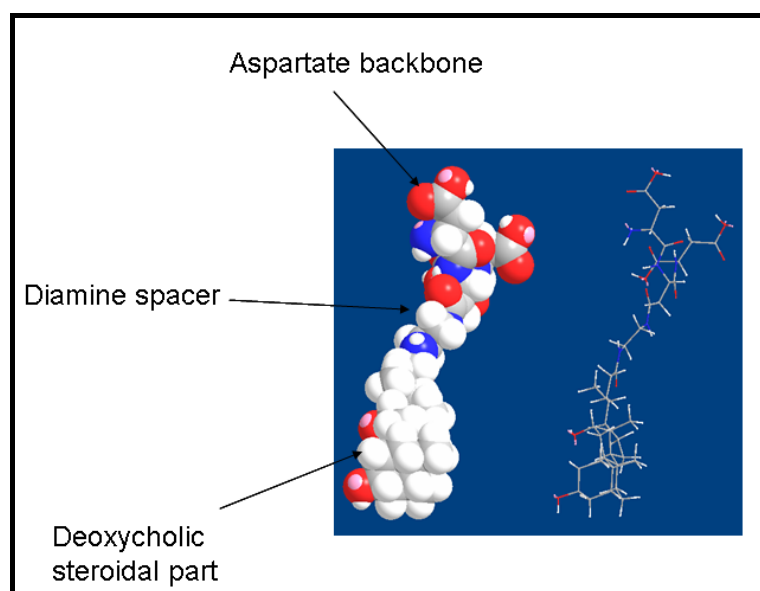


Figure 4.11. Structure of AEDOCA conjugated to Aspartic acid trimer as representative backbone.

The bile acids have a hydrophobic β side and a hydrophilic α side. They are known to form micelles, particulates and gels. Earlier reports showed that in the case of deoxycholic acid a right handed helical tape results from the OH (12) group on the right side and intermolecular hydrogen bonds between OH(3) and OH (2) groups (Kato 2004). The fit of COOH (24) between OH (3) and OH (12) of its own tape and the neighboring tape creates a chiral sheet which has a hydrophobic exterior and

hydrophilic interior. The van der Waal forces bring about the stacking of the hydrophobic surface producing bilayer crystals. Amidation of the Deoxycholic acid also produced a helical network. In biloproteins, AEDOCA units are conjugated to the polyaspartate which restrains mobility observed in monomeric amide derivative of Deoxycholic acid (Sada 1995). Biloproteins lack the crystallinity observed in their monomeric counterparts, stacking favors bilayer formation. In our case, incorporation of amide linked ethyl spacer favors hydrogen bonding between NH---NH, NH---CO, NH---OH sites present in AEDOCA units which were observed at 3310 cm^{-1} in IR spectra. Thus hydrophobic interactions are reinforced by hydrogen bonding, favoring lamellae formation. Similar findings of steroidal nucleus stacking led vesicles and tubules formation were reported in adamantyl or p – tert-butylphenyl group modified β aminated cholic acid (Tellini 2006, 2007).

The self assembly of the surfactant peptides containing aspartic acids at the C terminus and hydrophobic amino acid sequences with acetylated N terminus was correlated with the effect of head group on the packing parameter (Vauthey 2002).

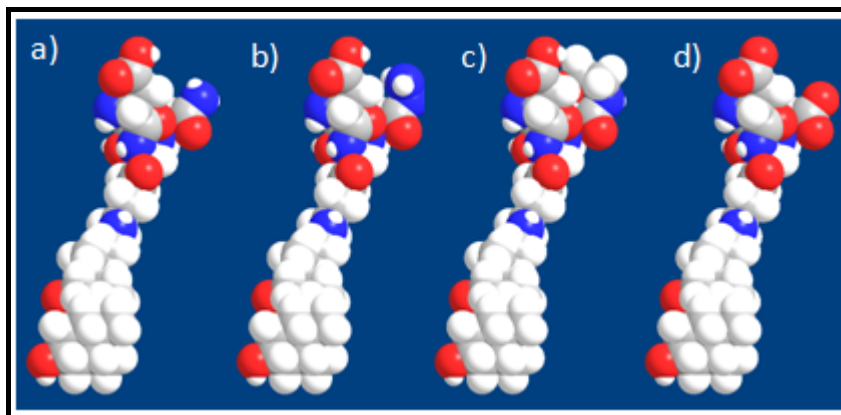


Figure 4.12. Spacefill model for functionalized PASP-AEDOCA unit of biloprotein.

We have already explained the formation of bilayer in polyaspartic acid AEDOCA conjugates. The fate of the bilayer will be governed by the hydrophilic functional group inserted between the AEDOCA units along the polymer chain.

The nature of the functional group and the degree of conjugation will influence molecule specific packing parameter, which governs aggregation behaviour of

amphiphiles. Conical molecules pack preferentially in spherical micelles, while cylindrical ones form flat lamellae (Antonietti 2003). Spacefill models indicate that Amino ethyl Deoxycholamide AEDOCA is almost cylindrical in shape. (Figure 4.12) It is therefore reasonable to assume that AEDOCA conjugated polyaspartate would form bilayer.

The role of size of hydrophilic head on shape and type of self assembly has been recognized in self assembly simulations (Bourov 2003, 2005). In an amphiphile with constant hydrophobicity, size of hydrophilic head influences CAC values. This is borne out by the effect of type of hydrophilic group and content on the CAC values of functionalized biloproteins summarized in Table 4.2. The size of hydrophilic substituent in biloproteins, measured as volume (\AA^3) was calculated. The size followed order Hydroxyl (318.50) > Hydrazide (242.86) > Amide (202.56) > Carboxylate (186.68). (Figure 4.13)

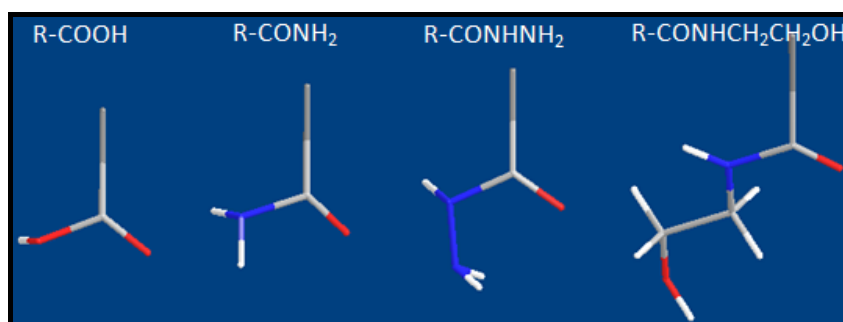


Figure 4.13. Chemdraw 3D view of functional groups in Biloproteins.

Hydrogen bonding favours lamellae formation leading to vesicular and tubular structures (Tellini 2006, Bong 2001, Kimizuka 1995, Roy 2003). In case of amide modified biloproteins amide head group being smaller and uncharged favour hydrogen bonding with other amide functionalities in the same and other backbones. This leads to lamellae formation. Amide functionalization leads to incorporation of asparagine in backbone. Asparagine and glutamine rich proteins yield fibrillar morphology (Tellini 2006, Bong 2001, Kimizuka 1995, Roy 2003). In biloprotein with high degree of amide functionalization (90 - 80 mole %) AEDOCA based lamellae closed and yielded vesicle. Further decrease in functionalization (60 - 40

mole %), increased rigidity in system inhibiting closure of lamellae, favouring extension of lamellae and rolling, leading to tubule formation. (Figure 4.14)

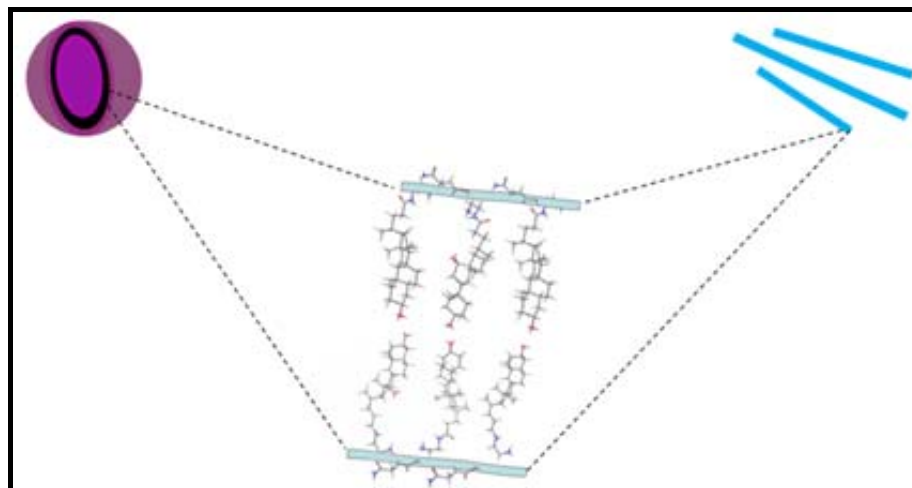


Figure 4.14. Schematic cross sectional view of lamella formed by AEDOCA in biloproteins

In hydroxyl and hydrazide functionalized biloproteins, hydroxyl and amine groups result in hydrogen bonding with diverse functionalities favouring lamellae formation. However larger size of hydrophilic head groups forces core segregation leading to micelle formation depending on the extent of functionalization (Bourov 2003, 2005).

In anionic biloproteins ionized carboxylate groups would contribute little to hydrogen bonding but result in repulsion. Some unionized COOH groups if present on backbone at neutral pH could still favour H bond formation between COOH --- COOH, COOH --- OH, COOH --- CONH. The balance of the hydrogen bonding and ionic repulsion leads to discontinuous lamellae formation which would close to form vesicle stabilized by carboxylate corona as in diblock copolymer vesicles of PSS-PAA (Zhang 1995). (Figure 4.14)

The calculated length of conjugated AEDOCA is 1.7 nm. TEM indicated that the bilayer thickness of vesicles formed by carboxylated and amidated biloproteins was 30 - 40 nm. Thus lamella formation results from steroidal stacking similar to that reported by Tellini et.al. (2007)

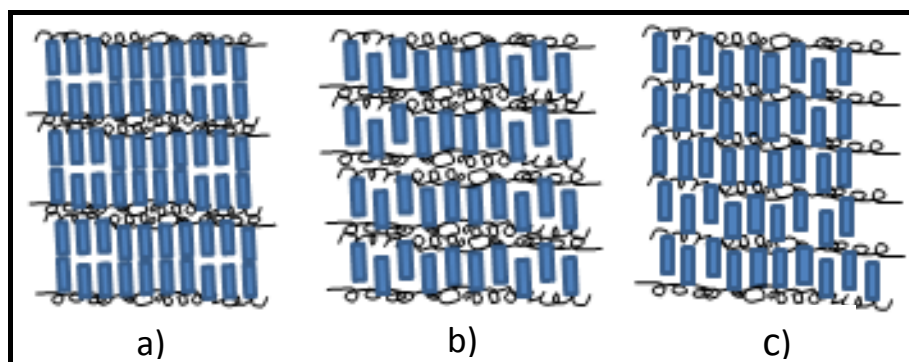


Figure 4.15. Models of lamella formation A) Juxtaposed; B) Interdigitated; C) model (Blue rectangles represent AEDOCA and black wire represent functionalized backbone)

According to Juxtaposed model, AEDOCA units would form a hydrophobic layer through intra chain hydrogen bonding and stack on other AEDOCA layer through inter chain hydrogen bonding. The peptide backbone and hydrophilic functionality would form hydrophilic layer and interact with other hydrophilic layer. Thus every two interacting layers of hydrophilic and hydrophobic nature would alternate to form lamella. As per this model approximately 15 layers of biloproteins formed lamella. In the interdigitated model, arrangement of layers is same as above but one AEDOCA layer would get interspersed in other AEDOCA layer. Hence a larger number of biloproteins would form lamella depending upon extent of interdigitation. As per lock and key model, AEDOCA units of one chain gets locked in AEDOCA units of other chain forming network which would stack to yield lamella. One hydrophobic layer would be held in between two hydrophilic layers. (Figure 4.15)

4.4 Conclusions

We have shown how hydrophilic functionalization mimicking post translational modification of proteins can be exploited to guide self assembly in Polyaspartic acid Deoxycholic acid conjugates. The diverse morphologies can be exploited for applications in nanobiotechnology such as drug delivery from micelles, vesicles, tubules and nanospheres. These morphologies have been explored for Amphotericin B delivery and synthesis of Silver nanoparticles as will be discussed in next chapters.

4.5 References

1. Antonietti M., Forster S. *Adv. Mat.*, 2003, 15, 1323-1333.
2. Azzam T., Eisenberg A. *Angew. Chem. Inter. Ed.* 2006, 45, 7443-7447.
3. Bong D. T., Clark T. D., Granja J. R., Ghadiri M. R. *Angew. Chem. Inter. Ed.*, 2001, 40, 988-1011.
4. Bourov G. K., Bhattacharya A. *J. Chem. Phys.*, 2003, 119, 9219-9225.
5. Bourov G. K., Bhattacharya A. *J. Chem. Phys.*, 2005, 122, 044702, 1-6.
6. Brownlee M., *Annu. Rev. Med.*, 1995, 46, 223-234.
7. Campanelli A. R., Sanctis S. C. D., Chiessi E., D'alagni, M., Giglio, E., Scaramuzza, L. *J. Phy. Chem.* 1989, 93, 1536-1542.
8. Cehelnik E. D., Cunall R. B., Lockwood J. R., Palmer T. F. *J. Phy. Chem.* 1975, 74, 1369-1376.
9. Checot F., Lecommandoux S., Gnanou Y., Klok H. A. *Angew. Chem. Inter. Ed.*, 2001, 41, 1339 – 1343.
10. Coldren B., Zanten R. V., Mackel M. J., Zasadzinski, J. A., Jung, H. *Langmuir*, 2003, 19, 5632-5639.
11. D'alagni M., D'Archivio A. A., Galantini L., Giglio E. *Langmuir*, 1997, 13, 5811-5815.
12. Discher D. E., Eisenberg, A. *Science*, 2002, 297, 962-973
13. Gutteridge A., Thornton J. M. *Trends biochem. Sci.* 2005, 30, 622-629.
14. Iozzo R. V. *PROTEOGLYCANS structure, biology and molecular interactions*, CRC press, 2000.
15. Kato K., Inoue K., Tohnai N., Miyata M. *J. Inclusion Phenom. Macrocyclic Chem.*, 2004, 48, 61-74.
16. Kimizuka N., Kawasaki T., Hirata K., Kunitake T. *J. Am. Chem. Soc.*, 1995, 117, 6360-6361 S. Roy, J. Dey, *Langmuir*, 2003, 19, 9625-9629.
17. Lamcharfi L., Meyer C. M., Lutton C. *Biospectroscopy*, 1997, 3, 393-401.
18. Lim Y., Moon K., Lee M. *Angew. Chem. Inter. Ed.*, 2009, 48, 1601-1605.
19. Malcolmson R. J., Higinbotham J., Beswik P. H., Privat P. O., Saunier L. J. *Memb. Sci.* 1997, 123, 243-253.

20. Matsuura K., Murasato K., Kimizuka N. *J. Am. Chem. Soc.*, 2005, 127, 10148-10149.
21. McMohan H., Gallop, J. *Nature*, 2005, 438, 590-596.
22. Mohanty A., Dey J. *Langmuir*, 2004, 20, 8452-8459
23. Montreuil J., Vliegthart J. F. G., Schachter, H. *Glycoproteins*, Elsevier, 1995.
24. Nelson R., Sawaya M. R., Balbirnie M., Madsen A., Riekel C., Grothe R., Eisenberg, D. *Nature*, 2005, 435, 773-778.
25. New, R. R. C. *Liposomes: A Practical Approach: Practical Approach Series*, Oxford University Press, 1990;
26. Persec, V., Ahn, C. H., Ungar, G., Yearley, D. J. P., Moller, M., Sheiko, S. S. *Nature* 1998, 391, 161-164.
27. Perutz, M. F., Windle, A. H. *Nature* 2001, 412, 143-144.
28. Ross, C. A., Poirier M. A., *Nat. Med.* 2004, S10-S17.
29. Roweton, S.; Huang, S. J.; Swift, G. J. *Environ. Polym. Degrad.* 1997, 5, 175.
30. Sada, K., Kondo, T., Miyata, M. *Supramol. Chem.*, 1995, 5, 189-191.
31. Saito, N., Sugawara, T., Matsuda, T. *Macromolecules*, 1996, 29, 313-319.
32. Saudek, V., Stokrova, S., Schmidt, P. *Biopolymers*, 1982, 21, 2195-2203.
33. Service, R. F. *Science*, 2002, 298, 2322-2323.
34. Shinoda H.; Asou Y.; Suetsugu A.; Tanaka K. *Macromol. Biosci.* 2003, 3, 34.
35. Tabata K., Abe H., Doi Y. *Biomacromolecules* 2000, 1, 157.
36. Taylor, K. M. G., Morris, R. M. *Thermochimica Acta*, 1995, 248, 289-301.
37. Tellini, V.H.S., Jover, A., Galantini, L., Pavel, N. V., Meijide, F., Tato, J. V. *J. Phy. Chem.B*, 2006, 110, 13679-13681.
38. Tellini, V.H.S., Jover, A., Meijide, F., Tato, J. V., Galantini, L., Pavel, N. V. *Adv. Mat.*, 2007, 19, 1752-1756.
39. Terech, P., Talmon, Y. *Langmuir*, 2002, 18, 7240-7244;
40. Torchilin, V. P., Weissig, V. *Liposomes: A Practical Approach*, Second edition, Oxford university press 2003.
41. Uchegbu, I. F., Florence, A. T. *Adv. Coll. Int. Sci.*, 1995, 58, 1-55.

42. Vauthey, S., Santoso, S., Gong, H., Watson, N., Zhang, S. Proc.Natl.Acad.Sci.USA, 2002, 99, 5355-5360.
43. Walsh, C. T., Tsodikova, S. G., Gatto Jr., G. J. Angew. Chem. Inter. Ed., 2005, 44, 7342-7372.
44. Wang W., Tetley L., Uchegbu I. F., J. Colloid and Interface Science 2001, 237, 200.
45. Wang, C., Li, G., Guo, R. Chem. Commun., 2005, 3591-3593.
46. Wang, C., Yin, S., Chen, S., Xu, H., Wang, Z., Zhang, X. Angew. Chem. Inter. Ed. 2008, 47, 9049-9052.
47. Wang, W., Qu, X., Gray, A. I., Tetley, L., Ichebu, I .F. Macromolecules, 2004, 37, 9114-9122.
48. Wasan, K. M., Brocks, D. R., Lee, S.D., Sachs-Barrable, K., Thornton, S. J. Nature 2008, 7, 84-99.
49. Whitesides, G. M., Boncheva, M. Proc.Natl.Acad.Sci.USA 2002, 99, 4769-4774.
50. Worrall, J. A., Gorna, M., Pei, X. Y., Sprint, D. R., Nicholson, R. L., Luisi, B. F. Biochem.Soc.Trans., 2007, 35, 502-507.
51. Yan, D., Zhou, Y., Hou, J. Science 2004, 65-67.
52. Yan, X., He, Q., Wang, K., Duan, L., Cui, Y., Li, J. Angew. Chem. Inter. Ed., 2007, 119, 2483 – 86.
53. Zhang, L., Eisenberg, A. J. Am. Chem. Soc. 1996, 118, 3168-3181
54. Zhang, L., Eisenberg, A. Science, 1995, 268, 1728-1731.
55. Zimmerberg J., Gawrisch, K. Nat.Chem.Biol., 2006,2,564-567.
56. Zimmerberg, J., Kozlov, M. Nat.Rev.Mol.Cell.Biol. 2006,7, 9-19.

Chapter 5

Drug encapsulation in biloprotein self assemblies for solubilization and toxicity reduction

Summary

Amphotericin B (Ampho B) in sodium deoxycholate (SD) micelle has been a useful antifungal formulation. Its usage is limited due to hemo and nephrotoxicity. In order to enhance drug solubilization and lower toxicity, synthetic Biloproteins were prepared by reaction of polyaspartic acid and ethylene diamine conjugate of deoxycholic acid (AEDOCA). These formed micelles and vesicles with increasing degree of substitution (DS). Solubilization of Ampho B in Biloprotein micelles and vesicles formed mixed micelles. At low DS, Ampho B in biloproteins was hemotoxic since Ampho B was held in loose structures much as in SD. At high DS, the hemotoxicity was lowered by 16% because of tightly packed environment conferred by Biloproteins. Ampho B loading and interactions with Biloproteins were studied using UV. Ampho B existed in aggregated state in all the Biloproteins as indicated by UV, CD and fluorescence spectroscopy. Minimum inhibitory concentration (MIC) values of Ampho B formulations against *Candida albicans* were same as that for Ampho B in SD micelles (0.38 $\mu\text{g} / \text{ml}$). Ampho B in Biloprotein mixed micelles also formed super aggregates on heat treatment. Super aggregated Ampho B in low DS Biloproteins and SD micelles exhibited lower hemotoxicity. Surprisingly, Ampho B super aggregates in high DS Biloproteins turned more hemotoxic.

5.1 Introduction

Ampho B is a broad spectrum antifungal drug used in systemic fungal infections arising due to forced immune compromised condition in AIDS, aggressive anticancer chemotherapy or organ transplantation etc (Yu 1998). Toxic side effects like chills, fever, nausea, vomiting, along with additional general malaise, phlebitis, anemia and nephrotoxicity limit its wide usage (Baas 1999, Graybill 1996, Laniado-Labori'n and Cabrales-Vargas 2009). Ampho B is water insoluble drug which need solubilizers like sodium deoxycholate (SD) to form clear solution for intravenous injection (Fungizone[®]). Ampho B toxicity in SD micelles is attributed to aggregated state of Ampho B (Barwicz 1992). In addition SD being surfactant also exhibits toxicity because of its membrane lytic activity (Rotunda 2004). To overcome solubility and toxicity limitations, other surfactants like Tween 80 and lauryl sucrose (Barwicz 1992) or complexing agents like cyclodextrins (Chakraborty and Naik 2003) have been explored in the past but the toxicity could be reduced marginally. Ampho B - Arabinogalactan conjugates although reduced toxicity also compromised efficacy to some extent (Ehrenfreund 2002, 2004, Falk 1999). The conjugation approach involved use of toxic reagents and organic solvents, which could only be removed through cumbersome and time consuming procedures. Liposomes and lipid complexes reduced Ampho B toxicity without compromising efficacy, but wide scale utilization of this approach has been limited by cost (Baas 1999).

Recently PEG-PBLA, (Yu 1998) PEG-PCL-TMC (Vandermeulen 2006), PEG-PLA (Yang 2007), PEG-PHASA (Adams 2003), Dextran- g – PLGA (Choi 2008) have been used as carrier for Ampho B delivery. Block copolymers like PEG-b-PAHA formed polymeric micelles which could retain Ampho B in monomeric state and reduce toxicity (Adams 2003). Synthesis of block copolymers needs elaborate procedures. The drug loading was comparatively low (10 w/v %) and procedure of drug loading needed organic solvents removal of which is cumbersome. Thus there exists a need for development of drug delivery system which would be easy to synthesize, economical, biocompatible and lower Ampho B toxicity.

Earlier reports suggested that Ampho B has to be maintained in monomeric state to reduce its toxicity. This could be achieved by using 25-50 folds higher mole ratio of surfactants such as SD or sucrose laurate to Ampho B than that needed for solubilization. High concentration of surfactant was difficult to maintain due to high CAC while membrane lytic activity caused toxicity (Barwicz 1992). So if one could enhance extent of conjugation of deoxycholate on the polymer backbone, then localized concentration of deoxycholate would be higher, lowering Ampho B aggregation.

On the other hand, Ampho B toxicity could also be reduced even when Ampho B was in aggregated state. These new findings explained that heat induced super aggregated Ampho B exhibited lower toxicity without compromising efficacy and loading (Gaboriau 1997).

We synthesized Biloproteins by conjugating Deoxycholic acid to polyaspartate backbone through imide – amine chemistry. This retained hydrophobic environment and carboxyl charge as in SD micelles. We intended to achieve Ampho B in monomeric or super aggregated state in order to reduce toxicity. These polymeric deoxycholates (Synthetic Biloproteins) would form self assemblies at low critical aggregation concentration in which Ampho B could be encapsulated. Synthetic Biloproteins exhibited micelles and vesicles with increasing DS. These Biloproteins solubilized Ampho B by forming mixed micelles. MIC and RBC hemolysis investigations were undertaken to quantify efficacy and toxicity of different Ampho B Biloprotein formulations. Effect of heat treatment on Ampho B state in Biloproteins was also investigated.

5.2 Experimental

5.2.1 Synthesis and characterization of synthetic Biloproteins

Polysuccinimide, Amino ethyl deoxycholamide (AEDOCA) and Biloproteins were synthesized as reported earlier. Briefly, Polysuccinimide was synthesized by dry blending at 180 ° C under nitrogen flow. AEDOCA was synthesized by reaction of

Deoxycholate NHS ester with excess of ethylene diamine. For Biloprotein synthesis, polysuccinimide was dissolved in DMF and reacted with varying mole ratios of AEDOCA at 70 ° C for 24 hrs. After purification, these conjugates were treated with aqueous NaOH to yield anionic synthetic Biloprotein (Figure 5.1.). These Biloproteins were characterized to establish aggregation by ¹H NMR in D₂O and critical aggregation concentration (CAC) by Pyrene fluorescence method (Table 5.1.).

5.2.2 Ampho B encapsulation in synthetic Biloprotein

Ampho B was loaded by solubilization method. Different Biloproteins were solubilized in 5 ml of phosphate buffer at pH 12. 50 mg of Ampho B was added to above solution and stirred to yield clear solution which was adjusted to 7.4 pH using 2 M phosphoric acid. Finally volume was adjusted to 10 ml with deionized water and pH was noted. In all cases, the ratio of Deoxycholic acid unit conjugated in Biloprotein to Ampho B was maintained at 2:1. All samples were filtered through 0.45 μ Acrodisc[®] Pall Gellman filter and stored at 4 ° C.

5.2.3 Ampho B content determination

Ampho B content in Biloprotein assembly was determined using UV spectrophotometer. 50 μl Ampho B containing Biloprotein solution was added to volumetric flask and diluted to 50 ml with DMSO. Samples were shaken for 5 minutes to ensure complete extraction of Ampho B from Biloprotein assembly. Using calibration curve for Ampho B in DMSO at 416 nm, concentration of Ampho B in Biloprotein assembly was determined.

5.2.4 Ampho B loaded biloprotein nano aggregate characterization

The static light scattering (SLS) measurements were performed using a Brookhaven Instruments corporation UK 90 Plus particle size analyzer. The scattering intensity was measured at 90°. Polymer aggregate solutions were prepared in double distilled water. The solutions were filtered through a Pall Gellman AcrodiscR syringe filter (0.45μ) directly into the scattering cell. Prior to the measurements, the scattering cell was rinsed

thrice with the filtered solution. The particle size measurements were done at 25 ° C in triplicate with each run of 1 min.

For zeta potential measurement electric field of 7.0 V/cm was applied across two electrodes and with inputs of pH, particle size and temperature. For each measurement 5 runs were averaged while each run employed 10 cycles for 3 minutes. Zeta pals software of Brookhaven instruments was used to analyze data.

Synthetic Biloprotein self assemblies were characterized for their size and surface charge before and after Ampho B loading.

5.2.5 Study of drug aggregation by UV, CD and fluorescence spectroscopy

In order to check Ampho B aggregation, different Biloprotein formulations were diluted to 10 µg/ml using phosphate buffer (pH 7.4) and their UV spectra were scanned in range 300 - 450 nm on Shimadzu UV spectrophotometer.

The CD measurements were performed using JASCO J-720 spectropolarimeter. The instrument parameters included a step resolution of 0.2 nm, a band width of 1.0 nm, scan speed of 200 nm/min and an accumulation of 3 scans with a 0.1 mm optical path cell. Spectra were recorded from 450 to 250 nm. Ampho B in Biloproteins and SD were prepared as stock at 145 mM in phosphate buffer (pH 7.4) which was used even for heat treatment studies. All the samples were diluted to 29 mM with deionized water for all final CD measurements.

A stock solution of Ampho B in Biloprotein 145 mM, prepared for previous studies was used as such for fluorescence studies but dilution was done before scanning to concentration of 5.17×10^{-2} mM. Fluorescence spectra were collected on Edinburgh spectrofluorimeter equipped with 450 W xenon arc lamp set with 2 nm excitation and emission band width with dwell time of 0.1 µS. Samples were scanned in 1 cm³ quartz cell with long axis perpendicular to the excitation beam.

5.2.6 In vitro antifungal activity

Biloprotein and SD self assemblies containing Ampho B were diluted with (pH 7.4) phosphate buffer saline to 50 µg /ml concentration. Ampho B (5 mg) was also dissolved in 0.5 ml DMSO and diluted with PBS to yield same concentration. The concentration of DMSO was less than 1% w/v in final preparation. MGYB broth was used as growth medium. *Candida albicans* count was adjusted to 5 x 10³ CFU in MGYB broth using microscopy technique. 150 µl of *Candida* suspension in broth was added in wells to which 50 µl of different samples were added to make final volume to 200 µl per well. Samples of Biloprotein at same concentrations along with medium were used as negative controls to check sterility while only *Candida albicans* in MGYB medium without Ampho B acted as positive control to check growth. 96 well plate was then incubated at room temperature for 48 hours protected from light. Samples were incubated in duplicate and results were averaged. The minimum inhibitory concentration was defined as the minimum concentration at which growth of *Candida albicans* was completely inhibited. The turbidity of samples was analyzed using UV plate reader at 600 nm.

5.2.7 Haemolytic activity

Human blood was collected in tubes containing EDTA and maintained at 2- 8 ° C. Buffy coat and supernatant were removed by centrifugation at 1000 g for 5 min at 4 ° C. The pelletized RBCs were washed with cold PBS and redispersed. An appropriately diluted RBC suspension on lysis with water released hemoglobin which gave absorbance at 576 nm in the range 0.4 - 0.5. All samples (30 µg/ml) were incubated with this RBC suspension at 37 ° C for 30 min and then placed in ice to arrest hemolysis. The unlyzed RBCs were removed by centrifugation (1000 g, 5 min) and the supernatant was analyzed for hemoglobin by UV/ VIS spectroscopy at 576 nm.

The percentage of hemolyzed RBCs was determined using following equation:

$$\% \text{ hemolysis} = (\text{Abst} - \text{Abso}) * 100 / (\text{Abs100} - \text{Abso})$$

Abst, Abso and Abs100 are the absorbance of test sample at 30 µg/ml, PBS control with no Ampho B and control of RBCs in the presence of deionized water.

5.3 Results and discussion

Drug delivery systems for Ampho B have to address two problems viz. solubilization and toxicity reduction. In the past solubilization of Ampho B has been achieved using SD, lauryl sucrose and phospholipids but reduction of hemotoxicity and nephrotoxicity using economically viable approaches has not been possible. Ampho B toxicity is mainly attributed to its aggregated state. Toxicity is also accentuated because of solubilizers like SD which are potentially membrane lytic. Lipid based Ampho B formulations like Amphotec[®], Amphocil[®], and Ambisome[®] could overcome solubility and toxicity problems but are rather expensive (Antoniadou 2005). Block copolymers like PEG-PBLA, PEG-PAHA, PEG-PLA and PEG-PCL overcame solubilization and toxicity limitations to a great extent. However, their synthesis and drug loading procedures are rather cumbersome hence have not attracted commercial usage limiting their practical utility. Heating of Ampho B loaded SD micelles for 20 min at 70 ° C forms Ampho B super aggregates which are less toxic but are of larger size (microns), which could be difficult to inject intravenously.

To overcome Ampho B toxicity, we synthesized Biloproteins i.e. polymeric deoxycholic acid, by conjugating Deoxycholic acid to polyaspartate backbone through amide linkage. By varying DS of deoxycholic acid on polyaspartic acid backbone, packing density of aggregates could be tailored. The ability of these structures to retain Ampho B in non toxic form was evaluated. The effect of heat treatment on Ampho B in these structures was also compared with heat treated Fungizone[®].

5.3.1 Synthesis and characterization of synthetic biloprotein

Bile acids have been explored extensively in drug delivery as solubilizing agents to enhance absorption of poorly soluble drugs (Gordon 1985). Deoxycholic acid, a major component of bile in human intestine has been used in commercial preparation of Ampho B. Its utility in drug delivery systems has been limited due to higher CAC and

hemolytic activity. Many approaches like preparation of different polymer bile acid conjugates, polymerization of bile acids, bile acid dendrimers have been explored (Zhu 2002, Vijayalakshmi 2006). The use of polymer bile acid conjugates is more interesting because of its ease of synthesis and ability to form micellar self assemblies retaining characteristics of deoxycholic acid. Bile acids have been conjugated to polysaccharides like Dextran, Chitosan and Heparin, mostly at low DS to yield micellar morphologies.

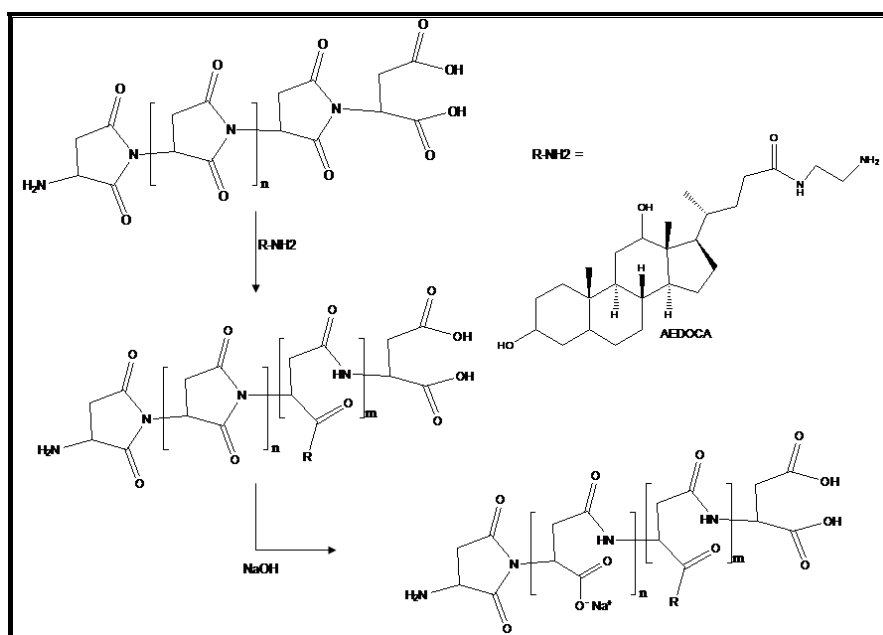


Figure 5.1. Reaction scheme for preparation of Biloproteins.

Polyaspartic acid is one of the most versatile synthetic polypeptides and is known to be biodegradable, biocompatible, and tailorable (Roweton 1997, Nakato 1998, Tabata 2000). It has also been reported to be nephroprotective (Swan 1991, Whitem 1996) which could reduce Ampho B induced nephrotoxicity to some extent. Hydrophobically modified polyaspartic acids with long alkyl chains, have been explored for encapsulation of poorly water soluble drugs (Yokoyama 1998, Kwon 1996). Poly hydroxyl ethyl aspartamide conjugates containing 10 mole % Dehydrocholic acid formed uncharged micelles. At higher DS those conjugates formed unstable morphologies due to secondary aggregation (Yang 2003). Synthesis of poly (Deoxycholamido ethylaspartamide co polyaspartate), containing DS up to 60 could be

achieved using Amino ethyl deoxycholamide. Depending upon the DS, micelles and vesicles formed, which were explored for Ampho B delivery.

For preparation of polymer conjugates, Polysuccinimide was synthesized by melt condensation and characterized by vapor pressure osmometry (VPO). Molecular weight was further confirmed by aqueous gel permeation chromatography (GPC), by converting PSI to Polyhydroxyethyl aspartamide, which had Mw 22,200, Mn 14,300 and PDI of 1.55. Poly(succinimide) (PSI), cannot be directly conjugated with Deoxycholic acid but is highly reactive towards amine because of the presence of imide in the succinimide ring. Deoxycholic acid was reacted with ethylene diamine through an NHS ester intermediate to yield AEDOCA which was then conjugated with Polysuccinimide to yield poly (Deoxycholamido ethylaspartamide-co-succinimide). The DS of AEDOCA was quantified by ^1H NMR in DMSO d_6 as reported earlier.

The polymer conjugates were treated with aqueous sodium hydroxide at 0 to 5 ° C to yield PASP-AEDOCA i.e. Synthetic Biloprotein, which was dialyzed against distilled water and then recovered by freeze drying.

The aggregates were prepared by dispersing PASP - AEDOCA in water by stirring for five minutes and characterized for CAC (Critical aggregation concentration), zeta potential and particle size. Except Biloprotein DS10, all other Biloproteins exhibited CAC values lower than that of SD (1.25 mg/ml). As reported in Table 5.1., Biloprotein DS 60 exhibits 35 folds lower CAC compared to that of SD.

Particle size for all Biloproteins ranged between 100 – 250 nm which indicated formation of higher aggregates like compound micelles and vesicles. All Biloproteins exhibited higher negative zeta potential values (-43 to -74 mV) which suggested that aggregates were stable and coated with anionic polyaspartate corona (Table 5.1.).

Table 5.1. Physico - chemical properties of Biloproteins

Sr.no	Name	CAC (mg/ml)	Zeta potential	Effective diameter (nm)
1.	Biloprotein DS10	1.297	-47.96	234.3
2.	Biloprotein DS20	0.257	-43.43	163.1
3.	Biloprotein DS40	0.0425	-60.93	147.7
4.	Biloprotein DS60	0.0372	-74.36	212.5

Transmission electron microscopic studies revealed loose micelles and vesicular structures at different DS in the range 10 to 60 (Figure 5.2.).

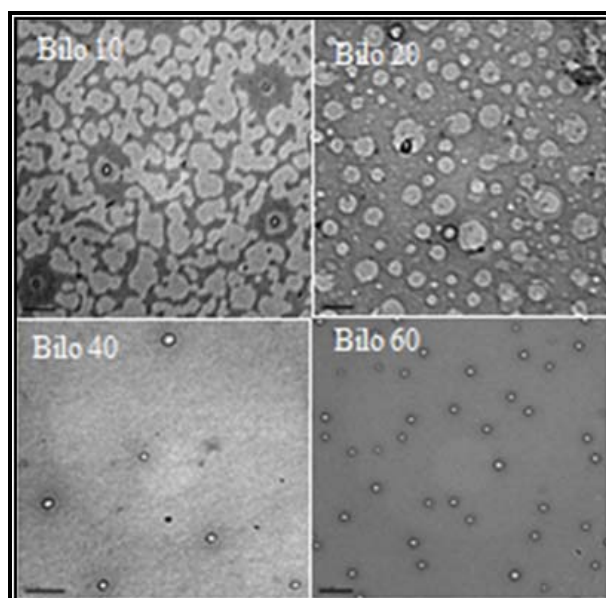


Figure 5.2. TEM images of synthetic Biloprotein (DS 10 to 60).

5.3.2 Ampho B encapsulation in Biloprotein

Ampho B was loaded in Biloprotein aggregates by mixed micellization method. The molar ratio of Ampho B : Conjugated Deoxycholate in polymer was 1 : 2, same as in FungizoneR. Loading of Ampho B in these Biloproteins was determined by dilution of these aggregates in DMSO and monitoring absorbance at 416 nm on a UV

spectrophotometer. The encapsulation efficiencies were high and comparable with those for SD micelles as shown in Table 5.2.

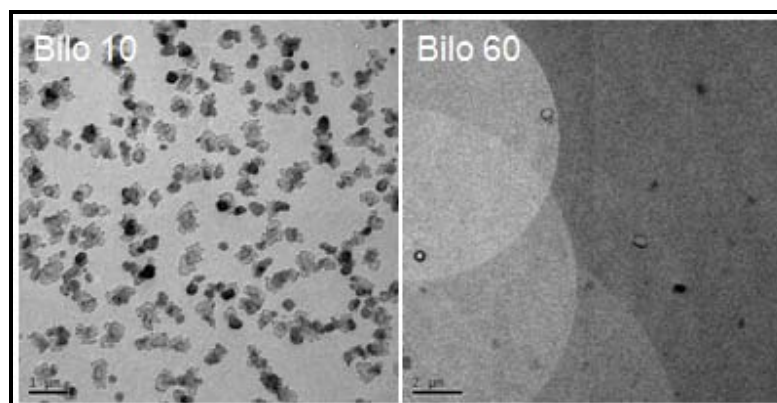


Figure 5.3. TEM images of Ampho B loaded synthetic Biloproteins (DS 10 and 60).

Table 5.2. Preparation of Ampho B loaded Biloprotein nanoaggregates

Sr.no.	Formulation	Amount (mg)	Ampho B (mg)	% loading	Encapsulation efficiency (%)
1.	Bilo 10	210	50	18.91	98
2.	Bilo 20	124	50	28.53	99
3.	Bilo 40	84	50	36.84	98
4.	Bilo 60	72	50	40.24	97
5.	SD	44	50	51.91	95

None of the samples showed any precipitation or aggregation during storage over 2 months. TEM images of Ampho B Biloprotein formulations suggested that on Ampho B loading, Biloprotein morphologies vanished and formed mixed micellar structures as seen in Figure 5.3.

5.3.3 State of Ampho B before and after heat treatment

Amphotericin B has been reported to exist in monomeric, dimeric, aggregated and super aggregated state, which determines the selectivity towards sterol binding and the ultimate toxicity. Hence state of Ampho B in biloprotein self assemblies was

investigated using different techniques like UV, CD and fluorescence spectroscopy. Effect of heat treatment on Ampho B state was also studied by heating all the samples at 70 ° C for 20 minutes.

5.3.3.1 UV spectroscopy

Absorption spectra of Ampho B indicated maximum at 330 nm and 332 nm in SD and Biloprotein solutions respectively. Other peaks at 364, 387, 409 and shoulder peak at 419 nm were also observed (Figure 5.4.).

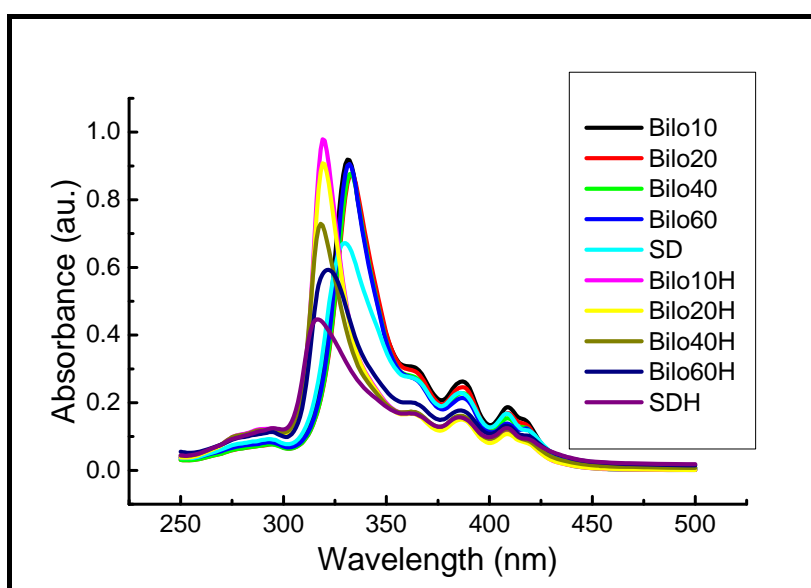


Figure 5.4. UV-vis absorption spectrum of aggregated and heat induced super aggregated form of Ampho B in SD and Biloprotein self assemblies at 0.01 mM in PBS pH 7.4.

The observed Peak at 332 nm matches well with that of reported value 326 nm (Gaboriau 1997, Stoodley 2007). This peak has been attributed to aggregated Ampho B in SD or super aggregated Ampho B. Ampho B self aggregate has been reported (Barwicz 1993) to absorb at 340 nm but in mixed micelles with deoxycholate, maxima blue shifts to 326 nm. In our set up, SD and Biloprotein based Ampho B aggregates exhibited maximum at 330 and 332 nm respectively. Thus Ampho B is in aggregated state in Biloprotein self assemblies. A small peak at 409 nm, comparable to earlier

reported peak at 411 nm, was observed in all Ampho B loaded Biloproteins and SD based formulation, which indicated presence of monomeric Ampho B (Gaboriau 1997).

Heat treated Biloprotein samples exhibited blue shift with peaks at 319 nm for Bilo 10 - 40, 322 nm for Bilo 60 and 316 for SD micelles. Biloprotein samples exhibited decreasing intensity for peak at 320 nm. Since Bilo 60 forms more compact assembly it hindered Ampho B super aggregation but less compact environment in loose aggregates of Bilo 10 favored super aggregation. Thus difference in interaction of Ampho B with deoxycholate groups in Bilo 10 and Bilo 60 affected aggregation.

Ratio of peak intensities at 348 nm and 409 nm (I / IV) can be used to determine degree of aggregation of Ampho B in formulation (Barwicz 1992). In our case, peak at 348 nm was not observed hence peak at 332 nm, a representative of aggregated state was used as peak I. The (I / IV) peak intensity ratios for all the samples were higher than 3.98, observed for SD. This indicated that Ampho B was more aggregated in any Biloprotein self assemblies as compared to that in SD. Within Biloproteins, degree of aggregation followed trend Bilo 60 (6.66) > Bilo 40 (5.71) > Bilo 20 (5.20) > Bilo10 (4.96).

On heat treatment, (I / IV) peak intensity ratios for all the biloprotein samples were higher than SD (3.48). This indicated that Ampho B was more aggregated in any Biloprotein self assemblies as compared to that in SD even after heat treatment. Surprisingly within Biloproteins, degree of aggregation followed the trend Bilo 20 (8.10) > Bilo 10 (7.99) > Bilo 40 (5.98) > Bilo 60 (4.39).

5.3.3.2 Circular dichroism spectroscopy

Circular dichroism has been used for investigation of Ampho B interaction with other components like lipoprotein, albumin etc. (Barwicz 2002) Ampho B presents CD signal in the range 250 - 450 nm, a region reported to be very sensitive to environment around Ampho B molecule in solution form. A strong dichroic doublet at 330 nm indicates formation of small aggregates. The intensity decreases as Ampho B interacts with lipids and completely disappears when Ampho B exists in monomeric form (Fujii 1997). This is because of exciton splitting resulting from preferred orientation of neighboring

molecules around Ampho B. Thus disruption of the organization of Ampho B molecules affects the signal around 330 nm (Figure 5.5.).

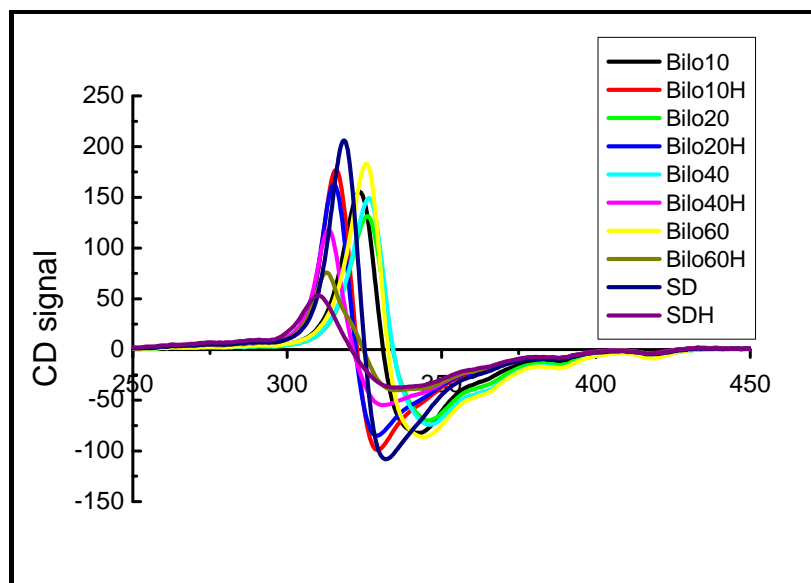


Figure 5.5. CD spectrum of aggregated and heat induced super aggregated form of Ampho B in SD and Biloprotein self assemblies at 29 mM in PBS pH 7.4.

The spectrum of Ampho B in SD presented strong dichroic doublet at 325 nm as against at 330 nm reported in literature (Hartel 2001). In contrast, Ampho B in Biloprotein samples exhibited dichroic doublet in range 331 - 334 nm. This difference in dichroic doublet position could be because of the differences in the extent of interaction between Ampho B and conjugated Deoxycholate units in different Biloproteins. The self aggregation peak intensity was highest for Ampho B in SD micelles and decreased in the order Bilo 60 > Bilo 10 > Bilo 40 > Bilo 20. This also suggested increasing extent of drug biloprotein interaction. In Bilo 20 and Bilo 40, lower intensity indicated mixed aggregation of Ampho B with Deoxycholate units. In Bilo 10, higher intensity observed, suggested Ampho B self aggregation due to loose micellar environment. In compact Bilo 60 structure, high intensity of dichroic doublet indicated that Ampho was not uniformly distributed amongst conjugated Deoxycholamide units but existed in self aggregated state.

Heat treated samples exhibited small blue shift in dichroic doublet position from 325 nm to 321 nm for SD. Large blue shift was observed for heated Biloprotein samples from 331-335 nm to 321-325 nm. The intensity of dichroic doublet also indicated extent of interaction between Ampho B and deoxycholate components in the system. The effect of heating was more prominent in case of SD micelles wherein dichroic doublet decreased substantially followed by Bilo 60 to Bilo 10 sequentially. This was not surprising since possibility of interaction of Ampho B with Deoxycholate was higher in Bilo 60 than in Bilo 10.

5.3.3.3 Fluorescence spectroscopy

In order to further ascertain above findings, fluorescence spectroscopy was employed (Gruszecki W.I. 2003). Typically 408 nm excites Amphotercin B monomer, 350 nm excites Ampho B dimer while excitation of higher aggregates has been suggested to occur at 325 nm, in agreement with UV absorbance of Ampho B self aggregate.

In Figure 5.6(a), emission spectrum (Ex 408 nm) displayed weak fluorescence with emission maximum at 562 nm corresponding to monomeric state for all Ampho B samples. Earlier reports attributed this large difference between absorption and emission to linearly conjugated polyene structure of Ampho B (Stoodley 2007). The spectra also displayed monomer emission transitions (0-0), (0-1), and (0-2) at 521 nm, 565 nm and 607 nm as reported earlier (Gruzecki 2003). Weak signal was observed possibly due to low concentration of monomeric Ampho B compared to aggregated Ampho B in the samples.

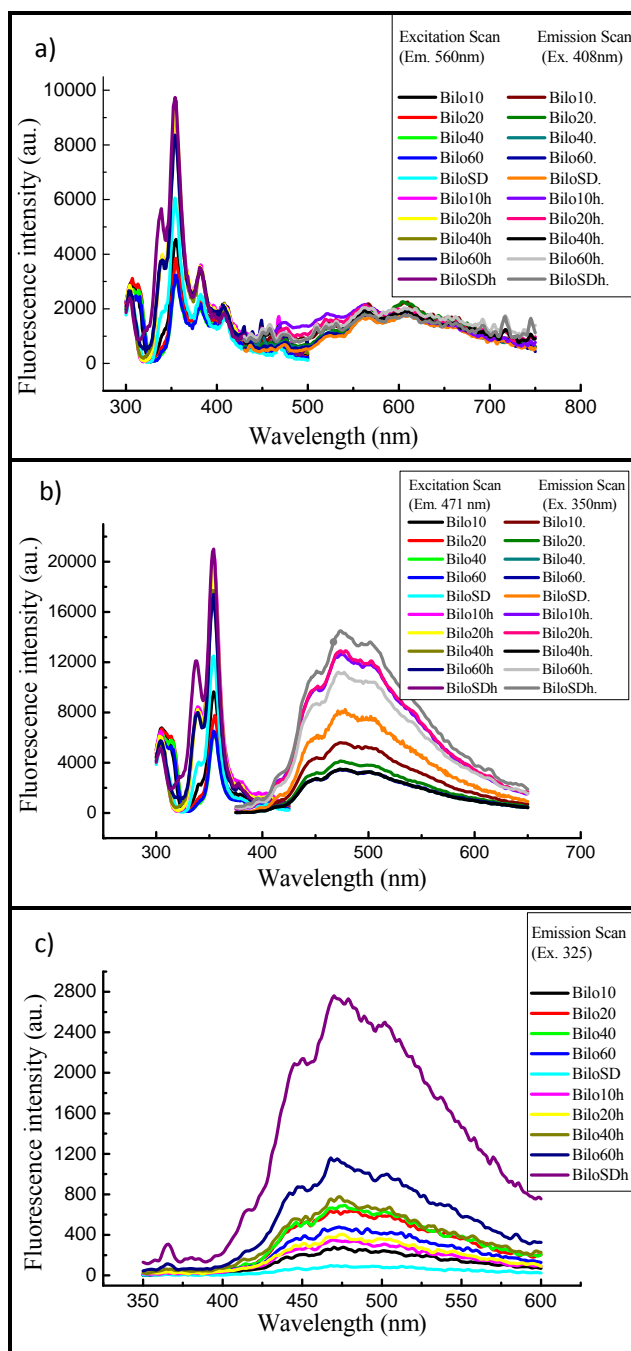


Figure 5.6. Fluorescence spectra (a) Excitation scan (Em. 560 nm), Emission scan (Ex. 408 nm); (b) Excitation scan (Em.471 nm.), Emission scan (Ex. 350 nm), (c) Emission scan (Ex. 325 nm) of aggregated and heat induced super aggregated form of Ampho B in PBS pH 7.4

Heat treatment induced new shoulder peak at 339 nm. This peak was more prominently observed in heat treated Ampho B in SD compared to that in Biloprotein samples. Intensities of all the peaks decreased, indicating further decrease in monomer content in samples. The excitation spectrum (Ex. 560 nm) of Ampho B in Biloproteins and SD displayed strong maximum peak at 355 nm with other peaks at 305, 382, 407 and 468 nm corresponding to different transitions as reported earlier (Stoodley 2007).

In Figure 5.6(b) excitation spectrum (Em. 471 nm) peaks at 305, 340, 355 and 378 nm were in agreement with the previously reported values at 338 and 356 nm (Gruszecki 2003). These bands result from excitation of Ampho B dimeric form or small aggregate form. Intensity of peak at 340 nm was highest in Bilo 10 and lowest in Bilo 60. This indicated presence of predominantly dimeric or small aggregate form in loose self assembly than in compact one.

On heat treatment, peak at 340 nm became prominent, indicating greater proportion of dimeric or small aggregated form. This signal was more intense than emission spectra at 408 nm excitation. Formation of dimers or small aggregates was more in Bilo 10 than in Bilo 60 as evident from the greater peak intensity in prior than later at the same Ampho B concentration.

An emission spectrum (Figure 5.6(b) Excitation 350 nm), displayed transitions as 450 nm, 474 nm and 503 nm which were in accordance with reported values of 452 nm, 473 nm and 494 nm indicating dimeric state. Heat treatment increased the intensity of characteristic peak at 474 nm in all the samples. Dimerization or small aggregate formation was more in Bilo 10 than Bilo 60 as noted from peak intensity. Ampho B in SD micelles exhibited 76% increase while the corresponding increase was from 225% to 331% for Bilo 10 to Bilo 60 as estimated from the peak intensity. Thus loose micelles (Bilo 10) favored dimeric or small aggregate form of Ampho B but extent of conversion was more in compact micelles of Bilo 60 possibly because of greater interaction of Ampho B with deoxycholic unit with increasing degree of substitution.

In Figure 5.6(c) the emission spectra of Ampho B on excitation at 325 nm, representative of aggregated state, indicated maxima at 468 nm with peaks at 447 nm and 502 nm. At same level of Ampho B in Biloprotein samples, peak intensity in spectra decreased from Bilo 10 to Bilo 60 while SD sample exhibited lowest intensity amongst all. This indicated that Ampho B is in more aggregated form in Biloprotein self assemblies compared to that in SD micelles. Within Biloprotein self assemblies Bilo 60 provided more compact environment which favored Ampho B aggregation exhibiting high emission intensity.

Heat treatment increased the intensity of all the peaks. In case of SD micelles, on heating the intensity of peak at 468 nm increased by 1000 %, suggesting increased aggregation. In Bilo 10, Bilo 20 and Bilo 40 heat treatment caused only 20-30 % increase suggesting heat did not further increase Ampho B aggregation. While in Bilo 60 the increase in peak intensity was 200 % suggesting that the extent of aggregation on heat treatment was greater than that observed in other Biloprotein samples but far lower than that observed in SD micelles. Thus in all heat treated samples, heat induced extent of aggregation might be different but final total aggregate content followed trend Bilo 10 > Bilo 20 > Bilo 40 > Bilo 60.

5.3.4 Effect of freeze drying and heat treatment on particle size and zeta potential

All the Biloprotein self assemblies containing Ampho B and SD micellar preparation were clear transparent solutions with particle size in the range 74 - 95 nm. Zeta potentials were negative in the range -20 to -40 mV indicative of stable formulations. The formulations were freeze dried and reconstituted with water for injection to check redispersibility. All the samples were redispersed easily without any visible aggregation. Particle size data indicated aggregation (Particle size 94 - 145 nm, ξ -16 to -40 mV) during freeze drying cycle which led to an increased particle size in almost all Ampho B containing Biloprotein samples (Table 5.3.).

Table 5.3. Effect of freeze drying on Ampho B loaded Biloprotein nanoaggregates

Sr.no.	Formulation	Particle size (nm)		Zeta potential (mV)	
		Before F/D	After F/D	Before F/D	After F/D
1.	Bilo 10	74 (0.350)	112 (0.276)	-20.01	-15.89
2.	Bilo 20	85 (0.384)	140 (0.401)	-28.45	-33.23
3.	Bilo 40	50 (0.299)	94 (0.392)	-44.64	-39.04
4.	Bilo 60	89 (0.335)	145 (0.302)	-45.12	-30.41
5.	SD	95 (0.325)	106 (0.374)	-20.15	-18.21

It has been reported in literature that size of Ampho B in Fungizone[®] increased substantially on heat treatment which was even difficult to analyze because of spongy aggregate formation but suggested an increase in particle size to 4 – 10 μ (Ettene 2000). Notwithstanding extensive aggregation and polydispersity, we determined particle size of all heat treated samples. Particle size as effective diameter indicated high polydispersity and bimodal particle size distribution as shown in Table 5.4. Particle size of Ampho based deoxycholate sodium micelles increased substantially to reach micron range as reported in literature. Biloprotein samples, Bilo 40 and Bilo 60 also aggregated to reach micron size but surprisingly heat treatment did not alter particle size of Bilo 10 and 20 significantly. Bilo 10 and 20 were transparent but Bilo 40, 60 and SD formulations turned translucent on heat treatment.

Table 5.4. Effect of heat treatment on particle size distribution

Sr.no.	Formulation	Effective diameter (nm)	Polydispersity [#]
1.	Bilo 10	71.6	0.230
2.	Bilo 20	124.8	0.162
3.	Bilo 40	8600	0.278
4.	Bilo 60	5635	0.330
5.	SD	12689	0.374

Distribution was bimodal in all the samples.

5.3.5 In vitro efficacy and RBC toxicity study

Ampho B encapsulated in all the formulations was active and exhibited activity against *Candida albicans*. Ampho B formulation on serial dilution in phosphate buffer from 12.5 to 0.19 $\mu\text{g/ml}$ exhibited complete inhibition of growth of *Candida albicans* till concentration of 0.38 $\mu\text{g/ml}$ after which slight growth was seen. Hence 0.38 $\mu\text{g/ml}$ was taken as MIC value. As per assay, all the formulations had almost same amount of Ampho B concentration hence exhibited identical MIC values as shown in Table 5.5.

Table 5.5. In vitro efficacy of Amphotericin B in Biloprotein nanoaggregates

Sr. no	Formulation	Conc. (mg/ml)	MIC ($\mu\text{g/ml}$)
1.	Bilo 10	4.90	0.382
2.	Bilo 20	4.89	0.381
3.	Bilo 40	4.88	0.380
4.	Bilo 60	4.85	0.378
5.	SD	4.77	0.371

Different Ampho B formulations were diluted to 10 $\mu\text{g} / \text{ml}$ and checked for their hemolytic potential by incubation with suitably diluted RBC's for 1 hour at 37 °C.

All Ampho B formulations were hemolytic (Figure 5.7.). In case of low DS Ampho B formulation Bilo 10, hemolysis was 100% which reduced to 84% in Ampho B formulation of Bilo 60 as shown in Figure 5.7. This decrease in hemolytic activity with increased DS can be attributed greater Ampho B - deoxycholate interaction in compact structure at high DS. This in turn causes slow release of Ampho B from Biloprotein self assembly.

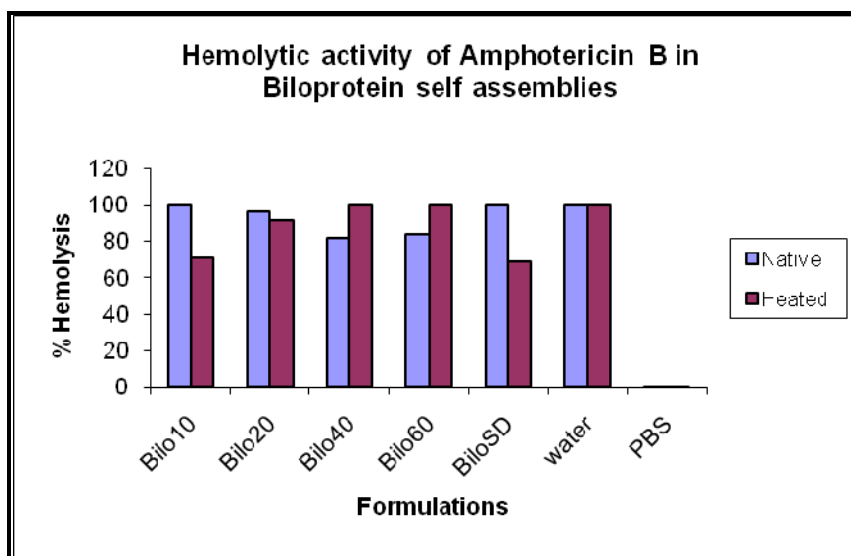


Figure 5.7. Hemolysis induced by Ampho B as a function of type of biloprotein and heat treatment in isotonic PBS, pH 7.4 at 37 ° C.

Biloprotein based self assembly could also form super aggregates when heated at 70 ° C for 20 minutes as reported earlier for Ampho B in SD micelles. Ampho B super aggregate formation could be observed by UV, CD and fluorescence studies for all Biloprotein samples. Hemolysis study of heated samples revealed that Bilo 10 which was most toxic prior to heat treatment, turned least toxic thereafter. On the other hand, Bilo 60 which was less toxic than its other compatriot became more toxic on heat treatment. We expected it to form more compact super aggregate further reducing its toxicity than its native form. SD based Ampho B which was used as a positive control, exhibited toxicity in native form but reduced toxicity on heat treatment as reported earlier in literature. It should be noted that even if heat treated SD exhibited 30 % lower hemotoxicity, its particle size increased to micron levels making it difficult to inject intravenously. On the other hand, Bilo 10 formulation exhibited same reduction in hemotoxicity without any increase in particle size, which is desirable from pharmaceutical and clinical application point of view.

5.4 Conclusions

This new approach based on synthetic Biloprotein has been developed as an alternative Ampho B drug delivery system since it enhanced solubilization of Ampho B through mixed micelle formation. The formed mixed micelles were more stable than Fungizone[®] towards storage led secondary aggregation. Detailed characterization of formulations indicated Ampho B existed in aggregated state in Biloprotein self assemblies. The type of Biloprotein self assembly also influenced Ampho B toxicity. Heat treatment led to Ampho B super aggregation as in Fungizone^R. Unheated Bilo 60 and heated Bilo 10 exhibited 16 – 30 % reduction in hemolytic activity without increase in size. Shell cross linking of these Biloproteins would stabilize these self assemblies towards dilution, yielding further toxicity reduction. These Biloproteins would be useful solubilizing agent for other hydrophobic drugs due to bile acid environment. Free carboxylates on surface of these aggregates could also be explored for conjugation of directing ligands for site specific drug delivery.

5.5 References

1. Adams M. L., Andes D. R., Kwon G. S., *Biomacromolecules*, 2003, 4, 750-757.
2. Antoniadou A., Dupont B., *Journal de Mycologie Médicale*, 2005, 15, 230–238.
3. Baas B., Kindt K., Scott A., Scott J., Mikulecky P., Hartsel S.C., *AAPS PharmSci.*, 1999, 1,3, 1-11.
4. Barwicz J., Christian S., Gruda I., *Antimicrob. Agents Chemother.* 1992, 36, 10, 2310-2315.
5. Barwicz J., Gruszecki W. I., Gruda I., *J. Colloid Interface sci.*, 1993, 158, 71-76.
6. Barwicz J., Beauregard M., Tancrede P., *Biopolymers*, 2002, 67, 1, 49-55.
7. Chakraborty K. K., Naik S.R., *J Pharm Pharmaceut Sci.*, 2003, 6, 2, 231-237.
8. Choia K., Bang J., Kim P., Kim C., Songe C., *International Journal of Pharmaceutics*, 2008, 355, 1-2, 224-230.
9. Ehrenfreund Kleinman T., Azzam T., Falk R., Polacheck I., Golenser J., Domb A. J., *Biomaterials*, 2002, 23, 1327–35

10. Ehrenfreund-Kleinman T., Golenser J., Domb A. J., *Biomaterials*, 2004, 25, 3049–3057.
11. Ettene W. M., Vianen W. V., Roovers P., Frederik P., *Antimicrob. Agents Chemother.*, 2000, 44, 6, 1598–1603.
12. Falk R., Domb A. J., Polacheck I., *Antimicrob. Agents Chemother.*, 1999, 43, 1975–81.
13. Fujii G., Chang J. E., Coley T., Steere B., *Biochemistry*, 1997, 36, 16, 4959-68.
14. Gaboriau F., Chéron M., Petit C., Bolard J., *Antimicrob. Agents Chemother.*, 1997, 41, 11, 2345-2351.
15. Gaboriau F., Chéron M., Leroy L., Bolard J., *Biophys. Chem.*, 1997, 66, 1, 1-12.
16. Gordon G. S., Moses A. C., Silver R. D., Flier J. S., Carey M. C., *Proc. Nat. Acad. Sci. USA.*, 1985, 82, 7419-7423.
17. Graybill J.R., *Ann. Intern. Med.*, 1999, 124, 921-923.
18. Gruszecki W. I., Gagoś M., Hereć M., *J. Photochem. Photobiol. B.*, 2003, 69, 1, 49-57.
19. Hartsel S. C., Baas B., Bauer E., Foree L. T., Kindt K., Preis H., Scott A., Kwong E. H., Ramaswamy M., Wasan K. M., *J. Pharm. Sci.*, 2001, 90, 124–133.
20. Kwon G. S., Okano T., *Adv. Drug Del. Rev.*, 1996, 21, 2, 107-116.
21. Laniado-Labori'n R., Cabrales-Vargas M. N., *Rev. Iberoam Micol.*, 2009, 26, 4, 223–227.
22. Nakato T., Yoshitake M., Matsubara K., Tomida M., Kakuchi T., *Macromolecules*, 1998, 31, 2107.
23. Roweton, S., Huang, S. J., Swift G., *J. Environ. Polym. Degrad.*, 1997, 5, 175-181.
24. Stoodley R., Wasan K. M., Bizzotto D., *Langmuir*, 2007, 23, 8718-8725.
25. Swan S. K., Kohlhepp S. J., Kohnen P. W., Gilbert D. N., Bennett W. M., *Antimicrob. Agents Chemother.*, 1991, 35, 12, 2591-2595.
26. Tabata K., Abe H., Doi Y., *Biomacromolecules*, 2000, 1, 157.

27. Vandermeulen G., Rouxhet L., Arien A., Brewster M. E., Pr'eat V.,
International Journal of Pharmaceutics, 2006, 309, 234–240.
28. Vijayalakshmi N., Maitra U., J. Org. Chem., 2006, 71, 768-774.
29. Whittam T., Parton K., Turner K., Antimicrob. Agents Chemother. , 1996, 40, 5,
1237-1241.
30. Yang S. R., Jeong J. H., Park K., Kim J. D., Colloid Polym. Sci., 2003, 281,
852.
31. Yang Z. L., Li X. R., Yang K. W., Liu Y., Journal of Biomedical Materials
Research Part A, 2007, 539-546.
32. Yokoyama M., Fukushima S., Uehara R., Okamoto K, Kataoka K, Sakurai Y,
Okano T., J Control Rel. ,1998, 50, 79–92.
33. Yu B. G., Okano T., Kataoka K., Kwon G., J. Control. Release., 1998, 53, 131-
36.
34. Zhu X., Nichifor M., Acc. Chem. Res., 2002, 35, 539-546.

Chapter 6

Biloprotein based preparation of gold and silver nanoparticles

Summary

Biloproteins formed by the reaction of polyaspartic acid and ethylene diamine conjugate of deoxycholic acid, on functionalization with carboxylate, hydrazide, amide and hydroxyl groups formed micelles, vesicles, tubules and nanospheres. Carboxylated biloprotein capped silver (Ag) nanoparticles (Nps). Increase in molecular weight of the backbone and hydrophobic content decreased particle size and polydispersity. Carboxylates were inherently most efficient capping agents amongst all functionalized biloproteins as evidenced from Nps synthesized by UV irradiation method. Reduction by NaBH₄ method, in the presence of different functionalized biloproteins yielded Nps in the range 5 – 15 nm. Silver Nps capped by amide functionality exhibited lowest size (4 nm) and polydispersity as indicated by TEM. Ag nanoparticles (Nps) were formed on biloprotein self assemblies to yield ring, necklace and rhizome like patterns. Carboxylated biloproteins also capped and stabilized gold (Au) Nps. These nano-patterned biloprotein self assemblies would find applications in laser / photo induced externally controlled drug delivery systems.

6.1 Introduction

Gold (Au) and silver (Ag) Nps have been gaining importance in physics, chemistry and biology owing to their unique optical, electrical, and photo thermal properties.(Daniel 2004, Yang 2006, Xiong 2007) Ag Nps also exhibit highest conductivity and reflectivity as well as antibacterial activity amongst all metals.(Xinyi 2009) Physicochemical properties of Nps which are of practical significance in the development of biosensors, chemical sensors, electro optical devices, data storage media and biological imaging (Radziuk 2007) strongly depend on particle size and shape as well as dielectric constant of dispersion medium. (Tao 2008, Prusek 2004, Hulteen 1999, Riboh 2003, Zynio 2002, Henry 2001, Yin 2002) Metal Nps also find applications in diagnostics and drug delivery because of ease of synthesis, affinity towards diverse biological molecules and high surface area for conjugating drugs and directing ligands. (Dhar 2009, Gibson 2007, Mukherjee 2007, Ding 2007, Huang 2006, Niidome 2006, Hirsh 2005)

Over the past two decades, Au and Ag Nps have been synthesized by the reduction of respective salts using ethylene glycol, sodium citrate, ascorbic acid and sodium borohydride using stirring, refluxing or UV exposure method. (Silvert, 1996, Henglein, A et.al. 1998, Van Hyning D. L. et.al. 1998) Use of capping agents along with external reducing agents or otherwise has also been investigated as to control growth, size, colloidal stability and functionalization of Nps. In order to disperse Nps in aqueous or non-aqueous media, wide range of capping agents have been investigated. These include alkane thiols, sugars, carbohydrates, peptides or proteins and polymers bearing functionalities like thiol, amide, amine, carboxylates etc. (Silvert 1997, Van Hyning 1998, Jana 2010)

The most common methodology for the synthesis of colloidal Ag Np is the reduction of AgNO₃ in the presence of polymers which yields stable nanostructures with controlled shapes and sizes.(Wiley 2005, Silvert 1996, 1997) Polymers also serve as suitable scaffolds for immobilization of metal Nps which prevent their aggregation (Chen 2006,

Morones 2007). Since the capping led stabilization effect of macromolecules also depends on the polymer architecture, linear, branched and dendritic polymers have been evaluated. The functional groups in macromolecules govern interaction with metal precursor through coordinate bond (amine, hydroxyl, carboxyl, amide), Hydrogen bond (hydroxyl) or ion-pair formation (carboxyl, sulfonate). Synthetic polymers like polyvinyl alcohol, poly(acrylic acid), poly(methacrylic acid), polymaleic acid, PVP, polyallylamine, polyNIPAM and PEG have been used for the synthesis of Nps. Similarly natural polymers like starch, dextran, gum Arabic, heparin, and hyaluronic acid have been evaluated in view of their biocompatible and biodegradable nature. (Suslick 1996, Zhao 1998, Raveendran 2003, Sharma 2009; Ershov 1998, Mayer 1998, Kemp 2009, Hussain 2003)

Apart from the polymers in solutions, self assembled polymer templates present size-confined, nanosized cavities for the controlled synthesis of Nps. The hydrophobic groups in main chain or pendant links on the polymer also assist in the synthesis of nanoparticles through stable template formation. (Voronov 2007, Samoilova 2009, Bukreeva 2008) For instance amphiphilic block copolymers like PS-b-P2VP (Osman 2010, Chang 2009), PEO-PPO-PEO (Sakai 2004), PEG-b-poly(DMAEMA) (Ishii 2004) have been widely explored for the synthesis of metal Nps. Depending upon type of solvent for dispersion, block lengths and block type. These polymers form colloidal structures such as micelles, vesicles and tubules of different size and geometry, within which Nps can be synthesized. (Antonietti 1995, Seregina 1997, Saptz 2000, Mo'ssmer 2000)

In nature, many biological systems control the deposition and structure of Nps. This has inspired biomimetic approaches for the synthesis of Nps (Lowenstam 1981, Cha 1999, Schueler 1999, Klaus 1999). Protein cages such as cowpea chlorotic mottle virus (CCMV) capsids, ferritins, and ferritin-like proteins have been used as substrates. (Meldrum 1991, Douglas 2002, Allen 2002) These supramolecular structures provide novel reaction vessels for the synthesis of nanostructures of controlled dimensions. The amino acids present on the surface of self-assembling cages of CCMV and ferritin were

used for the incorporation of novel functionalities or peptides useful in synthesis of silver Nps. (Klem 2003, Blum 2004) The limitations of these substrates are 1) need for highly purified proteins, 2) cumbersome techniques and expensive reagents, 3) undesirable modifications on protein motifs, 4) preservation of environment after functionalization, 5) limited availability of desired functionalities on natural protein self assemblies etc.

These limitations can be overcome by using synthetic proteins. Polyaspartic acid - deoxycholic acid conjugates based synthetic biloproteins were synthesized earlier. In this chapter we show that depending upon the hydrophobic content these biloproteins act as either capping agents in solution or serve as template for nano-patterning. At low hydrophobic content (10 mole %) biloproteins bearing carboxyl, hydroxyl, hydrazide and amide functionalities act as useful capping agents. These functionalized biloproteins having the same backbone exhibited varying capping abilities towards silver Nps. Carboxylate was found to be the most efficient capping agent amongst all the functionalities evaluated. At high hydrophobic content (60 mole %), the biloproteins exhibit diverse morphologies viz. micelles, vesicles, tubules and nanospheres which serve as templates for controlling nucleation, growth and eventual size distribution during Nps formation and yield different necklace and ring like nano-patterns.

6.2 Experimental

6.2.1 Synthesis and characterization of synthetic biloproteins

The functionalized synthetic biloproteins were synthesized and characterized as discussed in chapter 3. Briefly, PSI was dissolved in dry DMF to which different amounts of AEDOCA was added to achieve corresponding substitution and stirred at 65 - 70 ° C for 24 hrs under nitrogen. Solutions were then concentrated and precipitated in excess Acetone to remove unreacted AEDOCA. Reactive AEDOCA polymer conjugates of different DS were dissolved in dry DMF and each DS sample solution was divided into 4 portions and chilled to 5 - 10 ° C. Different functionalizing agents like amino ethanol, ammonia, hydrazine were diluted with dry DMF and added to each

of three portions and stirred overnight at RT then dialyzed against deionized water for 48 hrs using spectrapor 2K dialysis bags. For carboxylate functionalization, reactive polymer conjugate DMF solution was added to chilled aqueous sodium hydroxide solution and stirred for 3 hrs till clarity and dialyzed as mentioned above for other functionalities. Thus all functionalized biloproteins were prepared in one step at the same time. Biloprotein self assemblies were recovered by freeze drying and stored at RT in desiccators.

Biloprotein self assemblies were characterized by ^1H NMR, IR, static light scattering studies, zeta Potential measurements, and transmission electron microscopy as discussed in chapter 3.

6.2.2 Preparation of Au and Ag Nps

In order to study suitability of biloproteins for preparation Gold and silver hydrosols, 3 methods were investigated namely, thermal, photo and chemical reduction method.

1) Thermal reduction method: An aqueous solution of HAuCl_4 (50 ml, 1 mM) or AgNO_3 (50 mL, 3 mM) was refluxed for 5-10 min and a warm (50 - 60 °C) aqueous solution of carboxylated biloproteins (20 ml 0.2 g) was added quickly. Reflux was continued until a deep-red solution (for gold) and yellowish-brown solution (for silver) was observed (approximately 30 - 60 min). These solutions were then dialyzed against distilled water for 24 hrs. The solutions were filtered through 0.45 μm Pall Gelmann syringe filters to remove any precipitants, and the filtrates were stored at room temperature in the dark under nitrogen.

2) Photo reduction method: An aqueous solution of HAuCl_4 (50 ml, 1 mM) or AgNO_3 (50 mL, 3 mM) was mixed with aqueous solution of different functionalized biloproteins (20 ml 0.2 g) and stirred under UV light for 24, 48 and 72 hrs. Remaining procedure was followed as in thermal reduction method.

3) Chemical reduction method: An aqueous solution of HAuCl_4 (50 ml, 1 mM) or AgNO_3 (50 mL, 3 mM) was mixed with aqueous solutions of different functionalized

biloproteins (20 ml 0.2 g) and stirred for 30 min protected from light. Freshly prepared solution of NaBH₄ (10 mM) was added to them and stirred overnight. Remaining procedure was followed as in thermal reduction method.

6.2.3 Characterization

UV-visible adsorption spectra of gold and silver hydrosols were recorded on a SHIMADZU UV-2450 UV-vis spectrophotometer in the range 1000 – 200 nm. Aliquots of the solutions were taken out at different times during the synthesis for UV analysis. The static light scattering (SLS) measurements were performed using a Brookhaven Instruments corporation UK 90 Plus particle size analyzer. Thermo gravimetric analysis of freeze dried samples of gold and silver hydrosols was performed by heating till 900 ° C at heating rate of 10 ° C. Transmission electron microscopy (TEM) observations were carried out under high-resolution transmission electron microscopy (HR-TEM) at 300 kV with Technai- FEI machine. A drop of gold and silver hydrosol was placed on a copper grid coated with a carbon and polymer film. The grid was held horizontally for 5 minutes to allow the Nps to settle and then blotted with tissue paper from one edge point to allow the excess fluid to drain. Grid was then allowed to dry in air and stored in desiccator before visualization.

6.3 Results and discussion

Ag Nps have been synthesized in the presence of polymers or surfactants, which control the kinetics and preferential growth direction of Nps by acting as nucleating and stabilizing agents (Silvert 1997, Wiley 2005). In literature functional groups like amines (Kuo 2003), carboxylates (Hussain 2003), hydroxyls (Suslick 1996, Sharma 2009) and amides (Chen 2006) on carriers like polymers, proteins and solid surfaces have been explored for Np synthesis. These functional groups, depending upon their ability to share electron pairs form coordinate bond, hydrogen bond and ionic interactions with metal surfaces. To the best of our knowledge no attempt has been made to compare the efficiency of different functional groups on the same polymer backbone, to cap nanoparticles.

Functionalized biloproteins formed diverse morphologies like micelles, vesicles, tubules and nanospheres. Herein we show that these act as capping agents in the synthesis of silver hydrosols using irradiation and chemical reduction and templates yielding necklace and ring like patterns.

6.3.1 Synthetic biloproteins

Synthetic biloproteins bearing different hydrophilic functionalities were prepared and characterized as discussed in chapter 4. ¹H NMR indicated conjugation of amino ethyl deoxycholamide (AEDOCA) on polysuccinimide while IR confirmed incorporation of diverse hydrophilic functionalities. By increasing degrees of substitution (DS) of AEDOCA from 10 to 60 mole %, hydrophobicity in the self assemblies was enhanced. Exclusive hydrophilic functionalization to yield hydroxyl, hydrazide, amide and carboxylate corona was achieved. Depending upon the type and extent of functionalization with hydrophilic groups, the type and extent of interactions differ, which gives rise to diverse morphologies. Carboxylate functionalization yields micelles and vesicles, hydrazides yield micelles and vesicles, amides yield vesicles and tubules while hydroxyls form micelles and nanospheres.

6.3.2 Silver nanoparticles

6.3.2.1 Sodium borohydride reduction method

Silver Nps were prepared by reduction of silver nitrate with ice-cold sodium borohydride (mole ratio 1:10) in the presence of carboxylated biloproteins (DS 10). Biloproteins acted as capping agents and stabilized silver nanoparticles which exhibited an absorption peak around 400 nm, characteristic of silver Nps (Ji 1999, Sosa 2003).

Effect of molecular weight and hydrophobic content on preparation of Nps was investigated using carboxylated biloproteins synthesized from polysuccinimide of two molecular weights (Mn 2300 and 12000) and DS 10 – 60. The polymer without hydrophobe i.e. Polyaspartic acid sodium salt of low molecular weight capped silver Nps and exhibited lowest SPR maxima (395 nm). The SPR maxima for all the

carboxylated biloproteins of low and high molecular weight were in the range 412 – 419 nm.

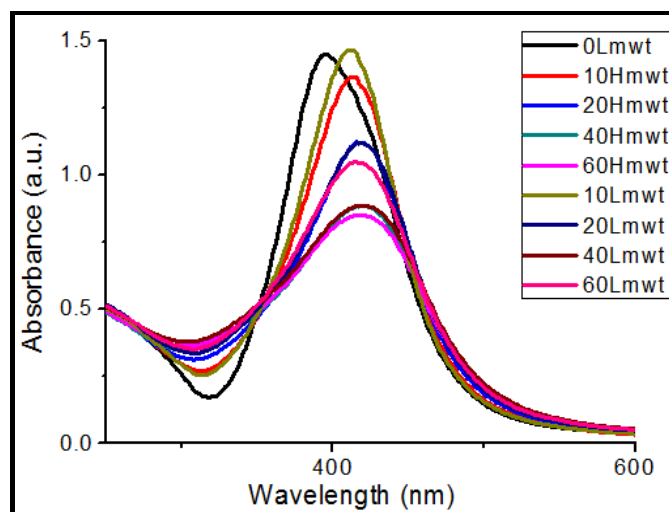


Figure 6.1. UV-visible spectra of Ag Nps in carboxylated biloproteins (NaBH₄ method).

Table 6.1. Silver Nps synthesized by carboxylated biloproteins.

Samples	SPR maximum (nm)	Absorbance (a.u.)	FWHM
0-Lmwt	395	1.45	85.883
10-Lmwt	411	1.46	79.88
20-Lmwt	418	1.12	102.7
40-Lmwt	420	0.88	108.84
60-Lmwt	416	1.046	111.26
10-Hmwt	413	1.36	85.58
20-Hmwt	418	1.12	96.05
40-Hmwt	420	0.88	129.33
60-Hmwt	418	0.85	137.885

Full width half maximum (FWHM) values of high molecular weight biloproteins (86 - 138) were higher than those obtained for low molecular weight biloproteins (80 - 111) (Table 6.1.). This is consistent with the reports that FWHM is inversely related to the particle diameter (Petit 2003). Similar effect was reported earlier in silver Nps prepared by chemical reduction method (NaBH_4) wherein sizes of Nps decreased from 6 nm to 3 nm with an increase in molecular weight of polyacrylic acid used as capping agent, from M_w 1200 to 15000 (Falletta 2008).

In both low and high molecular weight biloproteins with increasing DS from 10 – 60, SPR maxima intensity decreased and FWHM values increased from 85 - 138. Thus polydispersity and Np size decreased with increase in hydrophobic content of biloproteins (Table 6.1). Similar findings were reported in case of PEO-PPO-PEO capped gold Nps wherein increase in hydrophobicity of micelle stabilized gold efficiently resulting in uniform and spherical Nps (Chen 2006). In case of silicone grafted with hydrophilic diethanol tertiary amine, the size of Ag Nps decreased from 7 – 4 nm as the ratio of hydrophobe to silver increased from 2:1 to 9:1 (Kuo 2004).

Silver Nps were also prepared using reflux method. Carboxylated biloproteins differing in hydrophobic content and molecular weights capped Ag Nps which exhibited UV absorbance with two SPR maxima. The peak in the range 410 – 453 nm corresponds to excitation of surface plasmon vibrations in the silver nanoparticles and is responsible for the striking colours observed (Elechiguerra 2005). An additional absorption band at 514 nm was also observed. This has been attributed in the past to the formation of a) aggregation leading to coupling of the plasmon vibrations between neighbouring particles (Taleb 1998, Tan 2002) or b) anisotropic shapes (Jin 2003). In later study we demonstrate that this is result of aggregation of Nps.

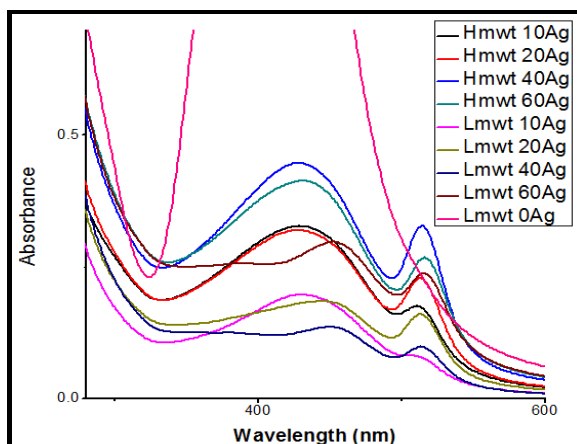


Figure 6.2. UV-visible spectra of Ag Nps in carboxylated biloproteins (Reflux method).

Biloproteins were also functionalized with hydroxyl, amide and hydrazide groups. To compare capping abilities of the functional groups, mole ratios of silver ions $[Ag^+]$ to $NaBH_4$ (1:10) and $[Ag^+]$ to functional groups (approx. 1 : 20 for DS 10 and 1 : 5 for DS 60) were used. UV- vis spectrum indicated that SPR maximum for silver Nps red shifted in all functionalized biloproteins as hydrazide (409 nm), hydroxyl (411 nm), carboxylate (425) and amide (429 nm).

Optical absorption spectra of metal Nps are dominated by surface plasmon resonances (SPR). The shift in SPR maximum to longer wavelengths is a result of increase in particle size (Brause 2002). Therefore particle size trend expected would be amide > carboxylate > hydroxyl > hydrazide. Frequency width half maximum (FWHM) values for all the silver Nps increased in the order hydroxyl (74.29), hydrazide (82.35), carboxylate (83.16), amides (101.10). Since full-width at half maximum (FWHM) is inversely related to the particle diameter (Petit 2003) particle sizes of Nps would be expected to follow order hydroxyl > hydrazide > carboxylate > amide. Actual particle size of all the samples by TEM also display similar trend as discussed later in more details.

6.3.2.2 UV irradiation method

Silver Np synthesis using chemical reduction method may not reflect inherent capping potential of the functional groups since NaBH_4 is also known to stabilize metal Nps. (Solomon 2007) Hence Nps were synthesized by UV irradiation method.

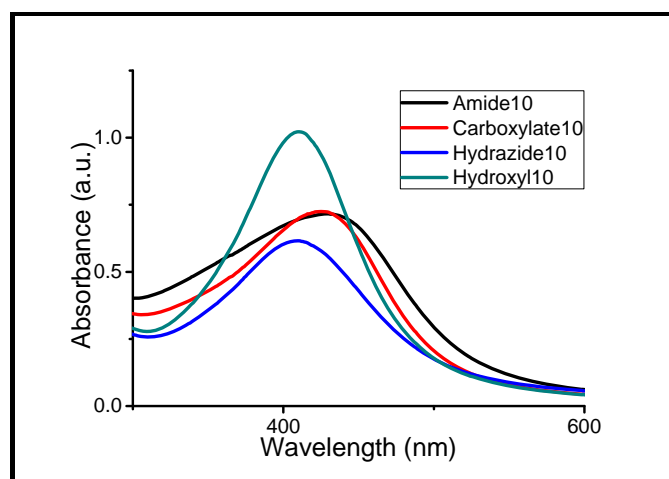


Figure 6.3. UV-visible spectra of silver Nps in functionalized biloproteins (NaBH_4 method).

Capping ability primarily depends on the interactions between the metal Nps and the functional groups in the capping agents. (Table 6.2.) Carboxyl group forms ion pair complex and coordinate bonds, amide forms coordinate bonds, hydroxyls forms coordinate and hydrogen bonds with hydrated metal surface. This bonding with metal surface passivates surface which prevents aggregation of metal nuclei resulting in nanoparticle stabilization.

Table 6.2. Mechanism of metal capping by different functionalities

Metal surface	Capping functionality	Carrier	Mechanism	Reference
Silver	NH ₂	Silica Polyallylamine	Coordinate bond	Lv 2009 Kuo 2004
Silver Gold	COOH	Myristic acid	Ionic bond Unidentate coordinate	Wulandari 2008
Silver	OH	Glucose	Hydrogen bond	Serra 2009
Silver	Pyrrolidone	PVP	Coordinate bond	Patil 2009
Silver	CONH ₂	PNIPAM	Coordinate bond	Chen 1998

Functionalized biloproteins at DS 10, in the presence of UV light, capped silver nuclei. Since the pH has been implicated in Np synthesis, pH values for all the samples at DS 10 were noted. The values were amide (7.6), hydroxyl (7.5), carboxylate (7.8), and hydrazide (8). Earlier reports indicated that the rate of reduction of the precursor was enhanced with increasing pH due to the higher activity of the citrate at high pH and altered coordinate bonding of Au(III) ions which mediated the nucleation and growth processes (Dong 2009). The observed pH difference in functionalized biloprotein solutions was not significant and hence was neglected. The UV exposure study was performed for 72 hrs and spectra were compared at 24, 48 and 72 hrs. As the irradiation time increased, solutions turned yellowish brown, light gray and yellow for carboxylate, amide and hydroxyl functionalized biloproteins. The solution containing hydrazide capped Nps turned grayish black to turbid and then slowly silver precipitated out. The SPR peak intensity decreased in the order carboxylate > amide > hydroxyl >>> hydrazide (Figure 6.4). With time, height of SPR maxima increased which indicated that completion of reduction takes time.

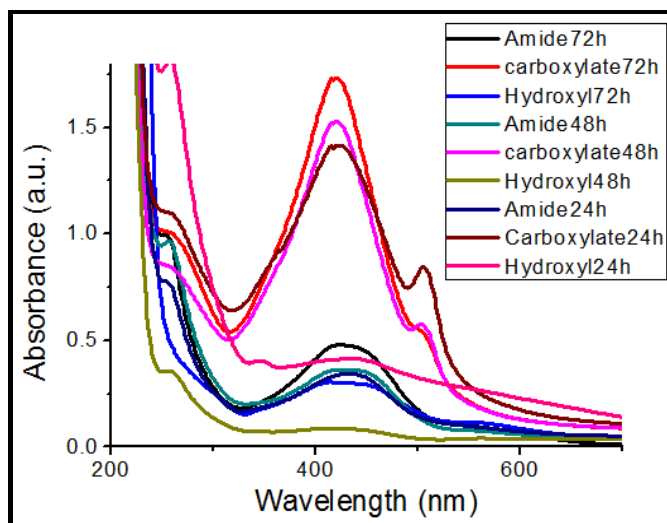


Figure 6.4. UV-visible spectra of Ag Nps in functionalized biloproteins (UV method).

SPR peak of Nps capped by carboxylated biloprotein (419 nm) evolved more rapidly compared to others. The negatively charged composite nanoparticles displayed a stronger tendency to form higher order aggregates, which explains the relatively high intensity of the absorbance at 420 nm in the UV-vis spectrum. Additional peak at 507 nm which is mainly due to aggregated silver Nps exhibiting coupling of Plasmon resonance. Amide groups form hydrogen bonds which lower their availability for capping silver nuclei hence intensity of SPR peak at 422 increased slowly with time. Hydroxyl groups are neutral and polar which also favours hydrogen bonding. The SPR peak developed slowly with time at 429 nm. In case of hydrazide functionalized biloprotein, silver salt precipitated out of solution with time since hydrazide groups could not cap silver nuclei formed by UV irradiation. Thus hydrazide functionality has got very weak inherent ability to stabilize silver. We expected hydrazide functionalized biloproteins to reduce silver faster and efficiently compared to others since hydrazine is well known weak reducing and stabilizing agent. (Nickel 2000) This inability of hydrazide functionalized biloprotein to cap silver is not understandable since the same biloprotein capped silver Nps by chemical reduction method and yielded uniformly distributed Nps.

6.3.2.3 IR spectra of composites

The freeze dried samples of biloprotein capped silver were ground with KBr, pelletized and analyzed on a Perkin Elmer Spectrum-1 in transmittance mode operating at a resolution of 1 cm^{-1} . (Figure 6.5) The peak in the range $3200 - 3500\text{ cm}^{-1}$ was assigned to COO-H, O-H, NH-NH₂, NH-H, CON-H stretching. Higher interactions were observed with carboxyl and amide functionalization since COO-H peak was shifted from 3290 to 3296 cm^{-1} and 3296 to 3316 . The weaker band at $1600 - 1660\text{ cm}^{-1}$ corresponds to amide I, arising due to carbonyl stretch in polyaspartate backbone of biloproteins. In particular, the carbonyl peak of amide which is present in all the biloproteins in main chain, shifts slightly to higher wave number on capping silver. The carbonyl peak shift from 1649 to 1653 cm^{-1} in carboxylated biloprotein and 1653 to 1660 cm^{-1} in hydrazide biloprotein is more prominent indicating greater interaction. Thus IR spectroscopic study confirmed that in all functionalized biloproteins the carboxyl, amide, hydrazide and hydroxyl groups on aspartic acid exhibited metal binding ability suggesting they could possibly form a layer which would coat the silver Nps and prevent agglomeration leading to stabilization.

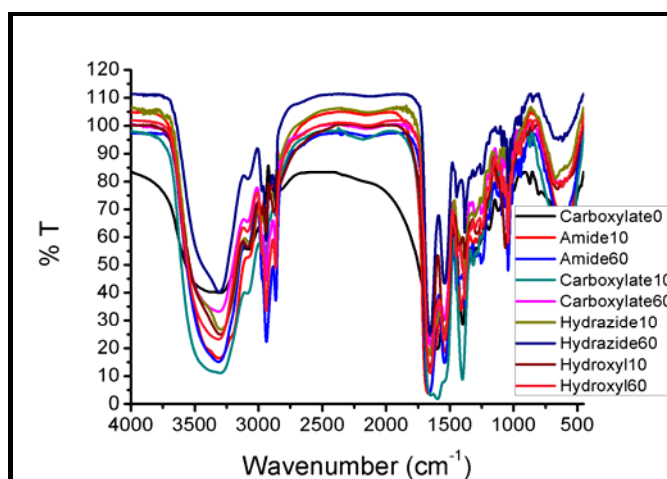


Figure 6.5. FTIR spectra of silver Nps in functionalized biloproteins (DS 10 and 60).

6.3.2.4 XRD analysis

The typical powder XRD pattern of silver Nps is shown in Fig. 6.6. The diffraction peaks at different 2θ angles, can be indexed to (111), (200), (220) and (311) planes of pure silver (Xu 2006). (Table 6.3)

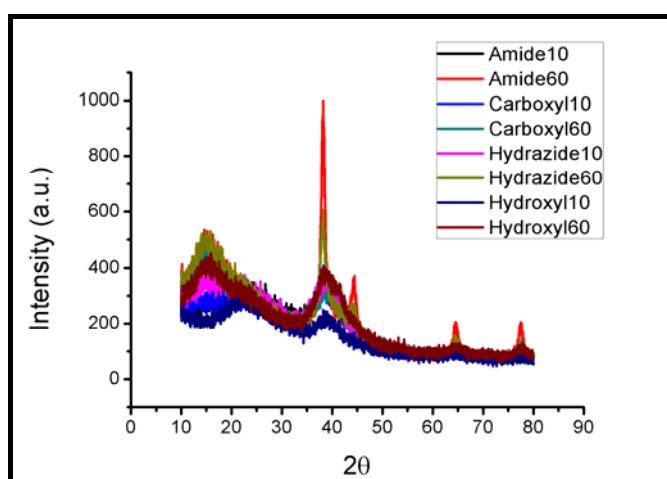


Figure 6.6. XRD pattern of silver Nps in functionalized biloproteins (DS 10 and 60).

Table 6.3. XRD angles of functionalized biloproteins coated silver Nps.

Sr. no	Biloproteins with Ag	Diffraction angles (2θ)	Diffraction planes
1.	Amide 10	38.95, 65.075	Ag 111, Ag 220
2.	Amide 60	38.26, 44.39, 64.54, 77.51	Ag 111, Ag 200, Ag 220, Ag 311
3.	Hydrazide 10	38.43, 65.075, 77.35	Ag 111, Ag 220, Ag 311
4.	Hydrazide 60	38.26, 44.21, 64.37, 77.51	Ag 111, Ag 200, Ag 220, Ag 311
5.	Carboxylate 10	38.26, 64.19, 77.68	Ag 111, Ag 220, Ag 311
6.	Carboxylate 60	38.43, 64.89, 77.34	Ag 111, Ag 220, Ag 311
7.	Hydroxyl 10	38.60, 63.84	Ag 111, Ag 220
8.	Hydroxyl 60	38.43, 64.54, 77.86	Ag 111, Ag 220, Ag 311

For the peak at 38 degrees, average particle size was estimated from Debye-Scherrer formula

$$D = 0.9 \times \lambda / W \cos \theta$$

Where ' λ ' is wave length of X-Ray (0.1541 nm), 'W' is FWHM (full width at half maximum), ' θ ' is the diffraction angle and 'D' is crystallite size. The crystallite sizes of Ag Nps obtained for functional biloproteins were amide (5.24), carboxyl (9.30), hydrazide (5.55) and hydroxyl (5.43). In TEM section, these are compared with particle size data and discussed.

XPS regions of various elements for the silver nanoparticles are shown in Figure 6.7. The occurrence of carbon and nitrogen signals confirmed the presence of biloproteins on the surface of the Ag Nps. XPS spectrum of C 1s (Fig. 6a) was fitted to multiple Gaussian curve. The C 1s spectrum is composed of two peaks. The binding energies of the two peaks were 286.5 and 289.5 eV, which can be assigned to C–C and C–N carbon atoms in the biloproteins respectively (Xu 2006).

In hydroxylated biloproteins the peak at 286.51 eV can be assigned to C–OH carbon atoms in the amino ethanol moiety. Similar peak was exhibited by 2-hydroxy-1, 3-bis(octadecyldimethylammonium) propane dibromide (18-3(OH)-18) a gemini surfactant capped silver Nps at 286.3 eV (Xu 2006). Curve in the N 1s region (Fig. 6b) shows a peak at 402 eV. In comparison to precursors, the N 1s peak shifts to a higher binding energy, implying decrease in electron density, probably due to interactions between functionalities and the silver nanoparticle core. Fig. 6c shows two peaks at 369.0 and 375.0 eV, resulting from Ag 3d_{5/2} and Ag 3d_{3/2}, respectively which indicates that silver is in Ag⁰ form (Xu 2006).

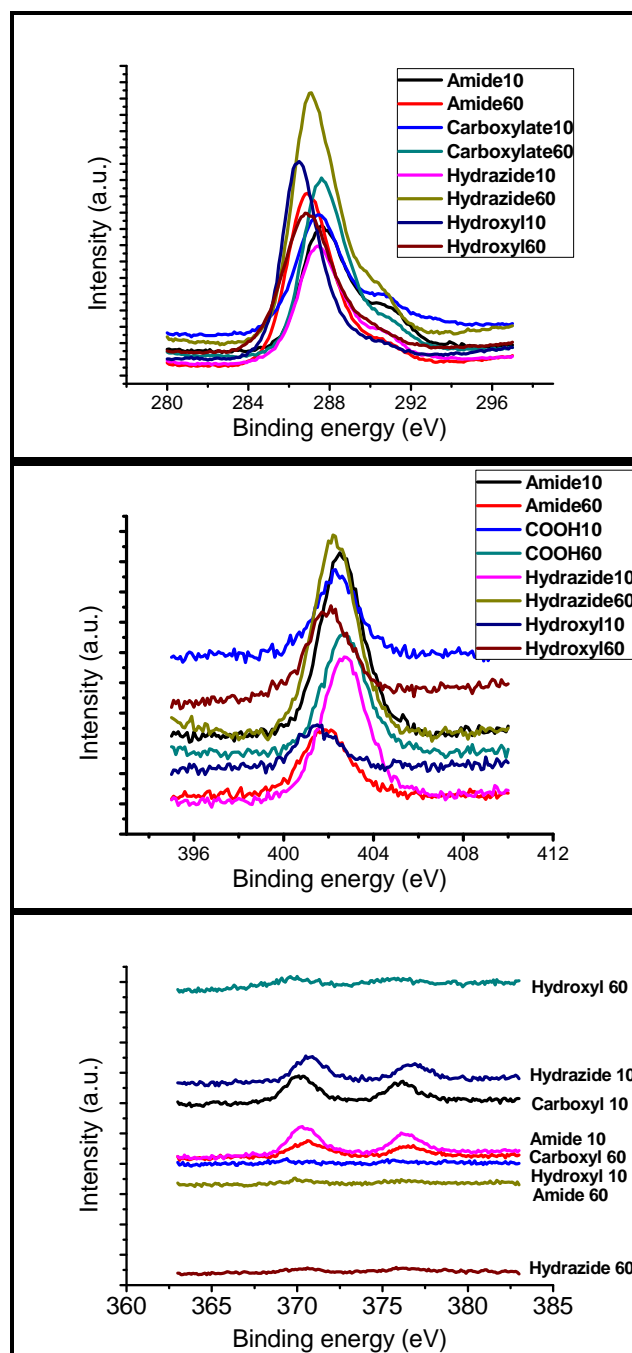


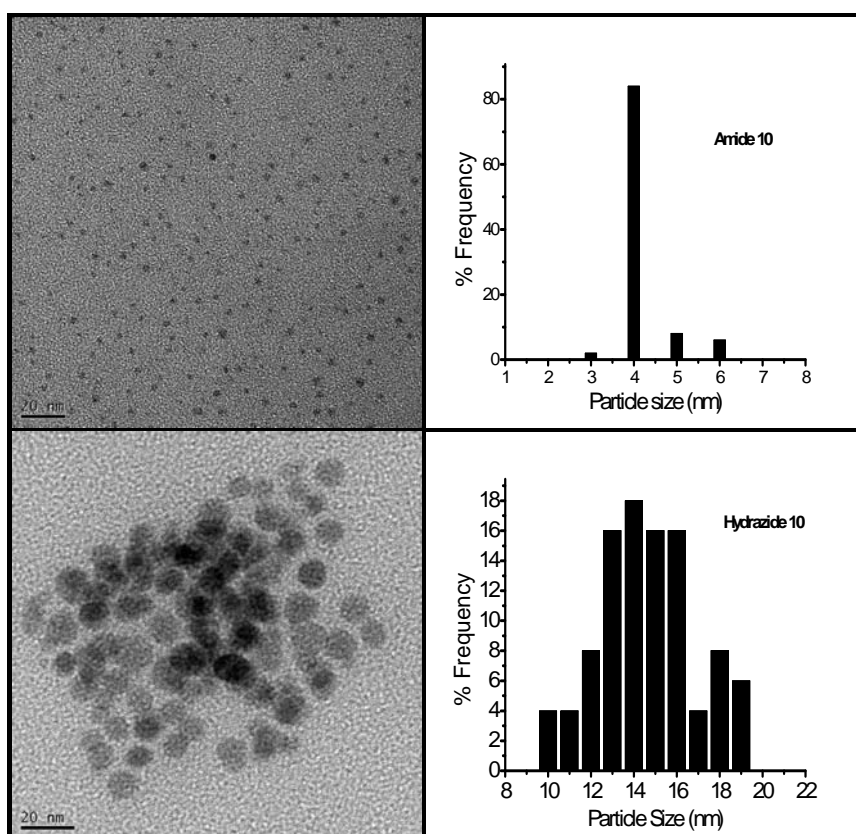
Figure 6.7. C 1s, N 1s and Ag 3d XPS spectra of Ag Nps in functionalized biloproteins.

The thermal stability and decomposition of biloproteins and silver Nps were investigated by TGA. In all the functionalized biloproteins, 7-15 % w/w of residue

remained when the samples were heated to 900 °C which corresponds to the loading of silver Nps.

6.3.2.5 TEM of nanoparticles

Morphology of silver Nps and distribution in biloprotein templates was investigated by TEM which showed the particle size in the range 5 - 20 nm. (Figure 6.8) Amidated biloproteins formed mono dispersed spherical Nps which had an average diameter of approximately 4 nm. Hydrazide functionalized biloproteins also formed monodispersed spherical Nps having average diameter 14 nm. Carboxylated and hydroxylated biloproteins formed polydispersed Nps of average diameter in the range 5 - 20 nm. From the XRD data and TEM particle size data, it is very clear that only Amide capped Ag Np are single crystallite Nps and others are formed from aggregates of crystallites.



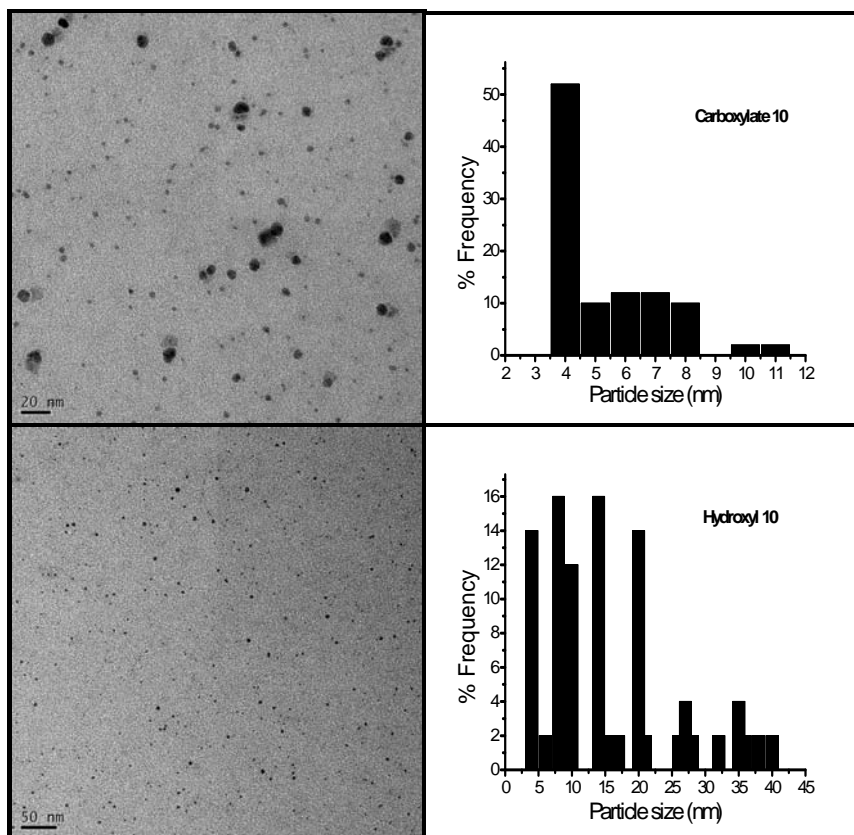


Figure 6.8. TEM of silver Nps capped by functionalized biloproteins at DS 10.

6.3.1 Nano-patterning of silver Nps

Patterning of functionalized metal nanoparticles (MNPs) into one-, two-, and three-dimensional assembled structures is very important in view of their potential applications in sensors, catalysis, optical and electronic nanodevices. In particular, the unique properties of one-dimensional assemblies of MNPs, such as photonic, electronic and energy transfer between the nanoparticles, make them desirable not only for the production of nanodevices, but also for the understanding of fundamental phenomena which occur in biological process at the nanometerscale.

However, arranging metal Nps into ordered arrays requires specific self-assembly technique. Recent studies reveal that nanoparticles often aggregate in solution or during TEM specimen preparation due to anisotropic and inhomogeneous distribution of

capping agents within the stabilizer coating and the lack of offsetting forces capable of positioning the agglomerated particles relative to one another. In order to control the assembly of Nps in solution, the interactions between nano building blocks need to be understood so that these could be controlled to design target structures. This could be achieved by using a template that can direct the assembly of monodispersed spherical Nps. Most of the current approaches for the preparation of assemblies of Nps use biomolecules such as DNA, fungi, virus, peptide, amyloid fibril, etc. as scaffolds due to their rigid structures (Bhattacharjee 2007).

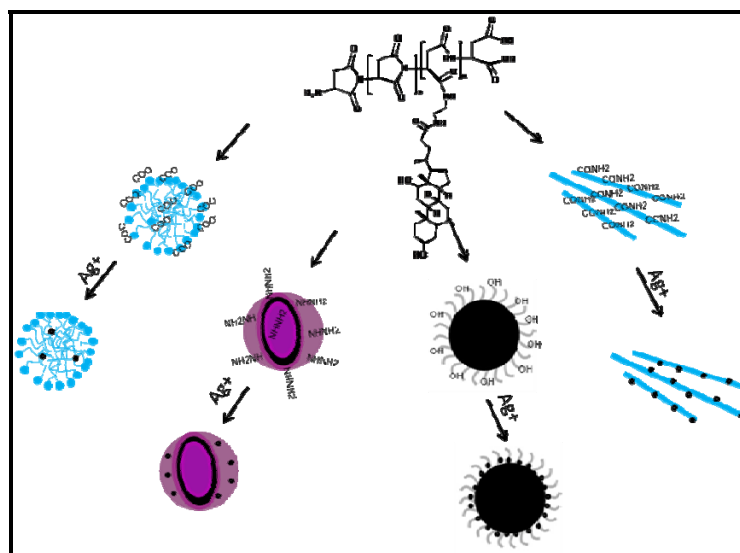


Figure 6.9. Schematic illustration of nanopatterned silver nanoparticles in biloproteins.

On increasing hydrophobic content further to DS 60, functionalized biloproteins formed higher order morphologies like micelles, vesicles, tubules and Nps depending upon size of head group as described in chapter 4. Those structures are used here as templates to nano-pattern silver (Figure 6.9).

Hydrazide functionalized biloproteins formed giant vesicles studded with silver Nps. The size of vesicle template was 1- 1.5 μ and silver Nps were 5 - 10 nm. The Nps were only present on the outer wall of vesicles and not inside wall or in the aqueous phase within the vesicle (See inset). This can be attributed to the fact that both AgNO_3 and

NaBH_4 do not diffuse into the interior of the vesicle because of the hydrophobic nature of the wall and also reduction has taken place on the surface.

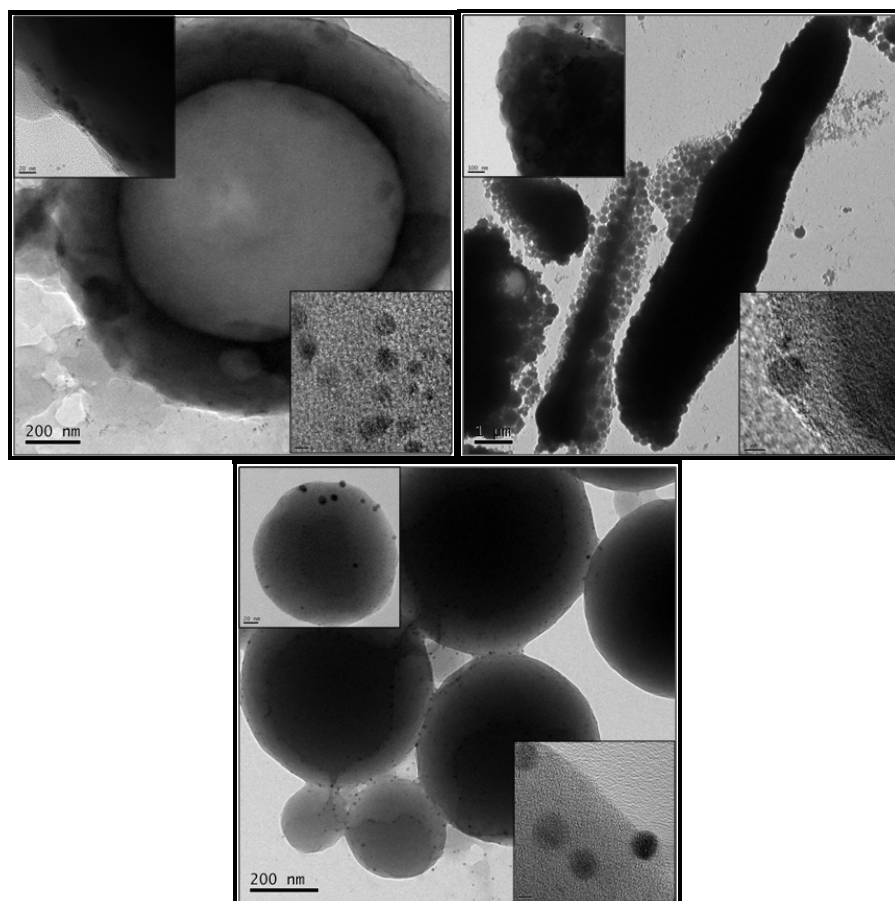


Figure 6.10. TEM of nano-patterned silver Nps in hydrazide, amide and hydroxyl functionalized biloproteins.

Amidated biloproteins formed elongated baton like structures of size 1 - 2 μ width and 10 - 20 μ length. Silver was reduced to yield Nps of size 5 – 10 nm uniformly distributed along the length of baton surface. (see inset) Hydroxylated biloproteins formed nano and microspheres of size 0.2 - 2 μ . Silver Nps of size 5 – 10 nm were studded on and within the microsphere structures to yield ring or necklace like patterns (See inset).

Similar approach has earlier been reported using different polymers and different block copolymers. However, templates comprising same polymer backbone and different functional groups have not been yet reported. PNIPAM coated Polystyrene microspheres were used as template for in situ formation of silver studded microspheres (Chen 1998). Poly(styrene-alt-maleic anhydride) self assembled to form tubes on which silver could be grown using AgCN to yield silver nanowires of size 5-200 nm width and more than 50 μm length (Lazzara 2009).

Recently layer by layer self assembly has been explored for nano-patterning of silver inside polymeric nanostructures. Laser induced hyperthermic character of Ag Nps leads to the rupture of nanostructures (Radziuk 2007). We believe that laser induced rupture of different silver studded biloprotein morphologies could be explored for stimuli sensitive drug delivery

6.3.2 Gold nanoparticles

Gold Nps exhibit lower toxicity and exceptional photo-thermal properties which find applications in diagnostics and drug delivery. Thiols have been most widely investigated capping agents for gold. Carboxylates are equally effective as evident from synthesis of citrate capped Au Nps with different shapes (Turkevich 1951, Dong 2009).

Carboxylated biloproteins were evaluated as capping agent by both thermal and chemical reduction methods. The effect of molecular weight as well as DS was investigated to evaluate the effect of contour length and rigidity of biloprotein self assemblies.

A strong absorption peak in the range 519 – 527 nm was observed for biloprotein capped Au Nps prepared by reflux and NaBH₄ method. (Figure 6.11) Low molecular weight biloproteins capped gold Nps more efficiently than high molecular weight counterparts as indicated by intensity of SPR peak. This is in contrast to that observed in case of silver Nps discussed earlier. However it is well in accordance with the report on preparation of Ag Np by γ irradiation using PVP as capping agent. According to

which more silver ions were in close proximity within a PVP molecule of MW 1,300,000 than in PVP chains of lower molecular weight 10000, which result in formation of aggregates of crystallites yielding larger silver Nps (Shin 2004).

Increasing degree of hydrophobicity enhanced the stabilization of Au Nps as observed by increased intensity of SPR maxima. This is in accordance with carboxylated biloproteins capped silver Nps.

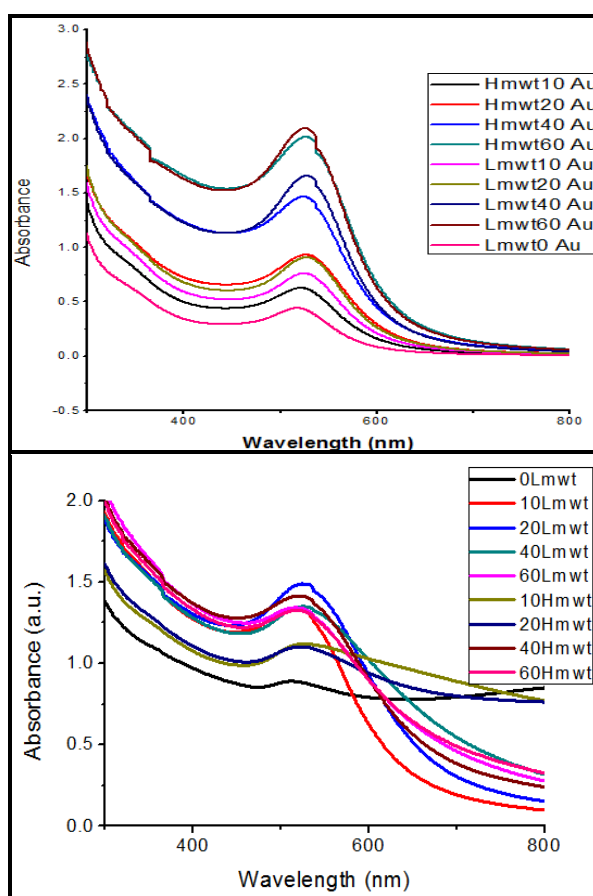


Figure 6.11. UV-visible spectra of Au Nps in carboxylated biloproteins (Reflux and NaBH₄ method).

Presence of biloproteins along with Au Nps was confirmed by IR spectroscopy as reported in Silver Nps. Typical XRD patterns of gold capped biloproteins display

diffraction peaks at 2θ angles of 38.4 and 64.5° which correspond to the (111), and (220) planes of the cubic phase of Au, respectively (Feng 2006).

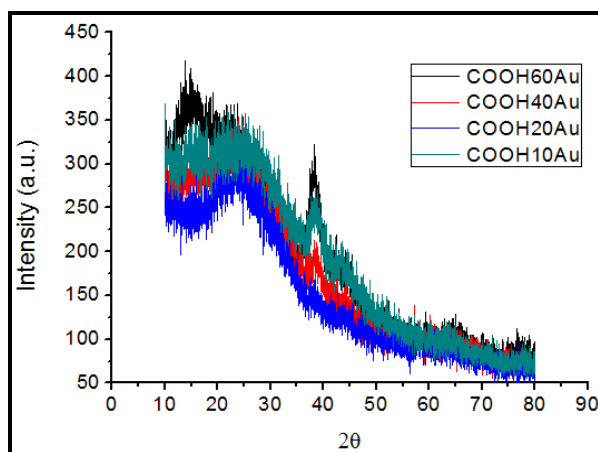


Figure 6.12. XRD spectra of Gold Nps with carboxylated biloproteins prepared by reflux method.

XPS spectra of Nps displayed 2 peaks with different binding energies. The values for Nps prepared by NaBH_4 method were 85.70, 89.47 and for Nps made by reflux method were 87.62, 91.44 eV.

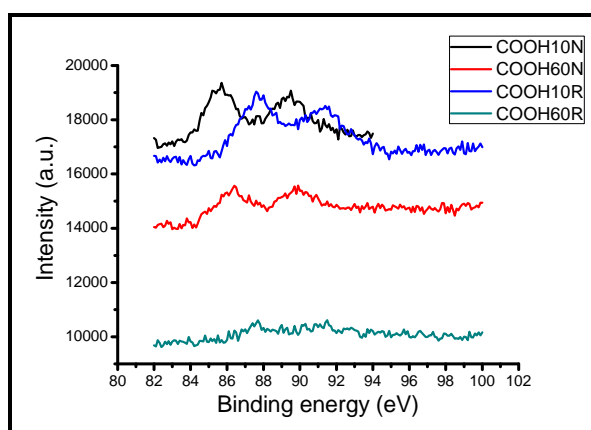


Figure 6.13. XPS spectra of Gold Nps with carboxylated biloproteins prepared by reflux and Chemical reduction (NaBH_4) method.

The line shape and peak-to-peak distance of the Au 4f doublet is consistent with the Au⁰ state, the binding energies 85.7, 87.62 (Au 4f7/2) and 89.47, 91.44 (Au 4f5/2) were slightly higher than expected for bulk Au (Au 4f7/2 84.0 eV and Au 4f5/2 87.6 eV) (Wang 2008).

TEM indicated that gold Nps were spherical in shape and ranged in size from 5 - 10 nm. It also confirmed earlier findings that size of gold Nps decreased with an increase in hydrophobicity.

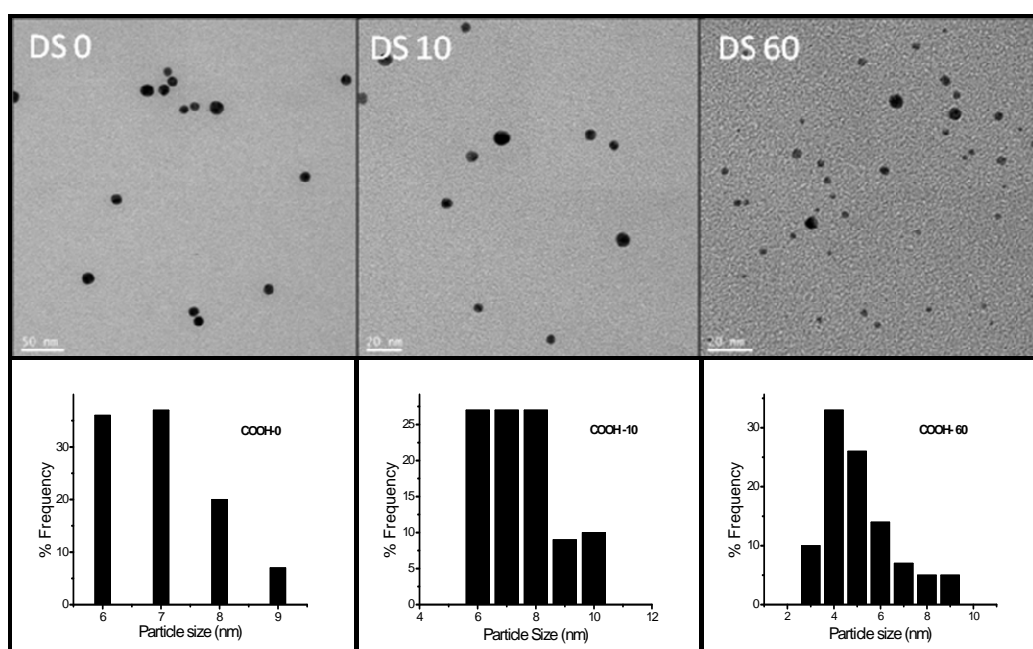


Figure 6.14. TEM of Au Nps capped by carboxylated biloproteins.

Thus Gold Nps were capped by carboxylated biloproteins (DS 10) and stabilized against aggregation. Molecular weight, hydrophobic content and method of preparation exhibited their effect on particle size distribution.

6.4 Conclusions

Carboxylated biloprotein mediated Silver Np synthesis could be explored using three different methods namely reflux, UV and chemical reduction which indicated that NaBH₄ reduction method yields complete reduction of metal salts with mono dispersed

Nps. In reflux and UV method observation of extra peak indicated polydispersed Nps of different size and shape due to aggregation. Similarly at low hydrophobicity, different functionalized biloproteins acted as capping agents but amidated biloproteins was the best with lowest silver Nps size 4 nm and low polydispersity. IR spectroscopy confirmed presence of biloproteins along with silver and gold Nps. With increase in hydrophobic content (DS 60) different functionalization like carboxylate, hydroxyls, amide and hydrazide formed morphologies like micelles, vesicles, tubules and Nps which were explored as templates for synthesis of silver Nps. The nano patterning followed ring and necklace like patterns which could be explored further for laser stimulated ablation studies. These nano-patterns would be useful for drug delivery of bioactives through pore generation using laser as stimuli.

6.5 References

1. Allen M., Willits D., Mosolf, J., Young, M., Douglas, T. *Adv. Mater.* 2002, 14, 1562-1565.
2. Antonietti M, Wenz E, Bronstein L, Seregina M. *Adv Mater.* 1995,7, 1000–5.
3. Bhattacharjee R. R., Mandal T. K., *Journal of Colloid and Interface Science* 2007, 307, 288–295.
4. Blum A. S., Soto C. M., Wilson C. D., Cole J. D., Kim, M. Gnade, B. Chatterji, A. Ochoa W. F., Lin T., Johnson J. E., Ratna B. R. *Nano Lett.* 2004, 4, 867-870
5. Brause R, Moeltgen H, Kleinermanns K *Applied Physics B: Lasers and Optics* 2002, 75:711-716.
6. Brust M., Merryl Walker, Donald Bethell, David J. Schiffrin and Robin Whyman J. *CHEM. SOC., CHEM. COMMUN.*, 1994, 801-802.
7. Bukreeva T. V., Parakhonskiy B. V., Marchenko I. V., Khlebtsov B. N., Khlebtsov N. G., Dementieva O. V., Savvateev M. N., Feigin L. A., Kovalchuk M. V., *Nanotechnologies in Russia*, 2008, Vol. 3, Nos. 1, 2, 85–93.
8. Cha J. N., Katsuhiko K., Zhou Y., Christiansen S. C., Chmelka B. F., Stucky G. D., Morse D. E., *Proc. Natl. Acad. Sci. U.S.A.* 1999, 96, 361-365.

9. Chang S., Srikanth Singamaneni, Eugenia Kharlampieva, Seth L. Young and Vladimir V. Tsukruk* *Macromolecules*, 2009, 42, 15, 5781–5785
10. Chen M., Wang L. Y., Han J. T., Zhang J. Y., Li Z. Y., Qian D. J. *J. Phys. Chem. B* 2006, 110, 23, 11224-11231.
11. Chen C., Chen M., Serizawa T., Akashi M. *Adv. Mater.* 1998, 10, 14, 1122-1126.
12. Copland J., Eghtedari M., Popov V., Kotov N., Mamedova N. Motamedi M., Oraevsky A. *Mol. Imaging Biol.* 2004, 6, 341-349.
13. Daniel M. C., Astruc, D. *Chem. Rev.* 2004, 104, 293-346.
14. Ding Y, Liu J, Wang H, Shen G, Yu R: *Biomaterials* 2007, 28:2147-2154. Huang SH *Clin Chim Acta* 2006, 373, 139-143.
15. Dong X., Ji X., Wu H., Zhao L., Li J., Yang W., *J. Phys. Chem. C* 2009, 113, 6573–6576
16. Dong X., Xiaohui Ji, Hongli Wu, Lili Zhao, Jun Li, and Wensheng Yang *J. Phys. Chem. C* 2009, 113, 6573–6576
17. Douglas, T., Strable, E., Willits, D., Aitouchen, A., Libera, M., Young, M. *Adv. Mater.* 2002, 14, 415-418.
18. Eby D. M. Schaeublin N. M., Farrington K. E., Hussain S. M., Johnson G. R., *ACS Nano* 2009, 3, 4, 984–994
19. Eghtedari M., Copland J., Kotov N., Oraevsky A., Motamedi M. *Lasers Surg. Med.* 2004, 164, 16.
20. Elechiguerra J. L., Burt J. L., Morones J. R., Camacho-Bragado A., Gao X., Lara H. H., Yacaman M. J., *Journal of Nanobiotechnology* 2005, 3, 6.
21. Ershov, B. G., Henglein, A., *J. Phys. Chem. B* 1998, 102, 10663.
22. El-Atwani O. C., Aytun T., Mutaf O. F., Srot V., van Aken P. A., Ow-Yang C. W., *Langmuir*, 2010, 26, 10, 7431–7436.
23. Etchegoin P., Liem H., Maher R., Cohen L., Brown R., Milton, M. Galop J. *Chem. Phys. Lett.* 2003, 367, 223-229
24. Falletta E., Bonini M., Fratini E., Nostro A. L., Pesavento G., Becheri A., Nostro P. L., Canton P., Baglioni P., *J. Phys. Chem. C* 2008, 112, 11758–11766

25. Feng X., C. Mao, G. Yang, W. Hou, Zhu J.J. *Langmuir* 2006, 22, 9, 4384–4389.
26. Feng Z., Liang C., Li M., Chen J., Li, C. J. *Raman Spectrosc.* 2001, 32, 1004–1007.
27. Gangwal J. J., Kulkarni M. G. 2010, Invited lecture in 6th Singapore International Chemical Conference Chemical Synthesis, Creativity and Applications.
28. Gao Y., P. Jiang, D.F. Liu, H.J. Yuan, X.Q. Yan, Z.P. Zhou, J.X. Wang, L. Song, L.F. Liu, W.Y. Zhou, G. Wang, C.Y. Wang, S.S. Xie, *J. Phys.Chem. B* 2004, 108, 12877.
29. Henglein, A., Giersig, M. *J. Phys. Chem. B* 1999, 103, 44, 9533-9539.
30. Henry, A., McCarley, R. *J. Phys. Chem.B* 2001, 105, 8755-8761.
31. Hirsch L.R., Halas N.J., West J.L., *Methods Mol Biol* 2005, 303, 101-111.
32. Housni A., Ahmed M., Liu S.,‡ Narain R., *J. Phys. Chem. C*, 2008, 112, 12282–12290.
33. Hulteen, J., Treichel, D., Smith, M., Duval, M., Jensen, T., Van Duyne, R. J. *Phys. Chem. B* 1999, 103, 9846-9853.
34. Hussain I., Brust M., Papworth A. J., Cooper A. I., *Langmuir* 2003, 19, 4831-4835
35. Ishii T.,† Hidenori Otsuka,‡§ Kazunori Kataoka,‡ and Yukio Nagasaki *Langmuir*, 2004, 20, 3, 561–564.
36. Jacob D. Gibson, Bishnu P. Khanal, and Eugene R. Zubarev *J. Am. Chem. Soc.*, 2007, 129, 37, 11653–11661.
37. Jana N. R., Erathodiyil N., Jiang J., Ying J. Y. *Langmuir*, 2010, 26, 9, 6503–6507
38. Ji M., Chen X., Wai C.M., Fulton J.L., *J. Am. Chem. Soc.* 1999, 121, 2631.
39. Kemp M. M., Kumar A., Mousa S., Park T., Ajayan, P., Kubotera N. Mousa S. A., Linhardt R. J., *Biomacromolecules* 2009, 10, 589–595.
40. Lazzara T. D., Bourret G. R., Lennox R. B., van de Ven T. G. M., *Chem. Mater.* 2009, 21, 2020–2026.

41. Jin R, Charles Cao Y, Hao E, Gabriella S M, George C S and Mirkin C A
Nature 2003, 425, 487
42. Kerker M. Journal of Colloid and Interface Science 1985,105, 297-314.
43. Klaus, T., Joerger, R., Olsson, E., Granqvist, C. G. Proc. Natl. Acad. Sci. U.S.A.
1999, 96, 13611-13614
44. Klem, M. T., Willits, D., Young, M., Douglas, T. J. Am. Chem. Soc. 2003,125,
10806-10807.
45. Kuo P and Wei-Fu Chen J. Phys. Chem. B, 2003, 107, 41, 11267–11272.
46. Lowenstam, H. A. Science 1981, 211, 1126-1130.
47. Lv Y., Liu H., Wang Z., Liu S., Hao L., Sang Y., Liu D., Wang J., Boughton
R.I. Journal of Membrane Science 331, 2009, 50–56.
48. Mayer, A. B. R., Mark, J. E., J. Polym. Sci., A: Polym. Chem. 1998, 35, 197
49. Meldrum, F. C., Wade, V. J., Nimmo, D. L., Heywood, B. R., Mann, S. Nature
1991, 349, 684-687.
50. Mo¨ssmer S, Spatz JP, Mo¨ller M, Aberle T, Schmidt J, Burchard W.
Macromolecules.2000, 33, 4791–8.
51. Morones J. R. and Frey W. Langmuir 2007, 23, 8180-8186.
52. Mukherjee P, Bhattacharya R, Bone N, Lee YK, Patra CR, Wang S, Lu L,
Charla S, Banerjee PC, Yaszemski MJ, et al J. Nanobiotechnology 2007, 5, 4.
53. Munro, C. H., Smith, W. E., Garner, M., Clarkson, J., White, P. C. Langmuir
1995, 11, 3712.
54. Nickel U., Castell A. Z., Pöpl K., Schneider S., Langmuir, 2000, 16, 23, 9087–
9091.
55. Niidome T, Yamagata M, Okamoto Y, Akiyama Y, Takahashi H, Kawano T,
Katayama Y, Niidome Y J Control Release 2006, 114, 343-347.
56. Patil S. S., Dhumal R. S., Varghese M. V., Paradkar A. R., Khanna P. K.,
Synthesis and Reactivity in Inorganic, Metal-Organic, and Nano-Metal
Chemistry, 2009, 39, 65–72.
57. Petit C, Lixon P, Pileni MP Journal of Physical Chemistry 1993, 97, 12974-
12983.

58. Pucek R., Kvi'tek L., Hrba'c', J. Phys. Chem. B 2004, 43, 1-5.
59. Radziuk D., Shchukin D. G., Skirtach A., Mo'hwald H., Sukhorukov G., Langmuir 2007, 23, 4612-4617
60. Raveendran P., Fu J., Wallen, S. L., J. am. chem. soc. 2003, 125, 13940-13941
61. Riboh, J., Haes, A., McFarland, A., Yonzon, C., Van Duyne, R. J. Phys. Chem.B 2003, 107, 1772-1780.
62. Sakai T. and Paschalis Alexandridis, Langmuir, 2004, 20, 20, 8426–8430.
63. Samoilova N., Kurskaya E., Krayukhina M., Askadsky A., Yamskov I., J. Phys. Chem. B 2009, 113, 3395–3403
64. Saptz J. P., Mo'ssmer S., Hartmann C., Mo'ller M., Herzog T., Krieger M., et al. Langmuir. 2000,16, 407–15.
65. Schueler, D., Frankel R. B., Appl. Microbiol. Biotechnol. 1999, 52, 464-473.
66. Serra A., Filippo E., Re M., Palmisano M., Vittori-Antisari M., Buccolieri A., Manno1 D., Nanotechnology 2009, 20, 165501-7.
67. Seregina M. V., Bronstein L. M., Platonova O. A., Chernyshov D. M., Valetsky P. M., Hartmann J., Chem Mater. 1997, 9, 923–31.
68. Sharma V. K., Yngard R. A., Lin Y., Advances in Colloid and Interface Science 145, 2009, 83–96.
69. Shin H. S, Yang H. J., Kim S. B., Lee M. S. Journal of Colloid and Interface Science 2004, 274, 89–94.
70. Silvert, P. Y., Herrera-Urbina, R., Duvauchelle, N., Vijayakrishnan, V., J. Mater. Chem. 1996, 6, 4, 573-577.
71. Solomon S. D., Bahadory M., Jeyarajasingam A. V., Rutkowsky S. A., Boritz C., Journal of Chemical Education 2007, 84, 2, 322- 325.
72. Silvert P. Y., Herrera-Urbina R., Tekaia Elhsissen K. J. Mater. Chem. 1997, 7, 2, 293-299.
73. Sokolov K., Follen M., Aaron J., Pavlova I., Malpica A., Lotan, R., Richards-Kortum, R. Cancer Res. 2003, 63, 1999-2004.
74. Sosa I. O., Noguez C, Barrera R.G. Journal of Physical Chemistry B 2003, 107, 6269-6275.

75. Suslick, K. S., Fang, M., Hyeon, T. J. *Am. Chem. Soc.* 1996, 118, 11960-11961.
76. Taleb A, Petit C and Pileni M P 1998 *J. Phys. Chem. B*, 102 2214
77. Tan Y, Jiang L, Li Y and Zhu D 2002 *J. Phys. Chem. B*, 106 3131
78. Tao A. R., Habas S., Yang P. D., *Small* 2008, 4, 310.
79. Tominaga J., Mihalcea C., Büchel D., Fukuda H., Nakano T., Atoda N., Fuji H., Kikukawa T. *Appl. Phys. Lett.* 2001, 78, 2417.
80. Van Hying D. L., Zukoski C. F. *Langmuir* 1998, 14 (24), 7034-7046.
81. Voronov A., Kohut A., Peukert W., *Langmuir* 2007, 23, 360-363
82. Wang Z. Zhang Q., Kuehner D., Ivaskab A., Niu L., *Green Chem.*, 2008, 10, 907-909.
83. Wiley B., Sun Y. G., Chen J. Y., Cang H., Li Z. Y., Li X. D., Xia Y. N., *MRS Bull.* 2005, 30 (5), 356-361.
84. Wulandari P., Nagahiro T., Michioka K., Tamada K., Ishibashi K., Kimura Y., Niwano M., *Chemistry Letters* 2008, 37, 8, 888-889.
85. Xiong Y. J., Wiley B., Xia Y. N., *Angew. Chem., Int. Ed.* 2007, 46, 7157.
86. Xu J., Han X., Liu H., Hu Y., *Colloids and Surfaces A: Physicochem. Eng. Aspects* 2006, 273, 179-183.
87. Yin Y., Lu Y., Sun, Y., Xia Y., *Nano Lett.* 2002, 2, 427-430.
88. Zhao M., Sun L., Crooks R. M., *J. Am. Chem. Soc.* 1998, 120, 4245-4246.
89. Zynio S., Samoylov A., Surovtseva E., Mirsky V., Shirshov. *Sensors* 2002, 2, 62-70.

Chapter 7

In situ biodegradable hydrogels from surface cross-linked supramolecular self assemblies

7.1 Reactive micelle based in situ hydrogels

Summary

Conjugation of fatty amines and amine derivatives of bile acids with polysuccinimides followed by reaction with amino ethyl piperazine (AEPz) yielded nanoaggregates bearing surface amino groups. Addition of polyethylene glycol diacrylates (PEGDA) in aqueous media yielded within 1 to 13 minutes, in situ biodegradable hydrogels containing hydrophobic domains. Triclosan was incorporated in these hydrophobic domains which were uniformly distributed in the hydrogels as demonstrated by confocal microscopy. Triclosan was released after a lag of 15 hours on degradation of the hydrogel. The release was sustained over 1 – 10 days from the hydrogels obtained by cross-linking with Jeffamine diacrylamide. Incorporation of hydrophobic domains enhanced hydrogel modulus 10 folds. High modulus and tunable hydrophilic hydrophobic balance, suggests potentials of these hydrogels as scaffolding materials for tissue engineering.

7.1.1 Introduction

Hydrogels formed *in situ* under physiological conditions are desirable in biomedical field as tissue adhesive, for hemorrhage control, tissue engineering and localized drug delivery because they are amenable to instantaneous preparation of complex shapes along with homogeneous loading of bioactives needing minimally invasive surgical technique (Yu 2008, He 2008). The functionalities used for *in vivo* cross-linking systems should be stable for storage, stable at site of application in an aqueous medium, nontoxic to surrounding tissues and spontaneously reacting with complimentary functionalities through addition mechanism to form nontoxic gel useful for clinical applications (Ossipov 2008).

In vivo physical cross-linking triggered by thermal (Yu 2008, Kiessel 2002), ionic (Kroll 1996, Tomme 2005), coordinate, (Roberts 2007) supramolecular (Schnepp 2006, Deng 2007) and stereo complexation (Jong 2000, Hiemstra 2006) is useful but weak mechanical strength and poor stability towards pH, temperature, ionic strength and dilution, limits their utility (Hiemstra 2007b). Photochemical cross-linking is undesirable due to limited accessibility of light in regions of interest, use of potentially toxic photo initiators, generation of highly reactive radicals *in vivo*, incomplete utilization of functionalities, and finally exothermic effect of photo reactions (Ossipov 2008).

Covalent cross-linking resulting from reactive functionalities has been useful for the preparation of injectable matrices, which deliver drugs in controlled manner at the sight of interest and deliver growth factors maintaining favourable environment for tissue regeneration. *In vivo* resorbable materials can be classified as (1) Synthetic scaffolds e.g. PVA gel (Ossipov 2008), (2) Semi synthetic scaffold e.g. Hyaluronate gel (Ghosh 2005) and (3) Natural scaffold eg. Fibrin gel (Ehrbar 2007).

In situ chemoselective cross-linking comprises set of reactive functionalities like electrophilic groups e.g. aldehyde, acrylates and epoxy and nucleophiles like thiols and

amines The polymers which bear above mentioned reactive functionalities are PEG (Viers 2000, Vernon 2003, Wetering 2005), Dextran (Hiemstra 2007a, Weng 2007), Hyaluronic acid (Ghosh 2005), Heparin (Tae 2007), Chitosan (Weng 2007), PVA (Tortora 2007, Ossipov 2008), Pluronics (Niu 2008) and peptides (Suk 2009, Ehrbar 2007).

The instability of aldehydes towards aqueous medium and their supposed toxigenic potential, limits utility for in vivo gel formation (Wallace 2001, Ossipov 2008). Epoxy functionality needs rigorous conditions like high temperature, longer duration and higher pH to execute cross linking reaction (Wang 2009), which is not feasible at in vivo conditions.

Michael addition between PEG thiols and acrylates or vinyl sulfones leads to in situ formed gels composed of cleavable ester linkages. The instability of thiols and potential to form disulfide linkage on oxidation causes premature cross-linking on storage which limits utility of the system for *in situ* use (Van Tomme 2008). Michael addition reaction between amines and acrylates in organic solvents has been reported earlier to develop a combinatorial library of polymers for applications in gene delivery (Lynn 2000). However the reaction is rather sluggish and takes few days to go to completion. Recently, Ranu et.al. (2007) reported that even at room temperature the rate of aza Michael addition can be accelerated significantly by mere use of water as reaction medium.

Ossipov et.al (2008) demonstrated gel formation within 30 sec through aza Michael addition between oxyamine and acrylate on PVA, suggesting the utility of the approach for clinical applications. Our group also demonstrated that the rates of aza Michael addition reaction can be dramatically accelerated in an aqueous medium to form *in situ* hydrogel instantaneously (Nair 2010). While the utility of these gels as scaffold material and depot for macromolecular drugs was demonstrated, it was realized that manipulation of hydrophilicity in microstructure of hydrogel, desirable for tissue

engineering (Haigh 2000, 2002, Rimmer 2005, Sun 2007) and hydrophobic drug delivery was not possible.

In order to control adhesion and drug release, micelles, nanoparticles, microspheres and emulsions have been incorporated in the hydrogel matrix (Chandra 2010, Shingel 2009, Chang 2010, Fang 2010, Cascone 2002, Yeo 2007). Thus there exists a need for *in situ* hydrogels which have hydrophobic domains within hydrogel matrix to enable uniform drug loading and sustained release.

In this chapter we describe the use of the same bile acid - polysuccinimide conjugates described in chapter 3 along with fatty amine - polysuccinimide conjugates and their modification with amino ethyl piperazine so as to form reactive micelles with bile or fatty core and amine corona. These micelles exhibit different CAC, anisotropy and particle size values depending upon the type of hydrophobe and its content. The biloprotein and lipoprotein micelles on mixing with PEG diacrylates formed *in situ* hydrogels through spontaneous aza - michael addition. The rheological studies indicated that hydrogels containing hydrophobic domains exhibit 10 folds higher modulus than control gels. These gels could act as useful scaffolding material because of high modulus and tunable hydrophilic hydrophobic balance within cross-linked hydrogel environment. In addition, the hydrophobic domains have been explored for encapsulation and release of Triclosan.

This approach offers following advantages over previous ones.

1. Efficient utilization of reactive functionalities for cross linking led gel formation.
2. Faster gelation owing to better presentation of reactive groups.
3. Viscosity contribution by both self assembly and cross linking mechanism yield higher modulus hydrogel, useful as a scaffold in tissue engineering.

4. Presence of hydrophobic domains in hydrogel offers hydrophobic surfaces for tissue adhesion and alignment also useful for hydrophobic drug solubilization and their delivery.
5. Delayed and timed drug release pattern depending upon rate of degradation of hydrogel matrix.

7.1.2 Experimental

7.1.2.1. General

L- aspartic acid, Amino ethyl piperazine (AEPZ), Deoxycholic acid, Polyethylene glycol diacrylate Mn 700 (PEGDA), amine terminated PPO-PEO-PPO (Jeffamine) diacrylamide, Pyrene, Diphenyl hexatriene (DPH), Nile red, 5/6 carboxy fluorescein, FITC dextran, Dicyclohexylcarbodiimide (DCC), Octadecylamine (C₁₈), Hexadecylamine(C₁₆) and Dodecylamine (C₁₂) were all purchased from Aldrich. N-hydroxysuccinimide (NHS) (SD fine India), o-Phosphoric acid (85%, Merck, India) Ethylene diamine (SRL, India), Dimethylformamide (DMF) (Merck, India) dried and stored on molecular sieves, Dry Methanol (SD fine India), Acetone GR (Merck, India), Hydrochloric acid (Merck, India), Sodium hydroxide (Merck, India)

7.1.2.2. Synthesis of polysuccinimide (PSI)

PSI was synthesized by dehydro polycondensation method under using o-Phosphoric acid as catalyst as described in chapter 3.

7.1.2.3. Synthesis of amino ethyl deoxycholamide (AEDOCA)

AEDOCA was synthesized through NHS ester of Deoxycholic acid and excess of ethylene diamine as described in chapter 3.

7.1.2.4. Synthesis of reactive bilo / fatty polymer conjugates

The reactive polymer conjugates were prepared as discussed in chapter 3. Briefly, 4 g of PSI was dissolved in 40 ml dry DMF to which different amounts of AEDOCA or C₁₂, C₁₆, C₁₈ fatty amine were added to achieve corresponding substitution. The suspension

was stirred at room temperature till solubilized and then maintained at 65 - 70 ° C for 24 hrs under nitrogen. Solution was then concentrated and precipitated in excess Acetone to remove unreacted AEDOCA or fatty amine. After sufficient washing with Acetone, the reactive polymer conjugates were dried in vacuum desiccator.

The DMF solutions of polymer conjugates were then added slowly with stirring to excess Amino ethyl piperazine solution in DMF at 2 - 8 ° C and stirred for 3 hours at RT. This DMF solution was then filled in dialysis tube and dialyzed against distilled water for 24 hours with intermittent change of outside water. Dialyzate was then freeze dried to yield AEDOCA or fatty amine substituted Piperazino ethyl aspartamide called henceforth as synthetic biloprotein or lipoprotein respectively. (Figure 7.1)

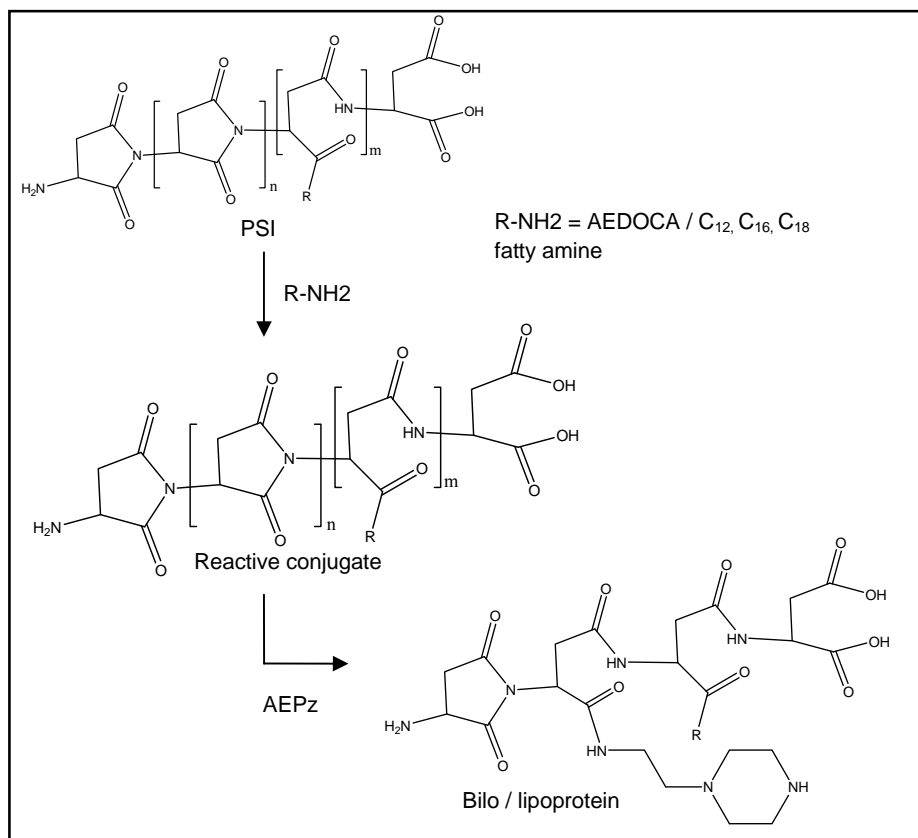


Figure 7.1. Synthesis of aminated bilo / lipoproteins.

7.1.2.5. Preparation of bilo / lipoprotein nanoaggregates

AEDOCA or fatty amine substituted Piperazino ethyl aspartamide (Synthetic biloprotein or lipoprotein) was added in Phosphate buffer 7.4 pH and stirred for 5 minutes on Spinix vertex stirrer at room temperature. It was then sonicated in bath sonicator to completely disaggregate particles.

7.1.2.6. Bilo / lipoprotein characterization

For determination of molecular weight of PSI, it was reacted with ethanolamine at 5 - 10 ° C in DMF to obtain Poly hydroxyl ethyl aspartamide, a water soluble analogue. Molecular weights were then determined at 25 ° C by aqueous Gel permeation chromatography (GPC), equipped with TSK- GEL columns using 0.2 M NaNO₃ at a flow rate of 1 ml/min. The columns were calibrated using PEO standards. Conjugation of AEDOCA or fatty amine on PSI and functionalization with amino ethyl piperazine was probed by ¹H NMR in DMSO d₆ at 200 MHz. Biloprotein and lipoprotein aggregates were characterized by static light scattering studies, Zeta potential measurements, Turbidity measurements, fluorescence spectroscopy and Transmission electron microscopy as reported earlier in chapter 3.

For surface tension measurements a stock solution of polymer conjugate (2 mg/ml) was prepared in deionized water. 25 ml of this solution was transferred to a beaker and surface tension was measured by Wilhelmy plate. For each measurement, at least three readings were taken and the mean γ (mN/m) value was recorded. Before each experiment, the instrument was calibrated and checked by measuring the surface tension of distilled water. Before every experiment Platinum plate was cleaned with deionized water and activated on gas burner to remove any adsorbed contaminant.

7.1.2.7. In situ gel preparation and its characterization

a) Gelation time

To determine the gelation time, each 250 μ L solution of aminated synthetic biloprotein or lipoprotein and PEG diacrylate (molar ratio of amine to unsaturated groups was kept

at 1.1) in isotonic Phosphate buffer (pH 7.4) was mixed by vortexing and held at 37 °C. The gelation time was determined by the vial tilting method. When the sample showed no flow on tilting and holding for 5 sec, it was regarded as a gel.

b) Rheological study

Rheology experiments were performed at 37 ° C on a US 200 rheometer (Anton Paar). Aminated synthetic biloprotein or lipoprotein and PEG diacrylate were dissolved separately in isotonic Phosphate buffer (pH 7.4). These two solutions were mixed at molar ratio of amine to unsaturated groups at 1.1 and quickly applied to the rheometer. The complex viscosity, storage and loss modulus were measured at constant amplitude of 2 % with angular frequency of 1 rad / sec as a function of time.

c) Morphological analysis by ESEM

Both the polymer solutions were placed in cup / sample holder of ESEM and field was applied for evaluation of surface morphology and nanoaggregate distribution inside hydrogel. Hydrogels were freeze dried and freeze fractured to study morphological patterns inside dried hydrogel matrix.

d) CLSM study

Hydrophobic domains in hydrogels were probed using confocal microscopy. Aminated lipoprotein solution was incubated with Nile red (hydrophobic dye) while FITC-dextran was solubilized in aqueous PEGDA solution. Both the solutions were mixed and placed on cavity silde covered with cover slip and sealed by nail lacquer. This slide was then mounted inverted on stage of Zeiss LSM510 confocal laser-scanning microscope (CLSM). Lasers of excitation wavelength at 484 nm and 650 nm were used to detect distribution of Nile red and FITC dextran in hydrogels.

7.1.2.8. Degradation study

The samples prepared for gelation time determination were weighed as zero hour reading and kept for degradation at 37 ° C with 3 ml of 0.1M isotonic Phosphate buffer

pH 7.4. For determining weight loss of gel, every 24 hrs buffer was removed, sample vials were inverted and allowed to dry on tissue paper and weighed. The same sample vial was then again filled with 3 ml of buffer and kept at 37 ° C. This procedure was repeated till gel was degraded completely. The time required for complete disappearance of gel in isotonic phosphate buffer at 37 ° C, pH = 7.4 was taken as complete degradation time.

7.1.2.9. Drug encapsulation and release

Triclosan (TCN) was dissolved in lipoprotein self assemblies (C₁₂-20, C₁₆-20 and C₁₈-20) in phosphate buffer (pH= 7.4) by bath sonication. The self assemblies were then cross-linked *in situ* using PEGDA and Jeffamine (PPO-PEO-PPO) diacrylamide to yield hydrogel. The hydrogels were placed in 10 ml Phosphate buffer (pH 7.4) with or without 2% SDS and studied TCN release. After each time interval 1 ml was withdrawn and same amount was replaced with phosphate buffer in order to maintain sink condition. In 1 ml sample, 0.25 ml of acetonitrile was added, vortexed and analyzed at 280 nm using standard calibration curve in UV spectrophotometer.

7.1.3 Results and discussion

In situ hydrogel formation, through physical cross-linking like ionic, stereo-complexation and coordinate complexes has been useful but limited due to gel instability towards dilution, pH, ionic strength and temperature. (Hiemstra 2007b) *In situ* cross-linking through chemical reaction between complimentary functionalities on PEG, Dextran, Hyaluronic acid, Heparin, PVA and peptides have been useful. Sequential cross-linking approach comprising both physical and chemical cross-linking is desirable for faster and complete gelation yielding high modulus gels. Stereo-complexed gel (e.g. PEG-PLA) was reinforced by photochemical cross-linking to increase modulus 6 folds (Murakami 2006, Hiemstra 2007b). Inherent drawbacks of photochemical crosslinking mentioned in introduction however renders the approach impracticable. In another approach aldehyde functionalized PEO - PLA micelles along with polyallylamine formed *in situ* gels which had tissue adhesion properties.

(Murakami 2006) Due to the presence of reactive functionalities on the surface of micelles, gelation was instantaneous which highlighted the importance of approach but aldehyde functionalities are known to be unstable for storage and toxic towards tissues limiting practical utility. Niu et.al. (2008) explored acrylated and thiolated Pluronic micelles, which on mixing at body temperature formed hydrogel through temperature induced physical gelation, followed by thiol- ene cross-linking reaction. In this approach only terminal thiol functionalities on polymer were reactive hence degree of cross-linking can be expected to be low. In addition premature cross-linking in thiols through disulfide linkage exists which further limits practical utility.

In order to overcome this problem, aza Michael addition involving amine functionality group has been introduced by our group, which indicated faster gelation and better storage stability.(Nair and Kulkarni 2010). In order to reduce amine content and achieve faster gelation, we synthesized hydrophobically modified polymer conjugates bearing reactive amine functionalities. These hydrophobically modified polymer systems are advantageous since they orient reactive amines towards surface of self assemblies because of natural segregation of hydrophilic and hydrophobic domains as evident from positive zeta potential values. The surface presented functionalities react easily with their counterparts causing faster and complete reaction. The synergy between hydrophobic association in self assembly and chemical cross linking exhibits high modulus and tunable hydrophilic hydrophobic balance within hydrogel indicating applications as scaffolding material in tissue engineering and controlled release matrix in drug delivery.

7.1.3.1. Synthesis and characterization of AEDOCA and fatty amine PSI conjugates

Polysuccinimide was synthesized by dry polycondensation method from aspartic acid using phosphoric acid as catalyst. The number average molecular weight as determined by Vapor pressure osmometry (VPO) was 2263. The polymer was further converted to polyhydroxyethyl aspartamide for the molecular weight determination by aqueous gel

permeation chromatography (GPC). M_w and M_n were 5171 and 2498 respectively with polydispersity index 2.07. Poly (succinimide) (PSI) cannot be directly conjugated with Deoxycholic acid hence amino ethyl deoxycholamide (AEDOCA) was synthesized by reacting Deoxycholic acid NHS ester with excess of ethylene diamine. AEDOCA was conjugated with Polysuccinimide through the amide linkage to yield poly (Deoxycholamido ethylaspartamide-co-succinimide). The conjugation was confirmed by ^1H NMR in DMSO d_6 : polysuccinimide CH (5.21 δ) and AEDOCA peaks, 18- CH_3 (0.60 δ), 19- CH_3 (0.86 δ), 21- CH_3 (0.94 δ) and CH_2 - CH envelope (1 - 2.3 δ)

Polysuccinimide was also reacted with fatty amines i.e. Octadecylamine, Hexadecylamine and Dodecylamine to yield fatty chain conjugates. The conjugation was confirmed by ^1H NMR in DMSO d_6 : polysuccinimide methine CH (5.25 δ) and fatty alkyl amine peaks, CH_3 - (0.85 δ), CH_3 - CH_2 - (1.23 δ), $-\text{CH}_2$ - CH_2 (2.31 δ), CH_2 - NH (2.69 δ)

With an increase in DS, intensity of methyl protons in AEDOCA at 0.60 δ and of fatty amine at 0.83 δ increased. The DS estimated from ^1H NMR analysis was in the range 7 - 58 mole % for AEDOCA and 8 - 55 mole % for C_{18} alkyl amine when the content in the feed was increased in the range 10 - 60 mole % (Nakato 2000).

7.1.3.2. Synthesis and characterization of synthetic bilo / lipoproteins

Polysuccinimide conjugates synthesized in the previous section were treated with amino ethyl piperazine at 5 to 10 $^\circ\text{C}$ to yield piperazino ethyl polyaspartamide (PEPAM) based synthetic biloproteins and lipoproteins which were recovered by freeze drying.

Slow addition of PSI - AEDOCA or PSI - fatty chain conjugates slowly to excess of AEPz in DMF at 5-10 $^\circ\text{C}$ ensured quantitative functionalization without cross-linking. AEPz conjugation to PSI and formation of PEPAM was characterized by ^1H NMR in D_2O as discussed later.

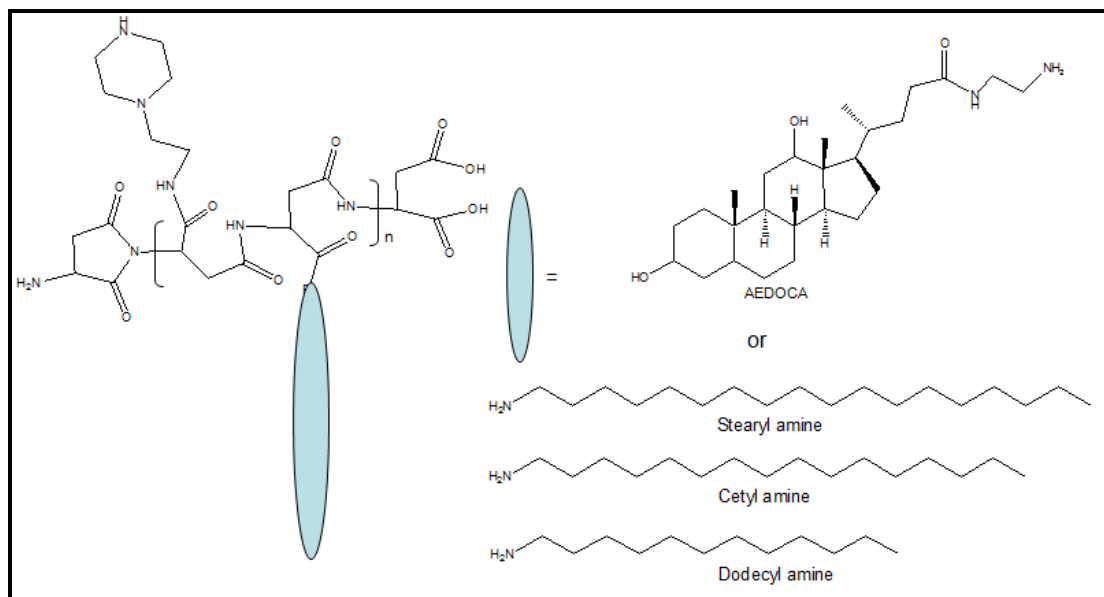


Figure 7.2. Synthetic bilo and lipoproteins.

7.1.3.3. Preparation and characterization of bilo / lipoprotein aggregates

The aggregates were prepared by sonicating synthetic bilo / lipoprotein in water. Macroscopic investigations of the aggregates included turbidity measurements, zeta potential measurements and ^1H NMR analysis. Microscopic investigations included fluorescence studies, light scattering and TEM measurements. Bilo / lipoprotein aggregates were evaluated for turbidity at 2 mg / ml by UV spectrophotometry at 500 nm. At DS upto 20 the samples were transparent while at higher DS turbidity was noted, primarily because of increase in particle size of the aggregates at higher hydrophobic content. All the conjugates coated with basic PEPAM corona exhibited positive Zeta potential (ξ) values in the range 7 to 30. (Table 7.2) Bilo and lipoproteins were dissolved in D_2O and $\text{DMSO } d_6$. The peaks of methyl protons in AEDOCA at 0.6 δ and 0.8 δ were very sharp in $\text{DMSO } d_6$ but decreased in intensity in D_2O . (Figure 7.3.)

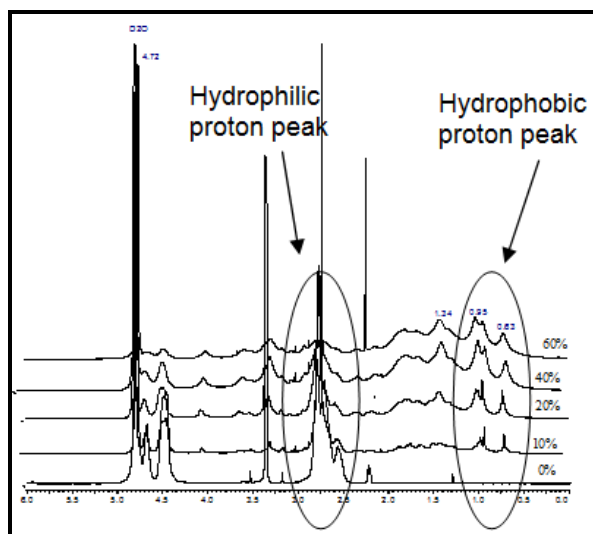


Figure 7.3. ^1H NMR of biloproteins at different DS in D_2O .

Thus NMR analysis revealed aggregation of bilo and lipoprotein, wherein AEDOCA or fatty chain is shielded as micro segregated segment and PEPAM segment is exposed to solvent. Similar decrease in intensity of AEDOCA peaks in ^1H NMR of Heparin aggregates in D_2O compared to that in $\text{CD}_3\text{OD} / \text{D}_2\text{O}$ has been reported by Park et.al (2004).

In order to further probe the aggregation, fluorescence studies were undertaken. Excitation and emission spectra of Pyrene in bilo or lipoprotein solutions revealed characteristic vibronic peaks of pyrene I_1 at 373 nm and I_3 at 385 nm which are a measure of hydrophobicity in microdomains of aggregate. The intensities of the vibronic bands strongly depend on the compactness of hydrophobic environment. Sigmoidal plots of intensity ratio (I_1/I_3) of pyrene as a function of biloprotein or lipoprotein concentration on a logarithmic scale. At 0.001mg/ml concentration the intensity ratio was 0.8, indicating very low hydrophobicity. Further at this concentration, with increasing degree of substitution of AEDOCA, the intensity ratio increased to 1 indicating increasing hydrophobic environment as a result of hydrophobic association. The concentration at which intensity ratio (I_1/I_3) showed an abrupt increase was denoted as critical aggregation concentration (CAC).

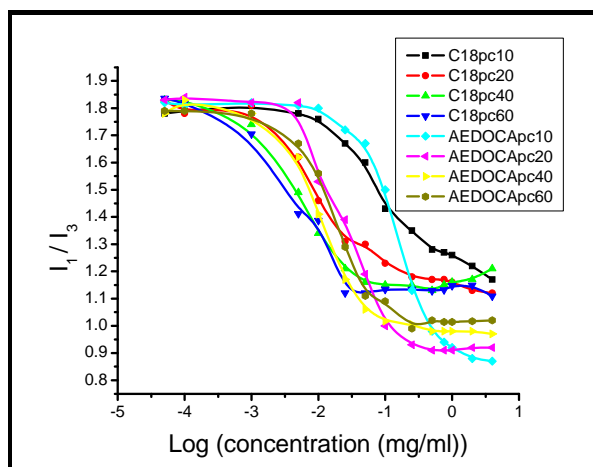


Figure 7.4. CAC of bilo / lipoprotein C₁₈ with DS 10-60

The CAC decreased with increase in DS (Figure 7.4, 7.5.). CAC values of bilo and lipoproteins summarized in Table 7.1 indicate that the CAC decreases with increasing DS. Further at a given DS the CAC values of lipoproteins are lower than those of biloproteins. This highlights the importance of the type of hydrophobe.

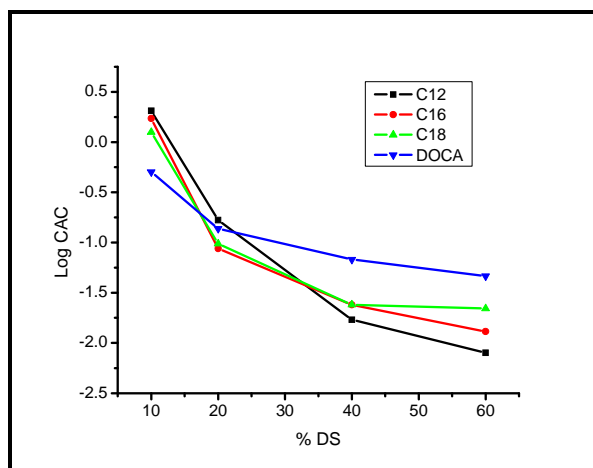


Figure 7.5. Effect of DS on CAC of bilo / lipoproteins.

Above CAC, fluorescence intensity increases due to the sudden increase in hydrophobicity in the system which enhances Pyrene binding. Equilibrium partition constants (K_v) for bilo and lipoproteins were determined as reported by Park et.al (Table

7.1) (Park 2004). In C₁₂ lipoproteins, an increase in DS enhanced K_v while in C₁₆ and C₁₈ lipoproteins K_v increased upto DS 40 and decreased thereafter. In Biloproteins too K_v increased upto DS 20 (Table 7.1). Compared to biloproteins, lipoproteins exhibited higher K_v values for Pyrene. This can be ascribed to greater hydrophobicity in fatty core compared to that in AEDOCA core.

The anisotropy values (*r*) of synthetic bilo / lipoprotein nanoaggregates evaluated using DPH as probe are listed in Table 7.1 (Cehelnik 1975)

Table 7.1. Bilo / lipoproteins characterization

Polymer conjugates	γ mN/m²	CAC mg/ml	η at 30 ° C	K v * 10⁵
Lp C ₁₂ -10	41.38	2.051	0.194	0.218
Lp C ₁₂ -20	45.92	0.167	0.181	0.273
Lp C ₁₂ -40	51.62	0.017	0.207	1.120
Lp C ₁₂ -60	61.17	0.008	*	2.594
Lp C ₁₆ -10	41.35	1.720	0.216	0.163
Lp C ₁₆ -20	45.89	0.087	0.228	0.420
Lp C ₁₆ -40	63.40	0.024	0.259	0.892
Lp C ₁₆ -60	65.29	0.013	*	0.837
Lp C ₁₈ -10	56.81	1.253	0.240	0.179
Lp C ₁₈ -20	56.99	0.097	0.242	0.413
Lp C ₁₈ -40	65.99	0.024	0.243	0.766
Lp C ₁₈ -60	66.26	0.022	*	0.577
Bp 10	45.41	0.505	0.239	0.053
Bp 20	43.79	0.137	0.243	1.078
Bp 40	43.33	0.068	0.256	0.303
Bp 60	51.66	0.046	*	0.104

* Highly turbid samples; Lp – Lipoprotein; Bp – Biloprotein; η - microviscosity

In synthetic biloprotein as DS increased from 10 to 60 mole %, anisotropy values increased from 0.239 to 0.256. These findings are in agreement with earlier increase in anisotropy values in Chitosan – Deoxycholic acid from 0.300 to 0.314 as the DS increased from 2.8 to 5.1 mole % (Lee 1998). The lower anisotropy values suggest micellar structure of biloproteins at low DS. Rigidity of the microenvironment results from more dense packing of steroidal moieties. C₁₂ and C₁₆ lipoproteins exhibited an increase in anisotropy values with an increase in DS which could be because of increase in packing density with increasing DS. Anisotropy values of C₁₈ lipoprotein were almost constant irrespective of DS in range of 240 - 243 which could be attributed to nonflexible nature of C₁₈ chains as reported by kang et.al. (2001).

Particle size of these reactive aggregates was determined using light scattering technique. At 2 mg/ml, synthetic biloproteins exhibited sizes in the range 57 - 2729 nm. Synthetic lipoproteins formed nanoaggregates in the range 67 - 635 nm. In synthetic lipoproteins an increase in DS from 10 to 20 resulted in decrease in the size but an increase thereafter. This initial decrease in particle size is because of more compact structure but further increase in DS increased size which could be attributed to multiple aggregation. Similar trend was observed for biloproteins. (Table 7.2)

TEM imaging of lipoprotein and biloprotein samples DS 40 at 2 mg/ ml, indicated micellar structures of different size and shapes. Lipoprotein C₁₂ formed spherical micelles, lipoprotein C₁₆ formed mixed oblong and spherical micelles, while lipoprotein C₁₈ formed oblong micelles. Biloprotein 40 formed larger aggregate structures of irregular shape.

Table 7. 2. Size and stability of bilo / lipoproteins

Type	D nm	PD	ξ mV	T	Type	D nm	PD	ξ mV	T
C ₁₂ -10	68	0.419	07.87	0.007	C ₁₈ -10	187	0.192	21.18	0.058
C ₁₂ -20	133	0.432	09.12	0.012	C ₁₈ -20	139	0.344	30.89	0.293
C ₁₂ -40	64	0.419	25.69	0.014	C ₁₈ -40	449	0.160	14.66	2.157
C ₁₂ -60	310	0.360	27.00	2.205	C ₁₈ -60	636	0.840	18.50	2.189
C ₁₆ -10	159	0.007	06.33	0.103	Bp 10	57	0.399	08.03	0.010
C ₁₆ -20	114	0.021	07.00	0.031	Bp 20	63	0.435	07.29	0.014
C ₁₆ -40	100	0.096	29.72	0.062	Bp 40	1627	0.030	25.58	2.156
C ₁₆ -60	431	2.075	20.37	2.175	Bp 60	2729	0.424	16.07	2.561

Bp – Biloprotein; PD – Polydispersity; D – Effective diameter; T - Turbidity

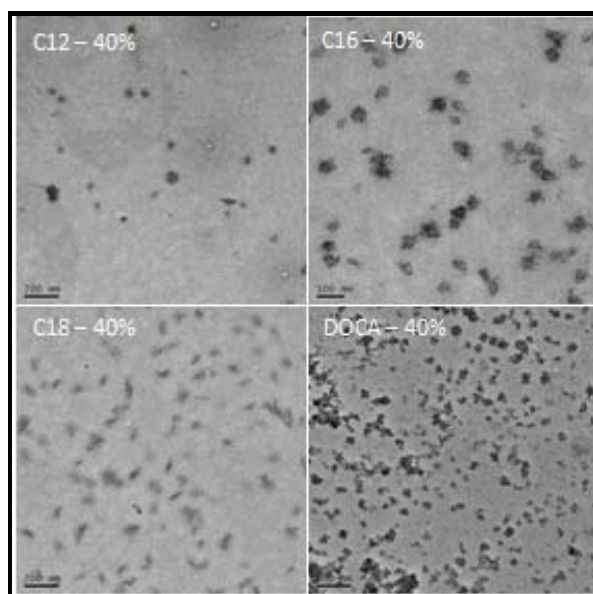


Figure 7.6. TEM of aminated lipoproteins and biloprotein at DS 40.

7.1.3.4. *In situ* Hydrogel Formation and characterization

In situ hydrogels were formed via Michael addition between synthetic bilo and lipoproteins with PEGDA in phosphate buffer at pH 7.4. poly β amino esters have been synthesized in non aqueous medium as synthetic vectors for gene delivery. These reactions were unusually slow and took 5 days at 50 °C (Lynn 2000). Recently it was reported that Michael addition between amine and acrylate is accelerated in an aqueous medium since water activates carbonyl group of acrylate esters which enhances its nucleophilicity and reactivity towards amine (Ranu 2007). Amino ethyl piperazine is a secondary amine which on Michael addition with acrylates ester converts into unreactive tertiary amine. This is the first report of rate enhancement of Michael addition between amine and an acrylate for polymer synthesis in an aqueous medium. Amine functionalization of the nanoaggregates has an advantage over thiols groups since the later are known to be susceptible towards oxidation and lead to premature cross-linking during synthesis and storage. Further the reactivity of thiol depends on pH since thiolate anion is the reactive species (Hiemstra 2007). Additionally amines being polar groups also act as hydrophilic corona on nanoaggregates formed by bilo or lipoproteins. Another advantage of the bilo and lipoproteins vis a vis natural and synthetic polymers bearing thiols is that because of lower molecular weights and high density of amino groups the cross linking densities can be expected to be high yielding high storage modulus.

Both bilo and lipoproteins have piperazino ethyl groups on the surface which are readily accessible for the addition to acrylates. The merits of a surface cross-linking reaction were demonstrated by Murakami et.al. (2006), wherein an aldehyde terminated polymeric micelle was reacted with polyallylamine and a tissue surface to form gel on a tissue surface by schiffs base formation. In general, gelation time increases with an increase in DS of hydrophobe in bilo and lipoproteins but decreases with increasing reactant concentrations (Table 7.3.).

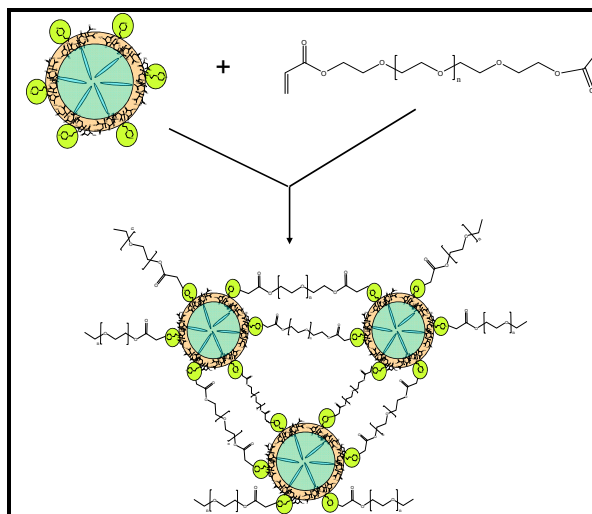


Figure 7.7. Schematic of in situ hydrogel Formation.

Table 7.3. Gel characteristics of synthetic bilo / lipoproteins

Sample	Gt (Sec)		Dt (days)		Gel	Sample	Gt (Sec)		Dt (days)		Gel
	10%	20%	10%	20%			10%	20%	10%	20%	
PEPAM	395	220	2	4	T _p	C ₁₈ -10	406	90	1	3	O
C ₁₂ -10	442	241	1	2	T _p	C ₁₈ -20	440	146	1	3	O
C ₁₂ -20	613	275	1	3	T _p	C ₁₈ -40	Pg	345	-	3	O
C ₁₂ -40	Pg	315	-	2	T ₁	C ₁₈ -60	Ng	Ng	-	-	-
C ₁₂ -60	Ng	Ng	-	-	-	Bp 10	602	253	1	2	T _p
C ₁₆ -10	327	66	1	3	T ₁	Bp 20	779	310	1	2	T _p
C ₁₆ -20	431	45	1	3	T ₁	Bp 40	Pg	Ng	-	-	-
C ₁₆ -40	Pg	210	-	3	O	Bp 60	Ng	Ng	-	-	-
C ₁₆ -60	Ng	Ng	-	-	-						

Bp – Biloprotein; PD – Polydispersity Gt – gelation time; Dt – Degradation time;
 T_p– Transparent; T₁ – Translucent; O – Opaque; Ng – No gel; Pg – partial gel



Figure 7.8. Bilo / lipoprotein aggregate dispersions and b) cross-linked Gels 10% w/v.

The aminated synthetic bilo or lipoprotein at DS 40 formed opaque gels while at lower DS yielded clear gels. This is because at low DS particle size was small and below 200 nm but at DS 40 multiple aggregations were noted. The turbidity experiments also indicated that at high DS nanoaggregates solutions were more turbid.

a) Confocal microscopy

Uniform distribution of hydrophobic domains within hydrogel was probed using confocal microscopy. Nile red was used as hydrophobic dye (Excitation wavelength at 484 nm) to stain hydrophobic interior of self assemblies and FITC dextran was used as the hydrophilic marker (Excitation wavelength of 650 nm) for continuous hydrophilic gel matrix. At DS 40 large aggregates could be seen which showed the presence of red interior due to Nile red and green continuous phase due to FITC dextran. In C_{12} synthetic lipoprotein aggregates also indicated some green fluorescence along with red which could be because of loose nature of aggregate which allowed FITC dextran to enter inside the aggregate along with Nile red. In C_{16} and C_{18} lipoproteins yellowish red (Orange) fluorescence was observed which suggested exclusive Nile red staining of compact nanoaggregates. (Figure 7.9.)

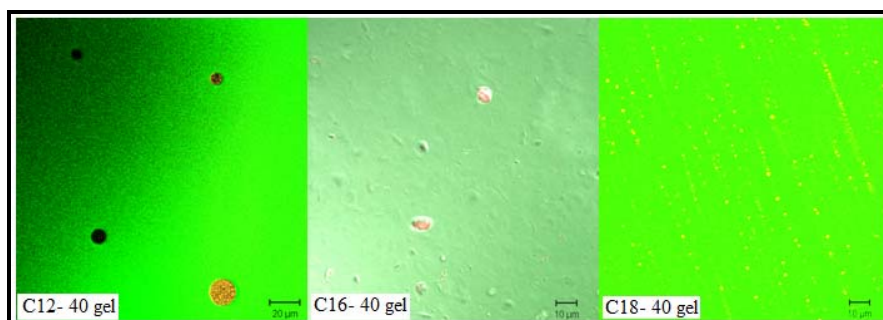


Figure 7.9. Confocal photomicrograph of Lp DS 40 gel stained with Nile red and FITC dextran.

b) ESEM analysis

It showed that the hydrogels based on lipoproteins (DS 40) were composed of a continuous gel phase comprising PEGDA in which the lipoprotein nanoaggregates were dispersed. (Figure 7.10.) In contrast, the biloproteins (DS 20) based hydrogels did not show the presence dispersed phase. This was because of very small size of nanoaggregates. (Table 7.3) *In situ* hydrogels of DS 20 with different hydrophobes like C₁₂, C₁₆, C₁₈, and AEDOCA were freeze dried and fractured to image microstructure and porosity for investigation of utility as scaffold for tissue engineering applications.

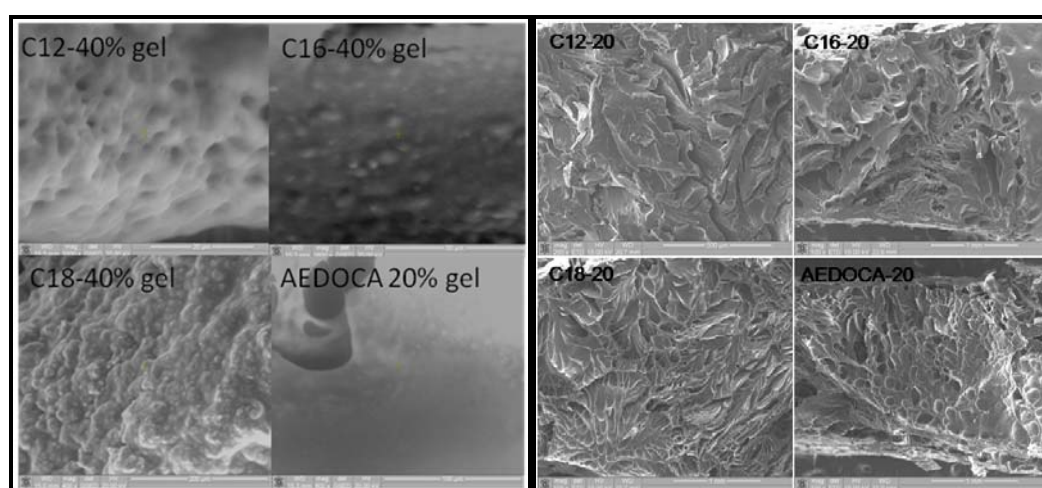


Figure 7.10. ESEM of bilo / lipoprotein in situ gels: a) hydrated b) freeze dried and freeze-fractured.

The structure indicated interwoven polymer phases with uniform distribution of porosity. The micro-channels can be observed in all the samples but channels were larger in C₁₂ and C₁₆ than C₁₈ and AEDOCA samples. The pores were uniformly distributed and structures were more compact in C₁₈ while discontinuity was more in AEDOCA samples.

c) Rheological characterization

The mechanical properties of self assembled and surface crosslinked hydrogels were studied by oscillatory rheology experiments on aminated bilo / lipoproteins and PEGDA 700 solutions in phosphate buffered saline (pH 7.4) at mole ratio of amine groups to unsaturated groups 1.1. Gel formation kinetics was followed by monitoring the storage (G') and loss modulus (G'') in time to establish when cross-linking reaction is completed.(Figure 7.11, 7.12, 7.13) For homogeneous systems starting from liquid precursors, the viscous behaviour dominates at the onset of cross-linking. Generally, after mixing the reactants due to the crosslinking through aza Michael addition reaction, elastic properties dominate hence G' increase more rapidly than G'' until reaching its plateau value, marking the end of cross-linking process. The loss modulus (G'') of all the hydrogels was intermittent (approx 0.1 – 1Kpa). Intermittent loss modulus indicated that the hydrogels were sufficiently elastic. Since the gelation process was very fast and it takes some time to run the experiment gelation time could not be determined from the crossover point of G' and G'' values. The gelation times were therefore determined by tube inversion method and were higher than those observed by rheology. This was also the case for dextran thiol and PEG diacrylate based gels (Hiemstra 2007a).

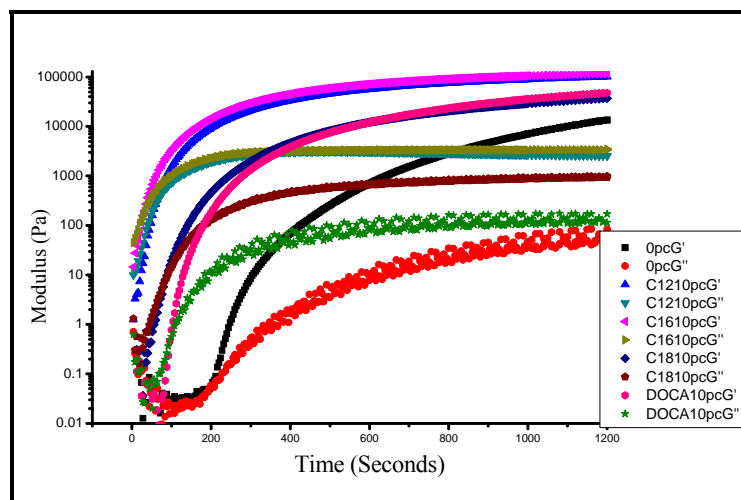


Figure 7.11. Storage and loss modulus of bilo / lipoproteins at DS 10.

Effect of type of hydrophobe

At DS 10, lipoproteins containing C_{16} chains exhibited highest storage modulus (115 Kpa) which was followed by C_{12} lipoproteins (101 Kpa) and biloproteins (47.7 Kpa). C_{18} lipoprotein exhibited lowest storage modulus (37.2 Kpa). The storage modulus of PEPAM was very low (13.6 Kpa) (Figure 7.11). This could be due to inefficient cross-linking and absence of reinforcement through micellar self assembly. The concentration of nanoaggregates during gelation is several folds greater than CAC. Thus nanoaggregates are linked together prior to gelation through inter micellar polymer links. This leads to higher modulus which is further enhanced by cross linking resulting from Michael addition reaction. This is similar to initial enhancement in modulus resulting from stereocomplexation of PLLA and PDLA chains which was further enhanced by photo cross-linking of terminal methacryloyl groups as reported by Hiemstra et.al. (2007b). The stereocomplexation was weak and progresses slowly for longer duration also methacryloyl groups were few at terminal of PLA for curing hence G' value were 31.6 Kpa for 17.5 % hydrogel (Hiemstra 2007b). The values in present case were significantly higher since the self associating network of nanoaggregates contributes to initial modulus which is further reinforced by the efficient crosslinking of surface functional groups through Michael addition on PEGDA. In comparison

Hyaluronic acid thiol conjugates took 24 hrs to complete 90% crosslinking as indicated by levelled G' . (Ghosh 2005) In present work, G' plateaued depending upon type of conjugated hydrophobe. At DS 10, the time needed for G' to reach plateau state decreased in the order AEDOCA > C_{18} > C_{12} > C_{16} . Overall in all the hydrogels G' plateaued within 20 minutes. This is due to faster reaction of amine groups on the surface of nanoaggregates. The plateau value of G'' were 0.1 – 1 Kpa which is 0.1 to 1% of G' indicating visco-elastic nature of cross-linked gels (Ghosh 2005).

Effect of DS of hydrophobe

For all the lipoproteins G' at DS 10 was higher than PEPAM at same concentration (10 %).

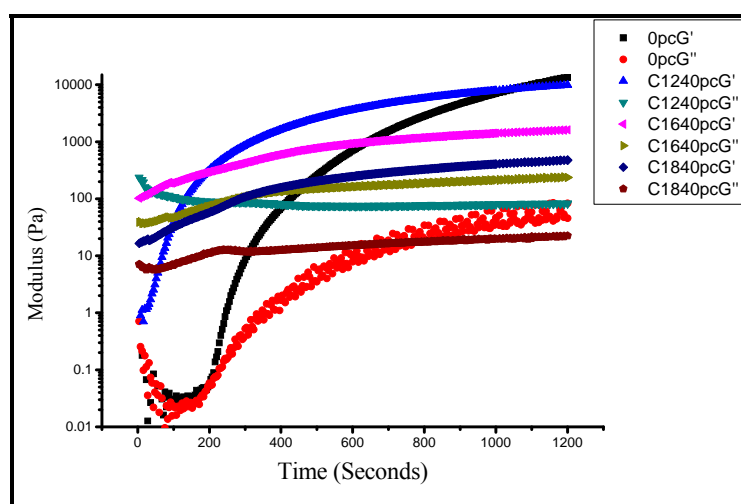


Figure 7.12. Storage and loss modulus of lipoproteins at DS 40

As the hydrophobicity content was increased, amine content on the backbone reduced which reduced degree of cross-linking. This led to formation of weak gel as reflected by lower modulus values. When the DS of hydrophobe was increased to 40 in lipoproteins, G' decreased in the order $C_{12} > C_{16} > C_{18}$ (Figure 7.12). This trend was expected since hydrophobicity decreased in the order $C_{18} > C_{16} > C_{12}$ making the gel network more discontinuous.

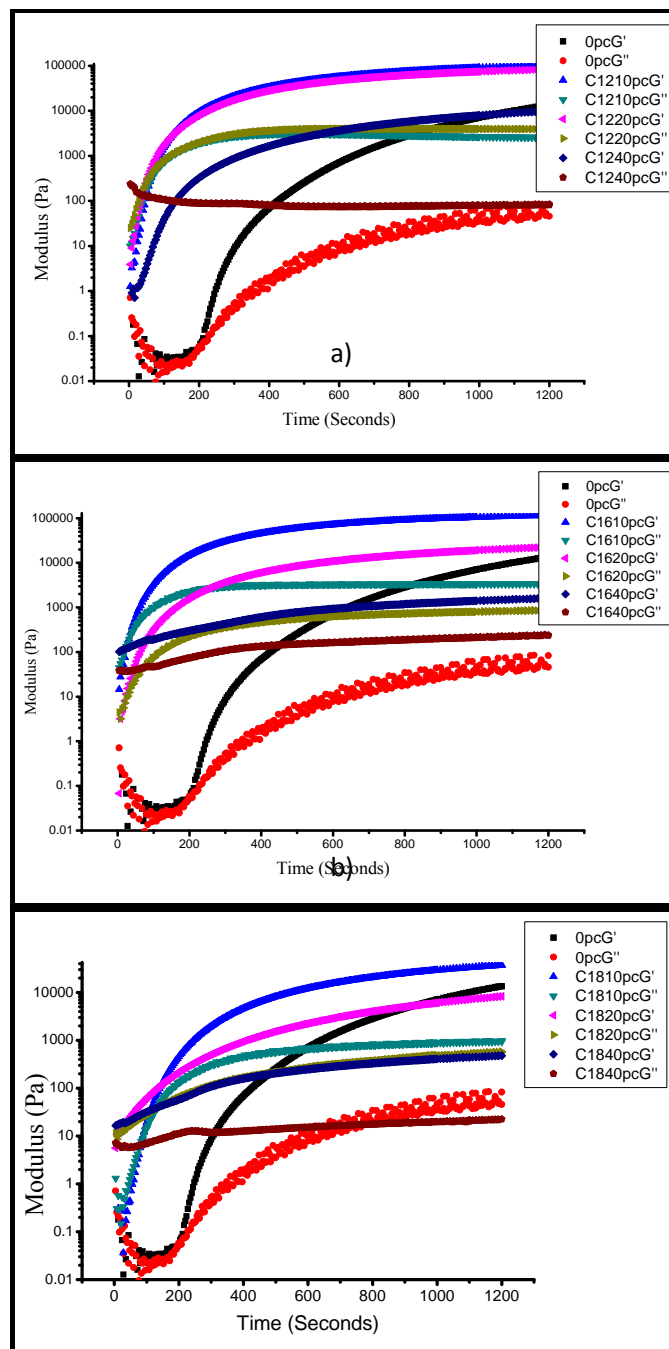


Figure 7.13. Storage and loss modulus of *in situ* lipoprotein gels: a) C₁₂, b) C₁₆, c) C₁₈ at DS 10, 20, 40 with PEGDA at 10% w/v.

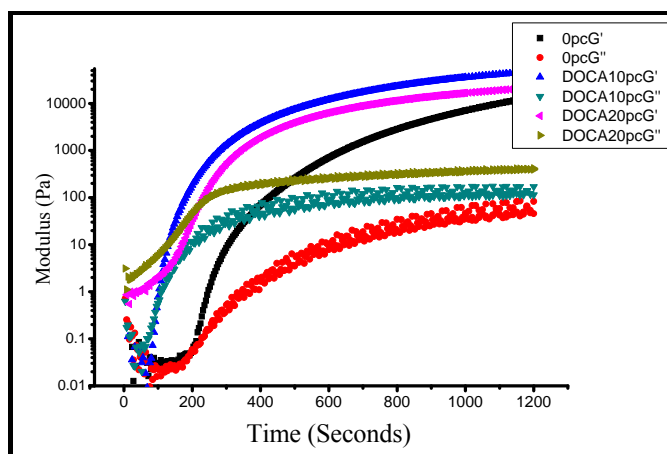


Figure 7.14. Storage and loss modulus of in situ biloprotein hydrogel at DS 10 and 20 with PEGDA at 10 % w / v.

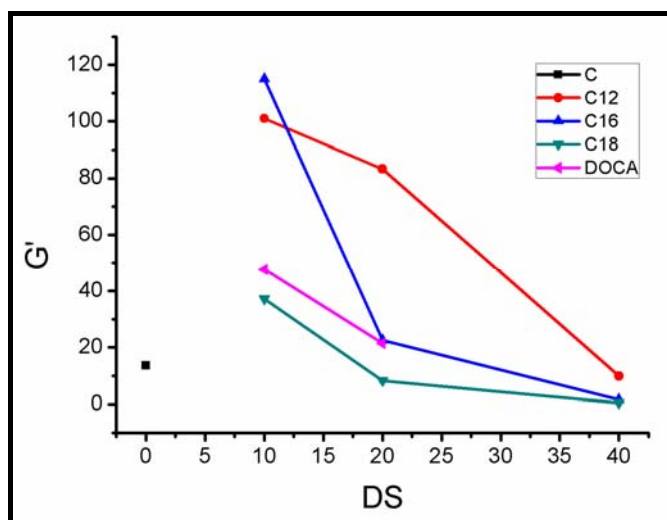


Figure 7.15. Effect of DS of type of hydrophobe in proteins on storage modulus (G') of in situ hydrogels.

The modulus of the hydrophobic domain enhances the modulus of the lipoprotein hydrogels initially. Since the degree of crosslinking is only marginally lowered at low DS 10 (Hiemstra 2007a). Hiemstra et.al. reported that varying the ratio of SH to vinyl

sulfone in the range 0.9 – 1.1, G' of formed gels did not change significantly, whereas further deviation in ratio to 0.75 decreased G' significantly due to decreased cross-linked density.

In the present case, an increase in DS of hydrophobic conjugates beyond 10% resulted in lower cross-link density which outweighed the enhancement in G' due to incorporation of hydrophobic domains yielding lower G' values. G' values of gels prepared by using DS 10 lipoproteins were higher as compared to the moduli of hydrogels with hydrophobic domains due to the contribution of self associating networks of hydrophobic domains. (Figure 7.13, 7.14, 7.15)

Table 7.4. Comparison of storage modulus of *in situ* gels in literature.

Precursors	G' (Kpa)	% w/v	Ref.
n-PEG-Gln with n-PEG-MMPLys, enzymatic gelation	38.50	10	Ehrbar 2007
HA-SH, PEGDA	5	10	Ghosh 2005
PEG-PLLA and PEG-PDLA	10	10	Hiemstra 2006
Dextran-SH and PEGDA / PEGTA	100	20	Hiemstra 2007a
PEG-PLA-MA	31.6	15	Hiemstra 2007b
Ploxamer 188 SH and acrylate	64	47.5	Niu 2008
Heparin SH and PEGDA	10	10	Tae 2007
PEGDA, TA with SH	10	75	Vernon 2003
P(NIPAAm-co-GMA) / PEI	10	4	Wang 2009
Oxid.Chitosan NCE Chitosan	1	3	Weng 2007
PCL-PEG-PCL	20	20	Bae 2005
PEPAM	13.6	10	Present work
Lipoprotein C ₁₂ DS10	101	10	
Lipoprotein C ₁₂ DS20	83.3	10	
Lipoprotein C ₁₆ DS10	115	10	
Lipoprotein C ₁₆ DS20	22.5	10	
Lipoprotein C ₁₈ DS10	37.2	10	
Lipoprotein C ₁₈ DS20	8.31	10	
Biloprotein DS10	47.7	10	
Biloprotein DS20	21.5	10	

The contribution of self associating network of hydrophobic domains is also evident from the starting point of modulus at time 0 for lipo or biloproteins and PEPAM. A

comparison of all the reported G' values at different percentage of precursors reported in literature with the values observed for lipo and biloproteins based hydrogels indicated that range of moduli have been achieved. DS 10 and 20 lipoproteins exhibit significantly higher storage modulus.

An examination of Table 7.4. reveals that by selecting appropriate fatty amine and DS, it is possible to synthesize hydrogels which offer wide range of moduli reported in the literature but degrade relatively rapidly. The modulus is governed both by the type and size of the nanoaggregates along with degree of cross-linking.

7.1.3.5. Mechanism of gel formation.

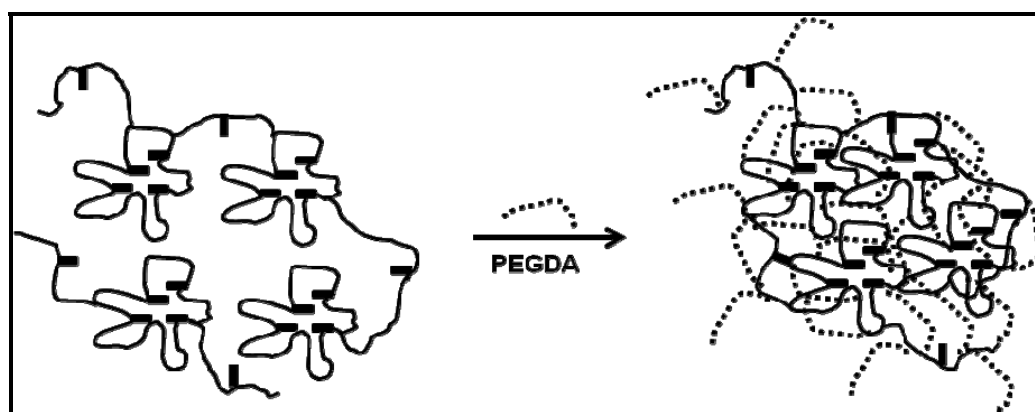


Figure 7.16. Schematics of gelation mechanism of bilo / lipoproteins with PEGDA

The gel formation follows hierarchy based mechanism wherein lipoproteins at many fold higher concentration of their CAC act as self associating polymers. This self associating behaviour is very similar to that observed by linear amine modified hyaluronic acid gels. The viscosity increase in present work is not significant to form standalone gel since the entanglements and chain entrapment in lipo and biloprotein are far less compared to hyaluronic acid due to low molecular weight. Similar findings were reported in low molecular weight heparin - thiol conjugate wherein even till 30% precursor content, viscosities were very low (Tae 2007). The self associating network formation seems to be favoured in low molecular weight C_{16} and C_{12} based conjugates

at DS 10, since micelle formation would be preferentially through intramolecular association. Their aqueous solutions also exhibited higher G' and G'' values at time zero, compared to PEPAM. C_{18} conjugate did not exhibit significant increase in G' and G'' values at time zero due to reported crystallized cores in C_{18} micelles which limits mobility inside hydrophobic core, necessity for formation of self associating networks (Kang 2001).

Surface amine functionalities on these self associating polymers were a result of segregation of hydrophobic and hydrophilic functionalities. These were further explored for aza Michael addition on PEGDA. This chemical cross linking was very fast and spontaneous and quantitative similar to those reported in case of aldehyde modified PEO- PLA micelles wherein aldehyde corona formed spontaneous hydrogels with polyallylamine. Thus chemical cross-linking further reinforced physical network formed by lipoproteins at low DS. The significant 10 fold increase in G' and G'' indicated viscoelastic nature in lipoprotein hydrogels at DS 10.

Similar sequential cross-linking approaches have been reported earlier in stereocomplex-photochemical cross-linking of PEG-PLA micelles, in thermo – michael addition based chemical cross-linking of pluronic micelles, in self assembly – Schiff base based chemical cross-linking of PEG-PLA micelles (Murakami 2006, Hiemstra 2007b, Niu 2008).

7.1.3.6. Hydrogel degradation study

The hydrogels degraded through hydrolysis of the β amino ester linkage under physiological conditions. The *in situ* gels were stored in the phosphate buffer solution and allowed to degrade at 37 ° C. The extent of degradation was calculated from the loss of hydrogel weight monitored as a function of time. The hydrogel degradation time was defined as the time required to transform matrix from gel to sol state. The concentration of bilo and lipoproteins as well as DS influenced the degradation time. For aminated bilo or Lipoproteins, the degradation time increased with increasing

concentration from 10 to 20 w/v % (Table 7.1.3). Degradation profiles as a function of hydrophobicity in aminated protein are as shown in Figure 17. All the samples degraded in 2-3 days time. The rapid degradation of the hydrogels irrespective of high cross-linking density and modulus can be attributed to the vulnerability of the labile β amino ester link and low molecular weight of precursors. Aminated protein DS 0 degraded relatively slower over 4 days. This was expected since the cross-linking density was highest in this case.

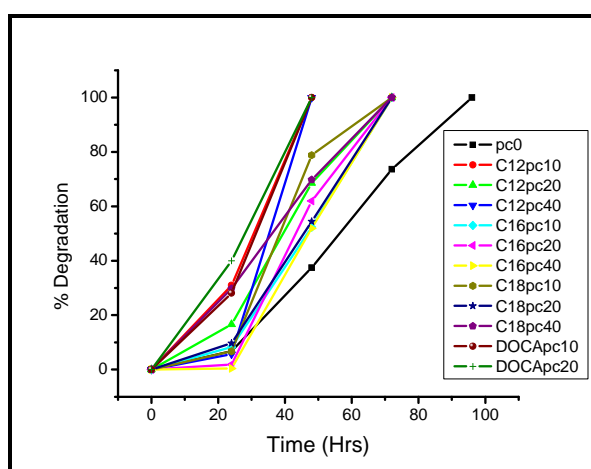


Figure 7.17. Effect of type of hydrophobe and its content on degradation of hydrogels

7.1.3.7. TCN release from in situ hydrogels

In situ hydrogels have been primarily explored for the release of hydrophilic as well as macromolecular drugs such as proteins and peptides. However these are not suitable for the release of hydrophobic drugs since the drugs have poor solubility. The release of such drugs is controlled primarily by dissolution and the hydrogel serves as a depot to immobilize drug. The incorporation of hydrophobic nanocontainers within cross-linked hydrogels helps to dissolve the hydrophobic drug within these nanocontainers which would then be released as the cross-linked hydrogel degrades and dissolves resulting in the release of the hydrophobic active due to the opening of the nanocontainers.

TCN is a hydrophobic bioactive which has poor solubility in water. It was solubilized in lipoproteins (DS 20) at 10 % loading. Nanoaggregates were cross-linked with PEGDA 700 using an amine to acrylate ratio of 1.1:1. Release of TCN from these gels at 37 ° C was monitored for 24 hours. (Figure 7.18.)

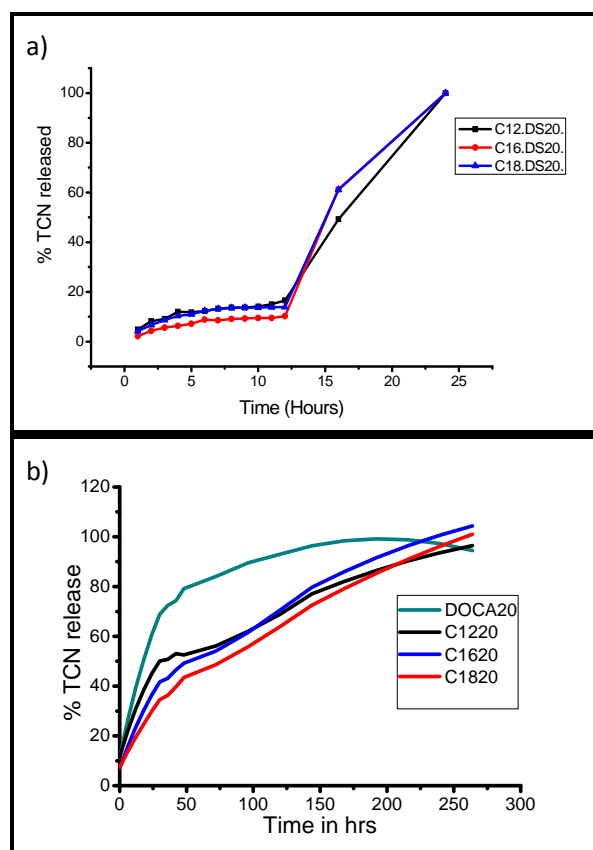


Figure 7.18. TCN release from lipo / biloprotein hydrogels prepared by cross linking with a) PEGDA 700, b) Jeffamine 600 diacrylamide, in PBS with 2% SDS (pH 7.4) at 37 ° C

Since the nanocontainers in which TCN is solubilized are dispersed within the degradable hydrogel matrix, no release was expected until the hydrogel surrounding the nanocontainers is degraded and let it open up and release the contents in the environment. The time for each nanocontainer to release TCN on degradation of hydrogel layer surrounding it would vary since the gel layer thickness can not be

expected to be uniform. After a lag of 12 hrs sustained release of TCN was observed over the next 12 hrs. The lag time cannot be directly correlated with the time for the degradation of the gels since the geometries in both the cases are not identical. In spite of the high crosslinking density, the lag times are short. This is because the crosslinker PEG diacrylate is only bifunctional. The lag time can be enhanced by the choice of the four and eight armed PEG acrylates and of increasing molecular weights.

To study the effect of crosslinker, Jeffamine 600 diacrylamide was used for nanoaggregates cross-linking led gel preparation. These gels released TCN continuously for 10 days. The drug release rate was dependent on the ability of core to hold it from extraction by SDS in release medium. AEDOCA core released drug very fast and release was completed within 4 days. Gels containing fatty cores released TCN over prolonged period of 10 days. The rate of TCN release was higher from hydrogels containing C₁₂ than C₁₆ and C₁₈. C₁₈ based lipoprotein gel released TCN at the lowest rate due to higher hydrophobicity coupled with possibly crystallized core as reported earlier by kang et.al. (Kang 2000)

7.1.4 Conclusions

Aminated Bilo and Lipoproteins prepared by the reaction of Polysuccinimide with amino ethyl deoxycholamide (AEDOCA), fatty amines and amino ethyl piperazine (AEPz) yielded self assembled nanoaggregates as established by morphological investigations. Michael addition reaction between the amines on the surface of these self assembled structures and the acrylates on PEGDA resulted in biodegradable hydrogels. The modulus of C₁₆ DS10 hydrogels was 10 folds higher at 115 Kpa than the hydrogel without hydrophobic domains. The presence of hydrophobic domains even after cross linking was evident from CLSM studies. Thus these hydrogels could be useful scaffolding material for tissue engineering. TCN could also be incorporated in hydrophobic domains, the release of which was controlled by the degradation of gels hence pattern shows lag phase followed by burst release. Using PPO-PEO-PPO diacrylamide cross linked hydrogels release could be extended to 10 days owing to

increase in degradation time. *In situ* hydrogels of this kind would be useful in delivery of anticancer and other hydrophobic drugs and would provide novel route to drug administration not possible hitherto.

7.2 Reactive emulsion based in-situ hydrogels (Emulhydrogels)

Summary

Emulsions have been used as vehicles for delivery of hydrophobic drugs. Since the drug is released as a result of partitioning, the release cannot be sustained over longer durations. A family of aminated biloproteins and lipoproteins has been described which emulsify soyabean oil and α tocopherol in water. These surface reactive emulsions on mixing with PEGDA 700 form biodegradable hydrogels termed emulhydrogels within 1 - 7 minutes. Uniform distribution of oil phase within the hydrogel matrix was confirmed by confocal microscopy and SEM. The moduli of emulhydrogels were several folds higher than the hydrogel without oil. These emulhydrogels degraded within 2 - 4 days. Paclitaxel loaded emulhydrogels exhibited sustained release over 15 hrs after a lag of 15 hrs. The degradation and release profiles can be extended by incorporating multifunctional cross-linkers.

7.2.1 Introduction

Emulsions constitute an important class of materials for the synthesis of polymers, catalysts, micro and nanocapsules, vehicle for hydrophobic actives and highly porous scaffolds through oil templating method. oil has been incorporated in gel matrix for the preparation of 1) highly porous gels useful for tissue engineering; 2) reactive cavities for reaction catalysis; 3) highly porous hydrogels useful as super absorbents and 4) drug encapsulated emulsions in hydrogels. Thus oil droplet inside hydrogel is used mainly as either template or as hydrophobic reservoir inside hydrogel.

Recently, microporous scaffolds are being developed by high internal phase emulsions pHIPE route for applications in tissue engineering and drug delivery (Gitli 2008). e.g. PHEMA synthesized within high internal phase emulsions (HIPEs) are highly porous which exhibit enhanced water absorption capacity that combine hydrogel water absorption and capillary action (Kulygin 2007). “smart” PNIPAM hydrogels containing Tetradecane (TD) incorporated emulsions prepared with SDS as emulsifier, released TD in response to thermal stimuli. This unique sponge like property of these composite thermoresponsive cryogels is reportedly useful for various biomedical applications and drug delivery of lipophilic actives from the gel under physiological conditions (Tokuyama 2007, Komarova 2008).

Synthesis of porous polyelectrolyte gels by oil templating method exhibited charged cavities useful as microreactors (Starodubtsev 2004, Komarova 2005). The same concept was extended recently to agarose gel containing oil domains for accelerating reaction between the hydrophobic mercaptans and esters (Komarova 2009).

Most of the new drugs introduced in the market are hydrophobic. This has propelled research to enhance their solubility and thus bioavailability. Among the various approaches explored oil-in-water nano and micro emulsions are the most promising (Lawrence 2000, Kreilgaard 2002, Spornath 2006) as they offer reduction in drug toxicity, protection to the active compounds from hydrolysis or oxidation, and the

relative ease of preparation (Shingel 2009). The hydrophobic active is released from these emulsions by partitioning into the contact tissues under *in vivo* conditions. Since this partitioning takes place at high rates the drug release from the emulsions can not be sustained.

Emulsion containing hydrogels have evolved as a new class of biomaterials (Graziacascione 2002, Gulsen 2005, Holtze 2005, Chen 2007). The polymer assemblies have been designed to integrate dispersed oil drops within the hydrogels for release of lipophilic drugs in sustained manner. These materials offer improved mechanical stability for easier handling and controlled release of even highly hydrophilic drugs since dispersion in oil helps to retard their release from the hydrogel matrix. The emulsifying surfactants used were not bound to the hydrogels hence were released along with the drug (Gulsan 2005) which limited the applicability of emulsion-containing hydrogels.

Recently, a series of solid emulsion gels which exhibit properties of both hydrogel and emulsion were reported. The gels were prepared by the reaction of activated p-Nitrophenyl carbonate poly(ethylene glycol) and protein stabilized oil-in-water emulsions. While the approach is useful in principle, p-Nitro phenyl carbonate chemistry is not desirable from a regulatory view point. Gelation is slow and applications are limited only to topical drug delivery system (Shingel 2009).

Thus there exists a need for emulsions which would encapsulate hydrophobic drugs at high loadings in oil core and have a reactive surface which can participate in the *in situ* cross-linking process to yield hydrogel depot containing oil *domains*. In this chapter we report the ability of synthetic biloproteins and lipoproteins to emulsify soyabean oil and α tocopherol. The emulsions contain emulsified oil droplets and amine functionality on the surface as indicated by positive zeta potential values. At 37 ° C, these reactive emulsions on mixing with water soluble PEG diacrylates formed biodegradable *in situ* hydrogels named “Emulhydrogels” within 1- 10 min. Paclitaxel was held in oily core and was released from emulhydrogels after the degradation of hydrogel matrix. This

resulted in sustained release of Paclitaxel over 15 hrs after a lag of 15 hrs. The release profile as well as the lag time can be enhanced by incorporating multifunctional polyacrylates.

7.2.2 Experimental

7.2.2.1 Materials

L- aspartic acid, Amino ethyl piperazine (AEPZ), Deoxycholic acid, Polyethylene glycol diacrylate Mn 700 (PEGDA), Pyrene, Diphenyl hexatriene (DPH), Nile red, 5/6 carboxy fluorescein, FITC dextran, Dicyclohexylcarbodiimide (DCC), α tocopherol, Octadecylamine (C_{18}), Hexadecylamine(C_{16}) and Dodecylamine (C_{12}) were all purchased from Aldrich. N- hydroxysuccinimide (NHS) (SD fine India), o-Phosphoric acid (85%, Merck, India) Ethylene diamine (SRL, India), Dimethylformamide (DMF) (Merck, India) dried and stored on molecular sieves, Dry Methanol (SD fine India), Acetone GR (Merck, India), Hydrochloric acid (Merck, India), Sodium hydroxide (Merck, India) and soya bean oil were used as received.

7.2.2.2 Synthesis and characterization of aminated bilo / lipoproteins

Aminated bilo and lipoproteins were synthesized and characterized for composition and self assembly behavior like critical aggregation concentration as in section 7.1 in this chapter. For surface tension measurements a stock solution of polymer conjugate (2 mg/ml) was prepared in deionized water. 25 ml of this solution was transferred to a beaker and surface tension was measured by Wilhelmy plate. For each measurement, at least three readings were taken and the mean γ (mN/m) value was recorded. Before each experiment, the instrument was calibrated and checked by measuring the surface tension of distilled water. Before every experiment Platinum plate was cleaned with deionized water and activated on gas burner to remove any adsorbed contaminant.

7.2.2.3 Preparation of reactive emulsion

Synthetic bilo / lipoproteins were added in phosphate buffer (pH 7.4) and sonicated in bath sonicator to achieve homogeneous dispersion. Soyabean oil or α tocopherol was then added to above solution and sonicated for 30 min at RT to form stable emulsion.

7.2.2.4 Characterization of reactive emulsion

Aminated emulsions were characterized for particle size, zeta potential and pH. For particle size determination, static light scattering (SLS) measurements were performed using a Brookhaven Instruments corporation UK 90 Plus particle size analyzer. The emulsion samples were diluted appropriately and scattering intensity was measured at fixed angles (θ) of 90°. For each measurement 3 runs were averaged with each run of 1 min.

For zeta potential determination, emulsion samples were diluted and analyzed at electric field of 7.0 V/cm. With the inputs of pH and particle size, zeta potentials were determined. For each measurement 5 runs were averaged with each run employing 10 cycles for 3 minutes. For analyzing data Zeta pals software of Brookhaven instruments was used.

7.2.2.5 Preparation of emulhydrogel and its characterization

a) Determination of gelation time

To determine the gelation time, each 250 μ L solution of reactive emulsion and PEG diacrylate (molar ratio of amine to unsaturated groups was kept at 1.1) in isotonic phosphate buffer (pH 7.4) were mixed by vortexing and held at 37 °C. The gelation time was determined by the vial tilting method. When the sample showed no flow on tilting and holding for 5 sec, it was regarded as a gel.

b) Rheological analysis of emulhydrogel

Rheology experiments were performed at 37 ° C on a US 200 rheometer (Anton Paar). Reactive emulsion and PEG diacrylate solution were prepared separately in isotonic Phosphate buffer (pH 7.4) and mixed (molar ratio of amine to unsaturated groups = 1.1) and quickly applied to the rheometer. The complex viscosity, storage and loss modulus were measured at constant amplitude of 2 % and angular frequency of 1 rad / s as a function of time.

c) Morphological analysis of emulhydrogel using ESEM

Emulsion and PEGDA 700 were mixed and placed in cup / sample holder of ESEM and field was applied for evaluation of surface morphology and oil globule distribution inside hydrogel.

7.2.2.6 Emulhydrogel degradation study

The samples prepared for gelation time measurement were weighed as zero hour reading and kept for degradation at 37 ° C with 3 ml of 0.1M isotonic Phosphate buffer pH 7.4. For determining weight loss of gel every 24 hrs buffer was removed, sample vials were inverted and allowed to dry on tissue paper and weighed. The same sample vial was then again filled with 3 ml of buffer and kept at 37 ° C. This procedure was repeated till gel was degraded completely. This time required for complete disappearance of gel in isotonic phosphate buffer at 37 ° C, pH = 7.4 was taken as complete degradation time.

7.2.2.7 Drug encapsulation and release from emulhydrogel

Paclitaxel (PTX) was dissolved in α tocopherol and emulsified by lipoprotein (C₁₂-20, C₁₆-20 and C₁₈-20) or biloprotein in phosphate buffer (pH= 7.4) by bath sonication. The emulsions were then cross-linked *in situ* using PEGDA to yield emulhydrogel. The samples were placed in 10 ml phosphate buffer and PTX release was studied over 30 hours. After each hour, 0.2 ml was withdrawn and same amount replaced with release

medium in order to maintain sink condition. The aliquots were diluted to 1 ml using ethanol, centrifuged and analyzed by HPLC [C_{18} column, Mobile phase - Acetonitrile : water (55:45), $\lambda_{\max} = 231\text{ nm}$].

7.2.3 Results and discussion

The advantages offered by *in situ* hydrogels have motivated researchers to explore newer applications like localized hydrophobic drug delivery (Cascone 2002, Yeo 2007, Gong 2009, 2010). Incorporation and uniform distribution of hydrophobic drugs, nanoparticles or microspheres inside hydrogel matrices has been a challenge. In the previous section of this chapter we discussed *in situ* cross-linked hydrogels containing hydrophobic domains. The aim was achieve faster gelation through aza - michael addition reaction. Synthetic bilo / lipoproteins bearing amine functionalities on the surface reacted with PEGDA to yield cross-linked hydrogels. These hydrogels released the drug held within the micelles once the matrix degraded.

During the characterization of bilo and lipoproteins we noted that they have ability to reduce surface tension of water similar to surfactants. Hence they could be explored for the emulsification of oil to form reactive O / W emulsions. In this section we report the potential of aminated bilo / lipoproteins to emulsify soyabean oil and α tocopherol and form emulsions. These emulsions stabilized by aminated bilo or lipoproteins also exhibited reactive amine functionalities on the surface of oil globules. These emulsified aminated globules were then cross-linked with PEGDA to form *in situ* hydrogels. Thus polymer conjugates act as emulsifiers for oil and then form *in situ* hydrogels with oil domains useful for delivery of hydrophobic drugs. The release profile of the drug depended upon relative rates of drug partitioning and degradation of emulhydrogel matrix.

7.2.3.1 Synthesis and characterization of bilo / lipoproteins

Bilo and lipoproteins were synthesized and characterized as discussed in section 7.1 of this chapter.

7.2.3.2 Preparation and characterization of biloprotein or lipoproteins

Synthetic bilo / lipoproteins were dispersed in water by sonication method and characterized by ^1H NMR analysis, fluorescence studies, zeta potential and particle size measurements as discussed in section 7.1 of this chapter.

Zeta potential (ξ) values for all bilo / lipoproteins were positive, indicating that the polymer conjugate is coated with cationic basic PEPAM corona. Synthetic bilo and lipoprotein exhibited zeta potential in the range from 7 to 30 with values increasing with increase in DS (Table 7.5).

Fluorescence measurements using Pyrene as probe were performed. The concentration at which intensity ratio (I_1/I_3) showed an abrupt increase was denoted as critical aggregation concentration (CAC). The CAC of synthetic proteins decreased with an increase in DS (Figure 7.19). CAC values exhibited by these bilo and lipoproteins have been compiled in Table 7.5. At a given DS, CAC values for biloproteins are lower than those for lipoproteins which highlights the importance of hydrophobe type and DS on CAC.

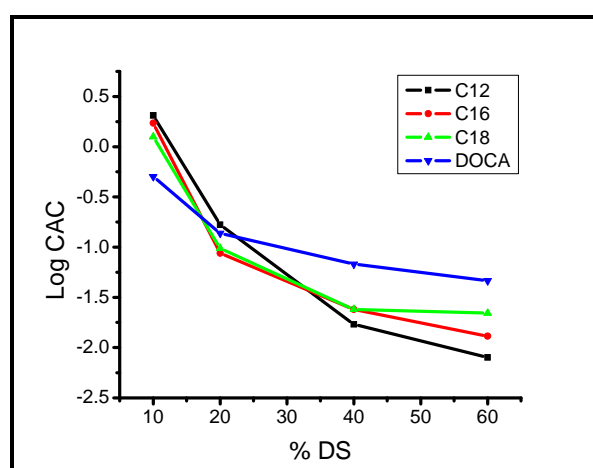


Figure 7.19. Effect of DS on CAC of synthetic bilo / lipoproteins.

Table 7.5. CAC and surface tension of synthetic lipo and biloproteins

Sr.no.	Emulsifier	Surface tension (γ)	CAC (mg/ml)
1.	Lp C ₁₂ -10	41.38 \pm 1.02	2.051
2.	Lp C ₁₂ -20	45.92 \pm 1.11	0.167
3.	Lp C ₁₂ -40	51.62 \pm 1.81	0.017
4.	Lp C ₁₂ -60	61.17 \pm 0.97	0.008
5.	Lp C ₁₆ -10	41.35 \pm 1.40	1.720
6.	Lp C ₁₆ -20	45.89 \pm 1.10	0.087
7.	Lp C ₁₆ -40	63.40 \pm 0.34	0.024
8.	Lp C ₁₆ -60	65.29 \pm 0.36	0.013
9.	Lp C ₁₈ -10	56.81 \pm 1.03	1.253
10.	Lp C ₁₈ -20	56.99 \pm 1.21	0.097
11.	Lp C ₁₈ -40	65.99 \pm 0.50	0.024
12.	Lp C ₁₈ -60	66.26 \pm 0.83	0.022
13.	Bp AEDOCA10	45.41 \pm 0.56	0.5052
14.	Bp AEDOCA20	43.79 \pm 0.68	0.1373
15.	Bp AEDOCA40	43.33 \pm 0.72	0.0677
16.	Bp AEDOCA60	51.66 \pm 0.37	0.0463

All bilo / lipoproteins at DS 10 and 20 lowered surface tension more effectively than DS 40 and 60. C₁₈ lipoproteins were less effective in this regard. This is because C₁₈ chains crystallizes and freezes chain mobility (Kang 2001) which reduces its efficiency as surfactant.

7.2.3.3 Preparation of reactive emulsion

Bilo / lipoproteins are composed of hydrophobic conjugates (AEDOCA or long alkyl chains), hydrophilic backbone (polyaspartamide) and hydrophilic amine functionality

(Amino ethyl piperazine). The backbone and functionality impart hydrophilicity which is balanced by hydrophobe conjugates yielding surfactant character as observed from surface tension measurements of their aqueous solutions.

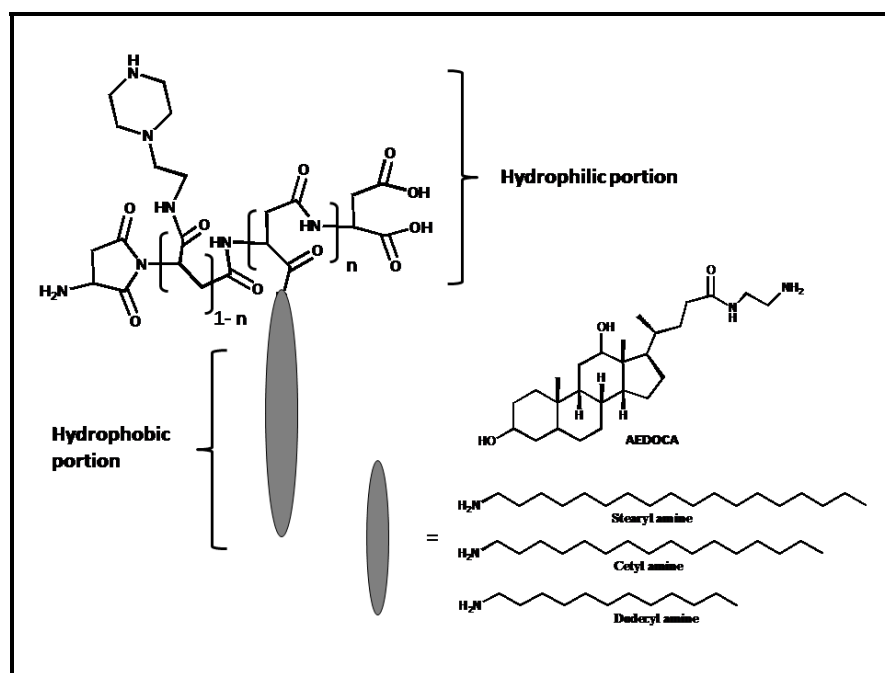


Figure 7.20. Synthetic biliprotein and lipoproteins.

Soybean oil and α tocopherol were emulsified by bilo / lipoproteins in sonication bath. Particle size measurements by light scattering revealed that the globule sizes of all the emulsions were in the range 318 – 550 nm (PD = 0.3). Irrespective of DS, lipoproteins bearing short alkyl chain were more effective and yielded smaller globule size with narrower distribution. (Table 7.6.)

Table 7.6. Characterization of synthetic bilo and lipoprotein based emulsions

Sr.no	Emulsifier	Effective diameter (nm)	PD	pH	Zeta potential (ξ)
1.	Lp C ₁₂ -10	385	0.299	7.65	27.22
2.	Lp C ₁₂ -20	379	0.295	7.76	41.25
3.	Lp C ₁₆ -10	405	0.315	7.70	27.18
4.	Lp C ₁₆ -20	406	0.266	7.56	22.24
5.	Lp C ₁₈ -10	403	0.328	7.76	23.26
6.	Lp C ₁₈ -20	555	0.103	7.61	19.10
7.	Bp DOCA-10	547	0.350	7.79	20.79
8.	Bp DOCA-20	318	0.319	7.65	23.20

Lp – lipoprotein; Bp – biloprotein; PD – polydispersity

7.2.3.4 Emulhydrogel preparation and characterization

In situ emulhydrogels were prepared by mixing bilo / lipoprotein stabilized emulsion with PEGDA in phosphate buffer pH = 7.4 at 37 ° C. (Figure 7.21) Bilo / lipoproteins emulsify and stabilize oil globules through segregation of lipophilic and hydrophilic segments on surface. Amine functionalities were on the surface of oil globules as evident from positive zeta potential values. These amine functionalities also stabilize emulsion droplets through charge repulsion. Amine functionalities on the oil globule surface on mixing with PEGDA reacted with acrylate functionalities similar to those reported in previous section of this chapter. The aza-michael addition led cross-linking reaction on the surface of oil globule formed network of interconnected globules which yielded *in situ* hydrogel with uniformly distributed oil domains.

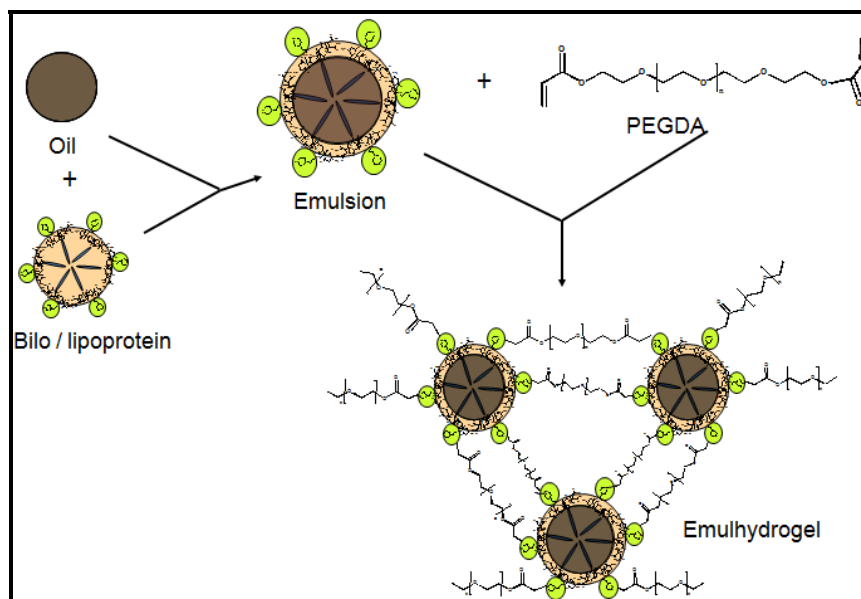


Figure 7.21. Schematic of emulhydrogel preparation.

All the biloprotein and lipoprotein DS 10, 20 based emulsions formed hydrogels in 1 - 7 minutes. In phosphate buffer the same gels degraded due to cleavage of β amino ester linkage network between oil globule surface and PEG within 3 - 4 days.

Table 7.7. Gel characteristics of synthetic bilo / lipoprotein Emulhydrogel

Sr. No	Emulsifier	Gelation time (sec)	Degradation time (days)
1.	Lp C ₁₂ -10	430	4
2.	Lp C ₁₂ -20	177	3
3.	Lp C ₁₆ -10	102	4
4.	Lp C ₁₆ -20	209	3
5.	Lp C ₁₈ -10	86	4
6.	Lp C ₁₈ -20	215	3
7.	Bp DOCA-10	72	4
8.	Bp DOCA-20	175	3



Figure 7.22. a) Synthetic bilo / lipoprotein based emulsion; b) Emulhydrogels.

a) Confocal microscopy

To demonstrate uniform distribution of hydrophobic *domains* inside hydrogel confocal microscopy was employed. Nile red was used to stain hydrophobic interior (Excitation wavelength at 484 nm) and FITC dextran stained continuous hydrogel matrix. (Excitation wavelength of 650 nm) In emulhydrogels, oil globules could be seen uniformly distributed inside gel matrix. (Figure 7.23)

Oil globules exhibited red fluorescence due to Nile red while continuous hydrogels matrix was green due to FITC Dextran. In few cases large globules were observed which we believe could have formed during cross linking led emulhydrogel formation. Emulhydrogel based on DOCA10 showed larger globular size compared to all other samples. Particle size distribution of the same sample had also exhibited broader distribution which can be attributed to weak emulsification capacity of biloprotein 10.

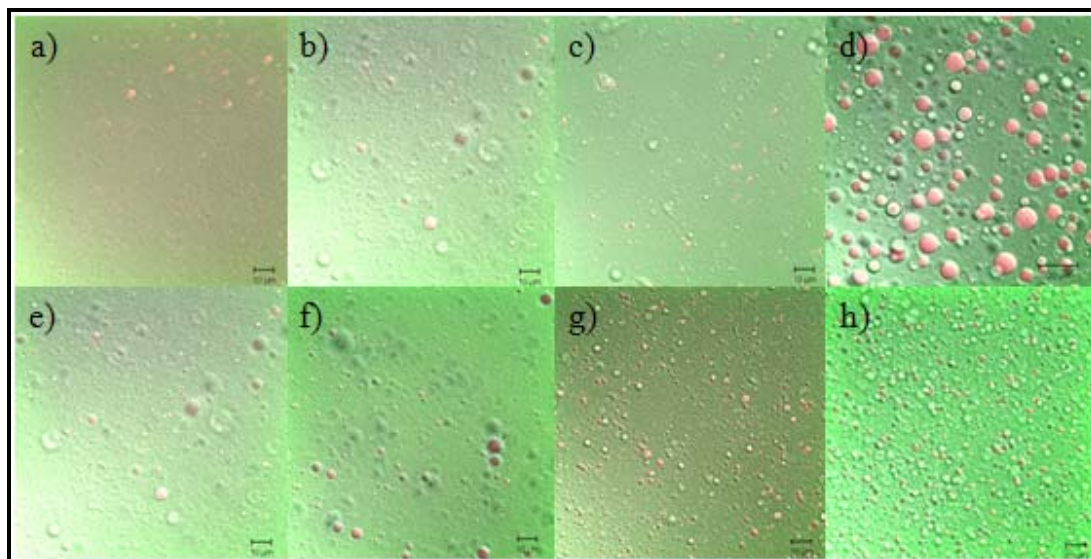


Figure 7.23. Confocal photomicrographs of emulhydrogels stained with Nile red and FITC dextran: a) C₁₂-10E; b) C₁₆-10E; c) C₁₈-10E; d) DOCA-10E; e) C₁₂-20E; f) C₁₆-20E; g) C₁₈-20E; h) DOCA-20E.

b) Rheological studies

The mechanical properties of emulhydrogels were evaluated at 25 °C by oscillatory rheology experiments. Aminated synthetic bilo or lipoprotein and PEGDA 700 solutions in phosphate buffered saline (pH 7.4, molar ratio of amine to acrylate 1.1) were mixed and placed in the plate of rheometer. Gel formation can be evaluated by monitoring storage modulus G' as a function of time. (Figure 7.24.) After mixing the reactants, G' increased and crossed G'' with time, indicating gel formation as a result of cross-linking reaction. However, the gel formation was too rapid to determine the gelation time by rheological measurements. After crossover, curves reach plateau stage indicating completion of cross-linking process as reported earlier (Hiemstra 2007a). Because of relatively fast gelation process, crossover point i.e. gelation time could not be determined accurately from rheological experiments.

Emulhydrogel (lipoprotein DS 10, C₁₂) exhibited 5 fold higher G' value (72.5 Kpa) than hydrogel without hydrophobic domains i.e. PEPAM hydrogels (13.6 Kpa). This

indicates the importance of hydrophobic domains in modulus. At any given DS the moduli of emulhydrogels were lower than the moduli of hydrogels containing hydrophobic domains discussed in previous section of this chapter. This lowering of modulus in emulhydrogels could be result of reduced cross-linking density along with increased fluidity in structures.

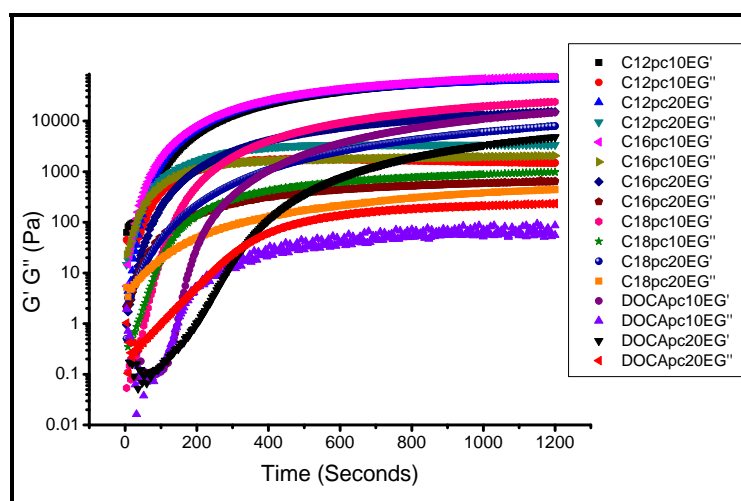


Figure 7.24. Storage and loss modulus of bilo / lipoprotein based emulhydrogels.

Thus overall these emulhydrogels exhibited G' in the range 14.7 - 72.5 Kpa which suggest sufficient gel strength to be used as *in situ* drug delivery system.

c) Morphological analysis of emulhydrogel using ESEM

Morphological analysis of emulhydrogel samples indicated smooth surface of all the emulhydrogels and presence of oil globule dispersed across hydrogel matrix. The oil globules exhibited higher contrast compared to hydrogel matrix. The oil globules in all the samples were larger than those observed in particle size experiments. This could be the result of coalescence taking place due to drying during imaging of emulhydrogels in ESEM (Figure 7.25).

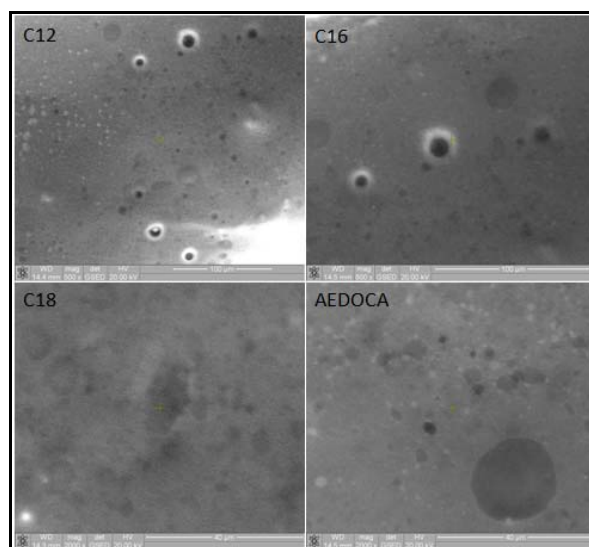


Figure 7.25. Morphological analysis of gels containing self assemblies.

7.2.3.5 Emulhydrogel degradation study

Emulhydrogels were prepared using aminated biloprotein or lipoprotein and soyabean oil. Reactive emulsions were mixed with PEGDA in phosphate-buffered saline at pH 7.4 and 37 °C to yield emulhydrogels. These samples were incubated in saline phosphate buffer (pH 7.4) at 37 °C.

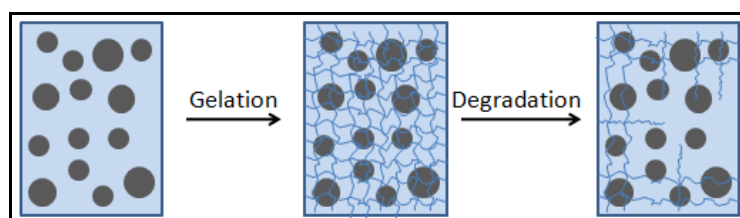


Figure 7.26. Emulhydrogel formation and degradation in phosphate buffer (pH 7.4).

The extent of degradation was calculated from the hydrogel weight before and after exposure to buffer at given time. Typical degradation pattern followed in emulhydrogels is schematically represented in Figure 7.26. The degradation is a result of hydrolysis of the β amino ester link between emulsifier on oil globule and PEG. In lipo and biloprotein emulhydrogels, complete degradation of gel matrix occurred within 3 - 4 days (Figure 7.27.). The degradation times of these hydrogels can also be tuned by

choice of other multifunctional cross-linkers as explained in previous section of this chapter.

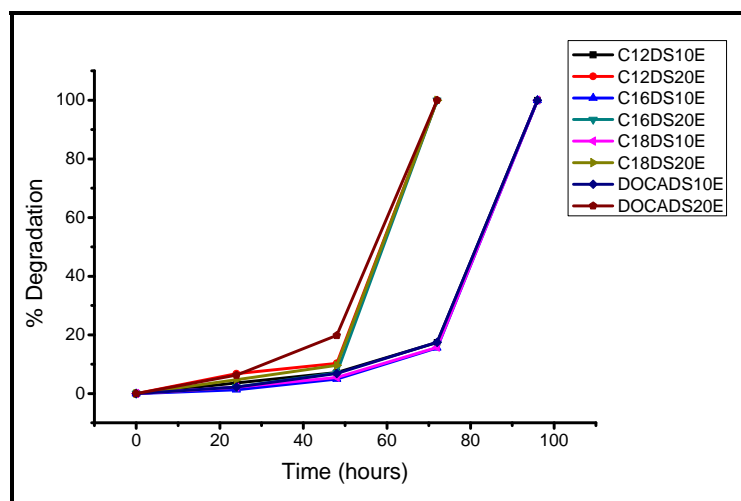


Figure 7.27. Degradation study of bilo / lipoprotein DS10 – 20 emulhydrogels.

7.2.3.6 PTX release from emulhydrogels

Paclitaxel is highly hydrophobic drug with limited or no solubility in an aqueous medium. Hence it was solubilized in α tocopherol, which on mixing and sonication with C_{12} lipoprotein and biloprotein (DS 20) solution formed emulsion.

These PTX loaded reactive emulsions formed emulhydrogels on mixing with PEGDA. PTX was released in phosphate buffer (pH = 7.4) at 37 °C over a period of 15 hrs after a lag of 15 hrs. Thus the release was governed by the degradation of hydrogel matrix encapsulating oil globules. The lag times were short and release relatively rapid since the cross-linker was PEG diacrylate. Instead, four or eight arm PEG acrylates can be explored further to sustain the release.

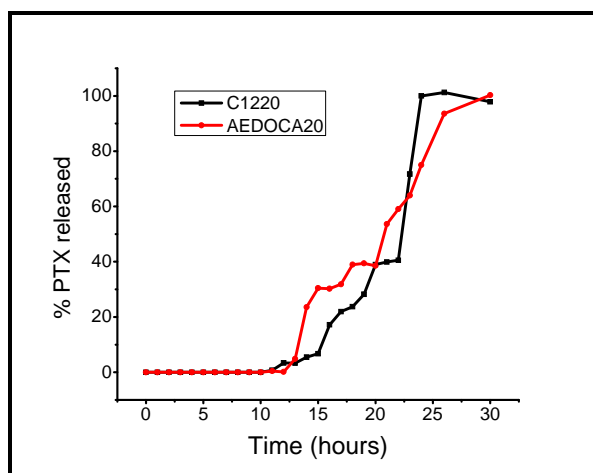


Figure 7.28. PTX release from bilo / lipoproteins (C_{12}) DS 20

7.2.4 Conclusions

Aminated bilo and lipoproteins emulsified soyabean oil and α tocopherol. PTX was incorporated in these reactive emulsions. The reactive emulsions spontaneously cross-linked *in situ* with PEGDA at 37 °C. Gelation times of these emulhydrogels were 1 - 7 minutes. Oil domains were uniformly distributed in hydrogel matrix as investigated by ESEM and confocal microscopy. Emulhydrogel degraded in phosphate buffer (pH 7.4, 37 °C) within 3 - 4 days. PTX was released over 15 hrs after lag phase of 15 hrs as a result of degradation of hydrogel matrix. The incorporation of multifunctional acrylates would enhance lag time as well as sustain the release over extended periods and would be useful in delivery of anticancer and other hydrophobic drugs and provide a novel vehicle for hydrophobic drug administration not possible hitherto. Formation of bicontinuous emulsions and extraction of oil from these hydrogels would yield porous biodegradable scaffolds useful for tissue engineering.

7.2.5 References

- 1 Balakrishnan B., Jayakrishnan A., *Biomaterials* 2005, 26, 3941-3951.
- 2 Cehelnik E. D., Cundall R. B., Lockwood J. R., Palmer T. F. *The Journal of Physical Chemistry* 1975, 79, 14, 1369 - 1376.
- 3 Chen, H., Mou, D., Du, D., Chang, X., Zhu, D., Liu, J., Xu, H., Yang X. *Int. J. Pharm.* 2007, 341, 78–84.
- 4 De Jong, S.J., de Smedt, S.C., Wahls, M.W.C., Demeester, J., Kettenes-Van den Bosch, J.J., Hennink, W.E. *Macromolecules* 2000, 33, 3680–3686.
- 5 Deng, W., Yamaguchi, H., Takashima, Y., Harada, A. *Angew. Chem. Int. Ed.* 2007, 46, 5144–5147.
- 6 Ehrbar, M., Rizzi, S. C., Schoenmakers, R. G., Miguel, B.S., Hubbell, J. A., Weber, F. E., Lutolf, M. P. *Biomacromolecules* 2007, 8, 10, 3000-3007.
- 7 Gangwal J. J., Kulkarni M. G. 10 th International symposium on advances in technology and business potential in NDDS Feb 2010.
- 8 Ghosh, K., Shu, X. Z., Mou, R., Lombardi, J., Prestwich, G. D., Rafailovich, M. H., Clark, R. A. F. *Biomacromolecules* 2005, 6, 5, 2857 - 2865.
- 9 Gitli T., Silverstein, M. S. *Soft Matter*, 2008, 4, 2475–2485.
- 10 Graziacascione, M.; Zhu, Z.; Borselli, F.; Lazerri, L.; *J Mater. Sci. Mater. Med.* 2002, 13, 29 - 32.
- 11 Gulsen, D., Chauhan, A. *Int. J. Pharm.* 2005, 292, 95–117.
- 12 Haigh, R., Fullwood, N., Rimmer, S. *Biomaterials* 2000, 21, 735 -739.
- 13 Haigh, R., Fullwood, N., Rimmer, S. *Biomaterials* 2002, 23, 3509 – 3516.
- 14 He, C., Kim, S.W., Lee, D.S. *J. Control. Release* 2008, 127,189–207.
- 15 Hiemstra, C., van der Aa, L. J., Zhong, Z., Dijkstra, P. J., Feijen J. *Biomacromolecules* 2007a, 8, 5, 1548-1556.
- 16 Hiemstra, C., Zhong, Z., Li, L., Dijkstra, P.J. , Feijen, J. *Biomacromolecules*, 2006, 7, 10, 2790-2795.
- 17 Hiemstra, C., Zhou, W., Zhong, Z., Wouters, M., Feijen, J. *J. Am. Chem. Soc.* 2007b, 129, 9918-9926.

- 18 Holtze, C., Landfester, K., Antonietti, M. *Macromol. Mater. Eng.* 2005, 290, 1025–1028.
- 19 Jo, Y. S., Gantz, J., Hubbell, J. A., Lutolf, M. P. *Soft Matter*, 2009, 5, 440–446.
- 20 Kang H. S., Yang S. R., Kim J. D., Han S.H., Chang I.S. *Langmuir* 2001, 17, 7501 - 7506.
- 21 Karlson, L., Nilsson, S., Thuresson, K. *Colloid Polym. Sci.* 1999, 277, 798-804.
- 22 Kissel, T., Li, Y., Unger, F. *Advanced Drug Delivery Reviews* 2002, 54, 99–134.
- 23 Komarova, G. A., Starodoubtsev, S. G., Khokhlov, A. R. *Macromol.Chem. Phys.* 2005, 206, 1752- 1756.
- 24 Komarova, G. A., Starodoubtsev, S. G., Khokhlov, A. R. *J. Phys. Chem. B* 2009, 113, 14849–14853.
- 25 Komarova, G. A., Starodoubtsev, S. G., Lozinsky, V. I., Kalinina, E. V., Landfester, K., Khokhlov, A. R. *Langmuir* 2008, 24, 4467-4469.
- 26 Kreilgaard, M. *Adv. Drug Deliv. Rev.* 2002, 54, S77–S98.
- 27 Kroll, E., Winnik, F. M., Ziolo, R. F. *Chem. Mater.* 1996, 8, 1594-1596
- 28 Kulygin, O., Silverstein, M. S. *Soft Matter*, 2007, 3, 1525–1529.
- 29 Lawrence, M.J., Rees, G.D. *Adv. Drug Deliv. Rev.* 2000, 45, 89–121.
- 30 Lee K. Y., Jo W. H., Kwon I. C., Kim Y., Jeong S. Y. *Macromolecules* 1998, 31, 378 - 383.
- 31 Li Y, Sun G, Xu J, Wooley KL. *Nanotechnology in Therapeutics.* 2007:381–407.
- 32 Lynn, D. M., Langer, R. J. *Am. Chem. Soc.* 2000, 122, 10761-10768.
- 33 Maia, J., Ferreira, L., Carvalho, R., Ramos, M. A., Gil, M. H. *Polymer* 2005, 46, 9604-9614.
- 34 Murakami, Y., Yokoyama, M., Okano T., Nishida, H., Tomizawa, Y., Endo, M., Kurosawa, H. *J Biomed. Mater. Res. Part A.* 2006, 80A, 2, 421 – 427.
- 35 Nair, H. R., Kulkarni, M. G. 10 th International symposium on advances in technology and business potential in NDDS Feb 2010.
- 36 Nakano, M. *Advanced Drug Delivery Reviews* 2000, 45, 1, 1-415.
- 37 Nakato, T., Tomida, M., Suwa, M., Morishima, Y., Kusuno, A., Kakuchi, T. *Polymer Bulletin* 2000, 44, 385-391.

- 38 Niu, G., Zhang, H., Song, L., Cui, X., Cao, H., Zheng, Y., Zhu, S., Yang, Z., Yang, H. *Biomacromolecules* 2008, 9, 2621-2628
- 39 O'Reilly RK, Hawker CJ, Wooley KL. *Chem. Soc. Rev.* 2006,35:1068–1083.
- 40 Ossipov, D. A., Piskounova, S., Hilborn, J. *Macromolecules* 2008, 41 11, 3971-3982.
- 41 Park, K., Kim, K., Kwon, I. C., Kim, S. K., Lee, S., Lee, D. Y., Byun, Y. *Langmuir* 2004, 20, 11726 -11731.
- 42 Rimmer, S., German, M.J., Maughan, J., Sun, Y., Fullwood, N., Ebdon, J., MacNeil, S. *Biomaterials* 2005, 26, 15, 2219 - 2230.
- 43 Roberts, M. C., Hanson, M. C., Massey, A.P., Karren, E. A., Kiser, P. F. *Adv. Mater.* 2007, 19, 2503–2507.
- 44 Schnepf, Z. A. C., Gonzalez-McQuire, R., Mann, S. *Adv. Mater.* 2006, 18, 1869–1872.
- 45 Shingel, K. I., Roberge C., Zabeida O., Robert M., Klemberg-Sapieha, J. E. *J Mater Sci: Mater Med* 2009, 20, 681–689.
- 46 Spornath, A., Aserin, A. *Adv. Colloid Interface Sci.* 2006, 128–130, 47–64.
- 47 Starodoubtsev, S. G., Khokhlov, A. R. *Macromolecules* 2004, 37, 2004- 2006.
- 48 Sun, Y., Collett, J., Fullwood, N.J., Mac Neil, S., Rimmer, S. *Biomaterials* 2007, 28, 4, 661 - 670.
- 49 Tae, G., Kim, Y., Choi, W., Kim, M., Stayton, P. S., Hoffman, A. S. *Biomacromolecules* 2007, 8, 6, 1979 - 1986.
- 50 Tokuyama, H., Kanehara, A. *Langmuir* 2007, 23, 11246.
- 51 Tortora, M., Cavalieri, F., Chiessi, E., Paradossi, G. *Biomacromolecules* 2007, 8, 1, 209 - 214.
- 52 Van de Wetering, P., Metters, A. T., Schoenmakers, R. G., Hubbell, J.A. *Journal of Controlled Release*, 2005, 102, 619– 627.
- 53 Van Tomme, S. R., van Steenbergen, M. J., De Smedt, S. C., van Nostrum, C. F., Hennink, W. E. *Biomaterials* 2005, 26, 2129–2135.
- 54 Vernon, B., Tirelli, N., Bächli, T., Haldimann, D., Hubbell J.A. *J. Biomed. Mater. Res. A.* 2003, 64, 3, 447 - 56.

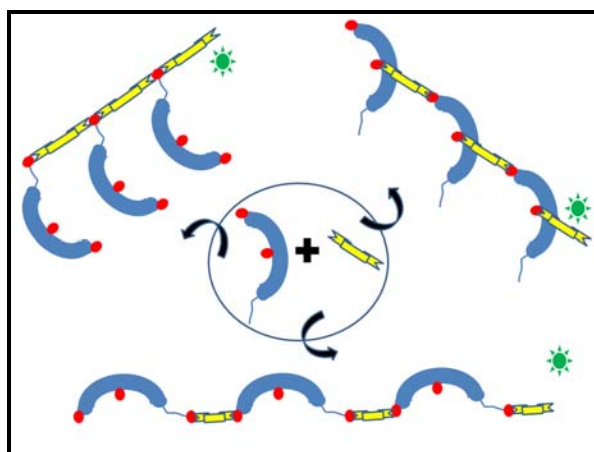
- 55 Viers, B. D., Bauer, B. J., Akpalu, Y., Gröhn, F., Liu, D., Kim G., Polymer Preprints 2000, 41, 1, 728 - 729.
- 56 Wallace, D.G., Cruise, G.M., Rhee, W.M., Schroeder, J.A., Prior, J.J., Ju, J., Maroney M., Duronio J., Ngo, M.H., Estridge, T., Coker, G.C. J Biomed. Mater. Res. 2001, 58, 5, 545-55.
- 57 Wang, Z., Xu, X., Chen, C., Wang, G., Cheng, S., Zhang, X., Zhuo, R. Reactive & Functional Polymers 2009, 69,14 - 19.
- 58 Weng, L., Chen, X., Chen, W. Biomacromolecules 2007, 8, 4, 1109 -1115.
- 59 Yoshida, T., Aoyagi, T., Kokufuta, E., Okano, T. J. Polym. Sci. Part A: Polym. Chem. 2003, 41, 779-787.
- 60 Yu, L., Ding, J. Chem. Soc. Rev. 2008, 37, 1473–1481.

Chapter 8

**Synthesis and characterization of bile
acid based oligo β amino esters for
drug delivery system**

Summary

New biodegradable poly β amino esters based on Deoxycholic acid were synthesized through polymerization of Deoxycholic acid (DOCA) in all the structural planes using same chemistry of 1, 4 addition of Trimethylene dipiperidine (TMDP) on C₃ - C₂₄, C₃ - C₁₂, Trimethylol propane - DOCA diacrylates. Bile acid based β amino esters were characterized for mol.wt., solubility, thermal stability, glass transition temperature, crystallinity & degradation. IR study indicated presence of amine and deoxycholyl units in polymers. XRD indicated that all the polymers were amorphous in nature. All the polymers were relatively thermostable and did not decompose till 300 ° C. DSC study indicated glass transition temperature in the range 70 – 80 ° C. The degradation study in buffers of pH (1.1, 7.4 and 10) indicated that polymers degraded very slowly due to hydrophobic nature of deoxycholate units. These polymers also exhibited pH sensitivity due to incorporation of amine in backbone structure. Release of p-nitro aniline indicated diffusion controlled release mechanism. Paclitaxel loaded nanoparticles prepared from these polymers were spherical and uniform with particle size in the range 75 – 500 nm and released 20 - 60 % of drug in 100 hrs.



8.1 Introduction

Designing materials for applications in biomedical engineering and pharmacy has always been a challenge for polymer chemistry in view of stringent requirements of mechanical strength, biocompatibility and biodegradability. The synthetic biodegradable polymers currently used are mostly polyesters like poly lactic acid (PLA), poly lactic glycolic acid (PLGA) & poly (caprolactone) (PCL). These polymers are approved by United States Food and Drug Administration (FDA) and have used as carriers in commercial products. Amongst them PCL is considered advantageous because it offers enhanced biocompatibility, higher hydrophobicity, and neutral biodegradation end products which do not alter the pH of the degradation medium unlike PLA and PLGA. (Pitt 1979, 1981, Cha 1990, Sinha 1998, Shenoy 2005)

Bile acids are biological compounds found in gastro intestinal tract. Their amphiphilicity and rigid structure makes them suitable building blocks for synthesis of degradable polymeric materials. These materials would exhibit tunable mechanical and interfacial properties along with better tolerability in biological environment especially gastrointestinal tract. (Ahlheim 1987, Gao 1997, Albert 1994, Pandey 1997) In the past bile acids have been polymerized as side chain pendants (Denike 1994, Benrebouh 2000, Zhang 1996), in main chain (Gouin 2000, Gautrot 2006), and as chain end groups (Kim 2000). However, reports on main-chain bile acid based polyesters, polyamides, and polyurethanes are relatively few in literature. (Gautrot 2006) Attempt to polymerize bile acid using p toluene sulfonic acid (PTSA) yielded branched polyester which had low molecular weight and limited solubility in organic solvents. Lipase and coupling agents like PTSA and Dicarboimidazole (DCI) with DMAP yielded rigid polymers of Deoxycholic acid and lithocholic acid with high crystallinity and reduced solubility in organic solvents. Degradation of polyanhydrides based on bile acid and sebacic acid could be tuned by varying comonomer ratios. These copolymers exhibited glass transition temperature (T_g) 13 ° C, which is low and limited their utility. (Gouin 2000) Cholic acid functionalized branched poly-caprolactones of different molecular weights were reported. These had melting points above room temperature and were

soluble in common organic solvents. They exhibited requisite molten viscosities, and good biocompatibility useful for tissue engineering applications (Fu 2007).

Synthesis of polyesters with bile acids in the main chain via entropy driven ring-opening polymerization using Grubbs catalyst yielded high molecular weight bile acid polymer without use of toxic chemicals and coupling agents. (Gautrot 2006) Drawbacks of this approach are 1) it involves preparation and use of catalyst, 2) bile acids with functionality on steroidal nucleus would need protections before lactone preparation and its polymerization. 3) polymers exhibited too low T_g to be useful in drug delivery applications.

More recently click chemistry was applied for the polymerization of bile acids which yielded high molecular weight main chain bile acid polymers. (Kumar 2010) Degradability of these polymers is compromised due to lack of readily hydrolysable linkage. The utility of these polymers has also not been explored for drug delivery applications.

Major factors which must be considered in developing new polymeric material are use of biocompatible monomers, presence of stimuli sensitive functionalities and maintenance of the hydrolysable backbone. Bile acids can be chemically modified on their hydroxyl groups or carboxylic side chain to introduce functional groups capable of polymerizing without toxic chemical agents and without drastic conditions or even heat.

Synthesis of linear poly(amino esters) and poly(amido amines) containing tertiary amines in their backbone has been reported by Ferruti et al (1985, 2002) and more recently by Lynn et al.(2000). These polymers have been synthesized by the addition of bifunctional amines to bisacrylamides and diacrylates. The synthesis of these polymers occurs via Michael addition. In this reaction primary and secondary amines add to chemically activated double bonds at the expense of an unshared electron pair at the Nitrogen atom. The chemical structures of poly(β aminoester), including main-chain structure and side-chain structure, greatly affect the degradation and transfection

efficiencies. Analogous poly (ester sulfides) and poly (amino esters) synthesized from diacrylates are potentially biodegradable due to the hydrolytic instability of the ester linkages. The absence of possibility of a retro-Michael addition in these systems eliminates the possibility of carcinogenic diacrylate production during degradation (Mather 2006).

Most of the poly (β amino esters) reported so far do not yield polymeric materials with high T_g which limits polymer processability and utility. Steroidal moieties are known to exhibit high T_g owing to rigid structure. To the best of our knowledge steroidal nucleus is not reported as building block in poly β amino ester synthesis. We have synthesized different diacrylates using hydroxyls on deoxycholate esters at Carbon 3, 12 and 24 position. β amino esters have been synthesized by Michael addition of trimethylene dipiperazine (TMDP) on deoxycholate diacrylates using Lewis acid $AlCl_3$ as catalyst. The β amino ester linkage would impart pH sensitivity to bile acid polymer and also incorporate hydrolysable linkages between deoxycholic acid units which might aid in faster degradation. Hydrophilicity in polymer backbone can be tuned based upon the position of acrylates on deoxycholate building block.

In this approach, bile acid has been polymerized using the Michael addition in three different dimensions i.e. 1) in backbone as head to side conjugated β amino ester, 2) head to tail conjugated β amino ester and 3) as a pendent through tail to β amino ester backbone. The steroidal diacrylates and poly β amino esters have been characterized by 1H NMR, GPC, IR, TGA, DSC and XRD. Degradability of these polymers has been investigated at different pH conditions (1.1, 7.4 and 10). Release of p- Nitro aniline a marker in phosphate buffer (pH 7.4) from these polymer matrices has been studied. Paclitaxel release from nanoparticles indicates the potential for drug delivery. Low molecular weight and cationic charge also suggest gene delivery application.

8.2 Experimental

8.2.1 Materials

Deoxycholic acid, acrylic acid, trimethylol propane and trimethylene dipiperidine (TMDP) were purchased from Sigma - aldrich and used as received. Triethylamine, methanol, dichloromethane (DCM), chloroform, ethylene glycol, benzoyl chloride were purchased from Merck India. Acryloyl chloride was freshly prepared from acrylic acid and benzoyl chloride. Paclitaxel was generous gift from Cadilla pharma, India.

8.2.2 Synthesis of bile acid based poly β amino ester

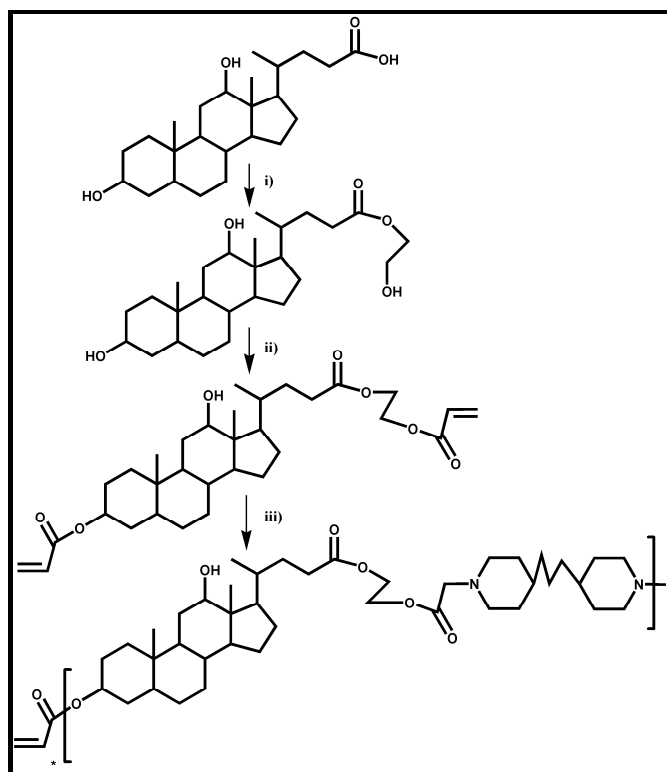
Different approaches have been undertaken to polymerize different deoxycholate diacrylate esters using 1, 4 michael addition of an amine i.e. TMDP. In the polymeric bile acids, deoxycholate units are incorporated in backbone as head to side conjugated β amino ester, head to tail conjugated β amino ester and as a pendent through tail to β amino ester backbone.

8.2.2.1 Poly (Deoxycholyl glycol β amino ester) (C₃-C₂₄ Head to tail conjugation)

a) Synthesis of deoxycholyl glycol ester

10 g of deoxycholic acid was dispersed in 100 ml ethane diol. The mixture was stirred for 10 minutes and 2 ml of concentrated hydrochloric acid was added. Stirring was continued for another 10 minutes and mixture was heated at 55 - 60 ° C for 8 hrs. Slowly this solution was added to 2 L of cold water and the resultant precipitate was filtered, washed and dried. This step was repeated once again to completely remove traces of ethane diol. Finally the product was completely dried under vacuum at 50 ° C for 2 days and stored in desiccator. (Melting point = 140 ° C, Yield = 11.3 g)

¹H NMR (200 MHz, CDCl₃) δ : 0.68 (s, 3H), 0.91 (s, 3H), 1 (d, 3H), 0.95-2.16 (m, steroidal CH, CH₂), 3.26 (m, 3H), 3.61 (m, 1H), 3.82 (d, 2H), 3.98 (t, 1H), 4.21 (d, 2H)



- i) Ethane diol, conc. HCl, 2 hrs, 80 °C; ii) Acryloyl chloride, TEA, THF, 24 hrs;
iii) TMDP, AlCl_3 , DCM, 24 hrs

Figure 8.1. Synthesis of Poly (Deoxycholyl glycol β amino ester).

b) Synthesis of deoxycholyl glycol diacrylate

10 g of deoxycholyl glycol ester was dissolved in 200 ml of dry THF. TEA was added to it and solution was stirred for 30 minutes under Nitrogen atmosphere at 2 – 8 °C. To this solution slowly acryloyl chloride solution was added drop wise for 1 hr and stirred overnight. Above solution was filtered to remove triethyl amine hydrochloride salt. The filtrate was concentrated and purified through silica gel column chromatography using ethyl acetate: petroleum ether as eluent. (Yield = 6.9 g)

^1H NMR (200 MHz, CDCl_3) δ : 0.68 (s, 3H), 0.93 (s, 3H), 0.99 (d, 3H), 0.95-2.16 (m, steroidal CH, CH₂), 2.46 (m, 2H), 4.00 (m, 1H), 4.40 (m, 4H), 4.58 (br d, 2H), 6.13 (br d, 2H), 6.41 (br d, 2H)

c) Synthesis of Poly (deoxycholyl glycol β amino esters)

2 g of deoxycholyl glycol diacrylate was dissolved in 20 ml of dry DCM and anhydrous AlCl_3 was added as a catalyst under nitrogen atmosphere. This solution was maintained for 15 minutes under stirring and cooled it to 5 - 10 ° C. Slowly a solution of 0.75 g TMDP was added to the activated deoxycholyl glycol diacrylate solution and stirred for 24 hrs at room temperature. Above solution was washed with brine and dried with anhydrous sodium sulfate and concentrate. The obtained polymers were washed with hexane and dried under vacuum for 8 hrs to yield poly (deoxycholyl glycol β amino esters) powder. (Yield = 2.34 g)

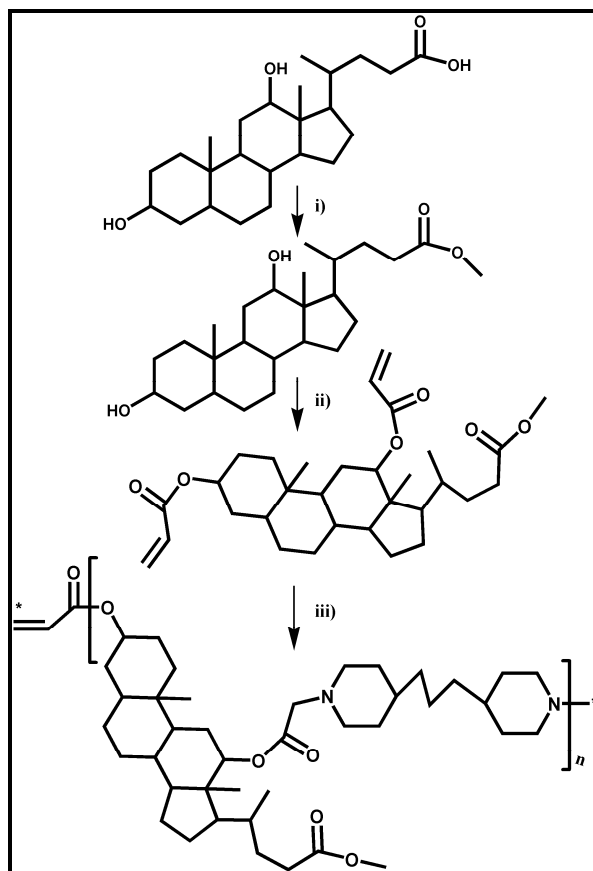
^1H NMR (200 MHz, CDCl_3) δ : 0.68 (s, 3H), 0.91 (s, 3H), 0.99 (d, 3H), 0.95-2.06 (m, steroidal and TMDP CH, CH₂), 2.33 (m, 2H), 2.51 (m, 4H), 2.68 (d, 4H), 2.85 (d, 4H), 4.00 (m, 1H), 4.40 (m, 4H), 4.80 (m, 1H), 5.83 (br d, 0.06H), 6.10 (d, 0.06H), 6.34 (br d, 0.06H)

8.2.2.2 Poly (methyl deoxycholate β amino ester) ($\text{C}_3\text{-C}_{12}$ Head to side conjugation)

a) Synthesis of methyl deoxycholate

50 g of deoxycholic acid was dissolved in 250 ml of dry methanol. 5 ml of concentrated hydrochloric acid was added to it and solution was refluxed for 1 hr. The reaction mixture was stored in refrigerator at 2 – 8 ° C to crystallize product. The product was filtered and washed with cold methanol to remove deoxycholic acid and acid impurities. Final product was dried under vacuum to ensure complete removal of residual methanol. (Melting point 120 ° C, Yield = 24 g)

^1H NMR (200 MHz, $\text{DMSO } d_6$) δ : 0.58 (s, 3H), 0.83 (s, 3H), 0.91 (d, 3H), 1-2.0 (m, steroidal CH, CH₂), 2.26 (m, 2H), 3.56 (s, 3H), 3.78 (s, 1H)



- i) Methanol, conc. HCl, 1 hr, reflux; ii) Acryloyl chloride, TEA, THF, 24 hrs;
iii) TMDP, AlCl₃, DCM, 24 hrs

Figure 8.2. Synthesis of Poly (methyl Deoxycholate β amino ester).

b) Synthesis of methyl deoxycholate diacrylate

10 g of methyl deoxycholate was added to 100 ml of dry DCM. 9.9 g of TEA was added to it and stirred for 30 minutes under nitrogen atmosphere and cold condition 2 - 8 ° C. Slowly acryloyl chloride solution in DCM was added to above solution for 1 hr and continued stirring for 24 hrs at room temperature. This solution was washed with 1N Hydrochloric acid and brine solution to remove triethylamine hydrochloride salt. The solution was concentrated and purified by silica gel column chromatography using ethyl acetate: petroleum ether mixture as eluent. (Yield = 3.7 g)

^1H NMR (200 MHz, CDCl_3) δ : 0.75 (s, 3H), 0.81 (d, 3H), 0.92 (s, 3H), 1 - 2.16 (m, steroidal CH, CH₂), 2.25 (m, 2H), 3.65 (s, 3H), 4.10 (m, 1H), 4.76 (m, 1H), 5.17 (t, 1H), 5.82 (br d, 2H), 6.15 (br d, 2H), 6.41 (br d, 2H).

c) Synthesis of Poly (methyl deoxycholate β amino ester)

2 g of methyl deoxycholate diacrylate was dissolved in 20 ml of dry DCM and pinch of anhydrous AlCl_3 was added as a catalyst under nitrogen atmosphere. This solution was stirred for 15 minutes and cooled to 5 - 10 ° C. Slowly to this solution 0.75 g TMDP in DCM was added and stirred for 24 hrs at room temperature. Above solution was washed with brine and dried with anhydrous sodium sulfate and concentrated. The obtained polymer was washed with hexane and dried under vacuum for 8 hrs to yield poly (methyl deoxycholate β amino ester) powder. (Yield = 2.25 g)

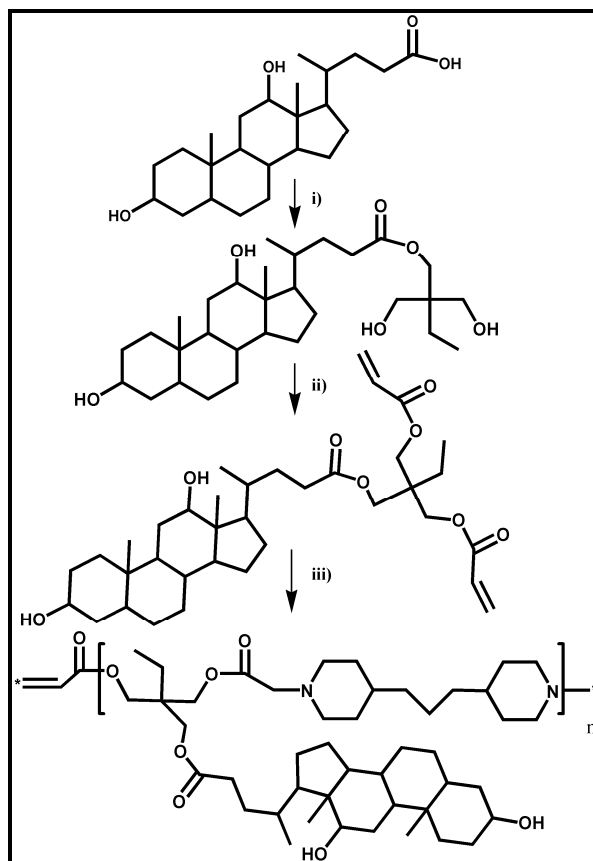
^1H NMR (200 MHz, CDCl_3) δ : 0.72 (s, 3H), 0.81 (d, 3H), 0.90 (s, 3H), 1-2.16 (m, steroidal CH, CH₂), 2.26 (m, 2H), 2.52 (d, 2H), 2.67 (m, 4H), 2.91 (t, 3H), 3.65 (s, 3H), 4.70 (m, 1H), 5.17 (d, 1H), 5.85 (br d, 0.3H), 6.25 (br d, 0.3H), 6.40 (br d, 0.3H)

8.2.2.3 Poly (trimethylolpropane deoxycholate β amino ester) (TMP-DOCA Pendent through tail)

a) Synthesis of trimethylol propane deoxycholate

15 g of deoxycholic acid and 150 g of trimethylol propane were mixed. Above mixture was heated at 75 ° C under nitrogen atmosphere. 2 ml of concentrated hydrochloric acid was added and stirred till complete solubilization of deoxycholic acid was achieved. Stirring was continued at 65 - 70 ° C for 15 hrs. Slowly this solution was added in 4 L of cold water, stirred and filtered. The product was washed and dried under vacuum. This step was repeated once again to completely remove traces of trimethylol propane and hydrochloric acid. Finally product was dried in vacuum oven at 50 ° C for 2 days and then stored in desiccator. (Melting point = 147 ° C, Yield = 15.9 g)

^1H NMR (200 MHz, CDCl_3) δ : 0.68 (s, 3H), 0.88 (m, 6H), 1 (d, 3H), 1.1-2.16 (m, steroidal CH, CH₂), 2.35 (m, 2H), 3.0 (s, 1H), 3.57 (m, 5H), 3.98 (t, 1H), 4.18 (s, 2H).



- i) Trimethylol propane, conc. HCl, 15 hr, 65 °C; ii) Acryloyl chloride, TEA, THF, 24 hrs; iii) TMDP, AlCl_3 , DCM, 24 hrs

Figure 8.3. Synthesis of Poly (trimethylolpropane deoxycholate β amino ester).

b) Synthesis of trimethylolpropane deoxycholate diacrylate

15 g of trimethylolpropane deoxycholate was dissolved in 300 ml of dry THF. 8 ml of TEA was added to it and stirred for 30 minutes under nitrogen atmosphere and cold condition 10 °C. Slowly acryloyl chloride in THF solution was added to above solution over 1 hr. This reaction mixture was stirred for 24 hrs at room temperature. This solution was filtered to remove triethylamine hydrochloride salt. The filtrate was

concentrated and purified by silica gel column chromatography using ethyl acetate: petroleum ether mixture as eluent. (Yield = 2.4 g)

^1H NMR (200 MHz, CDCl_3) δ : 0.68 (s, 3H), 0.92 (m, 9H), 1.12 (m, 3H), 1.15 - 2 (m, steroidal CH, CH₂), 2.33 (m, 3H), 2.82 (s, 2H), 3.43 (s, 2H), 3.99 (t, 1H), 4.04 (s, 1H), 4.11 (s, 1H), 4.78 (m, 1H), 5.82 (br d, 2H), 6.14 (br d, 2H), 6.37 (br d, 2H)

c) Synthesis of poly (trimethylolpropane deoxycholate β amino ester)

2.15 g of trimethylolpropane deoxycholate diacrylate was dissolved in 20 ml of dry DCM and pinch of anhydrous AlCl_3 as a catalyst was added under nitrogen atmosphere. This solution was maintained for 15 minutes under stirring and chilled to 5 - 10 ° C. Slowly 0.73 g TMDP in DCM solution was added to the activated trimethylolpropane deoxycholate solution and stirred for 24 hrs at room temperature. Above solution was washed with brine and dried over anhydrous sodium sulfate and concentrated. The obtained polymer was washed with hexane and dried under vacuum for 8 hrs to yield poly (methyl deoxycholate β amino ester) powder. (Yield = 2.33 g)

^1H NMR (200 MHz, CDCl_3) δ : 0.68 (s, 3H), 0.84 (s, 1H), 0.88 (s, 2H), 0.92 (s, 4H), 0.99 (d, 3H), 1.0 - 2.16 (m, steroidal CH, CH₂), 2.56 (t, 4H), 2.69 (m, 4H), 2.91 (d, 4H), 3.43 (s, 2H), 3.99 (t, 1H), 4.04 (m, 5H), 4.11 (s, 1H), 4.73 (m, 1H), 5.30 (s, 1H), 5.83 (br d, 0.11H), 6.10 (br d, J 0.11H), 6.34 (br d, 0.11H)

8.2.3 Characterization

8.2.3.1 ^1H NMR study

Nuclear magnetic resonance (NMR) spectra were recorded on a Bruker AMX-200 operating at 200.0 MHz for ^1H in CDCl_3 , which also served as an internal reference (chemical shifts BH = 7.27 ppm). All chemical shifts are relative to tetramethylsilane (TMS) set at 0 ppm.

8.2.3.2 Size exclusion chromatography

Molecular weight was determined by size-exclusion chromatography (SEC) performed on a Waters 410 system at 30 ° C at concentration 5 mg / ml in chloroform. The flow rate was 1 ml / min and calibration curve based on polystyrene standards was used.

8.2.3.3 IR spectroscopy

All the polymers were analyzed by FTIR using a Perkin Elmer, Spectrum One (Transmittance mode). 5 - 6 mg of sample was thoroughly mixed and triturated with potassium bromide (100 mg) and placed in the sample holder. The sample was scanned from 4000 to 450 cm⁻¹. The measuring conditions were resolution, 4.0 and number of sample scans, 5.

8.2.3.4 XRD

These samples were characterized by X-ray diffraction with a Philips PW1030 equipment running with CoK α radiation and an Fe filter at 40 kV and 30 mA.

8.2.3.5 Thermogravimetric analysis

All the samples were analyzed on thermal analyzer (TA Instruments, New Castle, DE, USA) and thermograms were obtained by heating about 5 - 7 mg of the polymer from ambient temperature to 700 ° C at a rate of 10 ° C / min. Weight loss with each temperature was plotted and decomposition trend was obtained.

8.2.3.6 Differential scanning calorimetry

The differential scanning calorimetry (DSC) thermograms were obtained on a DSC Quanta 100 Calorimeter (TA Instruments, New Castle, DE, USA). About 5 - 7 mg of the polymer was heated from ambient temperature to 300 ° C at a rate of 10 ° C / min and the glass transition temperature (T_g) values cited in this report were obtained from a second heating after quenching.

8.2.3.7 Polymer degradation study

Quantitative determination of degradation of polymers has been very difficult. Herein approaches like degradation study from film and compressed moulding led pellet were attempted but due to pH sensitivity and degradation led brittle nature interfered in the results. Hence only qualitative studies were undertaken by mere observation of the pellets. Three different pH conditions like 1.1, 7.4 and 10 were maintained using 1N HCl buffer, 1M Phosphate buffer and 1M sodium bicarbonate buffer respectively. Pellets of 100 mg were prepared at 8 tons of pressure on KBr press. To study degradation rate of all three approach polymers at pH 7.4, release of marker like p - Nitro aniline was undertaken.

8.2.3.8 Drug encapsulation in polymeric nanoparticles

PTX was loaded in poly bilo β amino esters nanoparticles by two methods namely

- 1) solvent diffusion precipitation (SD) and 2) solvent evaporation precipitation (SE) methods.

In solvent diffusion precipitation method, 15 mg of Paclitaxel (PTX) was dissolved in 6 ml of THF and 150 mg of poly bilo β amino ester (C_3 - C_{12} , C_3 - C_{24} , TMP-DOCA) was added to it. In 60 ml of chilled deionized water above solution is added drop wise over period of 15 minutes to yield PTX loaded nanoparticles. The residual THF was removed by rotary evaporation at room temperature and volume concentrated to 15 ml. Since these samples were larger in size they were centrifuged at 10000 rpm for 15 minutes, supernatant was removed and nanoparticles were redispersed. These nanoparticles were then freeze dried to collect drug encapsulated nanoparticles.

In solvent evaporation precipitation method, 15 mg of PTX was dissolved in 60 ml of THF to which 15 - 20 ml of water was added slowly over 15- 20 minutes. The addition was continued till some opalescence developed. In the end THF was removed by rotary evaporation. Final volume of nanosuspension was 15 ml. These samples were filtered

through 0.45 μ Acrodisc® (Pall Gellman) to remove precipitated PTX. This filtered solution was freeze dried to collect nanoparticles.

8.2.3.9 Scanning electron microscopy

All the samples were analyzed by drop casting sample solution on stub and then coating with gold vapor. The samples were imaged on FEI Quanta 200 – 3D model, dual beam SEM (ESEM) with EDAX. The electron source was Tungston filament. Resolution was 3 nm.

8.2.3.10 Particle size and zeta potential determination

The static light scattering (SLS) measurements were performed using a Brookhaven Instruments corporation UK 90 Plus particle size analyzer. The scattering intensity was measured at fixed angles (θ) of 90°. Nanoparticle solutions were prepared in double distilled water. The solution was filtered through a Pall Gellman PES syringe filter (0.45 μ) before analysing samples. Prior to the measurements, the scattering cell was rinsed thrice with the filtered solution. The entire particle sizing experiments were started at the room temperature and done in triplicate at concentration of 1 mg/ml. Same samples were also analyzed for zeta potential. Electric field of 7.0 V/cm was applied across 2 electrodes and with inputs of pH and particle size, zeta potentials were determined. For each measurement 5 runs were averaged with each run employing 10 cycles for 3 minutes. For analyzing data Zeta pals software of Brookhaven instruments was used.

8.2.3.11 Drug content determination

In order to determine total drug content, 5 mg of Paclitaxel loaded nanoparticles prepared by both method were weighed and 1 ml of THF was added to dissolve both polymer and PTX. Final volume was made up with ethanol. 25 μ l of this volume was injected in HPLC to determine total drug content. An isocratic reverse-phase HPLC (Agilent 1100 series, Agilent Technologies, Wilmington, DE) was used having a C₁₈

column at 25 °C and mobile phase acetonitrile-water (50:50 v/v) with a flow rate of 1.0 mL/min. The PTX concentrations in the samples were determined using a calibration curve obtained in the concentration range of 1 – 100 µg / ml, and the detection limit was 0.5 µg / ml.

8.2.3.12 Drug release studies

Precipitated nanoparticles (10 mg) were resuspended in 5 ml of 1M sodium salicylate in phosphate buffered saline solution (PBS; pH 7.4) and added in dialysis bag (molecular weight cut off 2000 daltons) and incubated at 37 ° C in 45 ml of sodium salicylate in PBS release medium under constant stirring. After every 12 hrs sample were withdrawn and the same volume of fresh release medium at the same temperature was added. The samples were assayed for drug content by HPLC according to the standard curve. The results were used to calculate cumulative drug release.

8.3 Results and discussion

8.3.1 Synthesis and characterization of poly bile β amino esters

Many approaches have been explored for the polymerization of bile acid. Main chain polymerization is one of the interesting areas since it would reduce dependence on the commonly used biodegradable polyesters like PLA, PLGA and PCL. The main problem with these polymers is generation of low molecular weight lactic and glycolic acid which causes acidic environment leading to inflammation in tissue region. On the other hand bile acid is high molecular weight compound having less acidic nature and high biocompatibility. This high molecular weight and hydrophobicity makes them suitable building blocks for synthesis of polymers useful in controlled release of actives. Use of coupling agents failed since they yielded branched polymer architectures having high crystallinity which limited their solubility (Zhu 2002). Bile acid based polyanhydrides degraded through surface erosion and exhibited zero order release (Gouin 2000). However, low T_g and lack pH sensitivity in the backbone limited their applicability. Ring opening polymerization of bile acid based lactones needs Grubb's catalyst and

need more drastic conditions (Gouin 2000). These polymers exhibited low T_g and high hydrophobicity but lacked pH sensitivity which limited their utility. Polymerization of bile acid derivatives through click chemistry, yielded high molecular weight polymers (Kumar 2010) but lack of pH sensitivity and readily hydrolyzable linkage limited their applications.

Synthesis of new steroidal diacrylates and their polymerization of them using β Michael addition of TMDP helps to incorporate pH sensitivity and degradability useful for the release of actives. The approach also involves polymerization of deoxycholic acid in different structural planes like head to tail, head to side and as tail pendent which alters the hydrophobicity of polymers.

Poly β amino esters based on the three approaches were synthesized by michael addition of michael donor like secondary diamines to michael acceptors like diacrylates. These reactions are like condensation polymerization and rates of these reactions can be increased by catalysts like lewis acid e.g. Aluminium chloride. No side products are generated which would control the rate of reaction. Here the rate of reaction is mostly controlled by steric factors and increasing viscosity of medium with the progree of reaction.

Deoxycholic acid has a steroidal nucleus with two hydroxyl and one carboxylate functionality. To polymerize deoxycholate in different structural planes selective acrylation of hydroxyls would be needed. Head to tail, head to side and pedant through tail has been achieved using michael addition.

8.3.1.1 C3-C24 polyaddition

C_{24} carboxyl group was esterified with excess of ethane diol to yield monogol ester with hydroxyl functionality. This monogol ester hydroxyl and steroid hydroxyl at 3β position were reacted with acryloyl chloride to yield deoxycholyl glycol diacrylate. Selective acrylation was possible since glycol hydroxyl is primary and steroidal 3β hydroxyl is comparatively more reactive than hydroxyl at C_7 position. This diacrylate helps to

incorporate deoxycholate moiety in polymer backbone as head to tail like conventional approaches reported earlier. Polymer molecular weight was determined from the ^1H NMR using ratio of one proton on C_{17} to diacrylate content. In deoxycholyl glycol ratio of C_{17} proton to diacrylate was 1 : 6. Since the stoichiometry of addition of amine to diacrylate was 1, the resulting polymer can be expected to have acrylate at one end and amine at another end like any other polymer prepared by polycondensation method. If we take reference of any completely resolved peak of deoxycholate unit and compare it with terminal acrylate protons then degree of polymerization of polymers can be determined. Herein ratio of three acrylate protons to single tertiary proton at C_{17} yields $\text{DP} = 15.96$. Thus for every three terminal acrylate protons 15.96 number of C_{17} proton were there, indicating 15.96 units present in chain. The calculated molecular weight was 11874. Molecular weight of the same polymer by GPC indicated M_w 2144 and M_n 563, PDI 3.8. This discrepancy cannot be explained but since molecular weight determination by GPC is relative and determined using calibration curve of polystyrene while molecular weight determination by ^1H NMR is absolute.

8.3.1.2 C3-C12 polyaddition

C_{24} carboxyl group of deoxycholic acid was esterified with methanol to yield methyl ester with two hydroxyl functionalities on C_3 and C_{12} . These two hydroxyl functionalities could be acrylated using acryloyl chloride. This methyl deoxycholate diacrylate could be polymerized in head to side structural plane due to Michael addition of TMDP like in C_3 - C_{24} polyaddition. In methyl deoxycholate diacrylate ratio of C_{17} proton to diacrylate was 1 : 6. On polymerization the ratio of three terminal acrylate protons to single C_{17} proton was found to be 3.4. Thus for every acrylate unit at terminal 3.4 units of deoxycholate units are present in chain indicating $\text{Dp} = 3.4$. The calculated molecular weight 2461. Molecular weight of the same polymer by GPC indicated M_w 2160 and M_n 1552, PDI 1.39.

8.3.1.3 TMP-DOCA polyaddition

C₂₄ carboxyl group of deoxycholic acid was esterified with excess trimethylol propane to yield TMP mono deoxycholate. In this monodeoxycholate four hydroxyls were present with two at C₃ and C₁₂ on steroidal unit and remaining two of trimethylol propane. Selective diacrylate could be prepared from this TMP monodeoxycholate using stoichiometric amount of acryloyl chloride. This was because trimethylol propane hydroxyls were primary, reactive and sterically unhindered compared to steroidal hydroxyls. This trimethylol deoxycholate diacrylate could be polymerized as pendent due to Michael addition of TMDP on acrylates. In trimethylol deoxycholate diacrylate ratio of C₁₇ proton to diacrylate was 1 : 6 as in other two approaches. On polymerization the ratio of three terminal acrylate protons to C₁₇ single proton was found to be 9.25 which indicated degree of polymerization 9.25. The calculated molecular weight was 7649. Molecular weight of the same polymer by GPC indicated M_w 9375 and M_n 5630, PDI 1.665.

Thus the three approaches yield M_w 2000 to 9000 indicating oligomers containing 4 to 16 steroidal moieties in chains.

All poly (β amino esters) were characterized by IR spectroscopy. The peak in the range 3400 to 3600 cm⁻¹ which corresponds to free hydroxyls is observed in TMP-DOCA oligomers at 3541 cm⁻¹ wherein both the hydroxyls are free on deoxycholate unit. In C₃-C₁₂ polymers, one hydroxyl is free and another is utilized for polymer preparation hence weak narrow peak at 3541 cm⁻¹ can be seen. In C₃-C₂₄ polymers both the hydroxyls are utilized during polymerization step hence no peak is observed at 3541 cm⁻¹. Another peak at 3445 cm⁻¹ can be observed in all oligomers which could be ascribed to β amino group. IR spectrum also displayed weak peaks acrylate esters at 1640 cm⁻¹ which can be ascribed to terminal acrylates on all the oligomers.

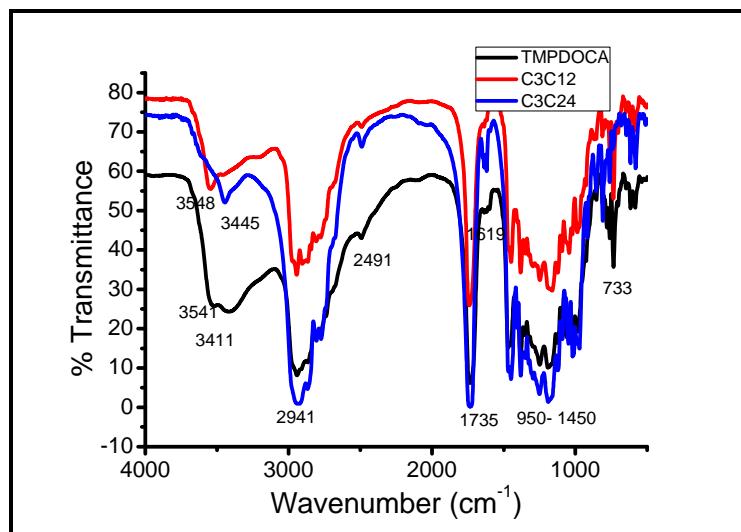


Figure 8.4. IR spectra of poly deoxycholyl TMDP β amino esters.

Bile acid based poly β amino ester swere also characterized by XRD. (Figure 8.5)

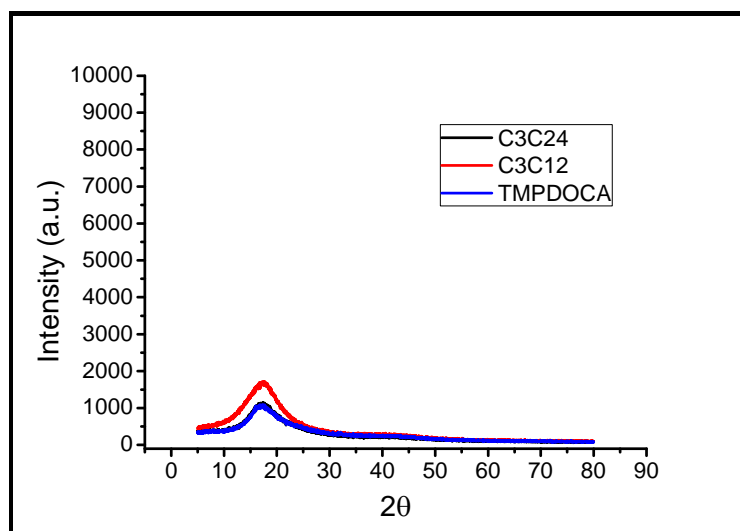


Figure 8.5. XRD spectra of poly deoxycholyl TMDP β amino esters.

Crystallinity of poly deoxycholyl TMDP β amino esters was investigated at low angles from 5 – 80 °. Earlier reports indicated that the bile acid polymers due to their rigid steroidal structure and stacking ability formed crystalline polymers which were difficult

to solubilize. Herein all the polymers are amorphous in nature with single weak peak at diffraction angle of 17.48°

Thermogravimetric analysis (TGA) of all poly β amino esters was performed at heating rate of $10^\circ\text{C} / \text{min}$. The thermograms indicated that all poly β amino esters were highly thermostable and only 10% weight loss was observed upto 300°C . The weight loss is complete at 450°C due to decomposition and degradation.

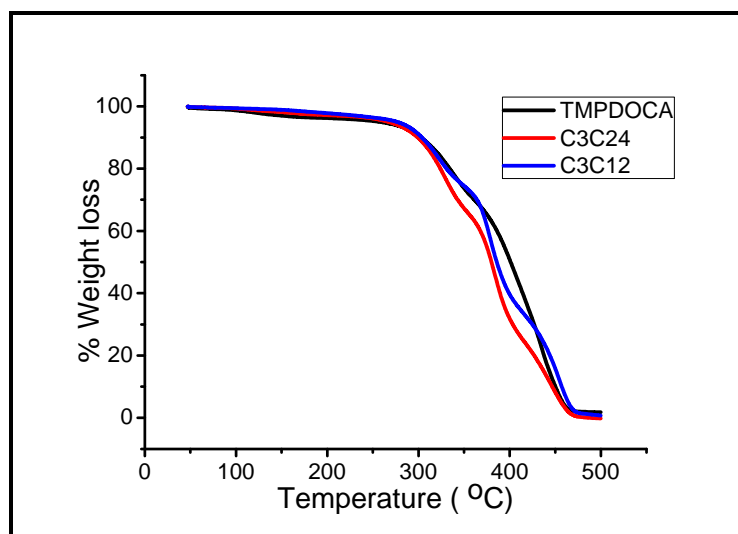


Figure 8.6. TGA curves of poly deoxycholylyl TMDP β amino esters.

Differential scanning calorimetry (DSC) of all poly β amino esters were performed at heating rate of $10^\circ\text{C} / \text{min}$ from -40 to 270°C . Poly Deoxycholylyl TMDP β amino esters prepared by different approaches exhibited different T_g values at 77.26 , 71.19 and 86°C for C_3C_{24} , C_3C_{12} and TMP-DOCA polymers respectively. These values are lower because of low molecular weight but still in the range of high molecular weight lithiocholic acid based polyanhydride homopolymer (M_n 18000) (85°C). These values are still higher than their copolymers with sebacic acid (13°C) (Gouin 2000). However the values are lower than bile acid polymerized through click chemistry which yielded high molecular weight polymers (M_n 25000 - 75000) having high T_g in the range $108 - 130^\circ\text{C}$ (Kumar 2010).

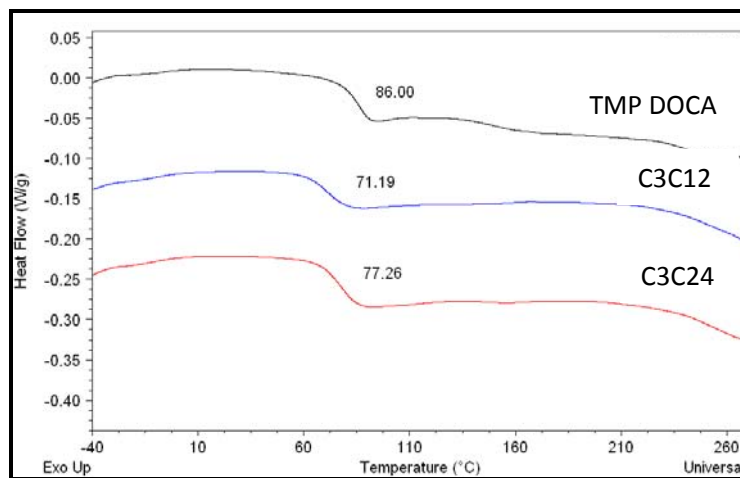


Figure 8.7. DSC thermograms of poly deoxycholyl TMDP β amino esters.

8.3.2 Degradation studies

Bile acid based poly (β amino esters) were highly hydrophobic due to deoxycholate moieties. pH sensitivity was observed in these polymers owing to incorporation of amine in the main chain backbone. These polymers formed films but when immersed in buffers, they turned brittle and were broken into pieces. Hence compression moulded disks were prepared. Disks collapsed and formed gelatinous mass at pH = 1 while pellets at pH 7.4 and 10 did not show any observable changes. With time gelatinous mass reduced and finally turbid solution remained at pH 1 while in other samples, fragments of disks increased with time. Quantitative degradation study was not possible since disks displayed abrupt weights even after removal, washing and drying. These disks due to presence of amine in the backbone adsorbed buffer salts and water so interference of many factors prevented degradation study quantitatively.

P- Nitro aniline release was studied in 7.4 pH phosphate buffer over a period of 1 month. Release study indicated decreasing release of p-Nitro aniline / day. At day 1 its release was approximately 25 mcg / ml which decreased to 2.5 mcg / ml at day 25. This clearly indicated release was not through erosion mechanism. In the present case since release rate is decreasing with time it can be attributed to concentration gradient led diffusion phenomenon.

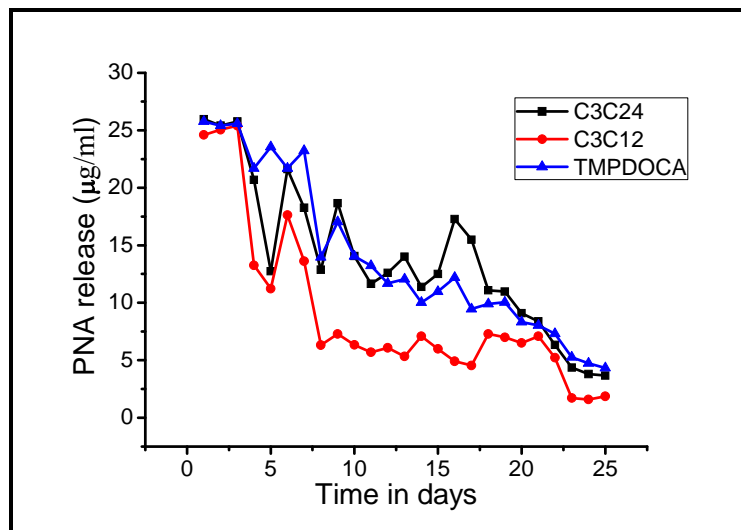


Figure 8.8. Release of p- nitro aniline from poly deoxycholyl – TMDP β amino esters.

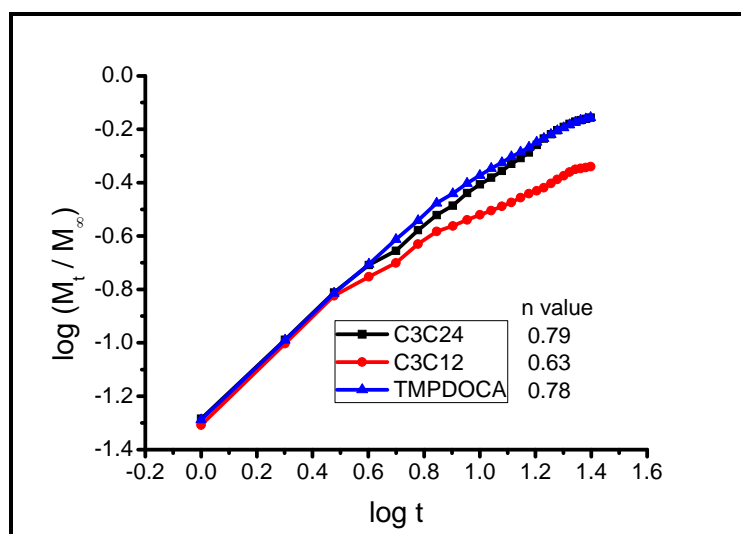


Figure 8.9. Mechanism of p- nitro aniline release from bile acid based poly (β amino esters) matrices.

Mechanism of pNA release from bile acid based poly β amino esters were elucidated using equation $M_t / M_\infty \propto t^n$. Plot of $\log M_t / M_\infty$ vs $\log t$ yielded slope values in the range 0.6 - 0.8 which indicate anomalous release kinetics.

8.3.3 Preparation of PTX loaded nanoparticles and characterization

In solvent diffusion induced precipitation method particle size of nanoparticles is smaller compared to solvent evaporation led precipitation method. Solvent evaporation led precipitation method yielded nanoparticles which were uniform and spherical in shape. The particle size ranged from 200 – 500 nm as observed in SEM micrographs. Further optimization of size could be achieved by controlling rate of addition of water, evaporation of solvent and concentration of polymer in solvent.

Nanoparticles prepared by solvent diffusion induced precipitation method were too small to be imaged by SEM. The particle size of these nanoparticles was determined by static light scattering method which indicated size in the range 75 - 270 nm as shown in table 8.1. C_3C_{24} and TMP-DOCA polymers yielded smaller nanoparticles compared to C_3C_{12} polymer. This could be explained by the bending inability of C_3C_{12} polymer. C_3C_{12} polymer is highly rigid since polymerization is between acrylates on head and side of steroidal nucleus.

Zeta potential values were positive and high which indicated that PTX loaded nanoparticles were stable and cationic in nature. The cationic nature can be attributed to β amino ester linkage present between deoxycholic acid units.

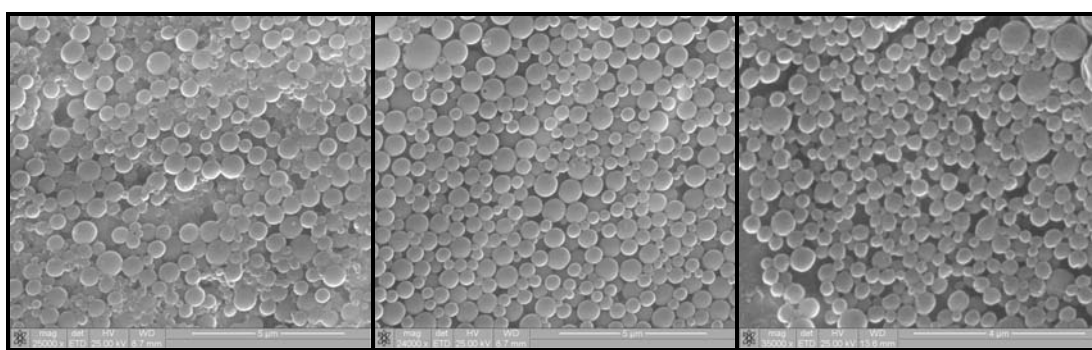


Figure 8.10. SEM micrograph of nanoparticles prepared from poly deoxycholyol – TMDP β amino esters a) C_3C_{24} , b) C_3C_{12} , c) TMP-DOCA.

Table 8.1. Partical size and zeta potential of PTX loaded nanoparticles

Polymer type	Effective diameter (nm)	polydispersity	Zeta potential (ξ) (mv)
C ₃ C ₂₄	118	0.156	37.52
C ₃ C ₁₂	267	0.226	42.39
TMP-DOCA	76	0.230	45.26

8.3.4 Drug loading and release

PTX is highly hydrophobic molecule which exhibits affinity towards deoxycholic acid unit for hydrophobic interaction. This is exploited for drug encapsulation inside poly β amino esters based on deoxycholic acid. Analysis indicated approximately 50 - 95 % drug was incorporated in nanoparticles. Drug loading was more in case of nanoparticles prepared by solvent evaporation led precipitation method. (Table 8.2.) This may be due to the larger size of nanoparticles which favoured more drug loading.

Table 8.2. PTX content in bile acid based poly (β amino ester) nanoparticles

Preparation method / polymer	% PTX loading
SD1	58.78
SD2	48.76
SD3	66.46
SE1	97.28
SE2	99.23
SE3	92.26

Drug release study carried out over 96 hrs indicated that at maximum 57% of drug was released from nanoparticles prepared from C₃C₂₄ polymer by solvent diffusion method. The release rates were dependent on type of polymer owing to different hydrophobic interactions of PTX inside nanoparticles and method of preparation.

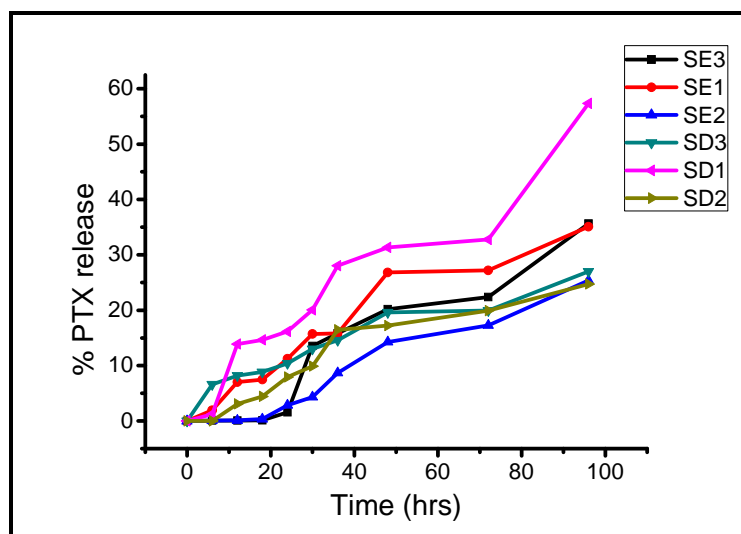


Figure 8.11. PTX release from nanoparticles prepared from bile acid based β amino esters of C_3C_{24} , C_3C_{24} , TMP-DOCA polymers by solvent evaporation (SE) and solvent diffusion (SD) methods.

In general irrespective of method of preparation, C_3C_{24} polymer released PTX faster compared to others. Except for sample of nanoparticles prepared from C_3C_{24} polymer by solvent diffusion method, nanoparticles prepared by solvent evaporation method released PTX faster than those prepared by solvent diffusion method.

8.4 Conclusions

Bile acid diacrylate monomers were synthesized in three different structural planes using different hydroxyl groups at C_3 , C_7 and C_{24} and characterized using 1H NMR and IR spectroscopy. These monomers were polymerized by 1, 4 Michael addition of TMDP catalyzed by Lewis acid i.e. Aluminium trichloride. The characterization of poly (Deoxycholyl TMDP β amino esters) indicated that they were mostly oligomeric, amorphous in nature and highly thermo-stable with T_g in the range from 70 – 80 °C. Qualitatively polymer degradation seems to be very slow at basic and neutral pH but fast in acidic condition. p-Nitro aniline release from the disks of poly (Deoxycholyl TMDP β amino esters) indicated diffusion controlled release pattern over 25 days.

Polymers yielded PTX loaded nanoparticles by solvent evaporation and diffusion led precipitation method in the range of 200 – 500 nm and 75 - 265 nm as indicated by SEM and particle size measurements. PTX encapsulation efficiency was approx 50-95% and 55% of drug was released over 96 hrs from these nanoparticles.

8.5 References

1. Ahlheim M., Hallensleben M. L., Wurm H. *Polym. Bull.* 1986, 15, 497 - 501.
2. Albert D., Feigel M. *Tetrahedron Lett.* 1994, 35, 565 - 568.
3. Allcock H. R., Pucher S. R., Scopelianos A. G. *Macromolecules* 1994, 27, 1 - 4.
4. Benrebouh A., Zhang Y. H., Zhu X. X. *Macromol. Rapid Commun.* 2000, 21, 685 -690.
5. Cha Y., Pitt C. G. *Biomaterials* 1990, 11, 108 - 112.
6. Denike J. K., Zhu, X. X. *Macromol. Rapid Commun.* 1994, 15, 459 - 465.
7. Ferruti P., Marchisio M. A., Duncan R. *Macromol Rapid Commun* 2002, 23, 332 - 55.
8. Ferruti P., Marchisio M. A., Barbucci R. *Polymer* 1985, 26, 1336 - 48.
9. Fu H. L., Yu L., Zhang H., Zhang X. Z., Cheng S. X., Zhuo R. X. *J. Biomed. Mater. Res. Part A* 2007, 81A, 186 - 194.
10. Gao, H.; Dias, J. R. *Synth. Commun.* 1997, 27, 757 - 776.
11. Gautrot J. E., Zhu X. X., *Angew. Chem. Int. Ed.* 2006, 45, 6872 – 6874.
12. Gouin S., Zhu X. X., Lehnert S. *Macromolecules* 2000, 33, 5379 – 5383.
13. Kim I. S., Kim S. H., Cho C. S. *Macromol. Rapid Commun.* 2000, 21, 1272 - 1275.
14. Kumar A., Chhatra R. K., Pandey P. S. *Org. Lett.*, 2010, 12, 1, 24 - 27.
15. Langer R., Peppas N. A. *Biomaterials* 1981, 2, 195 - 210.
16. Li A. M., Rashkov, I., Espartero J. L., Manolova N., Vert, M. *Macromolecules* 1996, 29, 57 - 62.
17. Lynn D. M., Langer R. D. *J. Am. Chem. Soc.* 2000, 122, 10761 - 10768.

18. Masar B., Cefelin P., Lipatova T. E., Bakalo L. A., Lugovskaya G. C. J. Polym. Sci. Polym. Symp. 1979, 66, 259 - 268.
19. Mather B. D., Viswanathan K., Miller K. M., Long T. E., Prog. Polym. Sci. 2006, 31, 487 - 531.
20. Mathiowitz E., Cohen M. D. J. Membr. Sci. 1989, 40, 67 - 68.
21. Pal A., Shah S., Devi S., Colloids and Surfaces A: Physicochemical and Engineering Aspects 2007, 302, 1-3, 51-57.
22. Pandey P. S., Singh R. B. Tetrahedron Lett. 1997, 38, 5045 - 5046.
23. Pitt C. G., Gratzl M. M., Kimmel G. L., Surles J., Schindler A. Biomaterials 1981, 2, 215 - 220.
24. Pitt C. G., Jeffcoat A. R., Zweidinger R. A., Schindler A. J. Biomed. Mater. Res. 1979, 13, 497 - 507.
25. Pitt C. G., Gratzl M. M., Jeffcoat A. R., Zweidinger R., Schindler A. J. Pharm. Sci. 1979, 68, 1534 - 1538.
26. Sinha V. R., Khosla L. Drug Dev. Ind. Pharm. 1998, 24, 1129 - 1138.
27. Shenoy D., Little S., Langer R., Amiji M., Pharmaceutical Research, 2005, 22, 12, 2107 - 2114.
28. Zhang Y. H., Zhu X. X. Macromol. Chem. Phys. 1996, 197, 3473 - 3482.
29. Zhu X.X., Nichifor M. Acc. Chem. Res. 2002, 35, 539 - 546.

Chapter 9

Conclusions and suggestions for future work

Post translational modification of proteins in body inspired the synthesis of bile acid – polyaspartic acid conjugates. The conjugates exhibited diverse morphologies like micelles, vesicles, tubules and nanospheres depending upon the type of hydrophilic functionalization. Amphotericin B was encapsulated in these morphologies and exhibited efficacy and reduction in hemotoxicity. These morphologies also acted as templates for nano-patterning of silver and gold nanoparticles in ring and necklace forms. The same conjugates with amine functionality formed *in situ* hydrogels with hydrophobic domains through aza - Michael addition on PEG diacrylate. Triclosan was released over 24 hrs to 7 days depending upon the type of cross-linker used for gel formation. Additionally *in situ* hydrogels formed by reactive emulsions has also been conceptualized. Bile acid based poly (β amino esters) were also synthesized in all structural planes of steroidal nucleus. These polymers formed nanoparticles in the size range 70 -500 nm which were investigated for Paclitaxel delivery.

Major conclusions arrived at from this investigation are summarized below.

1. Judicious selection and incorporation of hydrophilic functional groups governs the morphology of synthetic biloproteins. While hydrophobe AEDOCA was responsible for self assembly, hydrophilicity and hydrogen bonding ability of functional groups like carboxyl, hydroxyl, hydrazide and amide guided it to diverse morphologies like micelles, vesicles, tubules and nanospheres.
2. Ampho B solubilized in biloprotein self assemblies follows similar aggregation pattern like Fungizone[®] micellar form but exhibits lower haemotoxicity in more compact bilo 60 structures. All the compositions exhibited MIC values close to the values observed for conventional sodium deoxycholate micellar system. Ampho B super aggregates were observed on heating the formulations as confirmed by UV, CD and fluorescence spectroscopy. These are similar to those observed in heat induced super aggregates of conventional Amphotericin B in sodium deoxycholate micelle formulation. On heating, Ampho B in loose micelle

became less haemotoxic than Ampho B in compact structures which was an interesting observation, as this trend is exactly opposite to that reported in literature.

3. Biloproteins could form stable gold and silver nanoparticles with uniform and narrow particle size distribution. The gold and silver nanoparticles could be patterned on various morphologies.
4. Synthetic biloproteins and lipoproteins with amine functional groups could form self assembly with reactive surface. The surface amine groups could be cross linked in situ using water soluble PEG diacrylates to yield hydrogel. The hydrogels thus immobilized self assembled structures within the matrix. Cross linking prevents release of drug from the immobilized self assemblies.
5. The presence of self assembled structures within hydrogels was confirmed by confocal microscopic analysis of Nile red and FITC dextran loaded particles. Hydrogels containing hydrophobic domains were characterized for gelation time, viscosity and modulus as a function of time. The gelation times were 75 seconds to 15 minutes and increase in modulus was 10 folds compared to hydrogels without hydrophobic domains. Gel degradation in PBS (pH 7.4) was studied which showed complete degradation in 2-4 days.
6. Triclosan could be loaded in the self assembled structure by micellar solubilization. TCN loaded self assemblies were then cross linked to yield hydrogels which released drug over duration of 1 to 7 days depending upon the type of cross linker.
7. Synthetic biloproteins and lipoproteins could also act as emulsifier as indicated by emulsification of soya bean oil and α tocopherol. These emulsions were basic due to amine functionalities on the surface as indicated by positive zeta potential values.

8. *In situ* cross linked hydrogels could be achieved by reaction of these reactive oil droplets in emulsion form with PEG diacrylate. The formed hydrogels called “Emulhydrogel” contained oil droplet inside cross linked hydrogel matrix. Model compound Nile red could be dissolved in oil and held in hydrogel matrix as observed by confocal microscopy. Paclitaxel could be loaded in the oil phase of these reactive emulsions. It was released from *in situ* hydrogels over duration of 15 hrs following an initial lag phase of 15 hrs.
9. Deoxycholic acid based diacrylates could be prepared in different structural planes which acted as Michael acceptors along with TMDP to yield Poly (β amino esters) with deoxycholate units linked in head to tail, head to side and pendent through tail position.
10. The molecular weight investigations indicated oligomeric products with degree of polymerization in the range 5 – 20. Bile acid based poly β amino esters exhibited high hydrophobicity due to steroidal building units and pH sensitivity due to basic β amino ester linkage. The Oligomers were amorphous and exhibited high T_g in the range 70 – 80° C.
11. Bile acid based poly β amino esters formed nanospheres having size in the range 75 – 500 nm. These nanospheres could encapsulate paclitaxel and release 20 - 60 % over 100 hrs.

Any investigation of this kind addresses only some of the issues and opens opportunities for further investigations. Some of these are listed below.

1. The ability of functional groups studied in achieving diverse morphologies need to be further probed using different backbones with same hydrophobe used here.
2. The choice of drug and its efficient encapsulation in these morphologies should also be investigated in further details for utilization of benefits of morphology, type and shape in drug delivery system.
3. The biloproteins could also be modified with vinyl functionality and then cross linked by free radical mechanism using heat or light sensitive initiators. This would prevent mobility in hydrophobic core region of biloproteins holding drug in core region for extended time.
4. Taking advantage of high rate of reaction of amine with diacrylates demonstrated in hydrogel formation through Michael type addition mechanism, surface cross linking of aminated self assemblies using PEG diacrylates in dilute system can be developed like click chemistry.
5. Surface cross linking of these self assemblies using reducible disulfide cross linkers could further evolve this drug delivery system for targeted delivery of bioactives.
6. Surface reactive morphologies for in situ gel formation can be applied to wide range of applications wherever site specific controlled release of hydrophobic drug is needed. These drug delivery systems can also be developed by appropriately tailoring the degradation pattern for an in situ timed release hydrogel system.
7. Biloprotein capped gold and silver hydrosols can be explored further for drug targeting and imaging of carrier inside body.

8. Utility of diverse morphologies observed in biloprotein self assemblies for gold and silver reduction can be probed further. It would also help in achieving different gold and silver reduction patterns having applications in microelectronics, biosensors and drug delivery systems.
9. Drug delivery from bile acid based poly β amino ester based nanoparticles needs to be investigated more thoroughly. The cationic charge and high hydrophobicity with bile acid as building block imply better transfection ability which can be explored for applications in gene delivery.
10. The transport of bile acid based poly β amino ester nanospheres across intestinal mucosa needs to be investigated. If successful, these nanospheres could be used for the oral delivery of proteins and peptide drugs.

“Synthesis & Evaluation of Polymeric Drug Delivery Systems”

Synopsis

For the degree of Doctor of Philosophy

(Technology)

In

Chemical Engineering

Jitendra J. Gangwal

M.Pharm. (Pharmaceutics)

Polymer Science and Engineering Division

National Chemical Laboratory

Pune - 411008, India

**SYNOPSIS OF THE THESIS TO BE SUBMITTED TO THE UNIVERSITY OF
MUMBAI FOR THE DEGREE OF DOCTOR OF PHILOSOPHY
(TECHNOLOGY) IN CHEMICAL ENGINEERING**

Name of the Student	Mr. Jitendra J. Gangwal
Name of the Research Guide	Dr. Mohan G. Kulkarni
Place of Research	Polymer Science and Engineering Division, National Chemical Laboratory, Pune - 411008, Maharashtra, India.
Topic of Research	“Synthesis & Evaluation of polymeric Drug Delivery Systems”
Registration Number	02
Date of Registration	18 / 08 / 2006
Date of Submission of Synopsis	12 / 01 / 2010
Signature of Student Guide	Signature of Research
(Mr. Jitendra J. Gangwal)	(Dr. Mohan G. Kulkarni)

Introduction:

Molecular self assembly results in spontaneous formation of ordered aggregates as a result of non covalent interactions like hydrogen bonding, ionic and hydrophobic interactions. The molecular structure of basic component governs the structure and type of self assembly. Self-assembly is scientifically interesting and technologically promising. Importance of self assembly has been recognized in chemistry, physics, biology, materials science, nanoscience and pharmacy. Understanding dynamics of self-assembling systems is crucial to elucidate the role of self-assembly in biological processes. In nature, molecular self assembly of peptides, lipids and polysaccharides as lipoproteins, glycoproteins, lipoglycoproteins results in diverse supramolecular structures responsible for recognition in receptors, activity in enzymes, interaction motif in uptake and transport.

Present investigation was undertaken to devise new strategy for formation of diverse nano structures from the same polymer conjugates and illustrate their applications. We demonstrate that bile acid conjugates of polyaspartic acid exhibit diverse morphologies such as micelles, vesicles and tubules depending on the degree of conjugation of bile acid and the choice of hydrophilic functional moiety. Our strategy of manipulating hydrophilic groups tries to bring out importance of functional modifications which mimic post translational modifications in protein responsible for assignment of few functions, change in receptor recognition, binding and transportation or penetration etc.

Ampho B is an antifungal drug for systemic fungal infection however its acute and chronic toxicity limits its usage. We incorporated Ampho B in the micelles and evaluated the effect of encapsulation on toxicity and MIC of Ampho B. It was observed that Amphotericin B incorporation in biloproteins was possible with enhanced stability. Toxicity of Amphotericin B was same as that of Fungizone^R in micelle forming anionic biloproteins but reduced by 30% in vesicle forming biloprotein self assemblies.

The above mentioned anionic biloproteins which exhibited micellar and vesicular morphologies also formed Gold and Silver nanoparticles by reducing aqueous solutions

of respective metal salts. Biloproteins acts as capping and stabilizing agents for gold and silver nanoparticles. Effect of molecular weight of biloproteins on gold and silver nanoparticles was also studied.

In situ formed hydrogels have evoked considerable interest in site-specific drug-delivery systems. They exist as flowable aqueous solutions (or sol state) before administration and immediately turn to standing gels upon administration. Recent reports indicated formation of chemically cross linked in situ hydrogels through reaction of PEG diacrylates with PEG thiols in an aqueous medium. These in situ gels acted as depots for drug delivery and tissue regeneration.

The aminated biloprotein described in diversely functionalized biloproteins above form micelle which present reactive amine functionalities for reaction with the water soluble diacrylate monomers to yield biodegradable hydrogels containing hydrophobic domains. The release of Triclosan (TCN) from the hydrophobic domain can be controlled by the rate of degradation of hydrogel and / or by diffusion from the micellar domain.

To overcome the problem of limited hydrophobic drug loading in self assembled structures another well known approach is emulsion formation in which hydrophobic drug is solubilized in oil and then emulsified to form O / W emulsion. Synthesis of reactive emulsion droplet was achieved by emulsion formation using reactive amine functionalized bilo / lipoproteins as an emulsifier. Emulsification efficiency of synthetic biloproteins and lipoproteins (C₁₂, C₁₆, C₁₈) using soya bean oil or α tocopherol as oil phase were explored. Synthetic biloproteins formed weak emulsions while lipoproteins could yield stable emulsion with small globule size. Addition of polyethylene glycol diacrylates (PEGDA) to these reactive emulsions yielded hydrogels named "Emulhydrogel" in 45 seconds to 6 minutes as observed in case of reactive self assemblies discussed above. Oil pockets and their distribution within the hydrogel is demonstrated by Nile red distribution in oil as evidenced from fluorescent images by confocal microscopy.

The work is presented in nine chapters and a brief outline of each is given below.

Chapter 1: Literature Survey

The problems arising in formulating drugs having complex pharmacokinetic and physicochemical properties which compromise drug efficacy and drug toxicity are investigated and discussed. Formulation scientists are restricted in designing effective drug delivery systems because of lack of availability of versatile polymers which can solubilize hydrophobic drugs effectively by encapsulation and release them slowly at a rate adequate for efficacy mitigating toxic side effects. The most biocompatible and successful approach has been use of lipidic carriers like liposomes for drug encapsulation leading to reduction in toxicity. Formulation development troubles, long term stability and economic aspects limit their utility on large scale. This necessitated entry of polymers for fabrication of drug delivery systems. Most commonly used FDA approved polymers like PLGA, PLA, PCL could achieve controlled release in depot form but have limitation for not being able to deliver drug at the site of action with desired rate. Polymer based drug delivery systems based of principles of self assembly form diverse morphologies like micelle, vesicle, tubules and nanoparticles which exhibit promising applications in drug delivery systems.

Hydrophobic drug delivery using block copolymers like PEG-PLA, PEG-PCL, PEG-Polyamino acid etc has been an interesting approach. Hydrophobically modified polyaspartic acid has been explored as micellar drug delivery owing to biodegradability and biocompatibility. Poly hydroxyl ethyl aspartamide conjugates containing 10 mole % Dehydrocholic acid formed stable uncharged micelles. At higher degrees of substitution secondary aggregation resulted in unstable morphologies.

This literature survey reveals that a wide range of approaches have been adopted by researchers for solubilization and toxicity reduction of drugs. The specific issues which need to be addressed are as listed below

1. Drug loading capacities of micelles are generally limited and also need usage of toxic solvents for drug loading.

2. Elaborate synthesis and skillful manipulation of block lengths make these systems expensive and unattractive.
3. Lack of sufficient functional groups in PEG-PLA, PEG-PCL makes diblock copolymers unattractive for drug targeting since insufficient ligand attachment lowers efficient targeting.
4. Stability of monomeric biosurfactant systems is less owing to higher CAC values limiting their utility in drug delivery.
5. Grafts copolymers are easy to synthesize and functionalizable but do not show diverse morphologies needed for efficient drug delivery system.
6. Stabilization of self assemblies by chemical cross linking for preventing their opening below CAC due to dilution has been reported but most methodologies need high dilutions and particular reaction conditions followed by purifications.

Chapter 2: Objective and scope of work

The major focus of this work is to design and evaluate polymeric self assemblies which exhibit diverse morphologies with applications in drug delivery. This includes choice of hydrophobe, choice of biodegradable and biocompatible polymer backbone, and synthesis of polymer conjugates with examination of supramolecular self assemblies. It is also proposed to explore some of these morphologies for loading Amphotericin B (Ampho B) and explore reduction in toxicity.

It is also proposed to check feasibility of bridging fields of self assembly and hydrogels by introducing concept of an in situ hydrogels with hydrophobic pockets. Afore mentioned biloprotein self assemblies if appropriately functionalized with amine groups could be converted into in situ cross linked hydrogels by reaction of reactive self assemblies with polyethylene glycol diacrylate (PEGDA). Thus using hydrophilic cross linkers these self assemblies would be cross linked by exploiting Michael type addition reaction in water leading to formation of an in situ hydrogel containing hydrophobic pockets of self assembly. The release of drug from hydrogel depot would be triggered by

degradation of hydrophilic cross links. Hydrogel degradation would release self assembly which on dilution below CAC would open and release drug in medium. A model drug Triclosan would be used to probe above concept.

Ability of these reactive self assemblies formed by synthetic lipoproteins and biloproteins to act as emulsifier for soya bean oil or tocopherol would also be investigated. Using hydrophilic cross linkers these emulsified oil droplet would be cross linked in situ, forming hydrogel. If successful we believe this system would be useful for solubilization, in situ depot formation and delivery of hydrophobic drugs. The release of drug would be triggered by degradation of hydrophilic cross links and release of hydrophobic drug in emulsified form would be initiated by partition and dilution mechanisms.

The major objectives and scope of the proposed investigation are summarized below.

1. To identify biocompatible, biodegradable polymer and conjugate bile acids. Incorporate different functionalities, characterize synthetic biloproteins by different techniques and study the self assembly process.
2. To study Amphotericin B loading in these self assemblies and study its aggregation, solubilization and toxicity. Study effect of different parameters like hydrophobe content, type of self assembly and heat on aggregation and toxicity.
3. To probe ability of self assemblies for reduction of gold and silver forming stable nanoparticles.
4. To study in situ hydrogel formation using reactive self assemblies formed by various synthetic lipo and biloproteins. Characterize these hydrogels containing hydrophobic pockets for gelation time, degradation, rheology etc. Study solubilization of a model hydrophobic compound by encapsulation in self assemblies. Investigate in situ gelation by cross linking the self assemblies and release of the model compound encapsulated.

5. To explore emulsification ability of synthetic biloproteins and lipoproteins using soya bean oil or α tocopherol as oil phase. Monitor in situ cross linking of reactive emulsion droplets resulting in hydrogels containing oil pockets referred to as “Emulhydrogels”. Characterize these Emulhydrogels for gelation time, degradation time, rheology etc. and finally investigate the potential of these for the release of hydrophobic drug.
6. To explore polymerizability of bile acid using Michael type addition between diacrylated monomers of bile acids and Trimethylene dipiperazine (TMDP). Characterize oligo β amino esters for mol. Wt., degradability and drug loading. Study drug release from particulated drug delivery systems prepared from oligo β amino esters.

Chapter 3: “Synthetic biloprotein”: Synthesis and Characterization

The major focus of this work was to design and evaluate a new family of synthetic polymer conjugate which would disperse in an aqueous medium eliciting diverse morphologies depending upon the hydrophilic functional group incorporated in the backbone in addition to the hydrophobe. The polymer conjugates termed Synthetic biloproteins were prepared by exploiting amine - imide chemistry. Polysuccinimide prepared from aspartic acid by dehydro polycondensation polymerization technique was used as the backbone for preparation of polymer conjugate. Polymer backbone was characterized for molecular weight using water soluble polymer derivative PHEA. The polymer has been reported to be biocompatible and biodegradable.

Amino ethyl deoxycholamide, an ethylene diamine derivative of Deoxycholic acid, was used for reaction with succinimide rings in the polysuccinimide which yielded bile acid conjugate of polyaspartic acid. The amide link facilitates hydrogen bonding during self assembly process. The polymer conjugate was characterized for degree of conjugation and absence of free AEDOCA using ^1H NMR, TGA, DSC technique. Reactive intermediate polymer conjugate was treated with hydrazine, ethanolamine, ammonia and

sodium hydroxide to yield aminated, hydroxylated, amidated and carboxylated synthetic biloprotein having basic, neutral and acidic character respectively.

Chapter 4: Manipulating Self-Assembly in Synthetic biloprotein: Role of hydrophilic functional substitution

The chapter deals with the characterization of the various morphologies formed by self assembly of “synthetic biloproteins”. It has been shown for the first time that incorporation of different hydrophilic groups on bile acid conjugated polymers results in diverse morphologies *viz.* micelle, vesicle, tubule and compact nanoparticles. This is a result of different magnitudes of secondary valence forces like hydrogen bonding, charge interactions superposed on hydrophobic interactions which govern the self assembly process. The most interesting aspect of this approach is, once a polymer conjugate is prepared diverse synthetic biloproteins can be obtained by reaction with functional amines.

The self assemblies are characterized for Critical aggregation concentration (CAC), microviscosity and morphology. Transmission Electron microscopy (TEM), Optical microscopy and Static light scattering technique have been used for characterization of type of morphology and effective particle size distribution. Mechanistic analysis of self assembly process involved probing the role of polymer backbone, hydrophobe and functionality using IR, CD spectroscopy, DSC analysis indicated importance of type of functionality in achieving type of morphology along with hydrophobe content. The morphologies observed are summarized below.

Table 1. Hydrophilic functionalization guided self assemblies.

Sr. No.	Sample	Self assembly type
1.	Carboxylate 90 (C90)	Loose micelle
2.	Carboxylate 80 (C80)	Micelle
3.	Carboxylate 60 (C60)	Vesicle
4.	Carboxylate 40 (C40)	Vesicle
5.	Amide 90 (A90)	Vesicle
6.	Amide 80 (A80)	Vesicle
7.	Amide 60 (A60)	Tubules
8.	Amide 40 (A40)	Tubules
9.	Hydrazide 90 (Hz90)	Compact micelle
10.	Hydrazide 80 (Hz80)	Compact micelle
11.	Hydrazide 60 (Hz60)	Nanoparticles
12.	Hydrazide 40 (Hz40)	Nanoparticles
13.	Hydroxyl 90 (H90)	Aggregate micelle
14.	Hydroxyl 80 (H80)	Aggregate micelle
15.	Hydroxyl 60 (H60)	Aggregate micelle
16.	Hydroxyl 40 (H40)	Nanoparticles

Chapter 5: Drug encapsulation in biloprotein self assemblies for solubilization and toxicity reduction

Detailed investigation on drug solubilization by encapsulation in synthetic biloprotein assemblies is described in this chapter. The encapsulation is a result of mixed micelle formation of deoxycholamide units in synthetic biloprotein with Amphotericin B molecules. Ability of biloproteins to form mixed micelle varies owing to differences in

compactness in self assembly structures. Drug content in self assemblies was determined by UV spectroscopy. The influence of Biloprotein composition on mixed micelle formation with Amphotericin B determines release rate from structure which in turn governs toxicity. Investigation of aggregation using UV, CD and fluorescence spectroscopy reveals that the mechanism of mixed micelle formation of biloproteins with Amphotericin B is the same as in case of monomeric sodium deoxycholate. MIC values also confirm that in vitro efficacy of Ampho B aggregates against *Candida albicans* is comparable with sodium deoxycholate formulation. Amphotericin B formulation Bilo40 and Bilo60 are less hemolytic and toxicity follows trend:

Ampho 60 < Ampho 40 < Ampho 20 < Ampho10

Effect of heating (70 ° C for 20 min) is well documented for conventional sodium deoxycholate based formulation. Heat induced super aggregates of Amphotericin B prepared by us were found to be 30% less toxic towards isolated erythrocytes compared to unheated formulation. Biloprotein based Amphotericin B self assemblies were also investigated.. UV, CD and fluorescence spectroscopy proved that super aggregated Amphotericin B was similar to the one observed in heat treated conventional formulation. Heat treated Amphotericin B biloprotein samples exhibited reduced toxicity of previously toxic samples but displayed unusual increase in toxicity in less toxic samples. Toxicity of heat treated samples followed following trend:

Ampho 60 >Ampho 40 > Ampho 20 > Ampho10

Chapter 6: Biloprotein based preparation of Gold and Silver nanoparticles

This chapter illustrates use of biloprotein self assemblies for preparation of stable gold and silver nanoparticles. Nanoparticles were obtained by refluxing respective metal salts in presence of anionic biloproteins for 30 minutes to 1 hr.

Biloproteins act as capping and stabilizing agents for gold and silver nanoparticles. Effect of molecular weight, hydrophobe content in biloproteins on Gold and Silver nanoparticles formation was also studied. Size, shape and content were determined using

UV, IR, XRD, light scattering technique along with SEM and TEM. UV spectroscopy clearly indicated Plasmon absorption band at 523 nm for Gold and 432 nm for Silver nanoparticles. Gold and silver content in the biloprotein self assemblies was also determined using TGA and elemental analysis.

Chapter 7: In Situ Biodegradable Hydrogels from Surface Cross linked Supramolecular Self Assemblies

This chapter describes the in situ cross linked hydrogels formed under in vivo conditions. These hold promise in drug delivery, tissue engineering etc. Solubilization and uniform distribution of hydrophobic drugs in hydrogels is difficult. To overcome this limitation, biloprotein and lipoproteins were prepared by the reaction of polysuccinimide with amino ethyl deoxycholamide (AEDOCA) and fatty amines (C₁₂, C₁₆, C₁₈). Amination of both using amino ethyl piperazine (AEPz) yielded surface aminated self assembled structures such as loose micelles and nanoparticles, which were characterized for composition and morphology. Addition to polyethylene glycol diacrylates (PEGDA) resulted in biodegradable hydrogel in 45 seconds to 6 minutes.

Rheological characteristics of these hydrogels were compared with those containing no hydrophobic pockets. The biodegradable hydrogels containing hydrophobic nano reservoirs which degrade under physiological conditions in 2-4 days would be helpful for the sustained delivery of hydrophobic drugs as has been demonstrated by illustrative examples. Model drug Triclosan was dissolved in these reactive self assemblies and cross linked in situ to form hydrogel. TCN release from those hydrogels was studied in PBS (pH 7.4) and PBS containing SLS. Release pattern in PBS indicated no release for over 12 hours followed by burst after complete gel degradation. In PBS with SLS as release medium, 10% drug was released slowly for 12 hours followed by burst as observed above.

Synthesis of in situ hydrogels containing hydrophobic pockets for encapsulation and delivery of hydrophobic drugs was described above. Loading of hydrophobic drug in these systems was limited. Emulsions came into existence for delivery of highly

hydrophobic drugs with high drug loading inside hydrophobic oil pockets stabilized in an aqueous medium with suitable emulsifiers like lecithin, SLS, triglycerides etc. This chapter also describes synthesis of reactive emulsion droplet and check Michael type addition reaction on its surface. This was achieved by developing emulsions wherein reactive amine functionalized bilo / lipoproteins would be present at interface between oil and water. Efficiency of synthetic biloproteins and lipoproteins (C₁₂, C₁₆, C₁₈) in emulsification of soya bean oil and α tocopherol as oil phase was evaluated. Synthetic biloproteins act as weak emulsifier while lipoproteins were able to emulsify oil easily using sonication method. Addition of polyethylene glycol diacrylates (PEGDA) in these reactive emulsions resulted in formation of hydrogel termed “Emulhydrogel” in 45 seconds to 6 minutes as observed in reactive self assemblies above. Rheological characteristics of these “Emulhydrogel” were compared with in situ hydrogels. The biodegradable hydrogels containing oil nano reservoirs which degrade under physiological conditions in 3-4 days would be helpful for the sustained delivery of oil solubilized hydrophobic drugs.

Chapter 8: Synthesis and characterization of bile acid based Oligo β amino esters for drug delivery system

Materials based on bile acids show great promise for drug delivery and controlled release applications. Rigid steroidal backbone and amphiphilicity make them suitable candidates for fine-tuning mechanical and interfacial properties of synthetic degradable polymers. However, reports on main-chain bile acid based polyesters, polyamides and polyurethanes are few in literature and are not explored extensively. Poly β amino esters are new type of biodegradable polymers which are getting high attention because they present promising and efficient examples of hydrolysable polycations in nonviral gene delivery. They are easy to be prepared via the Michael type addition of primary amine or secondary amine to diacrylate. Different monomers based on deoxycholic acid were synthesized and characterized. Diacrylate monomers of deoxycholic acid were polymerized using Michael type addition of diamine. For the first time Deoxycholic acid was polymerized in all the structural planes using same chemistry of 1, 4 addition

of amine on Michael acceptor. Synthesized polymers were characterized for mol.wt., solubility & degradation. Particulate drug delivery system was prepared from synthesized bile acid based Oligo β amino esters and characterized for drug loading, drug release, size and stability etc.

Chapter 9: Conclusions and suggestions for future work

The important conclusions arrived at from the work are discussed in this chapter. Briefly these can be summarized as follows;

1. Judicious selection and content of functionality govern morphology of synthetic biloproteins. While hydrophobe AEDOCA was responsible for self assembly formation, hydrophilicity and hydrogen bonding ability of functional groups like carboxyl, hydroxyl, hydrazide and amide yielded diverse morphologies like micelles, vesicles, tubules and nanoparticles.
2. Ampho B solubilized in biloprotein self assemblies follows similar aggregation pattern like Fungizone[®] micellar form but exhibits lower haemotoxicity in more compact bilo 60 structures. All samples exhibited MIC values close to the values observed for conventional sodium deoxycholate micellar system. Super aggregate structure formation by heating of formulations was observed and confirmed by UV, CD and fluorescence spectroscopy. These are similar to those observed in heat induced super aggregates of conventional Amphotericin B in sodium deoxycholate micelle formulation. On heating Ampho B in loose micelle becomes less haemotoxic than Ampho B in compact structures which was an interesting observation, as this trend is exactly opposite to that reported in literature.
3. Biloproteins could form stable Gold and Silver nanoparticles with uniform and narrow particle size distribution.

4. Synthetic biloproteins and lipoproteins could form self assembly with reactive surface. The surface functionalities could be cross linked in situ using water soluble PEGDA to yield hydrogel. These hydrogels thus immobilize self assembled structures within the matrix. The cross linking prevents release of drug from the self assembly. The presence of self assembled structures within hydrogel was confirmed by confocal microscopic analysis of Nile red and FITC dextran loaded particles. Hydrogels containing hydrophobic pockets were characterized for gelation time, viscosity and modulus as a function of time. Gel degradation in PBS (pH 7.4) was studied which showed complete degradation in 2-4 days. TCN loading in the self assembled structure by micellar solubilization mechanism could be achieved. TCN loaded self assemblies could be cross linked to yield hydrogel which released drug over duration of 24 hours.

5. Synthetic biloproteins and lipoproteins could also act as emulsifier as indicated by emulsification of soya bean oil and α tocopherol. This also provided reactive functional coat on oil droplet which could be utilized for cross linking. Thus in situ cross linked hydrogels could be achieved by reaction of these reactive oil droplets in emulsion form with PEGDA. The formed hydrogel called as “Emulhydrogel” contained oil droplet inside cross linked hydrogel matrix. Model compound Nile red could be dissolved in oil and held in hydrogel matrix as observed by confocal microscopy.

Any investigation of this kind addresses only some of the issues and opens opportunities for further investigations. Some of these are listed below.

1. The ability of functional groups studied in achieving diverse morphologies need to be further probed using different backbones with same hydrophobe used here.

2. The choice of drug and its efficient encapsulation in these morphologies should also be investigated in great detail for utilization of benefits of morphology, type and shape in drug delivery system.
3. The biloproteins could also be modified with vinyl functionality and then cross linked by free radical mechanism using heat or light sensitive initiators. This would prevent mobility in hydrophobic core region of biloproteins holding drug in core region for extended time.
4. Taking advantage of high rate of reaction of amine with diacrylates demonstrated in hydrogel formation through Michael type addition mechanism, surface cross linking of aminated self assemblies using PEG diacrylates in dilute system can be developed like click chemistry.
5. Surface cross linking of these self assemblies using reducible disulfide cross linkers could further evolve this drug delivery system for targeted delivery of bioactives.
6. Novel concept of surface reactive morphologies for in situ gel formation can be applied to wide range of applications wherever site specific controlled release of hydrophobic drug is needed. These drug delivery systems can also be developed with appropriate tailoring of degradation pattern for an in situ timed release hydrogel system.
7. Biloprotein capped Gold and Silver hydrosols can be explored in more details for drug targeting and imaging of carrier inside body.
8. Utility of diverse morphologies observed in biloprotein self assemblies for gold and silver reduction can be probed further. It would also help in achieving different gold and silver reduction pattern with applications in microelectronics, biosensors and drug delivery systems.

References:

1. K. Kataoka et.al., *Advanced Drug Delivery reviews*, (2001), 47, 113-131
2. S. R. Yang et.al., *Colloid. Polym. Sci.*, (2003), 281, 852 - 861
3. W. Wang et.al., *Macromolecules*, (2004), 37, 9114 - 9122
4. G. M. Whitesides et.al., *PNAS* (2002), 99(8), 4769 - 4774
5. L. Zhang et.al. *Science*, (1995), 268, 1728 - 1731
6. Shinoda H. et.al. *Macromol. Biosci.* 2003, 3, 34
7. Y. Geng et.al. *Nature nanotechnology*, (2007), 2, 249 - 255
8. A. Antoniadou et.al., *J. mycmed.*(2005), 15, 230 - 238
9. A. Lavasanifer et.al., *Pharm. Res.* (2002), 19(4), 418
10. J. Barwicz et.al. *Antimicrob. Agents Chemother.* (1992), 36 (10), 2310 - 2315
11. P. V. D. Wetering et.al. *J. Controlled Rel.*, (2005), 102, 619 - 627
12. J. Turkewich et.al. *Discuss. Faraday soc.*, (1951), 11, 55 - 75
13. I. Hussain et.al. *Langmuir* (2003), 19, 4831- 4835
14. S. Gouin et.al. *Macromolecules*, (2000), 5379 – 5389
15. B. D. Mather et.al. *Prog. Polym. Sci.*, (2006), 31, 487 - 531

Signature of the Candidate

Signature of the Research Guide

Jitendra J. gangwal

Dr. M. G. Kulkarni